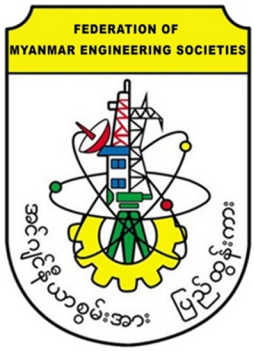

FEDERATION OF MYANMAR ENGINEERING SOCIETIES

THE FIRST NATIONAL CONFERENCE ON ENGINEERING RESEARCH

IN

COMMEMORATION OF ANNUAL GENERAL MEETING OF FEDERATION OF MYANMAR ENGINEERING SOCIETIES

PROCEEDINGS

January 16, 2020

FEDERATION OF MYANMAR ENGINEERING SOCIETIES

NATIONAL CONFERENCE ON ENGINEERING RESEARCH

IN

COMMEMORATION OF ANNUAL GENERAL MEETING OF

FEDERATION OF MYANMAR ENGINEERING SOCIETIES

16th January 2020

Fed.MES

Preface for AGM Proceeding

The First National Conference on Engineering Research has been organized by Annual General Meeting Paper Committee of Federation of Myanmar Engineering Societies (Fed.MES). The Conference will be held in Fed.MES Building on 16th January 2020.

The Conference intends to being together Engineers, Researchers form Education and Industry to Share and Exchange their Knowledge, Experience, Information and Research on Engineering and Technology.

The First National Conference on Engineering Research will be held in accordance with the objectives of Fed.MES as:

1. To develop the Engineering Profession
2. To Raise the competitiveness of Myanmar Engineers
3. To lift the work of Human Resource Development and Capacity Building
4. To enhance the infrastructure and industrial development to the nation.

The aim and objective of the papers for various engineering field, will be discussed at this conference and those who are interested in Engineering are warmly welcome to participate in this conference. Participants are sincerely requested to put up the questions related to concern Engineering Fields. But it should be notice that it would be allow 5 min for each paper.

This National Conference would encourage Researchers and Engineers to present and discuss the recent advances in engineering fields. The paper committee of this National Conference has collected papers of various Engineering fields as: Civil, Engineering Education, Electrical Power, Engineering Geology, Information Technology, Mechatronics, Mechanical, Metallurgy, Mining, Petroleum Engineering, Renewable Energy, Environmental Engineering, and Earthquake Engineering.

The AGM Paper Committee of Fed.MES assures the participants to gain very informative and invaluable knowledge and information.

FEDERATION OF MYANMAR ENGINEERING SOCIETIES

COMMEMORATION OF ANNUAL GENERAL MEETING OF FED.MES

16-1-2020

BUILDING OF FEDERATION OF MYANMAR ENGINEERING SOCIETIES

NATIONAL CONFERENCE ON ENGINEERING RESEARCH

Contents

Development of Flood Inundation Map for Upper Chindwin River Basin By Using HEC-HMS and HEC-RAS

Khaing Chan Myae Thu [1],

[1] Building Engineering Department, Nay Pyi Taw Development Committee, Nay Pyi Taw City , Myanmar

*chanmyaethu270@gtmail.com

Abstract — **Flood is one of the natural disasters which occur in Myanmar every year. Flooding of rivers has caused many humans and financial losses. Flood inundation mapping is an essential component of flood risk management because flood inundation maps not only provide accurate geospatial information about the extent of floods, but also, can help decision-makers extract other useful information to assess the risk related to floods such as human loss, damages, and environmental degradation. Chindwin River Basin is located in the western part of Myanmar and floods often occur seriously in monsoon season. In order to perform river flood inundation mapping, HEC-HMS and HEC-RAS were utilized as hydrological and hydraulic models, respectively. The model consists of a rainfall–runoff model (HEC-HMS) that converts precipitation excess runoff, as well as a hydraulic model (HEC-RAS) that models unsteady state flow through the river channel network based on the HEC-HMS-derived hydrograph. Three flood events were applied to calibrate and validate the results. The highest depth of inundation can seriously affect the Homalin and Mawlaik and U Yu tributary.**

Keywords: Flood Inundation Map, HEC-HMS, HEC-RAS

I. INTRODUCTION

Flooding is hazardous natural phenomenon happening worldwide and often causes a lot of damages on the earth's surface including human lives and infrastructure. Floods become the most significant natural disaster in Myanmar in terms of the population increased and the disruption to socio-economic activities. In the rainy season of Myanmar, the flooding in the river devastates the lives of the inhabitants and causes the socio-economic losses. The flood estimation that involves the development of hydrologic and hydraulic models may help to reduce the amount of damages incurred.

Besides, future flood-prone areas are identified, flood inundation maps are also useful in rescue and relief operations related to flooding. As floods are becoming an increasing menace throughout the world, it has become clearly that the problem has to be assessed at a river basin scale. This requires the evaluation of various hydrological and hydraulic parameters. Geographic Information System (GIS) linked the hydraulic numerical models that can provide the functionality capable of assessing and analyzing these parameters and visualization of the results.

The Chindwin River is naturally configured with tremendous segments of rivulets, streamlets and tributaries. It represents typical basins and flood plains that are prone to annual monsoon floods in Myanmar. Chindwin River Basin is blessed with abundance of rainfall that contributes to an average of 670 mm to 4200 mm a year. With an exception of extreme events, the annual average may exceed the above average. Heavy rainfall due to cyclonic storm crossing Myanmar and Bangladesh coasts during pre-monsoon and post-monsoon. The present condition of the Chindwin river basin is featured by its abundance of river water, large difference in rainfall, runoff and water level in a year, swift currents and whirlpools in the rainy season and chronic flood damages in the rainy season. In view of the above and severity of the damages caused by extreme events, it is therefore necessary to establish a hydrologic model to simulate flood levels [1].

In order to address this issue, hydrologic and hydrodynamic models and generated flood inundation

maps for the Chindwin River Basin are applied. Although this study is not new, this study is one of very few to be analyzed the flood inundation area in Myanmar. Furthermore, this study is significant because a local climate and hydrological dataset, as well as a topographic dataset, were used to assess the possible flood inundation in the data-scarce country of Myanmar. In this study, the HEC-RAS model was used for flood hazard map development.

II. LOCATION OF STUDY AREA

The Chindwin River is the biggest tributary of the Ayeyarwady River System and is located in the western part of Myanmar as shown in Figure 1. It is located between 21°30'N and 27°15'N latitudes and between 93°30'E and 97°10'E longitudes. The source of Chindwin radiates from the Kachin Plateau. The Saramali which is the second-highest mountain in Myanmar is also located on the upper Chindwin catchment area. Since it passes through the mountain region, there were numerous sterams, which is flowing into the Chindwin River. The important tributaries of Chindwin River is U Yu and Myitha, where U Yu flows into Chindwin near Homalin and Myithat near Kalewa respectively [2].

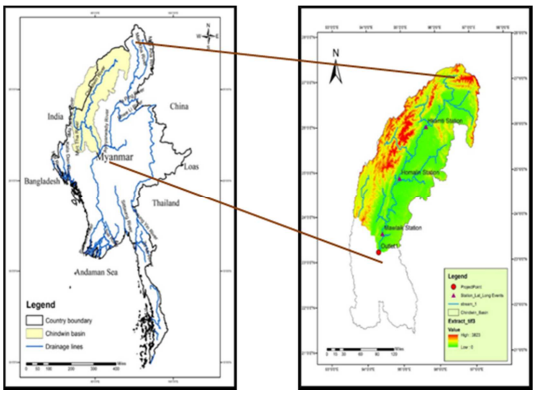

Figure 1. Location of Chindwin River Basin, Myanmar

III. METHODOLOGY

In this study, HEC-HMS and HEC-RAS were utilized as the hydrologic and hydrodynamic models using HEC-Geo HMS and HEC-Geo RAS for linking to a GIS environment. The procedure for developing the flood inundation maps consisted of four steps: (i) extraction of geospatial data, (ii) development of design flood hydrographs, (iii) computation of water surface profiles and (iv) flood Inundation mapping and visualization. The overall methodology is shown in Figure2.

The flood events were applied to the HEC-HMS model using calibration and validation approaches. The design flow hydrographs were generated by HEC-HMS. Water surface profiles were generated by HEC-RAS. The flood inundation map was generated for the along upper Chindwin River especially Homalin and Mawlaik. Three statistical criteria were used to evaluate the calibrated and validated model performance, namely Coefficient of determination (R2), Coefficient of correction(R), and Nash and Sutcliffe model efficiency (ENS). Flood inundation maps were developed for different return periods-2, 5, 10, 25, 50 and 100 year as future scenarios [3].

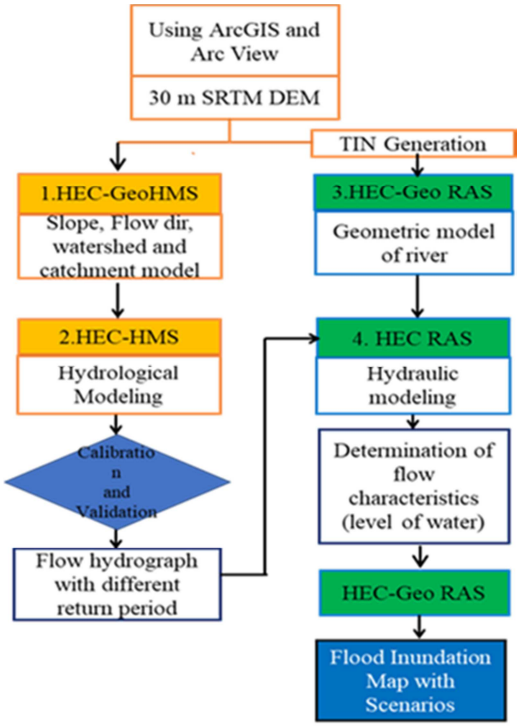

Figure 2. Overall methodology

Table 1 Sources of data

Used Dataset	Source
Digital Elevation Model SRTM 30m	https://earthexplorer.usgs.gov/
MODIS Land Cover	https://doi.org/10.5067/MODIS/MCD12Q1.006
(SSURGO) Soil Map	https://www.nrcs.usda.gov/
Daily precipitation (1967-2018)	Department of Metrology and Hydrology (DMH)
Daily Discharge (2011-2018)	
Daily Water Level (1967-2018)	
Rating Cuve Homalin Station	
PALSAR Satellite Imagery image of Advanced Land and Observing Satellite (ALOS) [2013]	https://scihub.copernicus.eu/dhus
Sentinel 1 Satellite Imagery (2015 & 2018)	

IV. HYDROLOGIC MODELLING

The Hydrologic Modelling System (HEC-HMS) is designed to simulate the rainfall-runoff process of watershed systems. It is designed to be applicable in a wide range of geographic areas to solve the widest possible range of problems [4]. HEC-HMS is physically based on a conceptual semi-distributed model design to simulate the rainfall-runoff processes in a wide range of geographic areas such as large river basin, water supply, and flood hydrology to small urban and natural watershed runoff. The basic components of the HEC-HMS are the basin model, meteorological model, control specifications, time-series data and pair data. The basin model is the physical representation of the watershed, the sub-basins, outlets, and river segments. Computation proceeded from the upstream elements in a downstream direction. The basin model has four basic components: Loss model, Direct runoff model, Base flow model and Routing model. These four methods are (1) loss method demonstrates the infiltration rate into the soil profiles, (2), runoff method represents the transformation of excess rainfall in the surface, (3) base flow method indicates the conveying groundwater into the stream and (4) routing method represents the conveying groundwater into the stream.

Initial and constant and SCS unit hydrograph were selected for the loss and transform methods, respectively. Recession and lag methods were assigned for the base-flow and routing methods [5].

The time of concentration was 4 hours, with the model parameter set optimized using individual event. In the calibration procedure, seven parameters which include initial loss, constant rate, impervious, base-flow initial flow rate, recession constant, base flow threshold ratio and SCS lag were adjusted. In this study, two flood events of 2011 and 2013 were selected for the calibration process and 2011 calibration result is shown in Figure3. 2015 and 2018 flood events were used for validation.

Design storms with different return periods were estimated from an intensity-duration-frequency curve as shown in Figure 5. Then design flood with different return periods were generated in HEC-HMS.

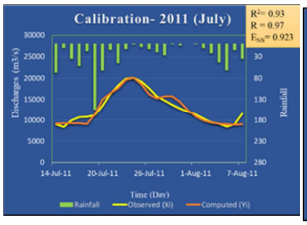

Figure 3. Observed and simulated hydrographs after calibration process for the 2011 flood event

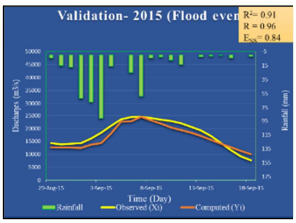

Figure 4. Observed and simulated hydrographs after the validation process for the 2015 flood event

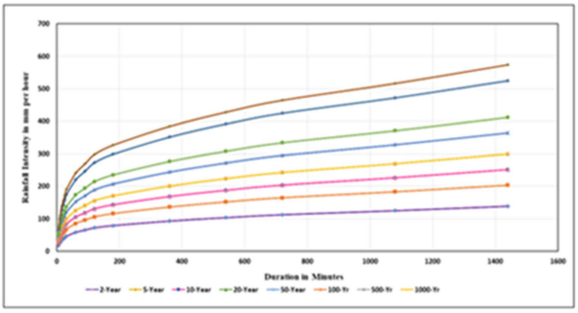

Figure 5. Intensity-Duration-Frequency Curve of Chindwin River Basin

V. HYDROLOGIC MODELLING

The Hydraulic Engineering Center-River Analysis System is a hydraulic modeling tool which is used to determine the flow behavior down a channel. HEC-RAS system includes steady flow water surface profile computations, unsteady flow simulation, sediment transport computations and water quality analysis. HEC-RAS application includes flood plain management studies, bridge, and culvert analysis and design, and channel modification studies [5].

The hydraulic model requires as input the output hydrography from HMS; its parameters are representative cross-sections for each sub-basin, including left and right bank locations, roughness coefficients (Manning's n) and contraction and

expansion coefficients. Roughness coefficients, which represent a surface's resistance to flow and are integral parameters for calculating water depth, were estimated by combining land use data with tables of Manning's n value such as that found in [6]. As present engineering studies are completed throughout the basin, more detailed cross-sectional data will be incorporated into the model. Due to the regional scale of the model, channel geometry was considered Chindwin mainstream and U Yu Tributary. In order to use the RAS model to develop floodplain maps, it must be geo-referenced to the basin.

a. RAS Geometric Data Creation

In ArcGIS, the DEM was converted into a TIN format file by using the 3 D analyst toolbox. RAS geometric data such as stream centerlines, bank lines, flow path lines, and XS cut lines were created using the TIN as base layer data in HEC-GeoRAS and delineated by enabling Editor Tool in ArcGIS. River reach name and flow pathname were also assigned. Finally, stream centerline attributes and XS cut line attributes were also generated. Created Geometric data was exported as RAS data to be used in HEC-RAS for modelling

b. Unsteady Flow Analysis

Unsteady flow analysis was done in HEC-RAS software based on the open flow channel. Boundary conditions at Hkanmti and Mawlaik station, the upstream end of the river system and U Yu, tributary were assigned to define flow hydrograph. The Mawlaik station, at the downstream end of the river system was assigned to define the normal depth and assume the friction slope of downstream. The simulated flow data with time series of flood events were used for calibrating the model [8].

c. Inundation Mapping

After steady flow analysis is being done in HEC-RAS, GIS data was exported and imported into ArcGIS for inundation analysis using RAS Mapping. Imported GIS data need to be converted from SDF format into XML format [8]. The calibration process was undertaken 2011 flood event and the result was shown in Figure6. The model was validated with the two different flood events of 2015 and 2018. The validated result of 2015 event was shown in Figure 7.

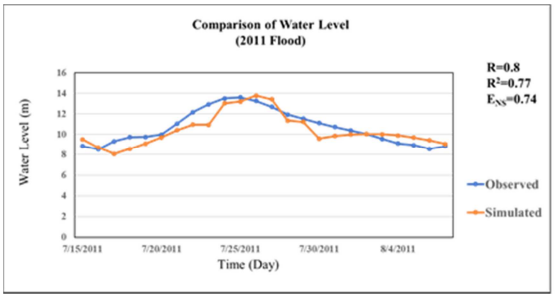

Figure 6. HEC-RAS Calibration Result of 2011 Flood Event

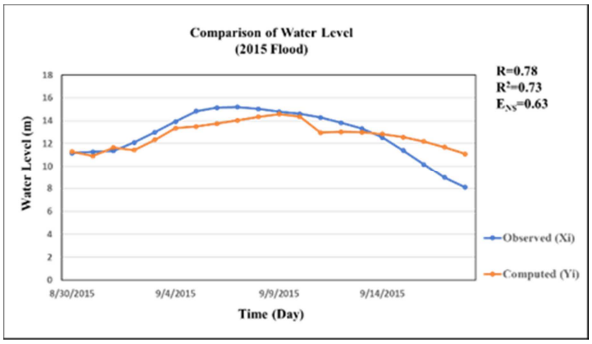

Figure 7. HEC-RAS Validation Result of 2015 Flood Event

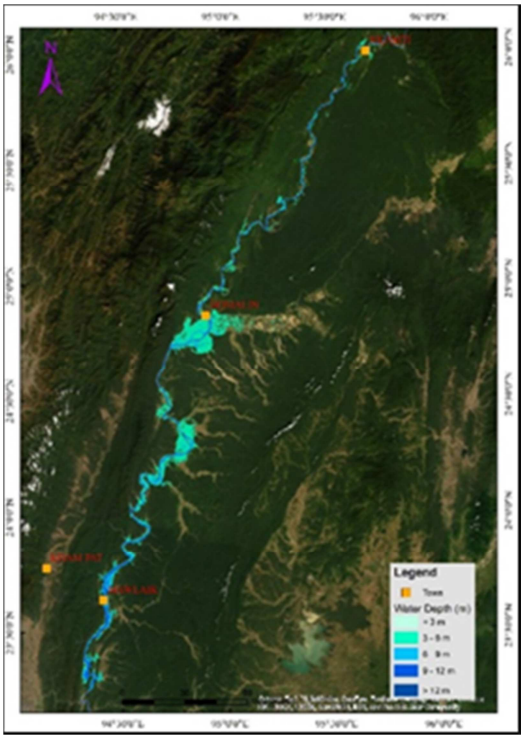

Figure 8. Simulated flood inundation depth and area for the 2011 flood event

Table2. Comparison of Flood Inundation Area of Simulated Result and Satellite Images

	Simulated by HEC-RAS Model	Estimate by Satellite Image	Ober-lapped Area	Over Estimated by model	Under Estimated by model
Inundation Area (km^2) (2011)	1613.7	1393.2	1155.2	401.3	57.3
Percentage (%) (2011)			**71.6**	24.9	3.5
Inundation Area (km^2) (2015)	1701	1380.4	1275	388.6	37.4
Percentage (%) (2015)			**75**	22.8	2.2
Inundation Area (km^2) (2018)	1097	892.7	842.3	232.8	21.9
Percentage (%) (2018)			**76.8**	21.2	2

VI. RESULT AND DISSCUSSION

The HEC-HMS model was calibrated for different flood events approach in order to determine the best fit between the model and observation. The model couldn't simulate well continuous flow of a one-year period for the Chindwin river catchment. HEC-HMS has an optimization feature that can be used to match the simulated flow with observed flow. The optimization feature was used to carry out the calibration process. Once the calibration was completed with two selected flood events, then the calibrated final parameters were taken as input in the selected two storms flood events of (2015 and 2018) for the model validation.

The validated result of 2015 flood event is shown in Figure 4. The coefficient of determination (R^2) and Nash Sutcliffe efficiency (ENS) and coefficient of correlation (R) values are obtained as 0.794, 0.89 and 0.403 respectively for the 2015 flood event. The coefficient of determination (R2) and Nash Sutcliffe efficiency (ENS) and coefficient of correlation (R) values are obtained as 0.6, 0.76 and 0.51 respectively for the 2018 flood event. These results are close and good correlation between the observed and simulated flow.

In HEC-RAS model, the simulated flood inundation maps for the 2011 flood event was validated by comparing the actual flood area derived by ALOS PALSAR images. Validation of results for 2015 and 2018 flood events were undertaken by comparing the model output with sentineal-1 image. Simulated flood inundation depth and area for 2011and 2015 flood events are shown in Figures 8 and 9.

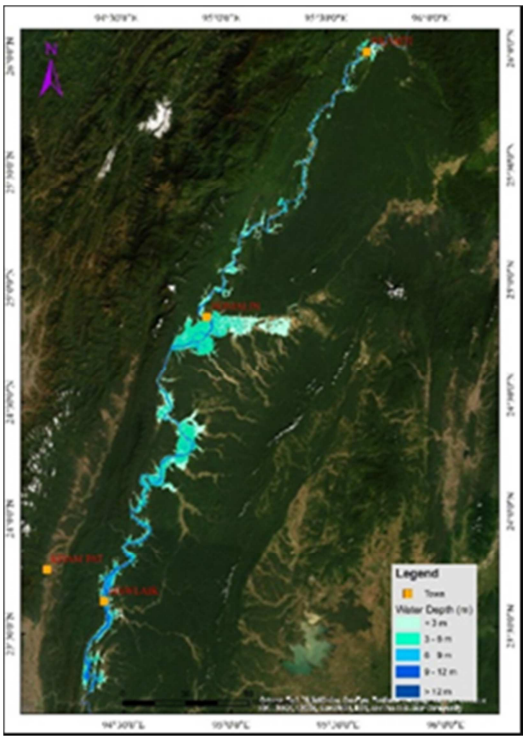

Figure 9. Simulated flood inundation depth and area for the 2015 flood event

Table3. Flood Inundation area with classified water depths in various return periods

Water Depth (m)	2 Year Flood		10 Year Flood		50 Year Flood		100 Year Flood	
	Area (km2)	%	Area (km2)	%	Area (km2)	%	Area (km2)	%
< 3 m	585.2	33.2	626.1	33.0	650.2	30.6	728.7	28.8
3 - 6 m	650.7	36.9	698.6	36.8	672.5	31.7	822.3	32.5
6 - 9 m	261.0	14.8	298.2	15.7	405.2	19.2	446.1	17.6
9 - 12 m	86.2	4.9	89.5	4.7	128.0	6.0	153.2	6.0
> 12 m	176.6	10.0	183.5	9.6	263.9	12.4	375.2	14.8
Total	**1760**	**100**	**1896**	**100**	**2120**	**100**	**2526**	**100**

Comparison of the predicted flood inundation area for 2011, 2015 and 2018 events are shown in Table 2.

For the inundation map of 100year flood frequency, the maximum depth of flood is extended to low terrain land and flood plain areas, especially in Homalin and some villages of Mawlaik Township. According to the result, the most flooded in 100 years return period is expended to the area of mid-stream

of river of study area due to the low terrain topography as shown in figure 11.

From a disaster reduction viewpoint, the information derived from this study can contribute to assess the possibility of flood damage for the local population and for those locations where data is limited, such as in Myanmar. Such an analysis would also be helpful in formulating and directing post-event relief efforts.

The obtained results representing the flood depth in the inundation area is categorized by six hazard classes corresponding to the inundation depth, named as 3, 6, 9 and 12 meters. The degree of flood hazard is classified as (D < 3 m) (3 m D < 6m), and extents of the flood water for 2, 10, 25, 50, and 100 year return period are increased gradually according to the recurrence interval. The most flooding extents and dangerous water depths are occurred for the flow conditions of 50 and 100 year due to the maximum flow conditions. For the inundation map of 50 years flood was shown in Figure 10.

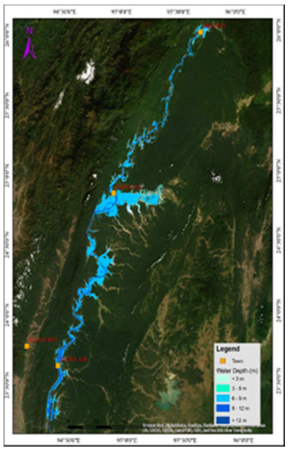

Figure 10. Flood Inundation Mpa of 50 Year Flood Event

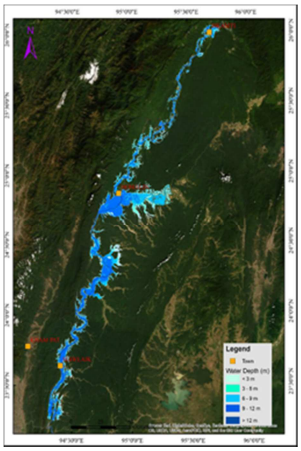

Figure 11. Flood Inundatin Map of 100 Year Flood Event

VII. CONCLUSION

The result of HEC-HMS model indicated the close and good correlation between simulated and observed flow in this study area. Despite difficulties, limitations and uncertainties associated with obtaining observations and measured parameters, this study ended-up with optimistic results for the simulation of the rainfall-runoff process in the Chindwin river basin.

In HEC-RAS model, food inundation map of the Chindwin river basin was developed and the result was validated by comparing the ALOS PALSAR image from the 2011 flood event. The analysis was undertaken to demonstrate that the model is currently at the limit of predictive ability for flood inundation, but the results of calibration and validation indicated acceptable results in terms of simulating flood events.

The process of creating flood inundation maps is affected by uncertainties in data, modeling approaches, parameters and geo-processing tools. The outcome of the study including the surrounding uncertainties in flood inundation mapping could be a powerful decision-making computational tool that would help in planning and prioritizing environmental actions in a pre-disaster stage. Such a tool would be widely applicable by agencies and decision-makers and would efficiently support planning and management of operations that are critical for human reservoirs, river channels, water conveyance systems, and environmental sustainability.

For the inundation map of 100year flood frequency, the maximum depth of flood is extended to low terrain land and flood plain areas, especially in Homalin and some villages of Mawlaik Township. According to the result, the most flooded in 100 years return period is expended to the area of mid-stream of river of study area due to the low terrain topography as shown in figure 11.

From a disaster reduction viewpoint, the information derived from this study can contribute to assess the possibility of flood damage for the local population and for those locations where data is limited, such as in Myanmar. Such an analysis would also be helpful in formulating and directing post-event relief efforts.

ACKNOWLEDGMENT(S)

First of all, the author would like to convey her thanks to Dr. Myo Aung, Mayor of Nay Pyi Taw, Nay Pyi Taw Development Committee, for giving the big opportunities to study the master course in Yangon Technological University. The author is deeply grateful to Dr. Myint Thein, Rector of Yangon Technological University, for his invaluable directions and management

The author wishes to thanks all persons who helped towards the successful completion of this paper.

REFERENCES

[1] Thet Hnin Aye, “Development of Flood Inundation Map for the Bago River Basin”, International Journal of Innovative Research in Multidisciplinary Field, Jan 2017, Volume 3, Issue 1, ISSN 2455-0620.

[2] Department of Meteorology and Hydrology. 2004. "Meteorological and Hydrological Data Agricultural Atlas of the Union of Myanmar". Department of Meteorology and Hydrolog, Food and Agriculture Organization of the United Nations.

[3] Zin, W. W. (2015). "River Flood Inundation Mapping in the Bago River Basin, Myanmar." Hydrological Research Letter 9 (4), 97-102 (2015). DOI:10.3178/hrl.9.

[4] Yusop, Z., Chan, C. & Katimon, A., 2007. Runoff characteristics and application of HEC-HMS for modelling stormflow hydrograph in an oil palm catchment. Water Science and Technology, 56, 41-48.

[5] Chen, Y., Xu, Y. & Yin, Y.,2009. Impacts of land use change scenarios on storm-runoff generation in Xitiaoxi basin, China. Quaternary International, 208, 121-128.

[6] Horritt MS, Bates PD.2002.Evaluation of 1D and 2D numerical models for predicting river flood inundation, Journal of Hydrology 268 (1-4), 87-89

[7] HEC,2002. River Analysis System: Hydraulic Reference Manual.US Army crops of engineers Hydrologic Engineering Center, Davis, CA.

[8] PANAGOULIA, D., MAMASSIS, N. and GKIOKAS, A., 2013. Deciphering the Floodplain Inundation Maps in Greece. In 8th International Conference Water Resource s Management in an Interdisciplinary and Changing Context, Porto, Portugal, European Water Resources Association.

Effect of Lime Content and Curing Condition on Strength Development of Lime-Stabilized Soil in Bogalay Township, Ayeyarwaddy Region

AUNG AUNG SOE[*1], Y. YAMADA[2], N. NAKAJIMA[3] and PHYU PHYU[4]

[1] PhD, Engineering Secretary, FUKKEN Co., Ltd. (Yangon Branch)
[2] PhD, General Manager, FUKKEN Co., Ltd. (Yangon Branch)
[3] Chief Engineer, Twister Sector, Civil Engineering Department, JDC Corporation
[4] Deputy Director, R & D Section, Department of Highways, Ministry of Construction
*Corresponding author – AUNG AUNG SOE, aungsoe@fukkenmyanmar.com

Abstract - Slaked lime was used to stabilize the cohesive soil, found in Bogalay Township to upgrade the rural road construction technique in Ayeyarwaddy Region, Myanmar. To achieve the stabilization purpose, this cohesive soil is mixed with slaked lime in different proportions, followed by different curing periods. The unconfined compression tests were conducted to investigate the strength characteristics of lime-stabilized clay soil, with respect to the lime content and the curing periods. From the test results, the strength of the lime-stabilized soil increases with the increase in lime content and curing period. However, the curing condition has the significant influence on the strength development of the lime-stabilized soil.

Keywords - **Lime stabilization, cohesive soil and unconfined compressive strength**.

I. INTRODUCTION

Ayeyarwaddy is one of the regions where play an important role for the development of Myanmar. To promote the development in this region, road networks are of importance. Originally, the region is covered by the alluvial deposit, which is soft cohesive soil containing clay minerals. For the road construction, this clay soil is not suitable as a foundation subgrade layer. One optimal solution is to improve the strength of cohesive soil by means of lime stabilization. According to National Lime Association [1], the effect of lime on soil can be generally categorized as (1) soil drying: a rapid decrease in soil moisture content due to chemical reaction between water and quicklime, (2) soil modification: modification of soil properties such as plasticity, density, compactability, etc., and (3) soil stabilization: production of long-term strength and the permanent reduction in shrinking, swelling, and soil plasticity. Regarding lime-soil mixture, a variety of proportioning procedures have evolved from various agencies, often reflecting local conditions and experience [2]. Therefore, due to the heterogeneous nature of soil, it needs to examine the local cohesive soil in Ayeyarwaddy Region and its reacting characteristics with the available lime. The trial road section was constructed in Bogalay Township, as presented in Figure 1.

According to Herrin & Mitchell (1961) [3], lime-soil mixtures are soil that have had their physical characteristics changed and/or the soil grains cemented together by action of lime with the aid of water. The production of cementitious materials between cohesive soil and lime can continue for ten years or more but the strength developed will be influenced by the materials and the environment [4]. This suggested that the local available materials need to be examined to achieve the proper mix-design. The cohesive soil was firstly tested to know its physical and chemical properties. Based on these properties, the cohesive soil was mixed with different amounts of lime. In this study, the unconfined compression tests were carried out to know the strength characteristics of the lime-stabilized specimens. The behavior of strength development was also analyzed, considering various curing periods.

Figure 1. Trial road section in Bogalay Township, Ayeyarwaddy Region, Myanmar.

II. TEST PROGRAM

This test program included the characterization of the cohesive soil and the slaked lime, and the strength determination of lime-soil mixtures. The characterization tests included physical tests such as

moisture content, Atterberg's Limit, Grain Size Analysis, Specific Gravity, Sulfate Content, pH and Lime Demand. Based on the index properties of cohesive soil, the slaked lime was added by weight percentages of 3%, 5%, 7%, 9% and 11%. For the strength determination, the unconfined compression tests were carried out after the curing periods of 7 days, 14 days, 21 days, and 28 days. The variation in the unconfined strength of lime-stabilized soil is analyzed with respect to the lime content and curing period.

III. MATERIALS

III-A. Cohesive Soil

The local cohesive soil was taken from the site in Bogalay Township, where a rural road will be constructed on the soft clay deposit. Laboratory tests were conducted to examine the index properties of this soil. These properties are summarized in Table 1. The particle size distribution of this soil is presented in Figure 2. As seen in this figure, the fine fraction (< 0.075 mm) in the cohesive soil is much greater than 50% and its liquid limit is also greater than 50%, as presented in Table 1. According to the Japanese Geotechnical Society Standard JGS 0051-2009, this cohesive soil can be classified as Clay with high liquid limit (CH). Since plasticity index of the soil is greater than 10, this soil can be a candidate for the stabilization with lime [1]. The required lime demand for this soil was determined in accordance with ASTM D6276, and it was estimated as 3% as seen in **Figure-3**.

III-B. Slaked Lime

The slaked lime, produced in Myanmar, was used to stabilize the cohesive soil. Some basic properties of this lime is presented in **Table-1**.

IV. TEST METHOD

IV-A. Sample Preparation

The cohesive soil was thoroughly mixed with the specific lime contents by weight at the respective optimum moisture contents, determined in accordance with JGS 0711-C. The mixed soil specimen was prepared in an air-tight disposable mold (Ø 50 mm) in three layers, with the compaction greater than 95% of maximum dry density. The specimen dimension had the height-to-diameter (Ø50mm) ratio of 2.0. Specimens were prepared for each lime content and the respective curing periods. The specimens were cured for the specific curing periods of 7 days, 14 days, 21 days, and 28 days. For 7 days and 14 days curing periods, specimens were kept at ambient temperature (≈ 30°C) under the shelter outside building. The purpose of this curing is to know the strength development characteristics during construction time. To understand the long-term strength development behavior after road construction, specimens were cured inside the room for 21 days and 28 days. For 28 days curing, specimens were cured in room for 21 days and cured in soak condition for the last 7 days, to examine the

Table 1. Index properties of Cohesive Soil and Slaked Lime

Material	Properties of Materials with Respective Testing Methods							
	JGS 0121	JGS 0141	JGS 0141	JGS 0141	JGS 0111	Land Use*	JGS 0211	ASTM D6276
	Moisture Content (%)	Liquid Limit (%)	Plastic Limit (%)	Plasticity Index	Specific Gravity at 15°C	Sulphate Content (meq/100gm)	pH	Lime Demand (%)
Soil	23.38	51.55	25.92	25.63	2.655	0.2	7.07	3
Lime	1.04	-	-	-	2.271	-	-	-

*Laboratory of Department of Agriculture (Land Use), Ministry of Agriculture, Livestock and Irrigation.

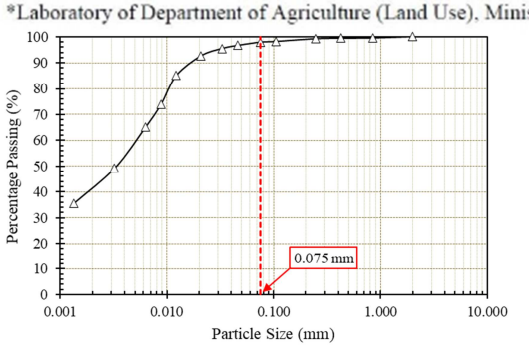

Figure 2. Particle size distribution of clay

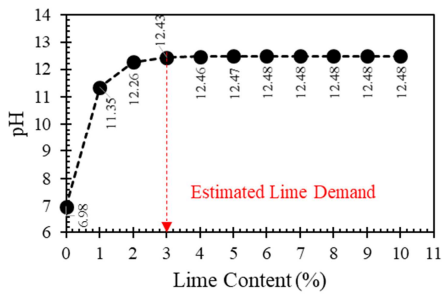

Figure 3. Estimated lime demand of clay

long-term strength behavior in severe weather condition.

IV-B. Testing Instrument and Test Procedure

To conduct the unconfined compression test, Humboldt Master Loader HM-5030 (50 kN Capacity) was used for loading. The deformation of the specimen was recorded by a displacement transducer. The cured specimen was firstly placed on the pedestal, followed by adjusting the loading arm to keep just in contact with specimen. The unconfined compression test was then carried out in accordance with the test procedure, described in ASTM D2166 standard. Once the specimen was ready to be tested, the loading was gradually increased in the strain controlled manner (1%/min) until the recorded load decreased with increasing strain or the strain reached 15%. The variations of load and deformation were recorded by the Humboldt mini-logger (HM-2325A). The schematic view of the unconfined compression test is illustrated in Figure 4.

V. TEST RESULTS AND DISCUSSION

V-A. Effect of Lime Content on Unconfined Compressive Strength

The variation in strength behavior of the lime-stabilized soil was analyzed with respect to the added lime contents. For the analysis of the short-term and the long-term strength development, the effect of lime content was examined for curing periods of 7 days and 28 days. The variations of stress-strain curve are presented in Figure 5 and Figure 6. The repeated curves show a good agreement with their respective curves, implying the reproducibility of the test specimens.

As seen in Figure 5, the stresses abruptly increased within 0.5% to 0.7% strains, with increasing strains. The peak strength generally increased with the lime content, greater than minimum lime demand (3%). The similar characteristics can be observed in Figure 6. In both curing cases, the curves of 11% lime content show insignificant increase in strength, compared to 9% lime content. This suggested that the upper limit of lime content might be 9% for the given cohesive soil. It is noticed that the curves of the larger lime content cases rapidly decrease after they had reached peak stresses. In case of high lime content, the amount of coarser particles might have been created due to flocculation, agglomeration and solidification processes. This would increase the resistance to the shearing. After it had reached to the peak, the interlocking between the coarser particles might have been reduced, forming shearing plane with low cohesion. According to Overseas Road Note 31 [4], the stabilized material will generally be non-plastic or only slightly plastic if the amount of lime added exceeds the initial consumption of lime. Here, this consumption was 3%.

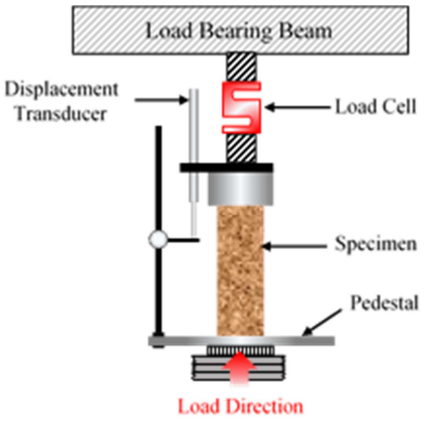

Figure 4. Schematic view of UCT

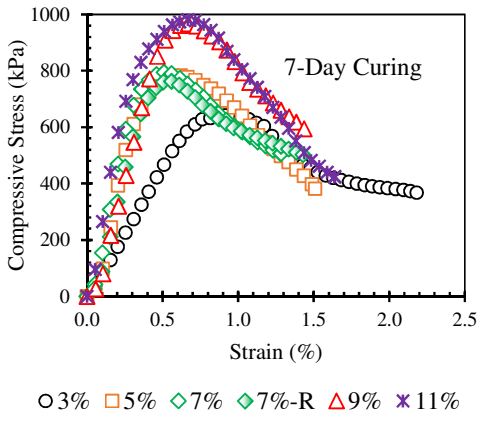

Figure 5. Stress-strain curves (7-day curing)

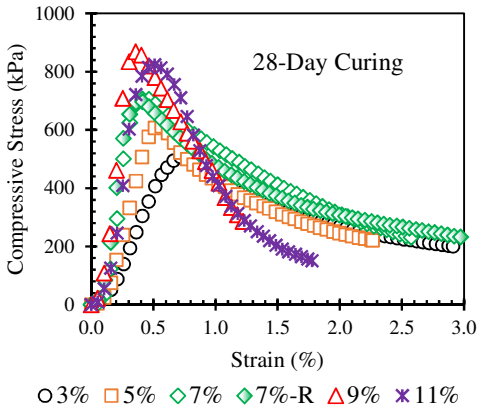

Figure 6. Stress-strain curves (28-day curing)

From the stress-strain curves presented in Figure 5 and Figure 6, the peak stresses were taken and analyzed their behavior. The change in characteristics of peak stresses are illustrated in Figure 7, together with the corresponding strains. As seen in Figure 7, the unconfined compressive strength increases with the increase in lime content. Regardless of curing time, the strength increases in a power trend, implying the rate of increase in strength declines with increase in lime content. It is noticed that the 28 days strengths are smaller than the 7 days strength with approximately 50 kPa offset. In the first 21 days curing of 28 days period, the soil drying in specimen would have been occurred, especially in the circumferential portions. When it was in the soaked condition in the last 7 days of 28 days period, this might result in the softening in these portions of specimen, thereby reducing strength when it was sheared. When the corresponding strains are examined, it is noticed that the strain decreases from 3% to 7% lime content. This implies that, with increase in lime content, the strength can be achieved at a smaller deformation of the lime-stabilized soil. After 7% lime content, a slight increase in the corresponding strain was observed in 9% and 11% lime contents. This might be due to the excess lime contents, creating non-plastic materials with coarser particle sizes. These specimens would need the larger strains to reach the corresponding peak stresses. Since the strength increases in a power trend, the rate of increase in strength becomes decline with further increase in lime content. From Figure 7, the strength increases until 9 % lime content, after which there is no obvious increase in strength. Therefore, this 9% lime content would be the upper limit for this particular clay found in Bogalay Township.

V-B. Effect of Curing Condition on Strength Behavior of Lime-Stabilized Soil

The effect of curing time was examined on the strength behavior of cohesive soil, stabilized with lime 3% (minimum lime demand) and 7 % of which test was performed for verification purpose. The variation in strength with curing periods can be seen in Figure 8 and Figure 9.

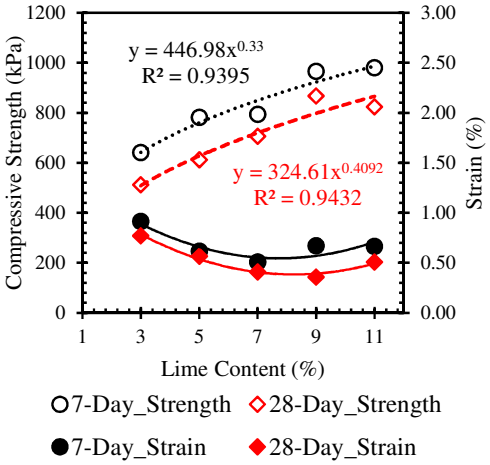

Figure 7. Strength development with lime

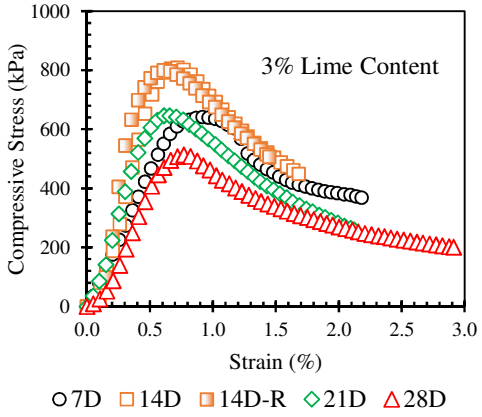

Figure 8. Strength development with curing days for 3% lime content

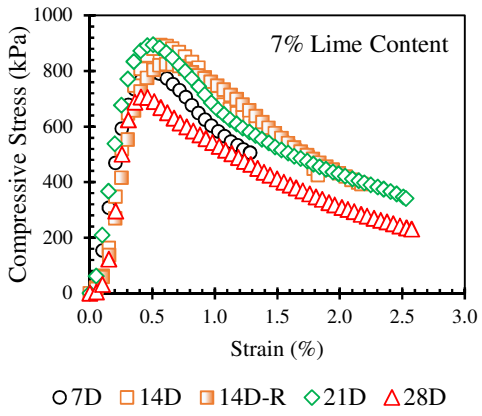

Figure 9. Strength development with curing days for 7% lime content

As seen in Figure 8, the peak stress increases with increasing curing period from 7 days to 14 days, of which curves show a good agreement of reproducibility. However, a decrease in peak stress was noticed when curing period was further increased to 21 days and 28 days. This was because, for those two curing periods, the specimens were cured at the room temperature (≈ 25°C), compared to 7 day and 14 day curing periods (≈ 30°C). This lower temperature might result in the slower rate of strength development. As seen in Figure 9, like 3% lime-stabilized case, the similar characteristics of stress-strain curves were observed for 7% lime-stabilized case. The variation of change in peak stress was analyzed and presented in Figure 10 with respect to the curing periods.

As seen in Figure 10, in both lime-stabilized cases, the compressive strength increased with curing

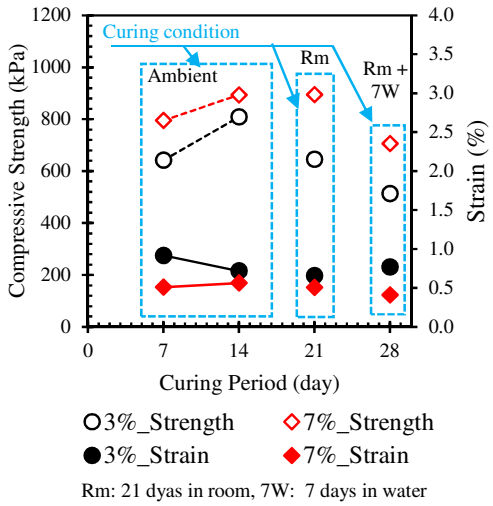

Figure 10. Change in compressive strength with curing condition and time

time from 7 days to 14 days. However, the strength declined after 14 days curing period. This was because the specimens were cured at room temperature, which was lower than the ambient temperature, for 21 days. The strength development in those specimens would take longer period at the lower temperature, compared to 7 days and 14 days specimens which were cured in a higher temperature environment. According to Jung and Bobet (2008) [5], the long-term reaction between lime and soil continues for years and, the strength and/or stiffness of this lime-treated soil increase with time. Hence, from the increasing tedency of strength development in 7 days and 14 days curing periods, it was realized that the strength of stabilized soil would increase with time under similar curing condition. For 28 days curing, the specimens were cured in soaked condition for the last 7 days, following 21 days curing in room. This latter 7-day curing would result in the softening of specimen, as discussed before.

When the characteristics of the strain at peak stress are examined, it is noticed that the effect of curing period and condition is insignificant on the strain behavior. This implies that, regardless of curing period, the certain amount of deformation would be necessary to achieve the peak value for the specific lime content as seen in Figure 7.

VI. CONCLUSION

To develope the road networks in rural areas, soil stabilization method was adpoted to improve the existing soft ground. The lime stabilization method was used to stabilize the cohesive soil encountered in Ayeyarwaddy Region. From the physical test results, it was known that the minimum lime demand was 3% for the given cohesive soil. Based on this, the slaked lime was mixed with the soil in proportion by weight of 3%, 5%, 7%, 9% and 11%. The unconfined compression test was conducted to investigate the strength development behavior with respect to the lime content and the curing condition and time.

From the analysis of test results, it was realized that the unconfined compression strength increases in a tendency of power trend with the increase in lime content, implying that the rate of increase in strength becomes slow with increase in lime content. Test results suggested that 9% lime content can be considered as the upper bound in regard of the strength development characteristics of the lime-stabilized cohesive soil, found in Bogalay Township. In general, the peak stress in case with higher lime content reaches at a smaller strain, compared to the smaller lime content case. This behavior is in regardless of the curing period. Regarding the curing period, it was realized that the strength increased with

the increase in curing period. However, the condition of curing has significant influence on the strength development behavior. It is recommended to investigate this behavior more in detail as a further study.

ACKNOWLEDGEMENTS

This study was conducted at the Soil Laboratory of FUKKEN Co., Ltd. with the supports of JDC Corporation. This work is a part of the program conducted under the Collaboration Program with JICA and MOC. Authors would like to express their sincere thanks and acknowledge the concerned parties and individuals for their continuous supports and help.

REFERENCES

[1] NLA, "Mixture design and testing procedures for lime stabilized soil," *Technical brief,* pp. 1-6, October 2006.

[2] TRB, "State of the Art Report 5 - Lime Stabilization," Transportation Research Board, 1987.

[3] M. Herrin and H. Mitchell, "Lime-soil mixtures," in *40th Annual Meeting of the Highway Research Board*, Washington DC, 1961.

[4] TRL, "Overseas road note 31: A guide to the structural design of bitumen-surfaced roads in tropical and sub-tropical countries," Overseas Center, Transport Research Laboratory, Crowthorne, Berkshire, United Kingdom, 1993.

[5] C. Jung and A. Bobet, "Post-construction evaluation of lime-treated soils," FHWA/IN/JTRP-2007/25, Indianapolis, IN 46204, 2008.

[6] JGS 0141, "Test method for liquid limit and plastic limit of soils," in *Laboratory testing standards of geomaterials (Vol. 1)*, Japanese Geotechnical Society, 2009.

[7] JGS 0111, "Test method for density of soil particles," in *Laboratory testing standards of geomaterials (Vol.1)*, Japanese Geotechnical Society, 2009.

[8] JGS 0211, "Test method for ph of suspended soils," in *Laboratory testing standards of geomaterials (Vol.3)*, Japanese Geotechnical Society, 2009.

[9] JGS 0121, "Test method for water content of soils," in *Laboratory Testing Standards of Geomaterials (Vol.1)*, Japanese Geotechnical Society, 2009.

[10] JGS 0051, "Method of classification of geomaterials for engineering purposes," in *Laboratory testing standards of geomaterials (Vol.1)*, Japanese Geotechnical Society, 2009.

[11] JGS 0711, "Test method for soil compaction using a rammer," in *Laboratory testing standards of geomaterials (Vol.1)*, Japanese Geotechnical Society, 2009.

[12] ASTM D6276, "Standard test method for using pH to estimate the soil-lime proportion requirement for soil stabilization," American Society for testing and materials, 2006.

[13] ASTM D2166, "Standard test method for unconfined compressive strength of cohesive soil," American society for testing and materials, 2006.

Investigation on Performance Level of 10-storey R.C Building with Pushover Analysis

Tin Tin Wai[1], Win Zaw[2], Ohnmar Khaing[3]

[1]*Master Candidate, Department of Civil Engineering, Technologic University (Taunggyi) Taunggyi, Myanmar*

[2]*Professor, Department of Civil Engineering, Technologic University (Taunggyi) Taunggyi, Myanmar*

[3]*Lecturer, Department of Civil Engineering, Technologic University (Mandalay) Mandalay, Myanmar*

waitintinaty@gmail.com,kowinzaw2007@gmail.com,ohnmarkhaing.mdy2019@gmail.com

ABSTRACT

This paper presents investigation on seismic performance of a 10-storeyed R.C building in Taunggyi region, southern Shan State. The main objective of this paper is to investigate their seismic performance levels, damage probabilities of proposed buildings under strong earthquake shaking. Taunggyi is located in MNBC Seismic Zone-4 and R.C type residential buildings are the most popular types. Its height is 110ft above ground level. The total length and width are 84ft and 54ft respectively. Basic wind speed 80 mph is used. This structure is composed of special moment resisting frame. Dead loads and live loads are used according to ACI code. The load combinations required for the whole structure is used according to UBC-97. This paper is an approach to do nonlinear static analysis in simplify and effective manner. This method determines the base shear capacity of the building and performance levels of each part of building under varying intensity of seismic force. The results of effects of different plan on seismic response of buildings have been presented in terms of displacement, base shear and plastic hinge pattern. The performance of the buildings is then assessed with the ATC 40 and FEMA 356 building acceptance criteria. From pushover analysis, the capacity curves for each building in two directions of the earthquake are obtained. The modeling and analysis is done by ETABS 9.7.1 software. The displacement control analysis is used and its value is 2% of total structure height. The lateral displacement of 2.48ft is subjected to roof level .After pushover analysis has been carried out, capacity spectrum curve is demonstrated in acceleration-displacement format. The graphical intersection of the two curves (capacity spectrum curve and demand curve) approximates the performance point of the structure. Based on analysis results, it was needed to strengthen for resisting up to earthquake shaking.

Keywords:R.C Building, Performance level, Displacement and base shear, Nonlinear static (Pushover) analysis and ETABS.

I.INTRODUCTION

Nowadays, Myanmar is still a developing country and there is a tendency to raise population in future. So, the high-rise building is the only answer to solve the problem of population dense. Buildings are commonly designed for lateral forces due to wind and earthquake. The primary objective of earthquake resistant design is to prevent buildings collapse during earthquake. structure must be safe against collapse and consequences of failure. So, the proposed building is intended to resist the level of LS during strong earthquake. Thus the performance based seismic design is a process that permits design of new buildings or upgrade of existing buildings with a realistic understanding of the risk of life, occupancy and economic loss that may occur as a result of future earthquakes .When structures are subjected to strong earthquake ground motion, safety of structures in the inelastic range, structural stability and nonlinear behaviour have to be carefully examined. The nonlinear pushover analysis is becoming a popular tool for seismic performance evaluation of existing and new structures. . In highly seismic area, it is important to design the building that will withstand moderate earthquakes without damage and serve earthquakes without collapse.

II.BACKGROUND THEORY

Linear

-Structure return to original form
-No change in loading direction or magnitude
-Material properties do not change
-Small deformation and strain

Nonlinear

-Geometry changes resulting in stiffness change
-Material deformation that may not return to original form
-Support changes in loading direction and constraint location
-Support of nonlinear load curves.

Pushover analysis

-Gravity analysis is force controlled.

-Pushover analysis is a displacement controlled.
-Behavior of structure characterized by capacity curve(base shear force vs roof displacement)
Nonlinear is subdivided by two classes.

Material Nonlinearity

a. Permanent Deformation
b. Cracking
c. Beam rotation
d. Energy dissipation

Geometric Nonlinearity

a. P-Delta analysis

Methods

-Capacity Spectrum method
-Displacement
-Modal plastic method

Control Case

-Brittle action(load 2ft from roof level)
-Ductile action(displacement 2% of overall height)

Methods of Analysis

Generally for analyzing the structure the following analysis methods are used depending upon the requirements.

(1)Linear static procedure
(2)Linear dynamic procedure
(3)Nonlinear static procedure
1.Pushover analysis
2.Capacity spectrum method
(4)Nonlinear dynamic procedure
1.Time history analysis

A pushover analysis to perform non-linear analysis is considered.

The analysis in ETABS 9.7.1 involves the following four steps. 1) Modeling, 2) Static analysis, 3) Designing 4)Pushover analysis. Steps used in performing a pushover analysis of a simple three-dimensional building.

1. Creating the basic computer model (without the pushover data) in the usual manner.
2. Define properties and acceptance criteria for the pushover hinges. The program includes several built-in default hinge properties that are based on average values from ATC-40 for concrete members and average values from FEMA-356 for steel members. These built in properties can be useful for preliminary analyses, but user defined properties are recommended for final analyses.
3. Locate the pushover hinges on the model by selecting one or more frame members and assigning them one or more hinge properties and hinge locations.
4. Define the pushover load cases. In ETABS 9.7 more than one pushover load case can be run in the same analysis. Also a pushover load case can start from the final conditions of another pushover load case that was previously run in the same analysis.

Typically a gravity load pushover is force controlled and lateral pushovers are displacement controlled.

5. Run the basic static analysis and, if desired, dynamic analysis. Then run the static nonlinear pushover analysis.
6. Display the pushover curve and the table.
7. Review the pushover displaced shape and sequence of hinge formation on a step-by-step basis.

Performance Level

A performance level describes a limiting damage condition which may be considered satisfactory for a giving building and a given ground motion.

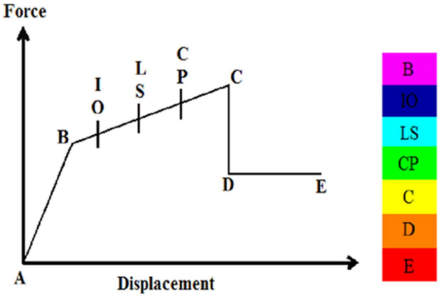

Figure 1.Performance Level of Structure

There are five levels of global structural response depending on the permissible amount of damage suffered by the structure when push-over analysis is performed. These are (1) Operational (O) level, (2) Immediate Occupancy (IO) level, (3) Live Safety (LS) level, (4) Collapse Prevention (CP) level and (5) Collapsed (C) level.[1] In the Operational level, the damage is Losses less than 5% of replacement value.[1] In the Immediate Occupancy level the damage is Losses less than 15%.[1] In the Live Safety level, the damage is Losses less than 30%.[1] In the Collapse Prevention level, the damage is Losses greater than 30%.[1] In the Collapse level, the damage is not exactly estimated.[1]

Pushover analysis, there need to define at least two types of static nonlinear case and the first case must be for gravity load and the other for lateral load. The structural model is modified to account for the reduced stiffness of yielded members and lateral forces are again increased until additional members yield. The process is continued until a control displacement at the top of building reaches a certain level of deformation or structure becomes unstable. Local nonlinear structure effects, such as flexural hinges at the member joints are modeled and the structure is deformed or push until enough hinges form to develop a collapse mechanism or until the plastic deformation limit is reached at the hinges.

III.Data preparation for Reinforced Concrete Structure

A. Site Location and Structural System

The proposed structure is a ten-storied reinforced concrete residential building. Details of the structure are described below,

- Height of structure = 124ft
- Length of structure = 84ft
- Width of structure = 54ft
- Typical storey height = 11ft
- Bottom storey height = 14ft
- Shape of building = regular

- Location = seismic zone 4
- Type of occupancy = Residential

B. Material Properties

Material properties for structural data are;

- Concrete cylinder strength = 3ksi
- Yield strength of main reinforcement = 50ksi
- Yield strength of shear reinforcement = 50 ksi
- Modulus of elasticity for concrete = 3122 ksi

C. Loading consideration

The applied loads are dead loads, live loads, earthquake load and wind load. Dead loads consist of the weight of all materials and fixed equipment incorporated into the building. Floor finishing, ceiling, partitions are considered as superimposed dead loads. Loads that are almost always applied horizontally are called lateral loads.

For dead load,

- Unit weight of concrete = 150 pcf
- 9" thick brick wall = 100 psf
- 4.5" thick brick wall = 55 psf
- Superimposed dead load = 20psf

For live load,

- Live load on floor = 40 psf
- Live load on stair case = 60 psf
- Live load on roof = 20 psf
- Weight of lift = 2 tons
- Weight of water = 62.4 psf

For earthquake load,

An earthquake level is defined with a probability of being exceeded in a specified period .The following three levels are commonly defined for buildings with a design life of 50 years by ATC 40:

- Serviceability Earthquake (SE): Ground motion with a 50 percent chance of being exceeded in a 50- years
- Design Earthquake (DE): Ground motion with a 10 percent chance of being exceeded in a 50- years
- Maximum Considered Earthquake (MCE): Ground motion with a 2 percent chance of being exceeded in a 50-years[3].

Mostly, the seismic hazard levels are determined by the probabilistic seismic hazard analysis (PSHA).The calculated results of the seismic hazards for Taunggyi city are;

- SE =0.22g
- DE =0.46g
- MCE =0.71g
- Soil profile type =SD
- Seismic important factor (I) =1
- Ct value = 0.03
- Seismic source type = A

1. Modeling Aspects of building elements:

Type of proposed building is ten storeyed rectangular shaped RC building and type of residential which is located in seismic zone 4. Typical story height and bottom story height are 11ft and 14ft. Total height of the whole building is 124ft. X direction length and Y direction length are 84ft and 54ft respectively. The material properties of structure are the strength of concrete is 3000 psi and yield strength of steel is 50000 psi. The plan view, elevation and 3D view of building is shown in figure 2, 3 and 4.Nonlinear plastic hinges are assigned to all of the primary elements. Default moment hinges (M3) are assigned to beam elements and default axial moment2-moment3 hinges (PMM) are assigned to column elements. The column sizes are defined as 20”x20”, 18”x18’, 16”x16”, 14”x14”, the beams are 12”x14”, 10”x12”, 10”x10” and shear wall is 12” and Stair thickness is 5”.

The design load combinations are used from UBC-97specification.

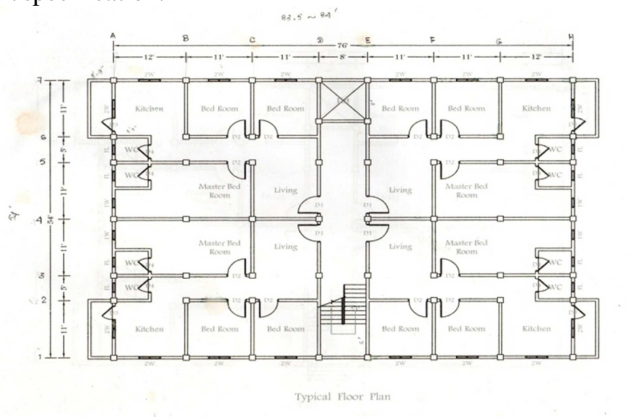

Fig-2, TYPICAL FLOOR PLAN

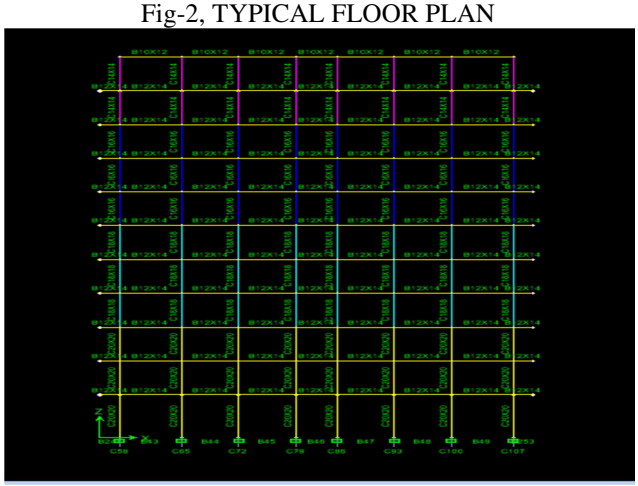

Fig-3, ELEVATION VIEW OF MODEL

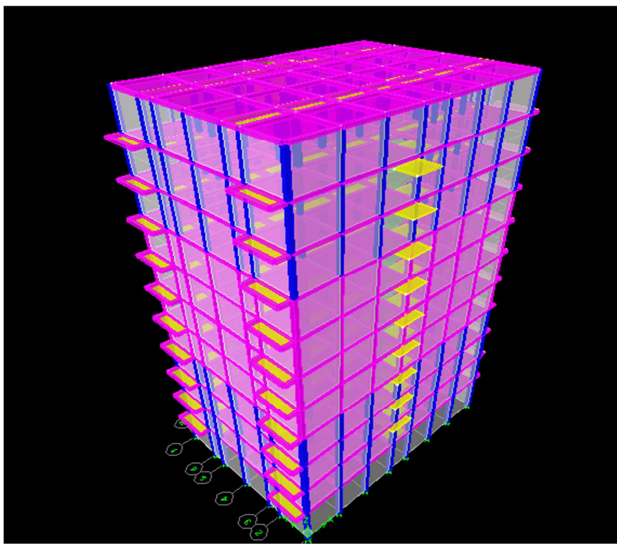

Fig-4, 3D VIEW OF MODEL

2. Loading condition for pushover analysis

Non-linear Static (Pushover) Analysis method is used to check performance levels of structure. To perform pushover analysis, there needs to define at least two types of static nonlinear case and the first case must be for gravity load and the other for lateral load.

For gravity load, it is zero initial condition and therefore the structure has zero displacement and velocity. And all elements are unstressed and there is no history of nonlinear deformation. Monitored story is at roof level with X and Y directions.

IV.Analysis Results

In this study, building is considered to resist earthquake effect by using Push-over analysis with ETABS 9.7.1.

For lateral load, lateral displacement of the building is considered in X and Y directions. Displacement control analysis is used. The 2% of total structure heights is used for displacement control value. The following figures 5,6,7 and 8 are the results of capacity spectrum curve and performance levels of TWO different cases for X and Y-direction by pushover analysis.

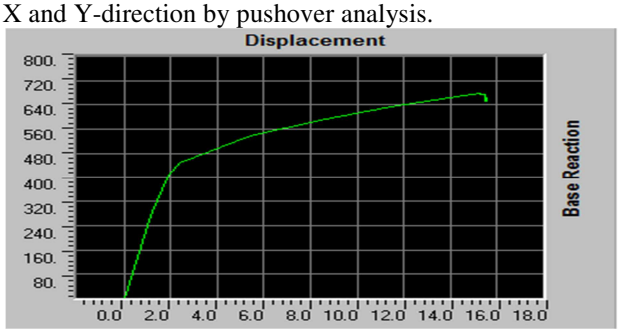

Fig-5, Case-1, Pushover curve for Displacement and base shear(X-direction)

This figure shows the hinges formation is reached maximum displacement and base shear in 15.53in and 649.8k at the level of collapse. The performance point(V,D)is 649.8 and 14.The effective period (T_{eff})is 2.775and the effective damping($ß_{eff}$) is 0.257.

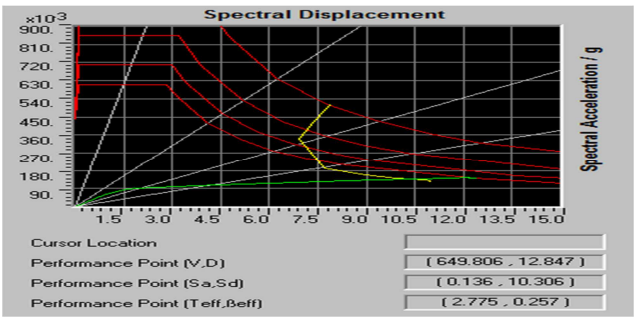

Fig-6, Case-1, Capacity Spectrum Curve For Zone 4 (X –direction)

This figure shows the performance point (Sa,Sd) is 0.136,10.306 and the structure is subjected to ground acceleration of 0.4 g, the performance level of structure is begun at Immediate Occupancy level. The structural ability is reached at the end of elastic limit stage and the consequence results of failure may be reached up to collapse level.

Fig-7, Case-2, Pushover curve for Displacement and base shear(Y-direction)

This figure shows the hinges formation is reached maximum displacement and base shear in 12.8546 in and 694.95k at the level of collapse. The performance point(V,D)is 701.418 and 12.192.The effective period (T_{eff})is 2.604and the effective damping($ß_{eff}$) is 0.255.

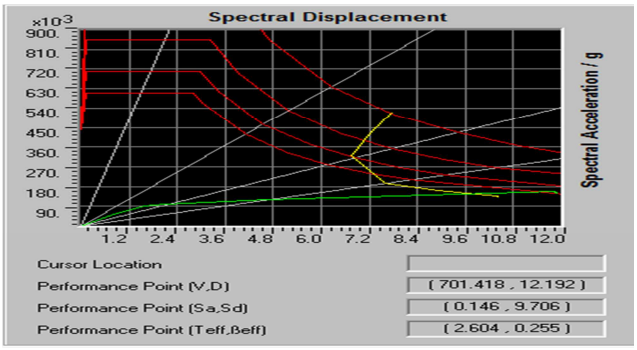

Fig-7,Case-2,Capacity Spectrum Curve For Zone 4 (Y-direction)

This figure shows the performance point (Sa,Sd) is 0.146,9.706and the structure is subjected to ground

acceleration of 0.4 g, the performance level of structure is begun at Immediate Occupancy level. The structural ability is reached at the end of elastic limit stage and the consequence results of failure may be reached up to collapse level.

V. DISCUSSIONS AND CONCLUSIONS

In this paper, the proposed building is ten-storeyed rectangular shaped RC building and it is located in seismic zone 4. The design codes used in this paper are the UBC-97 and ACI 318-05. Structural analysis and design is done by using ETABS software.

By the studying of plastic hinge mechanism of the structure, the structural performance levels and the first failed parts of the structure can be known. Total hinges formation of 3868 occurs in each case. The comparison of case 1 and case 2 are as follows:

- In case1, when the displacement reaches at 15.2574 in, the structure reaches at collapse prevention stage.
- In case 2, when the displacement reaches at 12.8546 in, the structure reaches at collapse prevention stage.
- To compare this stage, the structural capacity of Y-direction is less than in X-direction.
- Both case 1 and 2,more plastic hinges are found in beam than column face.

Moreover, according to figures the effective period (T_{eff})and the effective damping(β_{eff}) are in Case 1 is more than Case 2.This mean that Case 1 is safer than Case 2.S0,The weak points of structural elements in the building can be determined and The weak-beam & strong- column concept can be maintained. So, it can be concluded that the structure can resist high seismic force even in high seismic zone-4 according to the above results.

ACKNOWLEDGMENT

The author wishes to express her deep gratitude to his Excellency, Minister Dr.Myo Thein Gyi, Ministry of Education. The author is very grateful thanks to Dr.San San Yee, Rector of Technological University (Taunggyi), for her permission. The author would like to express deeply thanks to Dr.Win Zaw, Professor and Head, Department of Civil Engineering, Technological University (Taunggyi), for his guidance. The author is highly grateful to her co-supervisor, Daw Ohnmar Khaing, Lecturer, Department of Civil Engineering, Technological University(Taunggyi), for her keen interest, necessary advice, careful guidance and kindness. The author is very grateful thanks to all her teachers, Department of Civil Engineering, Technological University (Taunggyi), for helpful suggestions and necessary advices. Moreover, the author expresses the greatest thanks to her parents and friends for their support and encouragement. Finally, the author is very thankful to all teachers who taught her everything since her childhood.

REFERENCES

[1] ATC 40-"Seismic Evaluation and Retrofit of Concrete Buildings",Applied Technology Council, November 1996.

[2] Chopra AK. Dynamics of Structures: theory and applications to earthquake engineering. Englewood Cliffs, NJ; 1995.

[3] Federal Emergency Management Agency, *FEMA-356,* "*Prestandard and Commentary for Seismic Rehabilitation of Buildings*", Washington, DC, 2000.

[4] ETABS User's Manual, "Integrated Building Design Software",Computer and Structures Inc. Berkeley, USA.

[5] IS 1893(Part1):2002, *Criteria for earthquake resistant design of structures*.

[6] MNBC , Myanmar National Building Code(2016) Part 3 "Structural Design."

[7] Uniform Building Code(UBC),Vol-1and 2,1997 edition, Published by International Concrete of Building Officials.

Project Management and Construction Method for Different Types of Bridge in Various Locations of Myanmar. (From Naung Moon to Kawthaung)

Kyaw Myo Htun

Department of Bridge, Ministry of Construction
Naypyidaw, Myanmar

E-mail - ukyawmyohtun@gmail.com

Abstract **— This paper illustrates the duties & responsibilities of Ministry of Construction and especially describes the construction of bridges in Myanmar. Department of Bridge implements different types of bridges which were appropriated to related location. Due to the topography of Myanmar, northern part occupies mountains with cold & rainy weather, central lowlands have mostly flat terrain with hot & dry and southern coastal area with tropical weather. This paper presents how to plan and manage for bridge construction projects in various topography and weather of Myanmar and how to choose type of bridge with appropriate foundations and construction method to achieve successful outcomes.**

Keywords: Plan, Project, Construction Method, Types of Bridge, Topography, Foundation.

I. INTRODUCTION

Ministry of Construction is a focal Ministry for infrastructure development in the whole country. There are five departments in MOC , i.e Department of Building, Department of Highways, Department of Bridge, Department of Rural Road Development and Department of Urban and Housing Development. Among the Departments, Department of Bridge (DOB) implements the bridge infrastructures in Myanmar by 20 bridge construction units. Myanmar have many kinds of terrain such as mountain, hilly, flat and coastal with winter, summer & rainy seasons. Therefore type of bridges and construction method of bridges are varies depend on location of project site. This paper illustrates about the construction of some bridges which were located in Kachin State, Mandalay Region and Tanintharyi Region with mountainous and cold, flat & dry and hilly coastal area closed to Equator.

II. BRIDGE CONSTRUCTION PROJECT

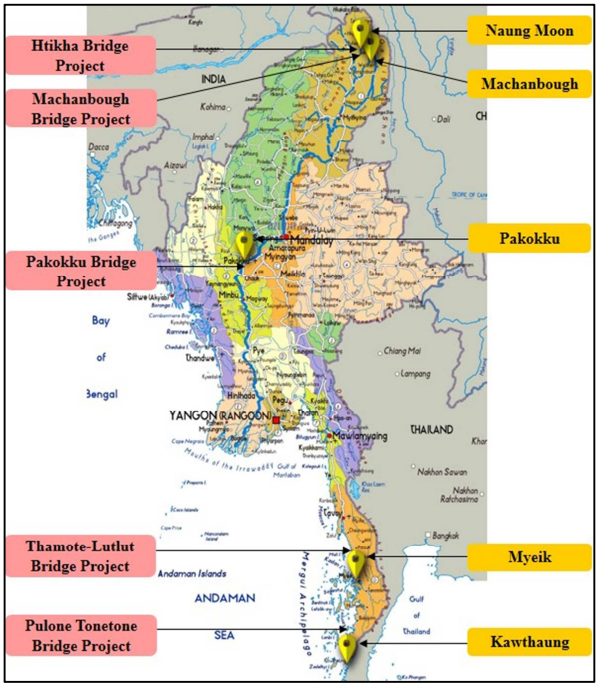

Fig.1 Location Map of Bridge Projects

There are many bridge infrastructure projects which are implemented by DOB in Myanmar and among them, the five projects described in Fig.1 are selected to study the project management and construction method. According to the location of that projects, they were constructed in different topography and weather with different condition of transportation to access project site.

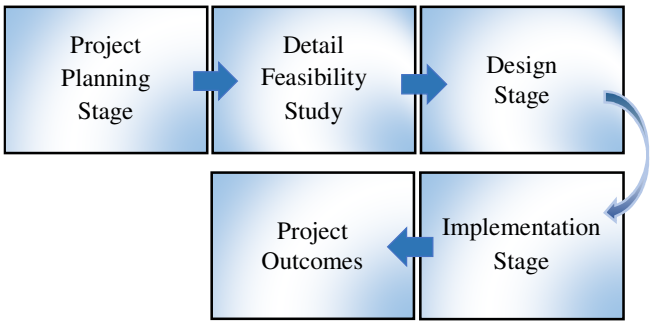

Fig.2 Flow Chart of Project Sequences

III. PROJECT PLANNING & FEASIBILITY STUDY

1. Htikha Bridge Project

Hitkha bridge is located on Machanbough-Hprukha-Naung Moon road and constructed crossed the Htikha creek. The local people across the Htikha creek with temporary suspension bridge with limited loading capacity. To reduce the poverty and upgrade the living standard of local people, the permanent bridge was need to construct to develop socioeconomic of this region.

1.1 Soil Investigation

Soil from surface to 10ft depth is silt trace clay & below 10ft depth is sandstone. N value is 44 at depth of 12ft.

1.2 Topography

Htikha creek is located in the valley of mountainous area, water level is decrease in summer, increase in rainy season with very rough flow velocity.

1.3 Transportation Condition

Htikha bridge is located in Northern part of Kachin State near Naung Moon town, the existing road is not all weathered road and automobile cannot travel in rainy season. Major Construction materials and equipments were supplied from Myikyina through Sumprabom-Putao road by using of two or three crown vehicle. Heavy construction machines could not be used because of road and weather condition.

2. Machanbough Bridge Project

Machanbough bridge is existed at starting mile post of Machanbough-Hprukha-Naung Moon road and acrossed Malikha river. There was a existing temporary suspension bridge which could be passed only small vehicle of less than one ton in weight. The asphalt pavement road form Putao to Machanbough was ended at Maylikha river and from river to Naung Moon was not all weathered road at that time. To developed socioeconomic of people who lived in upper region of Machanbough, the new bridge was needed which can carry more capacity than existing one.

2.1 Soil Investigation

Soil from surface to 20ft depth is sand with gravel and below 20ft are mostly Grey and Yellowish brown sand trace silt clay. N value is 65 at depth of 25ft.

2.2 Topography

Maylika river where the bridge constructed location is existed in valley and level of banks are high from low water level, but water level is flooded and flow velocity is also high in rainy season.

2.3 Transportation Condition

Machanbough bridge is located near Machanbough town, logistics condition is similar to Htikha bridge.

3. Pakokku Bridge Project

The Country is divided into east and west major portion by Ayeyarwaddy river which started from north of country and ended Ayeyarwaddy Region. The cities in east bank portion of Ayeyarwaddy were more developed than that of west bank because of good development of road infrastructure network. Bagan and Naung Oo are ancient cities and they are major tour destination of Myanmar and Pakokku town in a largest city in west bank of Ayeyarwaddy river which occupied many agricultural products especially onions, bean and cooking oil. The cargo vehicles, passenger vehicles and people crossed Ayeyarwaddy river with Z-Craft before Pakokku bridge was constructed and it took about 1:30 hours for one way trip excluding waiting time to aboard. Pakokku bridge was need to build to develop Pakokku town and also to develop west bank of Ayeyarwaddy river including Monywa town, Sagaing Region and Chin State.

3.1 Soil Investigation

There are mostly sand some silt and clay up to 85ft depth and below 85ft are Grey Sand trace gravel and silt. N=45 at depth 85ft.

3.2 Topography

Ayeyarwaddy river of bridge constructed area is located in flat and steady flow in summer and high currents velocity in rainy season. The island is existed near

Pakokku bank and temporary sand dunes are formed near Letpanchaepaw bank in summer.

3.3 Transportation Condition

Pakokku bridge is located in middle partion of Myanmar and having good road network for transportation of all materials, equipments and machines.

4. Thamote-Lutlut Bridge Project

Thamote-Lutlut bridge project which crossed Thamote river near Myeik is ongoing project and it is located on Dawei-Myeik-Tanintharyi-Kawthaung Road. (D-M-T-K) Road is No.1 National Highway (NH1) and (D-M-T) portion is also part of No.112 Asian Highway (AH112). Along this highway, Thamote-Lutlut bridge is only one bridge which remained to construct on NH1, also AH112. Therefore the regional governor proposed the plan to Union Government to implement Thamote-Lutlut bridge project in 2017-18 fiscal year. After the approval of Union Government, the project had been started on 1.8.2017.

4.1 Soil Investigation

Soil from river bed surface to 10ft depth is brownish grey clayey & sandy silt some gravel and below 10ft are light grey weathered GRANITE. N=66 at depth 12ft.

4.2 Topography

The bridge is being constructed near the end of Thamote river which flows to Andaman Sea. Therefore there are two tidal period by mean of sea water. The flow is rough in the case of tide water raised.

4.3 Transportation Condition

The bridge is located on NH1 and so there is good road network for transportation. The coastal marine transportation can be used for large and heavy construction machines and equipment.

5. Pulone Tonetone Bridge Project

Pulone Tonetone bridge project is ongoing project and which is existed on Kawthaung-Pulone Tonetone island road acrosses the Andaman sea. Kawthaung is mountainous and narrow spaced border city near Ranong city of Thailand. Pulone Tonetone island occupies small beach which is most visited by local people and Thai people by being passed through over the existing timber bridge. The island also occupies fisherman village and so, many sea products are unloading at that Pulone Tonetone village and then deliver to Kawthaung. Due to the load limit of timber bridge they carry fishery products from village and ice and other supporting materials from Kawthaung by using three wheel motorbike on the bridge. Due to existing of small beach and hilly terrain, the island can be developed into recreation area and tour destination by providing new bridge across the shallow sea between mainland and island.

5.1 Soil Investigation

Soil from bed level to 30ft depth are clayey silt some gravel some sand and below 45ft are Quartzose Sandstone and weathered Granite. N=63 at depth 40ft.

5.2 Topography

The bridge is being constructed in the Andaman Sea which will be connected Pulone Tonetone island to main land. The sea is shallow at the bridge project site and therefore there are no ship and large boat cross the bridge except small boat. Freeboad of existing timber bridge is 1m.

5.3 Transportation Condition

The bridge is located near NH1 and 4 mile away from Kawthaung. The access road to project site is in good condition. The marine transportation can also be provided for large & heavy construction machines & equipment.

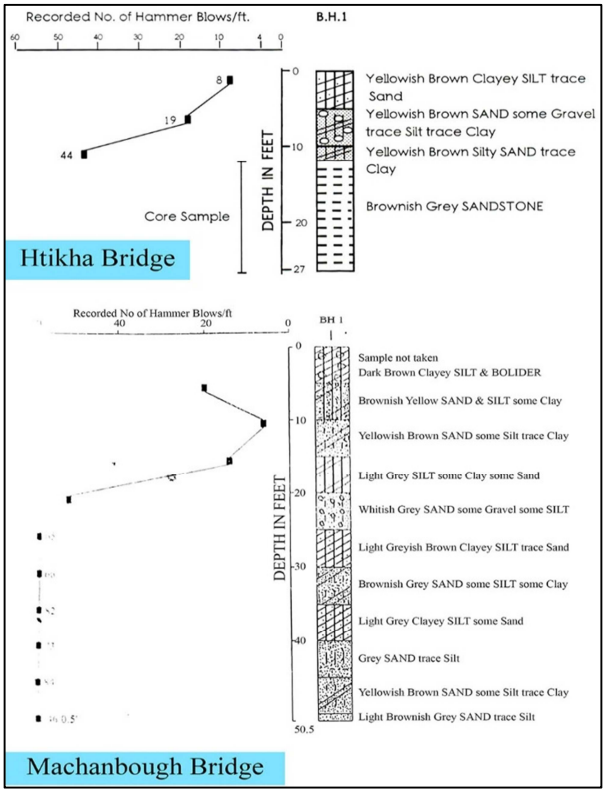

Fig.3 Soil Investigation Data

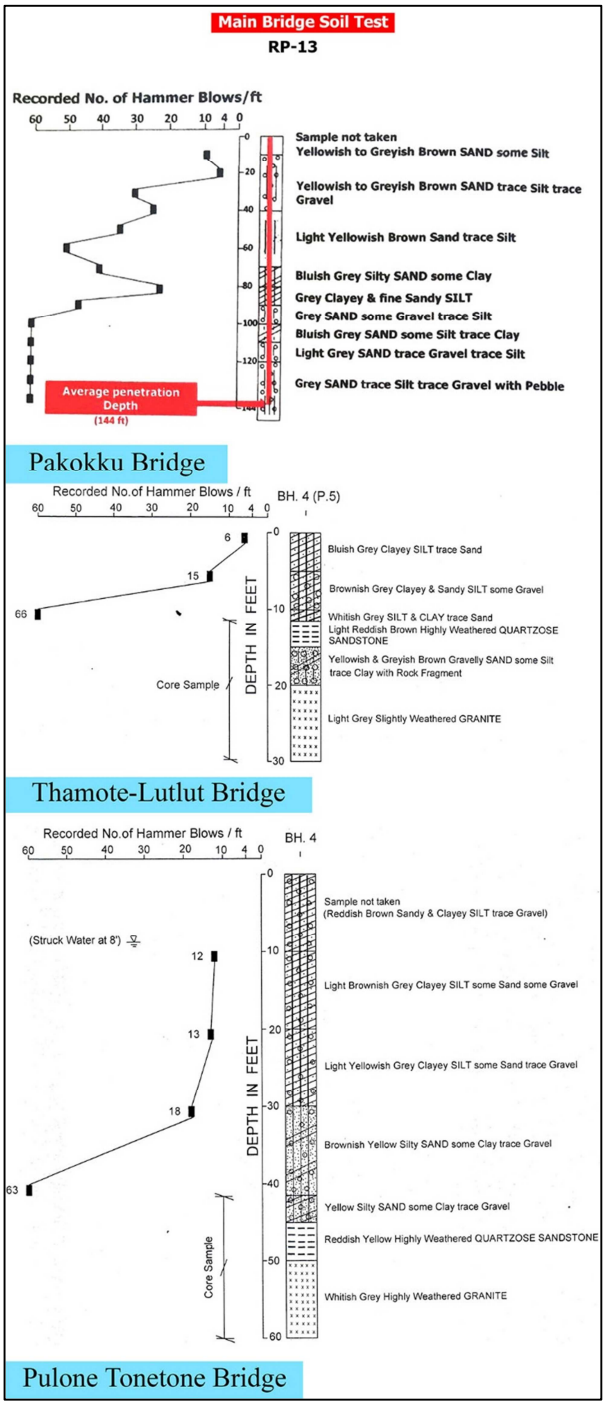

Fig.4 Soil Investigation Data

IV. DESIGN STAGE

When data were collected, the construction teams and designer made many discussions and site visits to provide most suitable conceptual design for projects. They reviewed about that, which materials could be got in local area, how to transport construction machines, equipments and major materials, which type of bridge is suitable for related project site, what kind of foundation would be defined and financial condition; etc.

After that, the designer proposed conceptual drawing with suitable spans arrangement and then the construction team set the layout at the project site to know that conceptual design is constructable or not. Designer provided complete detail design for the projects if conceptual is constructable and change alternative design when conceptual is not constructable. When deisngers and construction teams made final decisions, types of bridges, kinds of foundation, span length and span arrangement are designed as table (1).

Table-1 Design of Bridge Projects

Sr	Name of Brdige	Span	Type of Bridge			Location
			Foundation	Substructure	Superstructure	
1	Htikha Bridge	400 ft (100' x 4)	Caisson	R.C.C	Steel Plate Girder & R.C.C Decking	Machanbough-Hprukha-Naung Moon Road. (Naung Moon Twonship)
2	Machanbough Bridge	840 ft (50 + 70 + 600 + 70 + 50)	4'Ø Spun pipe	R.C.C	R.C.C Land Span and Bailey Suspension Main bridge	Machanbough-Hprukha-Naung Moon Road. (Machanbough Twonship)
3	Pakokku Bridge	4126 m Motor Way 6278 m Rail Way	Bored Pile (Cast in situe pile)	R.C.C	P.C Girder & R.C.C Decking Approach Bridge, Steel Truss & R.C.C Decking Main Bridge	Nyaung Oo-Pakokku Road
4	Thamote-Lutlut Bridge	1287'	Bored Pile	R.C.C	P.C Girder, Steel Box Girder & R.C Decking	Dawei-Myeik-Kawthaung Road. (Myeik Township)
5	Pulone Tonetone Bridge	2400'	Bored Pile	R.C.C	R.C.C, P.C Girder & R.C.C Decking	Kawthaung-Pulone Tonetone Island Road.

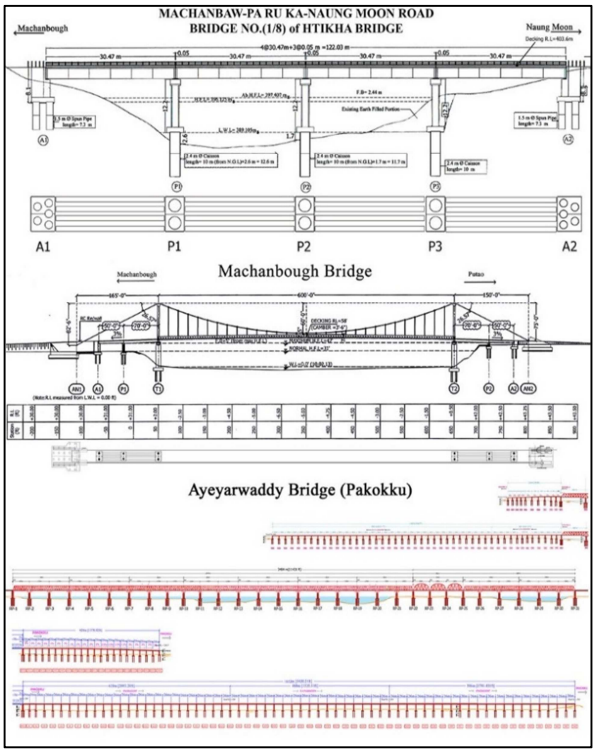

Fig.5 Conceptual Design Drawings

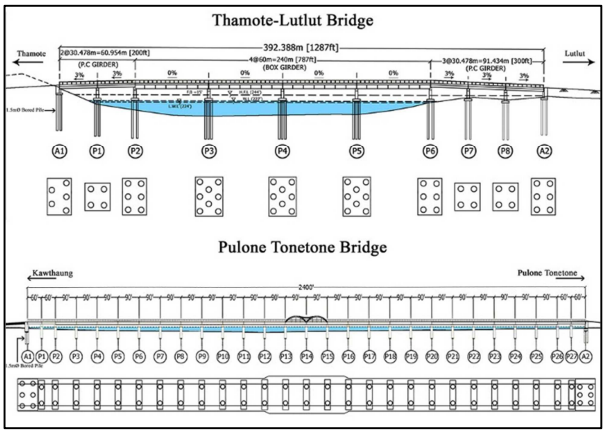

Fig.6 Conceptual Design Drawing

V. IMPLEMENTATION STAGE

Construction method and project management is very important in implementation stage to achieve successful outcomes. Therefore project director of each construction team need to do proper management on time, quality, cost and safety including project schedule, quality management system (QMS), cost control, safety measures, resources (human, material, machines, equipment), logistics, weather condition and communication; etc. Engineers in construction sites need to understand Standard Operation Procedure (SOP) of all kinds of works in implementation stage.

1. Htikha Bridge Project

Heavy machines and equipments were not available according to the difficulty of transportation. Therefore reinforced concrete caisson foundation type was chosen and provided by manpower by using of water pumps and concrete mixers only. Project Director carefully managed to maintain adequate human resources for foundation work which required to finish before rain fall in that region. 100 ft span steel plate girder type was chose to reduce number of pier and also no need to use scaffold for girder installation, it would be installed by launching method with less machines requirement. Therefore, experienced engineers and skill workers were required to complete this project successfully.

Fig.7 Recorded Photo of Htikha Bridge

Fig.8 Recorded Photo of Htikha Bridge

2. Machanbough Bridge Project

This bridge is bailey suspension bridge with steel pipe pylon. Foundation are 4'Ø spun pipe pile and therefore would be provided by manpower. Mobile Crane was required to install pylon of main bridge and bailey girder, therefore 15 tons mobile crane was delivered from Myitkyina in dry season through the Myitkyina-Sumprabom-Putao road. That delivery process took about 45 days to reach Machanbough bridge project site. Project director carefully managed to reach major construction material such as cement, M.S rods, bailey parts, main cable; etc in time. Project can be delayed if supply of material delayed. To collect or to get local labours was very difficult in Putao district and so engineers managed to maintain the adequate labours including skill labours in work site by being supplying from Myitkyina base camp.

In this type of bridge, installation process of main cable, suspender and baily girders were complicated to understand for unexperienced engineer and labours. Therefore project engineer explained method of statement or construction method to all participants and made many discussions to understand how to do without accident. Safety is very important in installation of suspension bridge because most workers would be worked on height places and narrow space.

Fig.9 Recorded Photo of Machanbough Bridge

Fig.10 Recorded Photo of Machanbough Bridge

3. Pakokku Bridge Project

Pakokku bridge is a longest bridge by eleven bridges which were constructed crossed the Ayeyarwaddy river. Project location was very good for supporting of all construction materials, machines, equipments and human resources. But key factor for this project was project duration because authority wanted to finish this project within two years. Therefore project director and project engineers were carefully monitored the project schedule and urgently provided correction for any delay of schedule. Construction of foundation, substructure and superstructure were carried out with times lapped schedule. Erection of steel truss of main bridge was started from four working points in six direction simultaneously in order to complete in specific schedule. Proper construction management was very important in this project and all participants could be followed the specific schedule and safety plan to achieve successful project outcome.

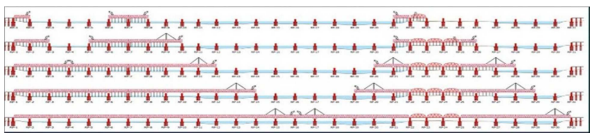

Fig.11 Steel Truss Erection Sequence

Fig.12 Recorded Photo of Pakokku Bridge

4. Thamote-Lutlut Bridge Project

The project site is located on Thamote tidal river near Andaman Sea. The soil condition under river bed is mostly granite layer and therefore special equipments which attached bored pile drilling machine were used in foundation work. To complete single bored pile took about 10 to 15 days due to rock layer. The main bridge is 60m x 4 spans continuous steel box girder types and which was installed by launching method by using of hydraulic jack. Project engineers managed carefully to achieve goal of project with clean sheet accident. Construction method is slightly different from above projects because p.c girder and main steel box girders are installed by launching method with bailey launching girder and steel plate launching nose girder respectively.

Fig.13 Recorded Photo of Thamote-Lutlut Bridge

Fig.14 Recorded Photo of Thamote-Lutlut Bridge

5. Pulone Tonetone Bridge Project

This bridge is bent pile type bridge with two 1.5mØ bored piles at each pier and 90ft girder 24 spans with 60ft R.C.C girder 2 spans at each side. In the middle spans of bridge, P_{12}-P_{13}-P_{14}-P_{15}-P_{16} Spans are designed innovatively with view deck and decorative archs for the purpose of visitors to feel relaxation by seeing open sea view with fresh breeze across the sea. There is no water in low tide level and the water depth become 3~4.5m at high tide level because of flat bed level and shallow portion of sea with mangrove trees. Construction method of foundation is different from other bored pile foundation in this bridge, because the ordinary working barge cannot carry bored pile machine and other loading without floating in water. Therefore coastal landing craft which can carry working bored pile machines on shore was used for foundation work. After that, prefabricated pre stressed concrete girders were installed in position by using of modified steel truss launching girder. Project director and engineers take care all steps of construction sequence not to deviate from schedule and quality and not to happen any accident.

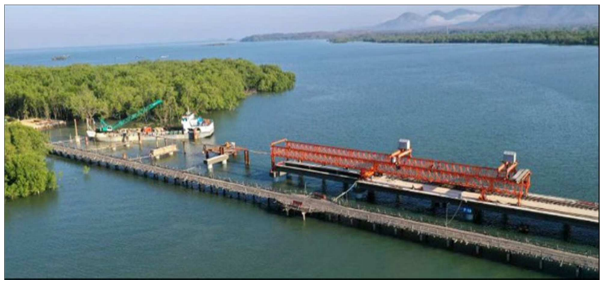

Fig.15 Recorded Photo of Pulone Tonetone Bridge

Fig.16 Recorded Photo of Pulone Tonetone Bridge

VI. CONCLUSIONS

By studying the bridge projects at different locations of Myanmar which were implemented by Department of Bridge, Myanmar engineers can construct any type of bridge with any kind of foundation by applying appropriate construction management knowledge. The constructors and engineers should consider proper alternative designs to comply with available resources. There are different construction methods for various topography of project location, the engineers should apply proper method to achieve successful outcomes. Modernized engineering technology, construction machines & equipments, safety rules & regulations and construction management knowledge should be studied and applied in all engineering societies to become our bright future Nation.

ACKNOWLEDGEMENT

Author would like to thank Director General U Shwe Lay for his kind advice to prepare this paper. Special thanks to U Saw Zarni Hla, U Myint Naing Oo, U Aung Kyaw Soe and U Wai Phyo for their kind support to collect required data for bridge projects. Also thanks to office staff of Bridge Construction (4) for their kind support during the period of this paper and the people who helped directly and indirectly to complete successfully this paper.

REFERENCES

(1) Construction Report of Pakokku Bridge, 2012.

(2) Completion Report of Machanbough Bridge, 2017.

(3) Construction Record of Htikha Bridge, 2019.

(4) Construction Record of Thamote-Lutlut Bridge and Pulone Tonetone Bridge, 2019.

INTEGRATED WATER RESOURCES MANAGEMENT PLANS FOR SITTAUNG RIVER BASIN

Shwe Pyi Tan [1], Toshio KOIKE [2,3], Mohamed RASMY [2,3]

[1]Irrigation and Water Utilization Management Department, Myanmar

[2] International Centre for Water Hazard & Risk Management (ICHARM) under auspices of UNESCO, Public Works Research Institute (PWRI), Japan

[3] National Graduate Institute of Policy Studies, Japan

Abstract - Sittaung River Basin (SRB) is one of the water-related hazards affected basins in Myanmar. To prevent and reduce socio-economic losses, both structural and non-structural countermeasures need to be considered in this basin. The overall objective of the research is to improve flood and drought analysis system in Myanmar using advanced spatial technologies, to understand on the past and future climate and to examine the effectiveness of existing and proposed countermeasures. In this study, past hydro-meteorological data analyzes by the Standardized Precipitation Index (SPI) method was used to understand the significant changes of hydro-meteorological condition of the area. The outputs of six models selected from the Coupled Model Inter-comparison Project Phase 5 (CIMP5) were used to identify signals of climate change. The Water and Energy based Rainfall-Runoff-Inundation (WEB-RRI) Model was used to estimate flood inundations and discharges, to analyze the effectiveness of existing countermeasures, and to propose new mitigation measures for future development works. The result of the assessment indicated that the discharge control by modifying the existing reservoir operations should be applied to an adequate water level to mitigate flood and drought damage. The proposed countermeasures can contribute to reduce the peak-inundation depth and thus reduce the agricultural damages.

Keywords: ***Flood Mitigation, CIMP5, Sittaung River Basin (SRB), SPI,WEB-RRI model***

I. INTRODUCTION

The Sittaung River Basin (SRB) is the 4th largest river in Myanmar and is located in the east-central zone, originating in Mandalay Region on the edge of the Shan Plateau and flowing south before it runs out into the Gulf of Martaban of the Andaman Sea. The catchment area of the Sittaung River is 34950 km^2 and it runs 450 km from upstream to the outlet. Every year, a monsoon rainfall event triggers a flood disaster. A state of emergency declared in the five regions; Bago, Taungoo, Phyu, Madauk and Shwegyin where devastated disasters often happen.

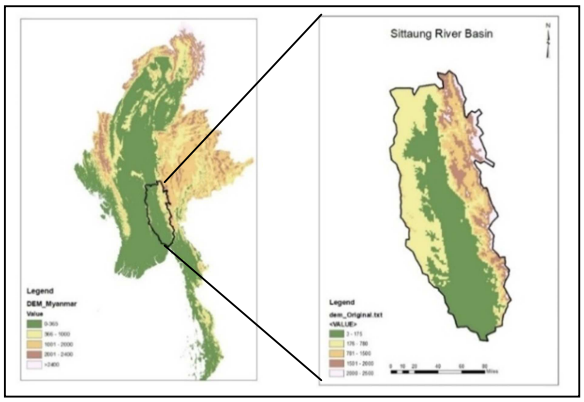

Figure 1 Topography of Myanmar and Location of SRB

Once a flood occurs, the agricultural fields are inundated, the major network of motor roads and railways passes through this region are blocked by flooding. Not only severe flooding but also drought is a major problem at some places. During the dry period, the amount of reservoir storage water decreases associated with climate change. The region often faces the shortage of water supply for hydro-power generation, the farmland and drinking water. Although local people encounter huge losses almost every year, there are lacks of systematic activities to prevent and mitigate of these damages. There are very few records for floods and no historical records for droughts and dam operations exist in this basin. An optimization-based approach for a multi-reservoir system operation is needed to mitigate flood damage and support stable water supply. Therefore, an integrated research is necessary to analyze climate change scenarios and seek lasting solutions for the flood and drought induced problems.

II. METHODS

The overall objectives are to analyze the changes in precipitation and floods and water scarcity in the past, to develop the countermeasures considering future climate change impact based on the flood and drought impact assessment and to integrate the efficient water allocation method by modifying the dam operation. Schematic diagram of the study

approach is shown in Figure 2. Past data analysis for extremely flood and drought were carried by the Standardized Precipitation Index (SPI) method. For identifying the past alternating wet and dry periods, the SPI method is primarily useful in the study of non-stationary associations using time-series data to provide the decomposition of precipitation time series. To improve the estimation of water and energy budget processes and initial soil storages, Rasmy et al.(2019) developed a Water and Energy based Rainfall-Runoff-Inundation (WEB-RRI) model by coupling the Simple Biosphere Model-2 (SiB2) (Wang et al. 2009) with the Rainfall-Runoff Inundation (RRI) model (Sayama et al. 2010). The WEB-RRI model was calibrated and validated by using the observed hydrograph at Taungoo and Madauk discharge measuring stations in 2011 and 2012, respectively. The selected six models of the Coupled Model Inter-comparison Project Phase 5 (CIMP5) under the Representative Concentration Pathways (RCP-8.5) scenario were used to investigate future climatology. To correct the biases in GCM precipitation, the daily precipitation data observed at six rain gauge stations were used for developing bias-corrected GCM rainfall data sets for 20 years in the past (1981 -2000) and for the future (2041 -2060) climate. The combination of the hydrological and climatological models illustrates excellent performances in simulations of the low flow, the timing of flood onset, flood peak discharges, and inundation extents and capabilities for identifying effectiveness of the existing countermeasures and proposing new mitigation measures for future development works. This research will focus on how to generate reliable and accountable information for supporting policy decision making related to integrated water resource management of the Sittaung River Basin (SRB) in the future.

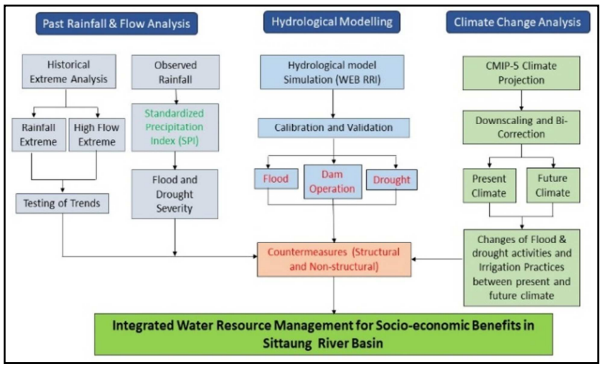

Figure 2 Schematic diagram of the study *approach*

III.DATA

Daily rainfall data were collected at six stations of the Department of Meteorology and Hydrology (DMH) and 22 stations from Irrigation and water utilization management Department (IWUMD). The seventeen dams released discharge data (maintained by IWUMD) were used for model validations, and the two observed discharge stations (maintained by DMH) were used to validate the model. The location of the dams and hydro-meteorological stations are shown in Figure 3.

Topographic data such as digital elevation models (DEM), flow direction (DIR) and flow accumulation (ACC) were collected from the U.S Geological Survey's Hydrological data (USGS) of 15 sec (450m) based on Shuttle Elevation Derivatives at multiple scales (Hydro-SHEDS) . Leaf Area Index (LAI) and Fraction of Absorbed Photo synthetically Active Radiation Data (FPAR) were obtained from NASA Earth Observation Data & Information System. Meteo-rological forcing inputs data such as Japanese 55-year Reanalysis Data (JRA55 Data) were obtained from the Japan Meteorological Agency (JMA).

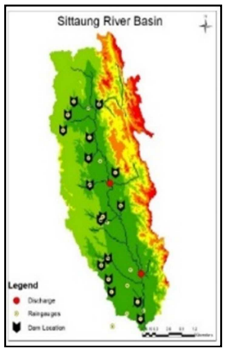

Figure 3 Dams and Hydrometeorological Stations

IV. TABLES AND FIGURES

The SPI values in a 3-months timescales were calculated using the six rain gauge data and plotted in Figures 4 to demonstrate wet and dry climate seasonality. In SRB, the SPI analysis values show that although floods are more severe than droughts, the duration of some drought events were longer and devastating in recent years. Droughts occurred in 1983, 1990, and 2010 as the SPI in those years indicates severe dryness.

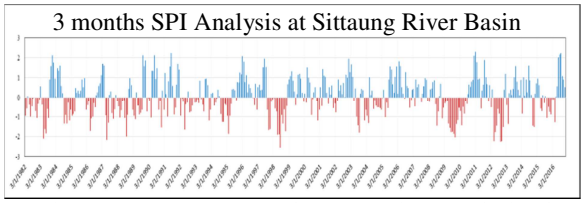

Figure 4 (3) Months SPI for wet and dry periods of Sittaung River Basin

The WEB-RRI model was set up for model calibration during 2012 flood events. The model sensitivity study was conducted to find the model calibrated parameter values. This simulation results showed the reasonable results for the model calibration at Taungoo and Madauk as shown in Figure 5.

Figure 6 demonstrates the observed and simulated discharge of the SRB at these two stations. At Taungoo station, the model outputs are similar to the observed values at the high flow and low flow condition of the year 2011 and 2012. Although there is a gap between the simulated and observed discharge at the Madauk station before and after the monsoon

periods due to the effect of the dams' release and storage, the result during flood events is nearly similar to observed discharge.

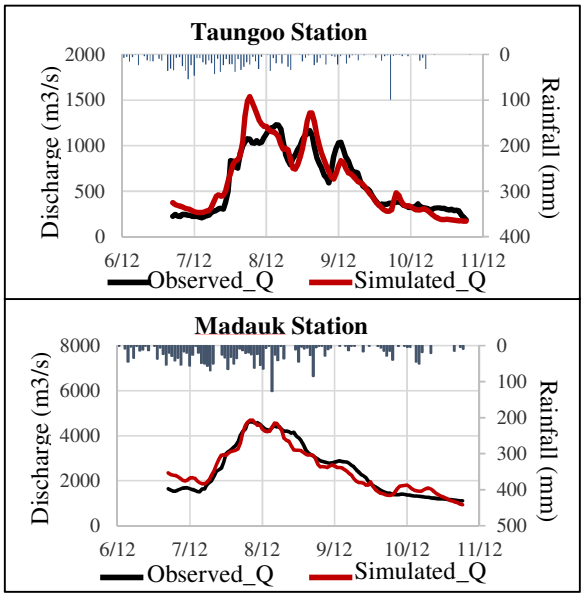

Figure 5 Simulated and Observed Discharge of Sittaung River Basin for 2012 Flood Event

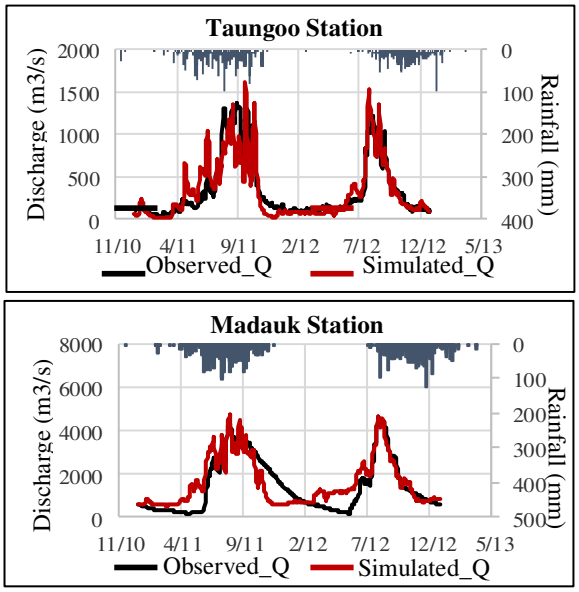

Figure 6 WEB-RRI Model Validation and Observed Discharge for 2011 and 2012

Even though many existing facilities such as reservoirs were established, new countermeasures are needed for flood mitigation because those facilities were not designed for flood management. Currently, three sluice gates and one retarding basin are proposed as shown in Figure 7**.** When the flood water enters, each sluice gate stores the water up to its designated level. The excess flood water overflows the sluice gate and flows down to the next one. At third one, the floodwater is transferred to the Ngabataing Lake that will act like a retarding basin. If we assume that discharge more than a threshold value of 2000 m^3/s can be diverted to the retarding basin, a total of 68 MCM of water can be stored to reduce the flood peak.

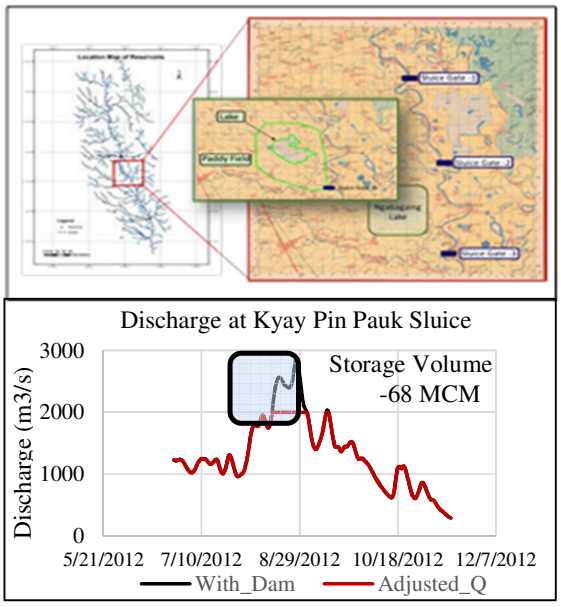

Figure 7 New Countermeasures for Flood Mitigation and Operation Capacity of Retarding Basin

Figure 8 illustrated the flood affected area and inundation depth in three cases, including without dams, with effective dam operations and with proposed countermeasures. Based on the simulated results, the total inundated area is reduced 20% and 40% by the existing counter-measures and the proposed countermeasures, respectively.

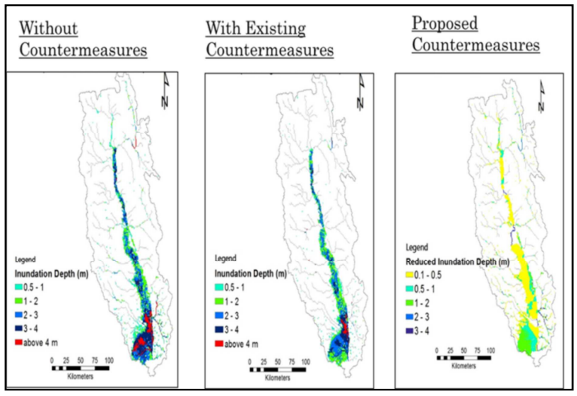

Figure 8 Inundation depth and area maps of different countermeasures

The paddy damaged area and value are estimated by analyzing the inundation depth with a stage of monsoon paddy and the production cost. Typical rice production cost to monsoon paddy is approximately USD 373. Table.1 shows the expected maximum area of the paddy damages and their values for different types of countermeasures.

On the other hand, the past and future climates were studied by using GCM of RCP8.5 Scenarios of the future climate, Six GCMs were selected and all the

Without countermeasure		Existing countermeasure		Proposed countermeasure	
Area (ha)	Value (US$ Million)	Area (ha)	Value (US$ Million)	Area (ha)	value (US$ Million)
82553	28.48	65961	22.75	32472	11.2
Reduced damage value			5.72		17.3

Table 1. Expected max paddy damage area and value

models showed that monthly precipitation would increase the wet season and three models showed that monthly precipitation would decrease in the dry period compared with the present climate. All six models show large increase rates of the daily extreme rainfall, 21% by ACCESS model, 33% by CMCC_CESM model, 29% by CMCC_CMS model, 4.78% by CMCC_CM5 model, 22.58% by MPI_ ESM_LR model and 42% by MPI_ ESM_MR model from the year 2040 to 2060 over the SRB (See as in Figure 9).

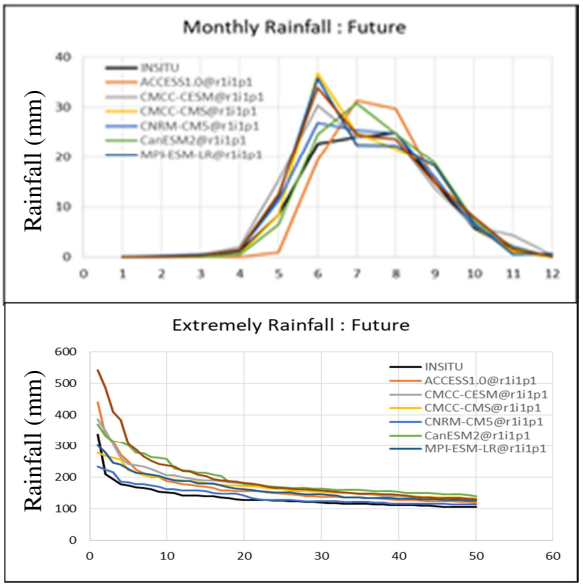

Figure 9 Monthly average and Probability of extreme precipitation under the *present and future*

Figure 10 shows probability distribution of precipitation and inflow at the downstream of SRB. All the models showed that extreme precipitation would increase in the future climate and that will subsequently lead to more inundation. However, three models showed that deficit rainfall would occur in the dry season in the future and meteorological drought also would occur in the dry period. According to the result of the WEB-RRI model simulation using the GCMs past and future data, inflow will increase in the future, that will lead to increase of inundation extents during flooding time. However, inflow will decrease in the dry season and that will lead to the hydrological drought condition.

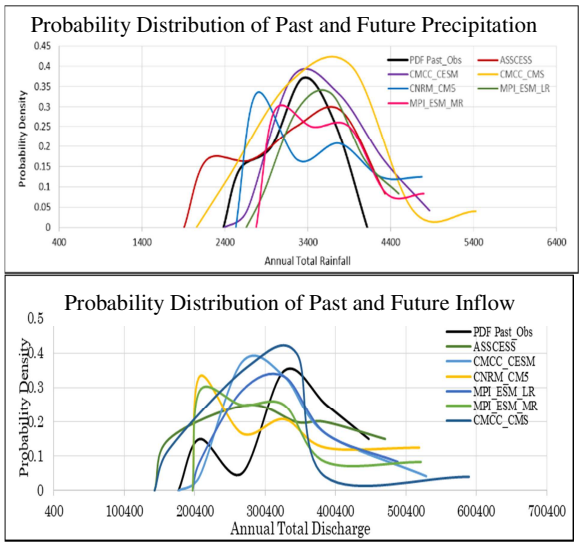

Figure 10 Probability Distribution of Precipitation and Inflow under Past and Future Climate

Keeping GCM model scenarios, the hydrological assessment of dams should be addressed as a prioritized project. Paung Laung Dam is selected to check the storage capacity and similar methodology to cope with other dams. Figure 11 shows the gap between past (1980-2005) and future (2040-2065) averaged inflows of the six GCM data. According to the figure, the inflow will decrease in summer and then increase in the rainy season

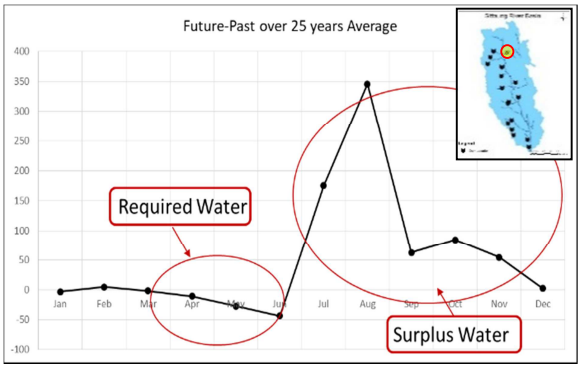

Figure 11 Future – Past over 25 years Average Inflow at Paung Laung Dam

(July to December). During the rainy season, there is an ample amount of water which may create flood and ultimately could reach the sea without any usage. Therefore the surplus water has to be stored to use for upcoming dry season (January to June). Hence the storage capacity of reservoir has to be increased to minimize the effect of drought during the dry season such as shortage of water for irrigation, hydropower and drinking water for the local people. Therefore, optimizing the water allocation management in the dam to improve the water storage capacity during the flood time is prime task in Paung Laung Dam. Subsequently the stored water will be made available for use in dry or summer season. Apart from the climate change, the population of this area under the dam is in increasing trend. Due to the demographic increase, the future water demand will also

increase. In that sense, irrigation, hydropower, drinking water, sanitation and industrial water usages will increase. Hence, the optimization of water usages is essential for decision makers of the SRB and this research will support them for timely decision making.

V. CONCLUSIONS

According to the SPI analysis, in most of the years, severe floods were recorded in the Sittaung River Basin. But some drought events were prominent and they lasted for long period of time in recent years. For the future climate assessments, the GCM rainfall data bias-corrected by using the in-situ data and indicated an increasing trend in the wet season and a decreasing trend in the dry period in the SRB. Therefore, the increasing precipitation will result in increasing water levels, and discharges during the wet season and vice versa in the dry season.

In this study, WEB-RRI modeled hydrographs showed acceptable performance in simulating flooding events, and the modeled discharge hydrographs correlated well with the observed discharge hydrographs. This study also examined the effectiveness of countermeasures for scenario flood events to minimize severe inundation damages by extreme rainfall events derived from the climate scenarios. To reduce the flood inundation area and inundation depth, the proposed cascade flood gate operations and diverting a peak discharges to the retention basin can reduce the flood damages during the rainy season, significantly.

As the SRB also plays an important role for the national agriculture production and hydropower generation, the projected water demand and seasonal water availability in dams for the future should be considered based on the present demand to improve the dam operation system. These outputs of this research, which based on natural science and advanced method of technology, can support policy and decision making to optimize the future water resources of the basin in an integrated approach.

ACKNOWLEDGMENTS

I would like to express my gratitude to my respected supervisor, Professor Koike and my co-supervisor, Associate Professor Dr.Mohamed Rasmy, for having time to supervise my research through his valuable comments, guidance and support. Also, I am grateful to Mr.Sawano, Dr.Shrestha and Dr.Takeda for their insightful comments and encouragement.

REFERENCES

[1] IPCC, 2007. *Climate Change 2007: The Physical Science Basis. Contribution of Working Group I to the 4th Assessment Report of the IPCC,* Cambridge, UK/New York, USA: Cambridge University Press.

[2] Yang, J. et al., 2008. Comparing uncertainty analysis techniques for a SWAT application to the Chaohe Basin in China. *Journal of Hydrology,* Volume 358, pp. 1-23.

[3] SAYAMA, Takahiro. *Rainfall-Runoff-Inundation (RRI) Model User's Manual.* Tsukuba: International Center for Water Hazard and Risk Management (ICHARM), 2013.

[4] United Nations. *Report on Sittaung Valley Water Resources Development* (Technical Report): Rangoon, Burma, 1964; (retrieved from the Irrigation Department, Myanmar on 2015)

Assessment of Crop and Irrigation Water Requirements for Some Selected Crops in Chaung Gauk Irrigation Scheme

Ei Khaing Zin Than [1], Kyaw Lin Htat [1], Ohnmar Tun Wai [2], Shwe War [3]

Department of Civil Engineering, Technological University (Thanlyin)
Yangon, Myanmar

eikhaingzinthan72019@gmail.com
kyawlinhtat@gmail.com
omtwai.30@gmail.com
shwewartutgi@gmail.com

***Abstract* - This study presents the estimation of irrigation water requirement (IWR) and crop water requirement (CWR) for some selected crops (monsoon paddy, summer paddy, green gram, sesame, chick pea, cotton) in Chaung Gauk irrigation scheme. The reference crop and actual crop evaporation (ET_o and ET_c) are estimated to evaluate the irrigation of water requirement of crops in study area. Necessary meteorological data (temperature, rainfall, humidity, wind speed, sunshine hour) and crop data have been collected for 10 years period from 2009 to 2018. Effective rainfall was calculated by using Fixed Percentage; 80 % Method. Crop evapotranspiration (ET_o) is calculated by multiplying the reference crop evapotranspiration with crop coefficient K_c. Irrigation requirement is different between the crop evapotranspiration under standard conditions (ET_c) and effective rainfall.**

Keywords: Reference crop evapotranspiration, effective rainfall, irrigation water requirement (IWR), crop water requirement (CWR), crop coefficient (K_c)

I. INTRODUCTION

Myanmar is an agricultural country. Therefore, assessment of crops water requirement is importance for all regions. The term water requirements of crop means the total quantity of all water and the way in which a crop requires water, from growing time to harvesting time. Different quantities of water at different times are required by different crops, till they grow up completely. The crop water requirement or crop evapo-transpiration is the depth or amount of water needed to meet the water loss through evapo-transpiration. It mainly depends on the climate, the crop type and the growth stages of the crop. In central Myanmar, rainfall is inadequate. So, irrigation system is necessary to supply the water where there is inadequate rain. The purpose of irrigation is to provide the best possible moisture contents required for the desired growth, yield and quality of plants. To achieve higher production of desired crops, the suitable water application programmes should also be adopted. The objective of this study is to evaluate the irrigation water needs for Chaung Gauk irrigated area, where are growing monsoon paddy, summer paddy, green gram, sesame, chick pea and cotton etc.

II. STUDY AREA

The study area, Chaung Gauk Dam impounds water from Chaung Gauk spring and the catchment area is 77.6 sq miles. It is located in the central dry zone of Myanmar, Pyawbwe Township, Yamethin District of Mandalay Region.

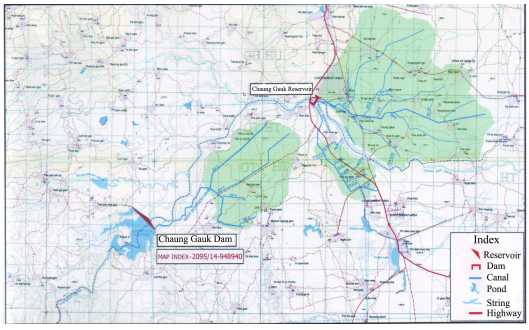

Figure 1 Chaung Gauk canal network
source: Irrigation Department

Geographical location of this irrigation area is

20.88º North (latitude) and 95.86º East (longitude) at an elevation of 244 meters. The type of dam is Earth. Its length is about 6800 ft and its height is 74 ft. Full tank capacity is 26,000 ac-ft and dead storage capacity is 5,000 ac-ft. Average annual rainfall is 33 inches. Chaung Gauk Dam project intends to provide the water for the 6493 acres irrigable area. Location of the reservoir and canal network system is shown in Figure 1.

III. METHODOLOGY

1. Collection of Meteorological Data

In this study a long recorded 2009 to 2018 (10years) meteorological data collected from Meiktila Station. These data are;

- Maximum Temperature and Minimum Temperature (Celsius)
- Mean Relative Humidity (%)
- Wind Speed (kmph)
- Sunshine Hours (Hrs)

The respective climatic data were collected from the Department of Meteorology and Hydrology under the Ministry of Transport and Communication.

2. Crop Stage Data

The major cultivated in study area are summer paddy, monsoon paddy, green gram, chick pea, sesame and cotton, etc. Crop coefficient values (Kc); rooting depth; length of plant growth stages; planting date and allowable depletion are taken from FAO Paper 56.Kc values for initial, mid and late growth stages of crops are used. Yield response factor for crops are taken from FAO paper 33.

(i) Crop coefficient (K_c)

Crop coefficient (K_c) varies during the growing period. As the crop develops, the ground cover, crop height and the leaf area change. Due to differences in evapotranspiration during the various growth stages, the K_c for a given crop will vary over the growing period. The changing characteristics of the crop over the growing season also affect the K_c coefficient.

(ii) Rooting depth (D)

The depth of soil water can be used effectively by the crop, defined as the Really Available Soil Moisture (RAM), depends directly on the rooting depth of the crop.

Two values are required;

- Rooting depth of initial stage normally taken as 0.25-0.3m, representing the effective soil depth from which the small seedling abstracts its water.
- Rooting depth at full development at start of mid-season. For most irrigated field crops values vary between land 1.4, vegetable crops 0.5-1.0.

  Rooting depth at development and late season are interpolated values and no input is required.

(iii) Allowable depletion (p)

Allowable depletion (p) represents the critical soil moisture level where first drought stress occurs affecting evapotranspiration and crop production. Values are expressed as a fraction of total available soil moisture and normally vary between 0.4 and 0.6, with lower values taken for sensitive crops with limited root systems under high evaporative conditions, and higher values for deep and densely rooting crops and low evapotranspiration rates.

(iv) Yield response factor (K_y)

Yield Response Factor (K_y) to estimate yield reductions due to drought stress; yield response factor have to be given for each growth stages.

3. Reference Crop Evapotranspiration (ET_o)

The reference crop evapotranspiration ET_o was calculated by FAO Penman-Monteith method, using decision support software CROPWAT 8.0 developed by FAO, based on FAO Irrigation and Drainage Paper 56. The Penman-Monteith equation integrated in the CROPWAT program is expressed by equation (1).

$$ET_o = \frac{0.408\,\Delta\,(R_n - G) + \gamma \frac{900}{T+273}\,u_2\,(e_s - e_a)}{\Delta + \gamma\,(1 + 0.34\,u_2)} \quad (1)$$

Where,

ET_o = reference crop evapotranspiration(mm/day^{-1})

R_n = net radiation at the crop surface (MJm^{-2}day^{-1})

G = soil heat flux density (MJm^{-2}day^{-1})

T = mean daily air temperature at 2m height ºC

U_2 = wind speed at 2 m height (ms^{-1})
e_s = saturation vapor pressure (kpa)
e_a = actual vapor pressure (kpa)
D = slope vapor pressure curve
γ = psychometric pressure curve (kPa/ ºC)

The FAO CROPWAT program incorporates calculation procedures for reference crop evapotranspiration and crop water requirements. The program allows the simulation of crop water use under various climate and crop conditions.

Meteorological parameters used for calculation of ET_o were latitude, longitude and altitude of the station, maximum and minimum temperature C, relative humidity (%), wind speed (km/day) and sunshine hours.

4. Effective Rainfall

Effective Rainfall defined as that part of the rainfall which is effectively used by the crop after rainfall losses due to surface runoff and deep percolation have been accounted for. The effective rainfall is the rainfall ultimately used to determine the crop irrigation requirements. To know the irrigation requirement, amount of effective rainfall data is needed.

5. Crop Evapotranspiration (ET_c)

The crop water need or actual crop evapotranspiration is defined as the depth or amount of water needed to meet the water losses through evapotranspiration which is calculated by multiplying ET_o by K_c as follow;

$$ET_c = K_c \times ET_o \quad (2)$$

Where,
ET_c = crop evapotranspiration under standard conditions
K_c = crop coefficient
ET_o = reference crop evapotranspiration

IV. RESULTS AND DISCUSSION

1. Reference Crop Evapotranspiration of the study Area

The results obtained when a ten years period was used with the FAO – Penman Monteith method to determine the reference crop evapotranspiration (ET_o).The table shows that ET_o varied from a minimum value of (2.98 mm/day) in January to the maximum value of (6.17 mm/day) in April. From the results, it can be seen that ET_o is the lowest during the peak of the rainy season and changes to the highest during the peak of dry season.

Table 1 Average reference crop evapotranspiration from the year 2009 to 2018

Month	Min Temp (°C)	Max Temp (°C)	Humidity (%)	Wind Speed (km/ day)	Sunshine (Hrs)	Radiation (MJ/m^2/day)	ET_o (mm/day)
Jan	15.1	30	74	94	7.4	15.6	2.98
Feb	17	34	59	109	7.9	18.1	4.03
Mar	21.5	36.9	57	163	7.7	19.8	5.37
Apr	25.3	38.4	63	195	7.9	21.4	6.17
May	25.8	35.7	71	207	7.2	20.7	5.66
June	24.9	33.2	81	248	5.7	18.5	4.65
July	24.7	32.8	81	249	4.4	16.4	4.26
Aug	24.5	32.3	84	187	4.8	16.8	3.97
Sept	24.5	33	83	142	5.9	17.5	4.04
Oct	23.4	32.2	83	96	5.9	15.8	3.5
Nov	20.3	31.9	77	115	7.0	15.5	3.41
Dec	16.5	29.5	76	128	6.9	14.4	3.0
Avg	22	33.3	74	161	6.6	17.5	4.25

2. Calculation Results of Effective Rainfall

The table 2 shows that the estimated rainfall and effective rainfall of the selected area for a ten year period. The maximum effective rainfall is 149.8 mm in September.

Table 2 Total effective rainfall data from the year 2009 to 2018

Month	Rainfall	Effective Rainfall
	mm	mm
January	8.8	7.0
February	0.9	0.7
March	5.3	4.2
April	33.9	27.1
May	116.4	93.1
June	125.9	100.7
July	84.4	67.5
August	140.2	112.2

Table 2 Continued

Month	Rainfall	Effective Rainfall
	mm	mm
September	187.2	149.8
October	173.7	139.0
November	22.3	17.8
December	10	8.0
Total	909	727.2

3. Crops and Cropping Patterns

In this study area, the crop and cropping patterns being cultivated in Pyawbwe and Meiktila Townships are collected from Ministry of Agriculture and Irrigation. The cultivated crops are monsoon paddy, summer paddy, sesame, chick pea, groundnut, green gram, onion, sunflower and cotton. Cropping patterns concerns with growing season describing planting date and harvesting date. Planting date is normally determined from climatic conditions and local agricultural practices. Planting date and crop cycle are required for harvesting date. The selected crop patterns from the study area are described in table 3.

Table 3 Existing crop pattern

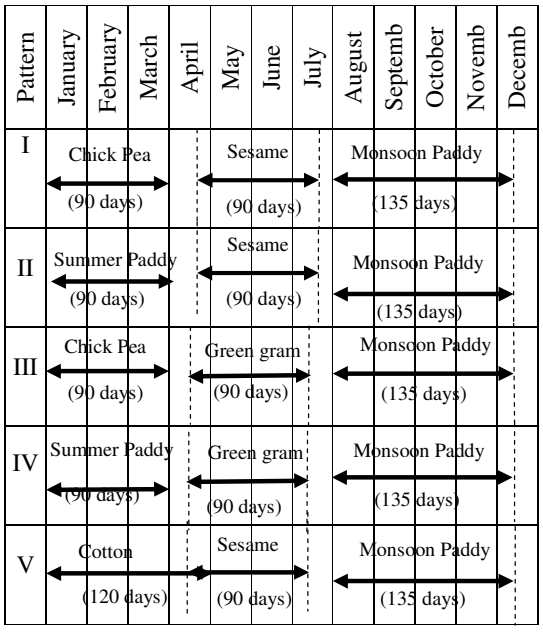

4. Calculation of evapotranspiration and irrigation requirement

In table 4, it will be seen that the minimum value of crop evapotranspiration (ET_c) for summer paddy is 14.4 mm/decade in January and the value of maximum is 56.7 mm/decade in second decade

Table 4 Evapotranspiration and irrigation requirement for summer paddy

Month	Decade	Stage	K_c (coefficient)	ET_c (mm/day)	ET_c (mm/dec)	Effective rain fall (mm/dec)	Irrigation Requirement (mm/ dec)
Jan	1	Init	0.50	1.46	14.6	2.6	12.0
Jan	2	Init	0.50	1.44	14.4	2.5	11.8
Jan	3	Deve	0.61	1.99	21.9	1.8	20.2
Feb	1	Deve	0.81	2.97	29.7	0.5	29.1
Feb	2	Deve	0.99	3.99	39.9	0.0	39.9
Feb	3	Mid	1.06	4.73	37.8	0.3	37.5
Mar	1	Mid	1.06	5.20	52.0	0.4	51.6
Mar	2	Mid	1.06	5.67	56.7	0.5	56.2
Mar	3	Late	0.88	4.97	54.7	3.4	51.3
					321.7	12.1	309.6

Table 5 Evapotranspiration and irrigation requirement for monsoon paddy

Month	Decade	Stage	K_c (coefficient)	ET_c (mm/day)	ET_c (mm/dec)	Effective rain fall (mm/dec)	Irrigation Requirement (mm/ dec)
Aug	1	Init	1.10	4.47	44.7	32.6	12.1
Aug	2	Init	1.10	4.37	43.7	37.7	6.0
Aug	3	Deve	1.10	4.39	48.3	41.8	6.6
Sep	1	Deve	1.11	4.46	44.6	47.2	0.0
Sep	2	Deve	1.12	4.54	45.4	52.2	0.0
Sep	3	Mid	1.14	4.39	43.9	50.2	0.0
Oct	1	Mid	1.14	4.20	42.0	51.0	0.0
Oct	2	Mid	1.14	4.00	40.0	51.5	0.0
Oct	3	Mid	1.14	3.96	43.6	36.3	7.3
Nov	1	Mid	1.14	3.93	39.3	15.9	23.4
Nov	2	Late	1.13	3.85	38.5	0.7	37.8
Nov	3	Late	1.09	3.57	35.7	1.4	34.4
Dec	1	Late	1.05	3.30	33.0	3.5	29.5
Dec	2	Late	1.03	3.08	9.2	0.7	8.1
					552.0	422.7	165

of March. Also, the highest requirement of irrigation is 56.2 mm/ decade and the lowest is 11.8 mm/decade just before the harvesting.

There is no irrigation requirement for monsoon paddy in August and September and the most irrigation requirement is 37.8 mm/decade at the second decade of November as shown in table 5. The table shows that the crop evapotranspiration changes from the maximum value of 48.3 mm/decade at the initial stage to the minimum value of 9.2 mm/decade.

For green gram, there is no irrigation requirement at the second stage of July shown in table 6. The maximum irrigation requirement is 21.9 mm/decade. The crop evapotranspiration varies from 55.6 mm/decade at the beginning of middle stage to 6.5 mm/decade at the end of late stage.

Table 6 Evapotranspiration and irrigation requirement for green gram

Month	Decade	Stage	K_c (coefficient)	ET_c (mm/day)	ET_c (mm/dec)	Effective rain fall (mm/dec)	Irrigation Requirement (mm/ dec)
Apr	2	Init	0.40	2.51	15.0	4.2	11.5
Apr	3	Init	0.40	2.42	24.2	15.0	9.2
May	1	Deve	0.45	2.64	26.4	25.5	0.9
May	2	Deve	0.69	3.91	39.1	33.8	5.3
May	3	Mid	0.95	5.05	55.6	33.7	21.9
June	1	Mid	1.03	5.15	51.5	34.0	17.5
June	2	Mid	1.03	4.80	48.0	35.5	12.6
June	3	Late	0.96	4.32	43.2	31.2	12.0
July	1	Late	0.69	3.02	30.2	23.8	6.5
July	2	Late	0.51	2.17	6.5	5.7	0.0
					339.8	242.4	97.3

For sesame, there is no irrigation requirements at the first stage of May and second stage of July shown in table 7. The maximum irrigation requirement is 19.3 mm/decade. The crop evapotranspiration varies from 2.2 mm/decade at the initial stage to 53.3 mm/decade at the mid season stage.

Table 7 Evapotranspiration and irrigation requirement for sesame

Month	Decade	Stage	K_c (coefficient)	ET_c (mm/day)	ET_c (mm/dec)	Effective rain fall (mm/dec)	Irrigation Requirement (mm/ dec)
Apr	2	Init	0.35	2.19	2.2	0.7	2.2
Apr	3	Init	0.35	2.12	21.2	15.0	6.2
May	1	Deve	0.40	2.34	23.4	25.5	0.0
May	2	Deve	0.63	3.55	35.5	33.8	1.8
May	3	Deve	0.88	4.70	51.7	33.7	18.0
June	1	Mid	1.07	5.33	53.3	34.0	19.3
June	2	Mid	1.08	5.01	50.1	35.5	14.6
June	3	Mid	1.08	4.87	48.7	31.2	17.5
July	1	Late	0.92	4.05	40.5	23.8	16.7
July	2	Late	0.44	1.89	15.1	15.1	0.0
					341.7	248.3	96.3

Table 8 Evapotranspiration and irrigation requirement for chick pea

Month	Decade	Stage	K_c (coefficient)	ET_c (mm/day)	ET_c (mm/dec)	Effective rain fall (mm/dec)	Irrigation Requirement (mm/ dec)
Jan	1	Init	0.40	1.17	11.7	2.6	9.1
Jan	2	Init	0.40	1.15	11.5	2.5	9.0
Jan	3	Deve	0.52	1.70	18.7	1.8	16.9
Feb	1	Deve	0.73	2.70	27.0	0.5	26.4
Feb	2	Mid	0.93	3.76	37.6	0.0	37.6
Feb	3	Mid	1.01	4.50	36.0	0.3	35.7
Mar	1	Mid	1.01	4.95	49.5	0.4	49.0
Mar	2	Mid	1.01	5.40	54.0	0.5	53.4
Mar	3	Late	0.68	3.82	42.0	3.4	38.6
					287.8	12.1	275.7

For Chick pea, crop evapotranspiration (ET_c) and crop water requirements are varied from 11.5 mm/decade to 54 mm/decade and 9.0 mm/decade to 53.4 mm/decade respectively in table 8.

Table 9 Evapotranspiration and irrigation requirement for cotton

Month	Decade	Stage	K_c (coefficient)	ET_c (mm/day)	ET_c (mm/dec)	Effective rain fall (mm/dec)	Irrigation Requirement (mm/ dec)
Jan	1	Init	0.35	1.02	10.2	2.6	7.6
Jan	2	Init	0.35	1.01	10.1	2.5	7.5
Jan	3	Deve	0.51	1.67	18.3	1.8	16.6
Feb	1	Deve	0.79	2.92	29.2	0.5	28.7
Feb	2	Mid	1.06	4.27	42.7	0.0	42.7
Feb	3	Mid	1.16	5.18	41.4	0.3	41.1
Mar	1	Mid	1.16	5.70	57.0	0.4	56.5
Mar	2	Mid	1.16	6.21	62.1	0.5	61.6
Mar	3	Late	1.14	6.42	70.6	3.4	67.3
Apr	1	Late	1.02	6.09	60.9	5.2	55.7
Apr	2	Late	0.89	5.58	55.8	7.0	48.7
Apr	3	Late	0.76	4.61	46.1	15.0	31.0
					504.5	39.3	465.1

For cotton, the most irrigation requirement is 67.3 mm/decade at the third decade of March as shown in table 9.The table show that the crop evapotranspiration changes from the maximum value of 70.6 mm/decade at the late season stage to the minimum value of 10.1 mm/decade.

V. CONCLUSION

The study mainly estimates the CWR and IWR for some selected crops as well as developing cropping pattern for the study area. The result shows that reference and crop evapotranspiration (ET_o and ET_c) were higher for crops with longer growing season than for those with shorter ones. Also ET_o and ET_c were more during the dry season than the rainy season. The maximum water requirement of crop is monsoon paddy and the minimum water requirement of crop is chick pea.

ACKNOWLEDGMENT

The author is deeply grateful to Dr. Nyan Phone, Professor and Head, Department of Civil Engineering, Technological University (Thanlyin), for his guidance. The author is sincerely thank to Dr. Kyaw lin Htat, Professor, Department of Civil Engineering , Technological University (Thanlyin), for his skillful guidance, helpful suggestions and editing of this paper. The author is profoundly grateful to Daw Ohnmar Tun Wai, Lecturer, Department of Civil Engineering , Technological University (Thanlyin), for her encouragement, helpful suggestion, true-line guidance and comment for preparing paper. The author would like to express her special thank to her co-supervisor Daw Shwe War, Assistant Lecturer, Department of Civil Engineering , Technological University (Thanlyin), for her support and invaluable comments.

REFERENCES

[1] FAO.1977.Crop Water Requirements: FAO Irrigation and Drainage Paper 24. Food and Agricultural Organization of the United Nation.

[2] FAO. 1998. Crop Evapotranspiration: Guidelines for Computing Crop Water Requirements, Irrigation and Drainage Paper 56. Food and Agricultural Organization of the United Nation.

[3] Smith, M,2006. Example of the Ues of CROPWAT 8.0. Food and Agricultural Organization of the United Nation.

COMPARATIVE STUDY ON SOFT STOREY EFFECT AT DIFFERENT LEVELS IN REINFORCED CONCRETE BUILDINGS

Aye Thet Mon[1], Kyaw Zeyar Win [2], Ni Ni Moe Kyaw[3], Ei Ei Kyaw[4]
s
Department of Civil Engineering
Technological University (Thanlyin), Yangon, Myanmar

[1]ayethetmon.tu@outlook.com
[2]kyawzeyarwin@ttu.edu.mm
[3]summerroseoneone@gmail.com[4]eekmtla@gmail.com

Abstract — According to social and functional needs, some high-rise buildings are constructed as soft storey because of the space occupancy considerations. The soft storey has one level that is considerably greater flexible than the storey above and below it. This type of building has no masonry wall in this level or it can also have a greater height than the rest of the other floors. In this study, the analysis of the superstructure for the selected model is carried out by using Extended Three-Dimensional Analysis of Building Systems software with static analysis. This study presents the comparison of structural behaviours of conventional and soft storey effect at different levels in multi-storey reinforced concrete buildings with six different cases. Firstly, the conventional model is analyzed by using software and storey stiffness, storey drift, P-Δ effect, overturning moment, storey shear and member forces are carried out from these results. Secondly, the structural analysis is made by change of storey height and without change of structural element size, seismic zone, exposure type and soil type. Finally, the analysis results of structural performance and member forces are compared. The results of present study indicate that if the soft storey condition is occurred in the ground floor, the storey stiffness, the storey drift, P-Δ effect, column moment and column torsion are more significant than the other structures and the structure is more economical and safe when soft storey is provided at third floor level for proposed models.

Keywords*: *Multi-storey, overturning moment, P-Δ effect, soft storey, storey drift.

I. INTRODUCTION

Nowadays, multi-storey or high-rise buildings are becoming increasingly common due to the rapid growth of the population and the high cost of land. Among them, some buildings are constructed as soft storey and it usually exists at the ground floor level for the purpose of parking and garage. However, soft storey can form any level of a high-rise building to fulfill the demands such as a multi-purposed hall, a large meeting room or series of retails business. According to Theory, a soft storey has stiffness less than 70 percent of the storey immediately above, or less than 80 percent of the average stiffness of the three storeys above. If the stiffness of the storey meets at least one of above two criteria, the structure is considered to have a soft storey. These structures can get soft storey effect and the effect of the seismic loading becomes more severe for heights above this floor level. This situation causes the structural damage but soft storey cannot be avoided in some buildings due to requirements. Therefore, the soft storey effect at different levels in reinforced concrete buildings are should be studied to consider the most appropriate location for this storey level.

II. METHODOLOGY

In this paper, the twelve multi-storey building will be analyzed by using Extended Three-Dimensional Analysis of Building Systems (ETABS) Software. All reinforced concrete members are designed with ultimate strength design using building code of American Concrete Institute (ACI 318-99). Wind and earthquake loads are considered according to Uniform Building

Code (UBC-1997). Exposure type (B) and soil type (D) are considered with design wind velocity 100 mph. Structural system is considered by concrete intermediate moment-resisting frame with over-strength factor 5.5. According to CQHP guide lines, static design load combinations are used. The proposed model is statically analyzed and the results are carried out for the superstructure and then these are compared.

1. Types of structure

The twelve storey reinforced concrete models are considered as a conventional structure and soft storey structures due to change of wall height. Table 1 shows different cases of six models for this study.

Table 1 Different cases of six models

Model-1	Conventional
Model-2	Soft storey at ground floor
Model-3	Soft storey at first floor
Model-4	Soft storey at second floor
Model-5	Soft storey at third floor
Model-6	Soft storey at fourth floor

2. Data preparation

The following Tables describe the analysis data for one conventional and five soft storey reinforced concrete models. Table 2 shows material specifications, Table 3 shows structural configurations and Table 4 shows structural element sizes. In this study, Table 5 shows storey heights of different configuration and M-1 is referred to conventional model. M-2, M-3, M-4, M-5 and M-6 are referred to soft storey models with soft storey effect at ground, first, second, third and fourth floor level respectively.

Table 2 Material specifications

Concrete compressive strength (f_c')	4 ksi
Bending reinforcing yield stress (f_y)	50 ksi
Shear reinforcing yield stress (fys)	50 ksi
Modulus of elasticity	3605 ksi
Poisson's ratio	0.2

Table 3 Structural configurations

Number of stories	12
Width of structure	68′-0″
Length of structure	95′-0″
Total height of structure	148′-0″
Number of bay's along X	8
Number of bay's along Y	6

Table 4 Structural element sizes

Column sizes	22″x22″, 20″x20″, 18″x18″, 16″x16″
Beam sizes for proposed buildings	18″x20″, 16″x18″ , 14″x18″, 12″x18″, 12″x14″, 10″x12″

Table 5 Storey heights of different configuration

Storey	Height (ft)					
	Model M-1	Model M-2	Model M-3	Model M-4	Model M-5	Model M-6
RT-1	10	10	10	10	10	10
RT	10	10	10	10	10	10
11F	10	10	10	10	10	10
10F	10	10	10	10	10	10
9F	10	10	10	10	10	10
8F	11	10	10	10	10	10
7F	11	10	10	10	10	10
6F	11	10	10	10	10	10
5F	11	10	10	10	10	18
4F	11	10	10	10	18	10
3F	11	10	10	18	10	10
2F	11	10	18	10	10	10
1F	11	18	10	10	10	10
GF	10	10	10	10	10	10
Total height	148	148	148	148	148	148

3. Model description

Figures 1 and 2 show the architectural floor plans and Figures 3 to 8 show the elevation of proposed models respectively.

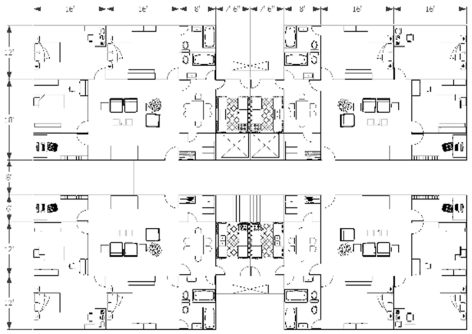

Figure 1 Typical floor plan for proposed model.

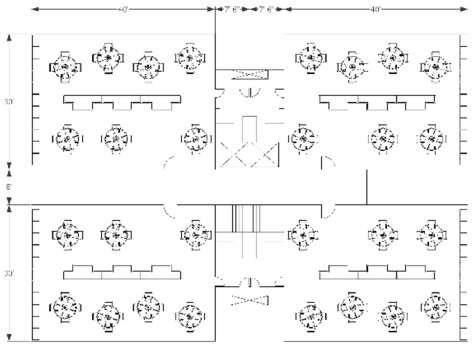

Figure 2 Soft storey floor plan for proposed model.

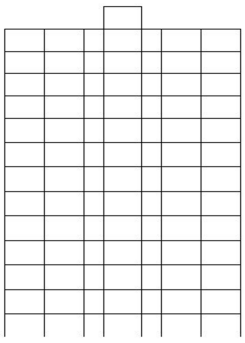

Figure 3 Elevation of (M-1).

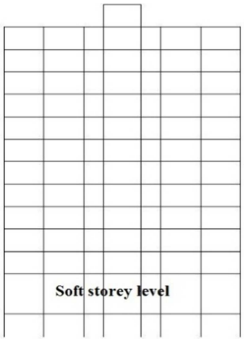

Figure 4 Elevation of (M-2).

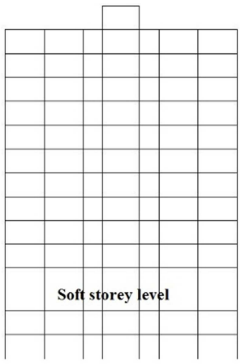

Figure 5 Elevation of (M-3).

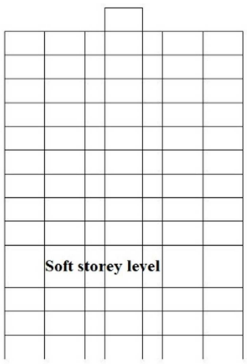

Figure 6 Elevation of (M-4).

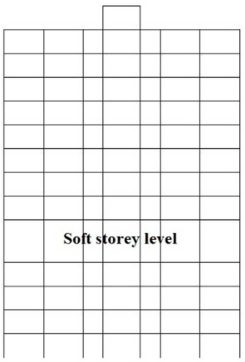

Figure 7 Elevation of (M-5).

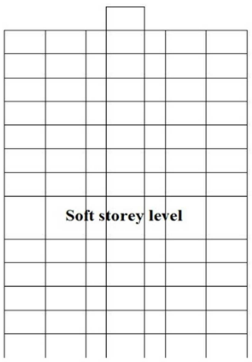

Figure 8 Elevation of (M-6).

4. Load combination

According to CQHP guide lines, the considerations of static design load combination are shown in Table 6.

Table 6. Load combination for proposed models

1	1.4DL + 1.4SDL
2	1.4DL + 1.4SDL + 1.7LL
3,4	1.05DL + 1.05SDL + 1.275 LL ± 1.275WX
5,6	1.05DL + 1.05SDL + 1.275 LL ± 1.275WY
7,8	0.9DL + 0.9SDL ± 1.3WX
9,10	0.9DL + 0.9SDL ± 1.3WY
11,12	1.05DL + 1.05SDL + 1.28LL ± EQX
13,14	1.05DL + 1.05SDL + 1.28LL ± EQY
15,16	0.9DL + 0.9SDL ± EQX
17,18	0.9DL + 0.9SDL ± EQY
19,20	1.27DL + 1.27SDL + 1.28LL ± EQX
21,22	1.27DL + 1.27SDL + 1.28LL ± EQY
23,24	0.68DL + 0.68SDL ± 1.02EQX
25,26	0.68DL + 0.68SDL ± EQY

III. RESULTS AND DISCUSSIONS

In this section, the results obtained from the analysis of one conventional and five soft storey reinforced concrete models using ETABS software have been tabulated and compared. The performance of structures on different criteria have

been analyzed and discussed as follow. In these figures, M-1 refers to normal building and M-2, M-3, M-4, M-5 and M-6 refer to soft storey buildings.

1. Comparison of Storey stiffness

The stiffness of a storey is generally defined as the ratio of storey shear to storey drift. Figures 9 and 10 show the comparison of storey stiffness in x direction and y direction.

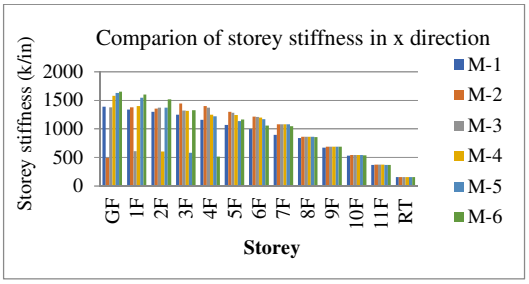

Figure 9 Comparison of storey stiffness in x direction.

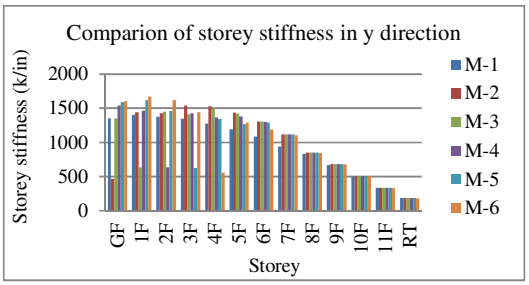

Figure 10 Comparison of storey stiffness in y direction.

In comparison of storey stiffness, it can be seen that the results for M-2, M-3, M-4, M-5 and M-6 suddenly decrease at soft storey levels. The stiffness of M-2 is about 35% and the results of other models (M-3, M-4 and M-5) are about 47% of M-1 at corresponding levels. In M-6, the stiffness is slightly decreased and its value is about 45% of M-1. Increasing the stiffness or rigidity of a structural element reduces its deflection under load. This can be done by strengthening its section or increasing its size and this will generally also increase its cost.

2. Comparison of Storey drift

Storey drift is the lateral displacement of one level relative to the level above or below. The Figures 11 and 12 show comparison of storey drift six proposed models in x direction and y direction respectively.

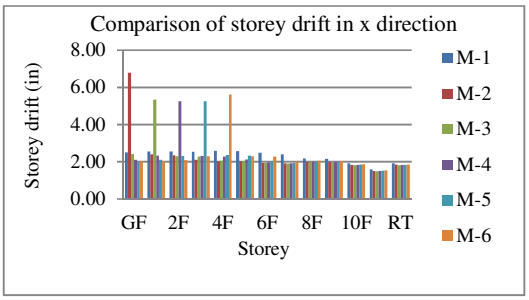

Figure 11 Comparison of storey drift in x direction.

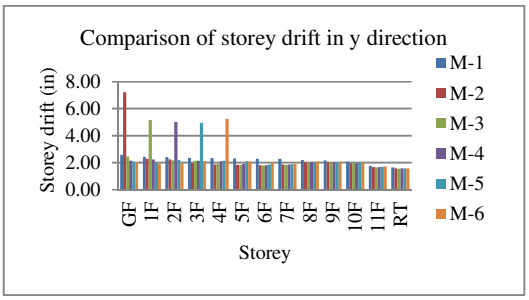

Figure 12 Comparison of storey drift in y direction.

The storey drifts for M-2, M-3, M-4, M-5 and M-6 obviously higher at each soft storey level than other levels. This means that the soft storey affects the storey drift at corresponding level. From this result, the storey drift of M-2 at soft storey level is about 2.75 times of M-1 and that of M-3, M-4, and M-5 are about 2% of M-1 in both directions. Then, this value of M-6 at soft storey level is slightly increase to 2.2% of M-1. The storey drifts in both direction at each soft storey level are more than drift limit so that the storey drift is significant in soft storey buildings.

3. Comparison of P-Δ effect

The P-Δ effect is the secondary effect on shears, axial forces and moment of frame members induced by the gravity load action on the laterally displaced structure frame. Figures 13 and 14 show the comparison of P-Δ effect in x direction and y direction respectively.

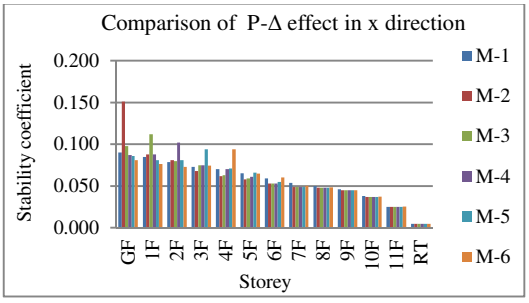

Figure 13 Comparison of P-Δ effect in x direction.

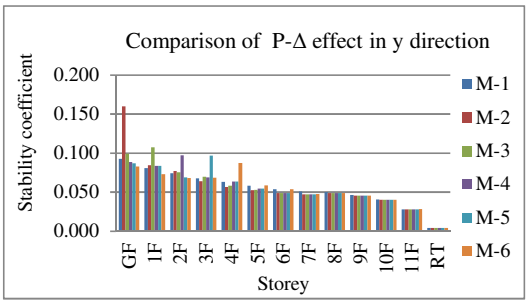

Figure 14 Comparison of P-Δ effect in y direction.

In comparison, the stability coefficient of P-Δ effect at soft storey level in each model is significantly higher than other levels. It can be seen that the stability coefficient of M-2 and M-3 in both directions and that of M-4 in x direction are more than allowable limit. However, the coefficient of M-4 in y direction and that of M-1, M-5 and M-6 in both directions are lower than allowable limit. The P-Δ effect results in additional forces and moment increases storey displacement and overturning moment and this effect influence at lower levels.

4. Comparison of Overturning moment

The summation of moments due to the the distributed lateral forces is the overturning moment and these values are shown in Figures 15 and 16.

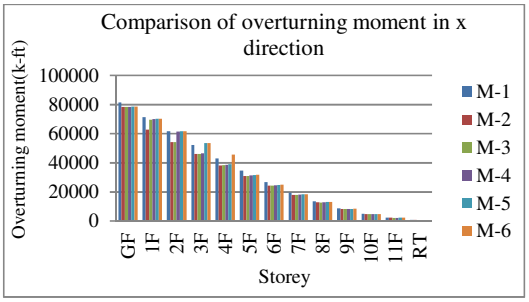

Figure 15 Comparison of overturning moment in x direction.

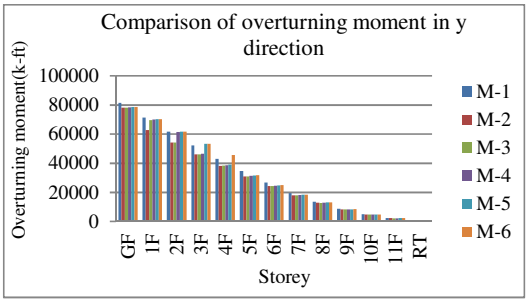

Figure 16 Comparison of overturning moment in y direction.

In this comparison, overturning moment of proposed models in x direction and y direction are nearly similar and it is decreasing from bottom to top. The overturning moment will increase the compressive stress in outer columns on the opposite side of the buildings. The safety factors of overturning moment for all models are greater than 1.5. Therefore, the overturning moment is no effect on soft storey for these proposed models.

5. Comparison of Storey shear

Storey shear is the summation of design lateral forces above the storey under consideration and the comparison of this value in x direction and y direction are shown in Figures 17 and 18.

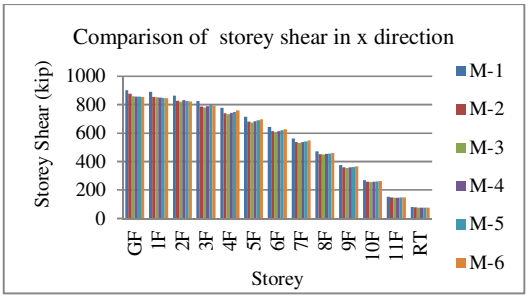

Figure 17 Comparison of storey shear in x direction.

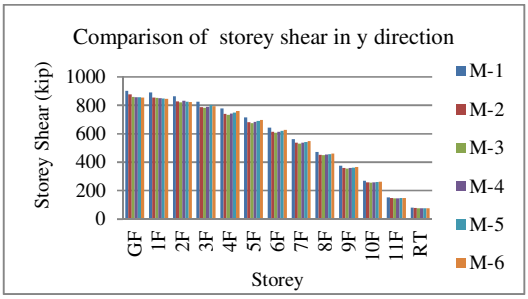

Figure 18 Comparison of storey shear in y direction.

From these comparisons, it can be seen that the storey shear is larger in bottom and then declines gradually to top. The results of proposed models are nearly equal in x direction and y direction and this value of M-1 is slightly larger at each level of other models. The results of all models other than M-1 at corresponding levels are nearly similar in both directions.

6. Structural member forces in Columns

Structural member forces in columns such as moment and torsion are shown in Figures 19 and 20 respectively.

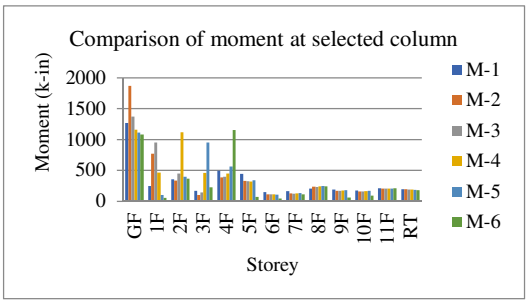

Figure 19 Comparison of moment at selected column.

In comparison, it can be seen that the column moment at soft storey level for each model is obviously higher than others. The maximum value is occurred at soft storey level of M-2 and the minimum value is in that of M-3 and M-5 at each soft storey level. These values of M-4 and M-6 are nearly similar.

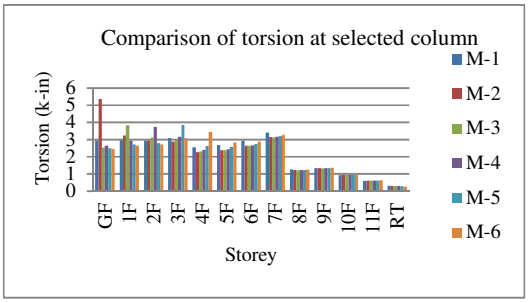

Figure 20 Comparison of torsion at selected column.

In comparison, the higher torsion is occurred at soft storey level of each model in which the maximum value occurs in M-2. The torsions of M-3, M-4 and M-5 at soft storey levels are nearly similar and this value of M-6 is minimum.

7. Structural member forces in Beams

Structural member forces in beams such as moment and torsion are shown in Figures 21 and 22 respectively.

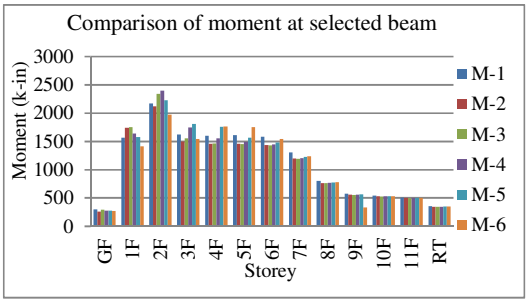

Figure 21 Comparison of moment at selected beam.

In comparison of moment in beams, it can be seen that the minimum value is occurred at ground floor of all models and this value is suddenly increased from ground floor to first floor. The moment at first floor, second floor, third floor and fourth floor of M-3, M-4, M-5 and M-6 are increased about 10% of M-1 due to soft storey effect. The maximum moment is occurred at the second floor of all models and the largest value is occurred at that floor of M-4.

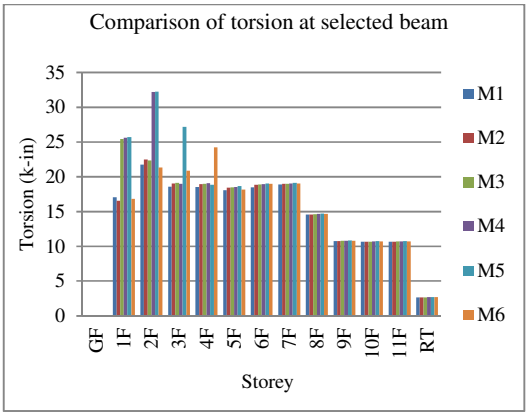

Figure 22 Comparison of torsion at selected beam.

From comparison of torsion in beams at soft storey level, the minimum value is occurred at ground floor of all models and this value is suddenly increased from ground floor to first floor. The torsion at first floor, second floor, third floor and fourth floor of M-3, M-4, M-5 and M-6 are increased about 50% of M-1 due to soft storey effect. The maximum torsion is occurred at the second floor of M-4 and M-5, and these values are nearly similar.

IV. CONCLUSIONS

If the soft storey condition is occurred in the ground floor, the storey stiffness, the storey drift, P-Δ effect, column moment and column torsion would be more significant than the other structures. The maximum moment of the beam is occurred at the second floor of M-4 and the maximum torsion is occurred at the second floor of M-4 and M-5. The structural member forces on columns are more significant than on beams. The present study indicates that soft storey located at ground, first and second floor cause higher forces in the structure. Therefore, the soft storey should be avoided at that level and the structure is more economical and safe when soft storey is provided at third floor level for proposed models.

ACKNOWLEDGMENT(S)

The author wishes to express grateful thanks to Dr. Theingi, Rector of Technological University (Thanlyin). The author wishes to express the deepest thanks and gratitude to her supervisor Dr. Kyaw Zeyar Win, Professor of Civil Engineering Department of Technological University (Thanlyin). The author special thanks go to her co-supervisor Dr. Ni Ni Moe Kyaw, Lecturer of Civil Engineering Department of Technological University (Thanlyin), for her invaluable advice and effective suggestion throughout the study. The author would like to express her thanks to her teacher Daw Ei Ei Kyaw, Assistant Lecturer of Civil Engineering Department of Technological University (Thanlyin), for her valuable comments and indispensable guidance during this study. Finally, her special thanks to all who helped her towards the successful completion of this study.

REFERENCES

[1] IS 1893 2002, "Indian Standard Criteria for Earthquake Resistance Design of Structures Part I General Provisions and Buildings" Bureau of Indian Standard, New Delhi, 2002.

[2] American Concrete Institute Committee, "Building Code Requirements for Structural Concrete, ACI-99," 1999.

[3] International Conference of Building Officials, Uniform Building Code, Vol II", Structural Engineering Design Provision, UBC-97, 1997

[4] Dogan, Mizan, Kirac, Nevzat and Gonen, "Soft Storey Behaviour in Earthquake and Samples," August, 2012.

[5] Murty, C.V.R. "Why are Open Ground Storey Buildings Vulnerable in Earthquakes," August 2012.

[6] Committee for Quality Control of High-Rise Building Construction Projects, 2017.

Design of Water Distribution System Using Hydraulic Analysis Program (EPANET 2.0) for Tatkon Town in Myanmar

Aung Myo Wai [1], Haicheng Liu [2]

[1] Engineering Department (Water and Sanitation)
Naypyidaw Development Committee, Naypyidaw - 15011, Myanmar

[2] School of Environmental Science and Engineering
Suzhou University of Science and Technology, Suzhou - 215000, People's Republic of China

[1] amyowai.dec@gmail.com, [2] 183973079@qq.com

Abstract - **Water is one of the plentiful things in the world. If the water cannot be available, the living things cannot grow and live. It is a basic requirement and it influences social, economic and living standard of human beings. Nowadays Sustainable development is a major interest. High-quality infrastructure of water system takes part in a key role for any kind growth of a city. Here in this paper, medium town in Naypyidaw of Myanmar, Tatkon has been emphasized for design purpose. Although new towns in Naypyidaw have proper water supply system for inhabitants, there is no strategic plan yet to develop the water supply system for that town. Supply water distribution network of Tatkon town area was selected for detail analysis and design. The area has been modeled using EPANET software on the basis of data surveyed by Tatkon TDC. Assessment of required pressure head, velocity coverage, water age and residual chlorine (chemical) concentration has been done. In addition, the design is made keeping in view of the population growth rate, and the developing town up to 2048. Finally, this paper offers a modeling strategy of Tatkon town which intends at proposing solutions to the challenges of lacking proper water supply system and reducing menace associated with waterborne disease.**

Keywords: EPANET software, network analysis, pressure head, residual chlorine (chemical) concentration, velocity, water distribution system.

1. INTRODUCTION

Water and related services must be as part of the economic development business. Many of the major problems that humanity is facing in the twenty-first century are related to water quantity and/or water quality issues, and which currently affects more than a third of the people in the world (Schwarzenbach et al., 2010). In developing countries, where most of the sewage is discharged without treatment, the improvement of sanitation and access to safe drinking water are primarily important. In the report of Myanmar demographic and health survey (2015-2016), 80% of all households have access to an improved drinking water source, as do 89% of urban households and 77% of rural households. However, distribution of households by the source of drinking water is only 6% of Myanmar's population as safe and piped water into their residence (MOHS, 2017).

Water distribution networks play an important role in modern societies being its proper operation directly related to the resident. Naypyidaw, capital city of Myanmar, is very imperative in modern society to insure the availability of potable water and to plan and design for a sustainable economic suitable pipe network system or water supply schemes. Tatkon town is an inaccessible water supply area of Naypyidaw and people use only tube well or insufficient water supply system. With the aim of understanding the nature of progress, looking carefully is important of the way that improvements in water and sanitation have benefited different socioeconomic groups.

At the present time, marketable computer software applications are accessible to characterize configuration of distribution system and pipe network where detailed information with the pipe properties like “Diameter, Length, Pipe material etc.” and devices like “Pumps, Valves etc.” are provided.

The analysis of design is done by using the software EPANET. It is such a computer based program that performs extended period simulation of hydraulic and water quality behavior within pressurized pipe networks. The overall objective of this project is to construct a distribution system model using EPANET and assesses system criteria and limitations. The main objective of water distribution system is to supply water at acceptable pressure and velocity to meet the requirement. In support of suitable assessment of a distribution system computation of flow, velocity and pressure is essential. These parameters can be calculated competently with the aid of EPANET. Despite the fact that EPANET has some limitations, such as it does not account phenomena such as water hammer, pipe bursting, behavior of non-return valves and starting a pump or stopping it.

The primary goal of the distribution systems is to maintain adequate water pressure at various points i.e., at the consumer's tap and the selection of the distribution and its elevation regarding the location of the water treatment plants.

2. STUDY AREA

Tatkon is located on the central basin of Myanmar. It is about 60 km far from Naypyidaw (capital city of Myanmar) and 422 km from Yangon. It is located between 19°- 55′ and 20°-21′ of North latitude and 95°-20′ and 96°-30′ of East longitude and at the altitude of 2250′ above sea level. Location map of Tatkon is shown in figure 1.2. Located to the South of the town is Pobbathiri (Naypyidaw), to the North is Yamethin (Mandalay Region), to the West is Myothit (Magway Region) and to the East is Pinlaung (Shan State). It includes 5 Numbers of District Meter Area (DMA) which is mainly central part of Tatkon starting from Moekaung pagoda and ending to township football field.

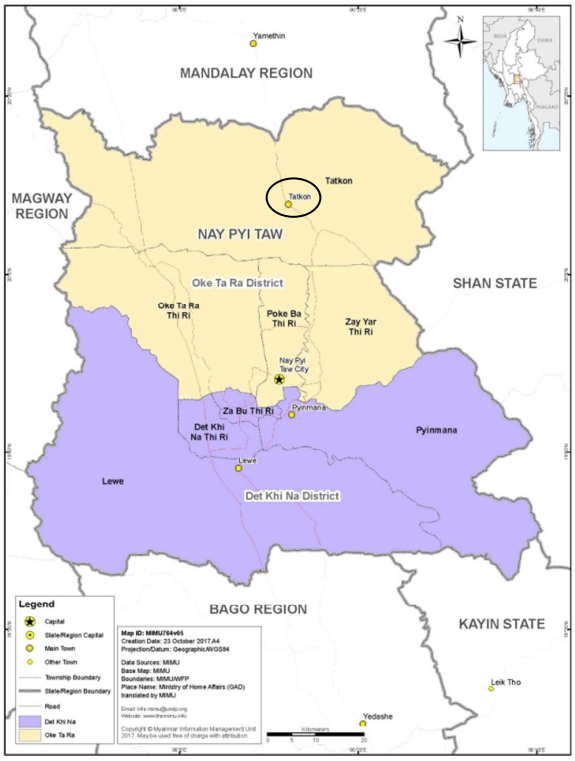

Fig.1 Location Map of Tatkon in Naypyidaw

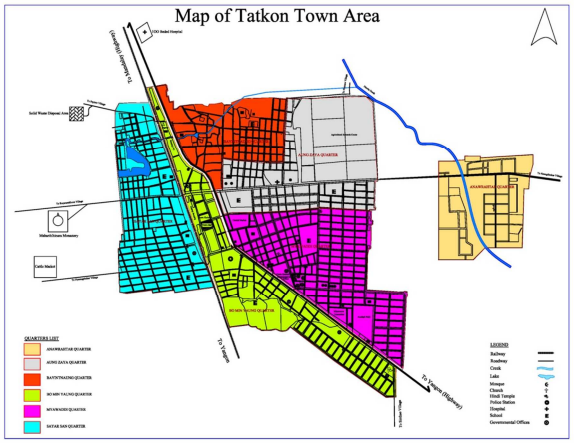

Fig.2 Map of Study Area

2.1 Data collection

The data was provided by Tatkon Township Development Committee (TDC). Data of individual ID and Labels of Pipes along with specified length, diameter& material was obtained. Data of individual Nodes with specified elevation and demand was also provided.

3. METHODOLOGY

3.1 Population and water demand forecast for Tatkon town

Tatkon is divided into six quarters. The total population of Tatkon changes during each past decade according to the births, deaths, migration in and out. In this study, the calculation of population estimation is computed by arithmetical increase method. Data is got population per decade and design population is calculated by the following equation.

$$P_n = P_0 + n\,I \quad (1)$$

where, P_n = future population at the end of n decades

P_0 = present population

I = average increment for a decade

n= No. of decades between now and future

So, P_3= 41737 + (3 x 5726.5) = 58916.5 (Say = 59000)

The estimated population in Tatkon town for the next three decades computed by Arithmetical Increase Method along with water demand is plotted in Figure-3. The population was forecasted up to the year of 2048. For the same the water demand has been calculated as well. The population forecasting is carried out from the projection of the year of 1978, 1988, 1998, 2008 and 2018 from the Department of Population, Government of Myanmar. From the results, Arithmetical Increase Method gave good idea about the growth of population. The results for the future decade population are 2018 (41737), 2028 (47464), 2038 (53190) and 2048 (59000).

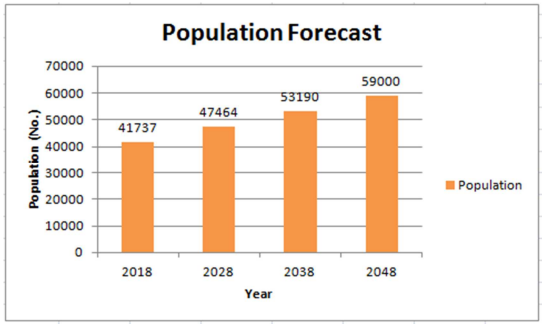

*Per capita water demand = 135 lpcd

Fig.3(a) Chart of population forecast

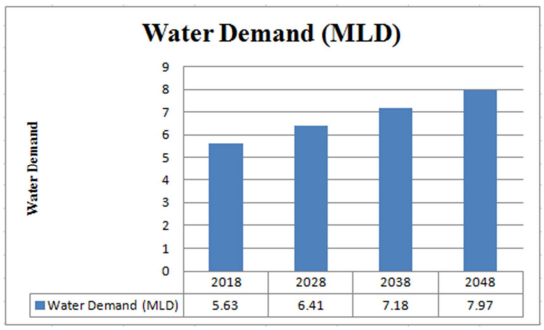

Fig.3(b) Chart of water demand

3.2 Water distribution system

There are four principal methods of lay-out distribution system:

1. Dead-end system or Tree system,
2. Grid-iron system or Reticular system,
3. Circular system or Ring system and Radial system.

The roads of Tatkon town are designed and developed in a Grid Iron pattern so that Grid-iron system is appropriate and the pipelines in such places can simply track along the road.

3.3 EPANET

EPANET is developed by the US Environmental Protection Agency. It is a computer program that performs extended period simulation of hydraulic and water quality behavior within pressurized pipe networks. A network consists of pipes, nodes (pipe junctions), pumps, valves and storage tanks or reservoirs. EPANET tracks the flow of water in each pipe, the pressure at each node, the height of water in each tank, etc. Sinthe dam is selected as a water source for water supply in Tatkon town which has been situated at a distance of 12.93 km. The most common pipe flow formula used in the design and evaluation of a water distribution system is the Hazen-Williams shown in Equation 1 and 2:

$$V=0.849CR^{0.63}S^{0.54} \quad (2)$$

In which V= average velocity of flow in m/s, C_{HW} = Hazen-Williams coefficient, R=hydraulic radius (=A/P) in m, S = Slope of the energy line (=h_f/L).

$$Q = 0.278\ Cd^{0.63}S^{0.54} \quad (3)$$

In which C_{HW} = Hazen-Williams coefficient and D is diameter in metres and Q is in m^3/s, S = Slope of the energy line ($=h_f/L$).

Pipe network and nodes are created on the AutoCAD file and water demands at each junction were provided as the demand homogeneously using EPANET. The elevation of the nodes and length of each pipes are confirmed from the Google Earth Image as seen in Figure-4. In which all the nodes are provided at each junction of roads and pipes have been provided connecting to nodes. The expected material selected for the pipe distribution analysis was HDPE (High Density Polyethylene) with the roughness coefficient for Hazen-Williams is 140. These pipes are sufficiently resistant to corrosion and may be last as long as 50-100 years.

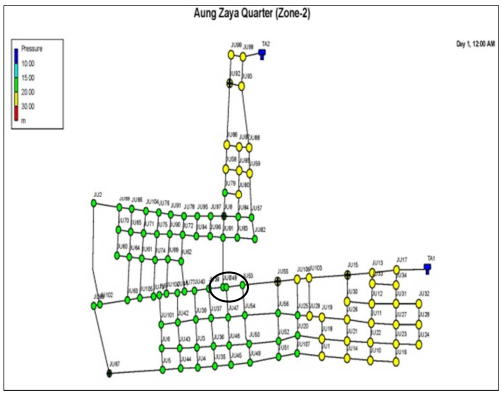

Fig.4(a) EPANET image showing Node

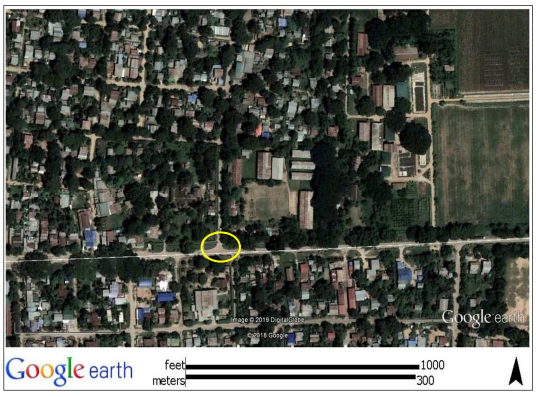

Fig.4(b) Google Earth Image showing Node

Here one of the examples is given in Figure-4 showing the identification of node JU38 and its elevation taken from Google Earth Image. Then the length of the pipe was recorded. The same procedure has been taken to each pipe and node.

3.4 Brief description of the model

In relation to the road pattern, the area is divided in five quarters like as five District Metered Area (DMA) and one quarter is for future plan. The whole distribution network is made by 706 Nodes, 1172 Pipes and 13 Tanks. Distribution system of the study area contains HDPE pipes having different diameters (i.e. 100mm to 500mm). As a result design life of the model has been considered up to year 2048.

3.5 Procedure of method

The procedure of method is as per following steps:

- Design population of the Tatkon town is computed with the estimated design period.
- The system of distribution and methods of supply are considered.
- Measurement of distances and elevations of proposed pipe networks with measuring device and satellite images is done.
- The background of design outline was prepared in AutoCAD relating to the road condition.
- The raw file of AutoCAD was transformed to EPANET file with the aid of EpaCAD software.
- 706 Nodes, 1172 Pipes, 13 Tanks were allocated by data obtained.
- After assembling and loading the model, EPA's Network Modeling is implemented to determine the nodal pressure and flow in the pipe with given design parameters and nodal demand with the assumption.
- After the necessary calibration the final results are generated.

3.6 Design assumptions

Design assumptions are as per following points:

- Hazen Williams Roughness Coefficient "C" value has been used as 140 for HDPE pipe materials.
- Pressure is prioritized over the rest of the design criteria.
- For the Loss Coefficient, a value of 1.2 has been used for standard tee flow through pipes. Bulk Coefficient and Demand pattern are considered.

- Demand has been opted to assign homogenously as assignment by grids.

4. ANALYSIS AND RESULTS

The intention of the system of pipes is to supply continuous water at adequate pressure and flow. On the other hand, pressure is lost by the action of friction at the pipe wall and it also depends on the water demand, pipe length, hydraulic gradient and diameter.

With the data like elevation, length, demand, diameter, after selecting the layout of water distribution system for Tatkon town, the results had been achieved for velocity, head loss, pressure from EPANET which meet the requirement for the optimal water supply system. Aung Zaya quarter (DMA-2), one of the analysis parts of Tatkon town, is described here. The analysis of DMA-2 is given below in Figure-5.

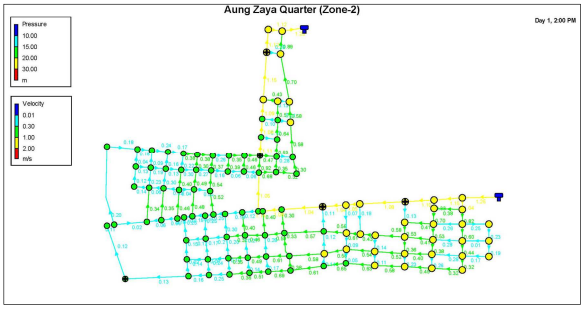

Fig.5(a) Pressure and Velocity distribution network diagram of DMA-2

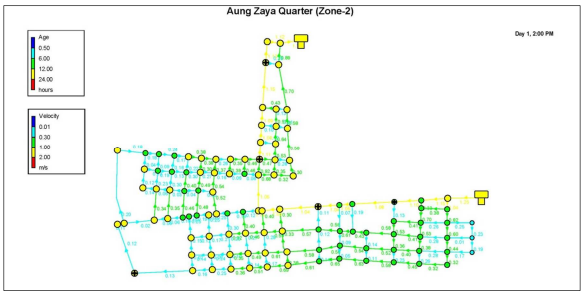

Fig.5(b) Water age and Velocity distribution network diagram of DMA-2

With the connection of Elevation and Pressure, the graph in Figure-6 gives good indication of the type of land and pressure into the pipes. Here for one of the Node Id JU57, the elevation was 151.8 m which is less in a particular road and the outcome result from the EPANET for the pressure was 19.51 m (1.95 bars). In general the analysis results show that if the elevation is less, then the pressure is higher for those particular nodes. On the other point of view, it could be clearly recognized that unit headloss depends primarily on the flow rate and its velocity if the pipe diameter is small for more flow, the head loss would be higher through high pressure. Accepted values are 5 m/km and occasionally 10 m/km. It can be reduced by increasing pipe diameter. Then finding is come out that the flow in the pipe, diameter, velocity, pressure and headloss are correlated to each other.

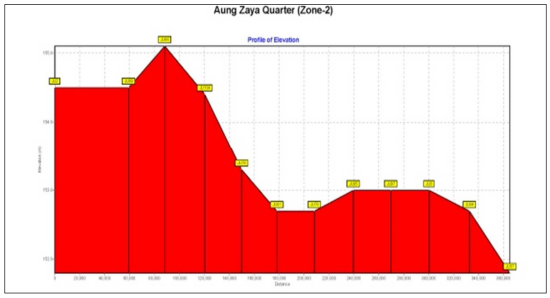

Fig.6 (a) Elevation profile graph

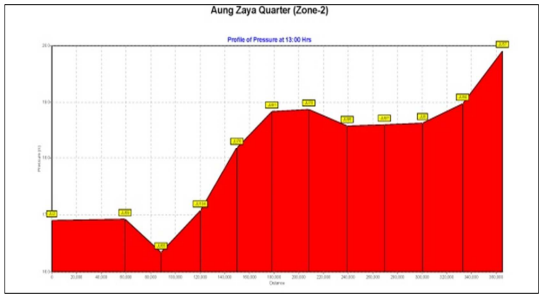

Fig.6 (b) Pressure profile graph for a particular road

The Figure-7 shows the representation of water age (hrs) and residual chlorine (chemical) concentration (mg/L) in each node of DMA-2. From the analysis result, it can be clearly identified that it is in the furthest and most isolated areas of a network where quality problems are greatest, mainly because:

- The journey time is longer. Chlorine concentration decreases through internal reactions with time, increasing the possibility of contamination. Recirculation or dilution is not possible as the water only travels one way.

Some of link results and node results of DMA-2 are as shown in Table-1 and Table-2.

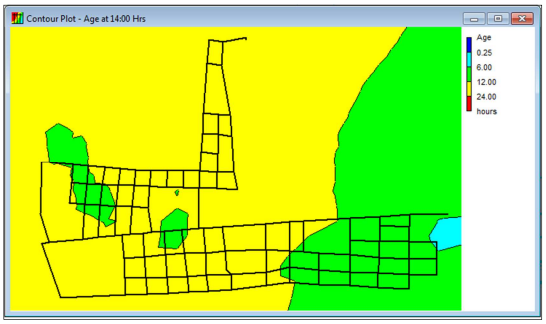

Fig.7 (a) Water age contour graph

Table-1: Link Results

Zone-2 Network Table – Links at 10:00 Hrs

Link ID	Length (m)	Diameter (mm)	Flow (LPS)	Velocity (m/s)	Unit Headloss (m/km)
Pipe PI115	65.5	150	-1.73	0.10	0.10
Pipe PI117	58	150	-9.18	0.52	2.25
Pipe PI118	59.5	150	-2.31	0.13	0.17
Pipe PI119	102.5	150	-7.35	0.42	1.41
Pipe PI120	102.5	100	-1.84	0.23	0.75
Pipe PI121	102.5	100	-1.52	0.19	0.53
Pipe PI122	102.5	150	4.10	0.23	0.47
Pipe PI123	102.5	150	-9.12	0.52	2.10
Pipe PI124	65.5	150	2.32	0.13	0.17
Pipe PI125	83	150	6.85	0.39	1.25
Pipe PI126	83	150	4.99	0.28	0.69
Pipe PI127	83	150	-4.27	0.24	0.52
Pipe PI128	65.5	150	-1.32	0.07	0.06
Pipe PI129	65.5	150	2.99	0.17	0.27
Pipe PI130	59.5	150	6.64	0.38	1.23
Pipe PI131	56	100	1.14	0.15	0.32
Pipe PI132	83	150	-5.19	0.29	0.75
Pipe PI133	86.7	100	-0.82	0.10	0.17
Pipe PI134	110.6	100	2.65	0.34	1.48
Pipe PI135	69	100	1.73	0.22	0.68
Pipe PI136	94	150	8.06	0.46	1.68
Pipe PI137	69	150	6.89	0.39	1.29
Pipe PI138	69	150	3.85	0.22	0.43
Pipe PI139	55.5	150	2.25	0.13	0.16
Pipe PI140	69	150	5.97	0.34	0.99
Pipe PI142	55.5	150	-7.27	0.41	1.46
Pipe PI143	87.7	150	2.26	0.13	0.16
Pipe PI144	69	150	8.37	0.47	1.86
Pipe PI145	69	150	5.22	0.30	0.77
Pipe PI146	55.5	150	3.50	0.20	0.37
Pipe PI11	69	150	6.78	0.38	1.25
Pipe PI190	69	150	7.89	0.45	1.66
Pipe PI1	104.5	400	138.80	1.10	3.25

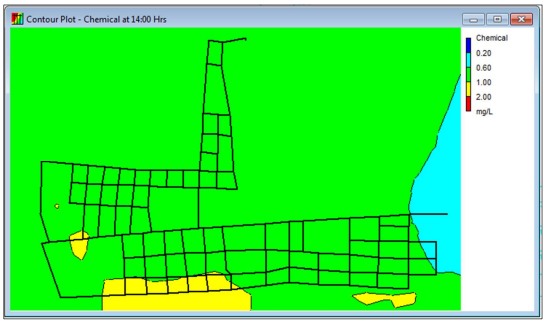

Fig.7 (b) Chemical contour graph for DMA-2

Table-2: Node Results

Zone-3 Network Table – Nodes at 10:00 Hrs

Node ID	Elevation (m)	Demand (LPS)	Head (m)	Pressure (m)	Chemical (mg/L)
Junction JU1	151.2	0.60	171.30	20.10	0.57
Junction JU2	151.2	0.60	171.30	20.10	0.57
Junction JU3	150.9	0.60	171.30	20.40	0.58
Junction JU4	154.5	0.60	171.26	16.76	0.63
Junction JU5	153.9	0.60	171.26	17.36	0.60
Junction JU6	153	0.60	171.27	18.27	0.50
Junction JU7	154.8	0.60	171.18	16.38	0.70
Junction JU8	154.8	0.60	171.20	16.40	0.68
Junction JU9	154.8	0.60	171.18	16.38	0.65
Junction JU10	154.5	0.60	171.18	16.68	0.58
Junction JU11	154.2	0.60	171.22	17.02	0.56
Junction JU12	155.1	0.60	171.20	16.10	0.68
Junction JU13	154.5	0.60	171.25	16.75	0.63
Junction JU14	153	0.60	171.26	18.26	0.55
Junction JU15	152.7	0.60	171.28	18.58	0.65
Junction JU16	152.1	0.60	171.28	19.18	0.58
Junction JU17	150.6	0.60	171.28	20.68	0.56
Junction JU18	150	0.60	171.29	21.29	0.54
Junction JU19	150	0.60	171.30	21.30	0.45
Junction JU20	150	0.60	171.30	21.30	0.47
Junction JU21	152.4	0.60	171.29	18.89	0.61
Junction JU22	151.2	0.60	171.29	20.09	0.57
Junction JU23	150	0.60	171.30	21.30	0.56
Junction JU24	150	0.60	171.30	21.30	0.54
Junction JU25	149.3	0.60	171.31	22.01	0.51
Junction JU26	153.6	0.60	171.25	17.65	0.63
Junction JU27	152.4	0.60	171.27	18.87	0.55
Junction JU28	151.2	0.60	171.29	20.09	0.58
Junction JU29	151.8	0.60	171.30	19.50	0.57
Junction JU30	152.7	0.60	171.28	18.58	0.63

5. CONCLUSION

The projected distribution network of Tatkon town consists of five zones. This network is arranged according to those days's requirement to the future (2048) needs and demands. The design capacity of the distribution network is 11.43 MLD which is sufficient for the future design demand of 2048. Hence the 13 elevated tanks (452.6 m^3) must support a capacity to suppress the future demand. So a new network is to be designed to meet future demands and to reach the user's door step. The new network is placed according to the road pattern using master plan in view of the town in future.

Main problems to be paid attention to when using the software are to meet all design criteria for optimization and to define phases like as net tracing and dimensioning the elements. The deficiency of software is to leave out phenomena such as water hammer, pipe bursting, behavior of non-return valves and starting a pump or stopping it. But this work hopes to be a good step toward further understanding of comprehensive design and research.

The design of water distribution system of Tatkon town showed suitable and provides minimum head loss, maximum pressure and efficient diameter. The

results of the analysis are confirmed by hydraulic equations. Finally, this study would assist the water supply engineers in saving time under one umbrella because this process is fast, more attractive, easy to integrate the changes.

ACKNOWLEDGEMENTS

I would like to express my gratitude to my supervisor, Associated Professor Haicheng Liu, School of Environmental Science and Engineering, Suzhou University of Science and Technology, Suzhou, China for supporting me in completing my work successfully by providing the required facilities and advices. I am also grateful to our School of Environmental Science and Engineering for their cooperation during my academic days and providing guidance. I would like to thank The Chinese Ministry of Commerce, Chinese Government Scholarships to students from developing countries, for providing me the necessary fund for the paper. Special thanks are due to Naypyidaw Development Committee and Yangon Technological University for encouragement of the study. Finally, I am grateful to my family for their kind support and encouragement.

REFERENCES

[1] Anisha, G., Kumar, A., Kumar, J. A., & Raju, P. S. (2016). Analysis and Design of Water Distribution Network Using EPANET for Chirala Municipality in Prakasam District of Andhra Pradesh. *International Journal of Engineering and Applied Sciences*, *3*(4).

[2] Dave, B. H., Rajpara, G., Patel, A., & Kalubarme, M. H. Analysis of Continuous Water Distribution System in Gandhinagar City Using EPANET Software: A Case Study of Sector-8.

[3] Ministry of Health and Sports. (2017). *Demographic and Health Survey Myanmar 2015-2016*. Ministry of Health and Sports, Naypyitaw, The Republic of the Union of Myanmar.

[4] Montasir, M., Abrar, A. C., Rifat, M., & Mahommad, S. R. (2015). Water Distribution System Modelling By Using EPA-NET Software. In *International Conference on Recent Innovation in Civil Engineering for Sustainable Development, Gazipur, Bangladesh* (pp. 960-964).

[5] Muranho, J., Ferreira, A., Sousa, J., Gomes, A., & Marques, A. S. (2014). Technical performance evaluation of water distribution networks based on EPANET. *Procedia Engineering*, *70*, 1201-1210.

[6] Ramesh, H., Santhosh, L., & Jagadeesh, C. J. (2012, January). Simulation of hydraulic parameters in water distribution network using EPANET and GIS. In *International Conference on Ecological Environmental and Biological Sciences (ICEEBS'2012) Jan* (pp. 7-8).

[7] Rossman, L. A. (2000). EPANET 2 users manual, water supply and water resources division. *National Risk Management Research Laboratory, US Environmental Protection Agency, Cincinnati, Ohio*.

[8] Schwarzenbach, R. P., Egli, T., Hofstetter, T. B., Von Gunten, U., & Wehrli, B. (2010). Global water pollution and human health. *Annual Review of Environment and Resources*, *35*, 109-136.

STUDY ON THE BEHAVIOR OF SPUN PILE FOUNDATION DUE TO SEISMIC LOADING

Chan Myae Kyi[#1], Dr.Nyan Phone[#2], Myat Thidar Tun[#3]

Department of Civil Engineering

Technological University (Thanlyin), Yangon, Myanmar

Abstract- This aim of the paper is the study on the behavior of spun pile foundation due to effect of seismic loading. This foundation describes the lateral deflection and settlement due to seismic load by applying static load case and dynamics load case. These results are described by using ETABS software. To design the foundation, the super structure of sixteenth storeyed R.C building with basement is analyzed by applying static load case and dynamics load case of ETABS software. The two results of unfactored load are used to study the behavior of spun pile by applying the superstructure from two different load combinations. According to the result of unfactored load of superstructure, the same number of pile is divided into three groups. Allowable bearing capacity is gained from the soil report of Inya Lake Residence Project in Yangon. The allowable bearing capacity of soil is calculated by Terzaghi based on Meyerhof's Method. The smallest area of spun pile foundation is used. The size of spun pile is outside diameter 400 mm and thickness 75mm slender shape. The pile working load from materials for spun pile is 54 tons. The required length for 54 tons spun pile regard to 85 ft according to calculation of the allowable bearing capacity .The analyzing results of deflection and settlement for spun pile are within allowable limits. The results of deflection and settlement of spun pile foundation due to the effect of two load combinations are compared.

I. INTRODUCTION

Pile foundation is the part of a structure used to carry the applied column load of a super structure to the allowable bearing capacity of the ground surface at the same depth. The common used shape of pile is rectangular and slender which applied the load to the stratum of high bearing capacity. In the case of heavy construction, the bearing capacity of shallow soil will not be satisfactory; the construction should be built on pile foundation. It is used where soil having low bearing capacity respect to loads coming on structure or the stresses developed due to earthquake cannot be accommodated by shallow foundation. To obtain the most economical and durable foundation, the engineers have to consider the super structure loads, the soil condition and desired to tolerable settlement. Pile foundations are convened to construct the multi-storeyed building and work for water, such as jetties as bridge pier. The types of prestressed concrete pile are usually of square, triangular, triangle, circle and octagonal section which are produced in suitable length in one meter interval between 3 and 13 meters. Nowadays, most people use spun pile foundation one of the most prestressed concrete pile to construct most of the buildings and bridges. Spun piles are widely used in construction. Prestressed concrete cylinder pile is a special type of precast concrete pile with a hollow circular cross section. Advantage of using spun pie are spun pile is less permeable than reinforced concrete pile, thus it has a good performance in marine environment. So the design of spun pile foundation can be based on the deflection and settlement due to earthquake.

II.PREPARATION DATA FOR ANALY-SICS OF SPUN PILE FOUNDATION

Information of structure and material properties is prescribed as follows. Dead load, live load, wind load and earthquake loads are considered in proposed building. The typical beam plans and 3D view of the proposed buildings from ETABs software are shown in Figure 1 and Figure 2.

A. Site location and Profile of structure

Type of structure: 16th storyed R.C Building

Location : Seismic zone (4)

Soil Type : Silty Sand, SD

Type of Occupancy : Residential

Shape of Building : Rectangular shape

Size of Building : Length = 81 ft

: Width = 65 ft

: Height =162 ft

Height of Building: Typical story height = 10ft

Bottom story height = 12ft

B. Design Codes

Design code applied for superstructure are ACI (318-99) and UBC-97 There are 26 numbers of load combinations which are accepted for beam, column and slab etc

(1)Material Properties

Analysis property data

Weight per unit volume of concrete= 150 pcf

Modulus of elasticity = 3.12×10^6

Poisson's ratio = 0.2

Design property data

Reinforcing yield stress (f_y) = 50000 psi

Shear reinforcing yield stress (f_y) = 50000 psi

Concrete strength (f'_c) = 3000 psi

Concrete cylinder strength (f'_c) = 3500 psi

C. loading Considerations

The applied loads are dead loads, live loads, earthquake load and wind load.

(1) Gravity Loads: Data for dead loads which are used in structural analysis are as follows;

Unit weight of concrete = 150 pcf

4½ inches thick wall weight = 50 psf

9 inches thick wall weight = 100psf

Light partition weight = 20 psf

Finishing Weight = 20 psf

Weight of elevator = 2 ton

Data for live loads which are used in structural analysis are as follows:

Live load on slab = 40 psf

Live load on lift = 100 psf

Live load on stairs = 100 psf

Live load on corridors = 60 psf

Live load on roof = 20 psf

Weight of water = 2ton

(2)Lateral loads: Data for wind loads which are used in structural analysis are as follows;

Exposure Type = B

Basic wind velocity =100mph

Important factor, Iw = 1.0

Windward Coefficient = 0.8

Leeward Coefficient = 0.5

Data for earthquake load are as follows:

Soil profile type = SD

Seismic Zone = 2B

Seismic Zone Factor = 0.2

Building period coefficient, Ct = 0.03

Important Factor, I = 1

Seismic coefficient, C_a = 0.28

Seismic coefficient, C_v = 0.4

The magnitude of earthquake loading depends upon the weight or mass of building, dynamic properties of the building and difference in stiffness of adjacent floors along with the intensity and duration of the earthquake.

(3)Lateral Load Combination: According to (ACI 318-99) codes, the design of load combination are as follows

Table 1 Load Combination for Static

No	Load Combination
1	1.4 DL
2	1.4 D + 1.7 LL
3	1.05DL + 1.275LL + 1.275WX
4	1.05DL + 1.275LL – 1.275 WX
5	1.05DL + 1.275LL + 1.275 WY
6	1.05DL + 1.275LL - 1.275 WY
7	0.9DL + 1.3 WX
8	0.9DL -1.3 WX
9	0.9DL + 1.3 WY
10	0.9DL - 1.3 WY
11	1.05DL + 1.28LL + EX
12	1.05DL + 1.28LL - EX
13	1.05DL + 1.28LL + EY
14	1.05DL + 1.28LL - EY
15	0.9DL + 1.02 EX
16	0.9DL - 1.02 EX
17	0.9DL + 1.02 EY
18	0.9DL - 1.02 EY
19	1.16DL + 1.28 LL + EX
20	1.16DL + 1.28 LL - EX
21	1.16DL + 1.28 LL + EY
22	1.16DL + 1.28 LL – EY
23	0.79DL + 1.02 EX
24	0.79DL - 1.02 EX
25	0.79DL + 1.02 EY
26	0.79DL - 1.02 EY

Table 2 Load Combination for Dynamics

No	Load Combination
1	1.4 DL
2	1.4 D + 1.7 LL
3	1.05DL + 1.275LL + 1.275WX
4	1.05DL + 1.275LL – 1.275 WX
5	1.05DL + 1.275LL + 1.275 WY
6	1.05DL + 1.275LL - 1.275 WY
7	0.9DL + 1.3 WX
8	0.9DL -1.3 WX
9	0.9DL + 1.3 WY
10	0.9DL - 1.3 WY
11	1.05DL + 1.28LL + 1 SPEC X
12	1.05DL + 1.28LL – 1 SPEC X
13	1.05DL + 1.28LL + 1 SPEC Y
14	1.05DL + 1.28LL – 1 SPECY
15	0.9DL + 1.02 SPEC 1
16	0.9DL - 1.02 SPEC 1
17	0.9DL + 1.02 SPEC 2
18	0.9DL - 1.02 SPEC 2
19	1.16DL + 1.28 LL + SPEC X
20	1.16DL + 1.28 LL – SPEC X
21	1.16DL + 1.28 LL + SPEC Y
22	1.16DL + 1.28 LL – SPEC Y
23	0.79DL + 1.02 SPEC X
24	0.79DL - 1.02 SPEC X
25	0.79DL + 1.02 SPEC Y
26	0.79DL - 1.02 SPEC Y

III.DESIGN RESULTS OF PROPOSED BUILDING

The design results of beam and column for proposed building are described.

Table 3. Design Results for Column, Beam and Slab

Section	Size (Static)	Size (Dynamics)
Column	(12″ × 12″) (14″× 14″) (16″ × 16″) (18″ × 18″) (20″ × 20″) (22″ × 22″) (24″ × 24″) (26″ × 26″) (28″ × 28″)	(14″× 14″) (16″ × 16″) (18″ × 18″) (20″ × 20″) (22″ × 22″) (24″ × 24″) (26″ × 26″) (28″ × 28″) (30″ × 30″)
Beam	(9″ × 9″) (9″ × 12″) (12″ × 16″) (12″ × 18″) (12″ × 20″) (14″ × 18″) (14″ × 20″)	(9″ × 9″) (9″ × 12″) (10″ × 12″) (12″ × 16″) (12″ × 18″) (12″ × 20″) (14″ × 18″) (14″ × 20″)
Slab	4 ″, 4.5″, 5″	4 ″, 4.5″, 5″
Wall	8″, 12″ & 16″	8″, 12″ & 16″

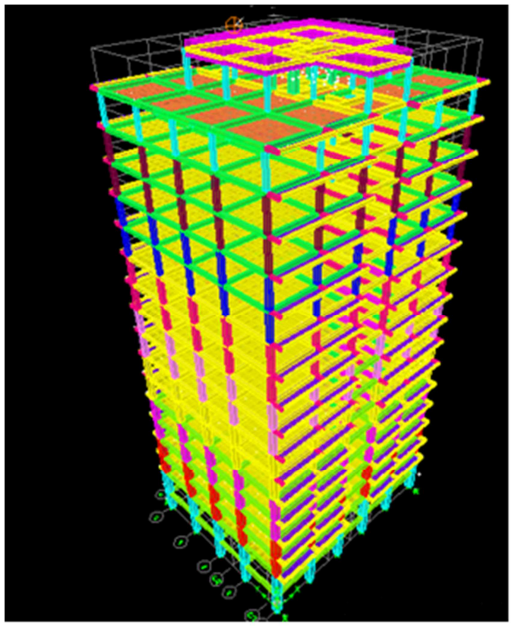

Figure.1 3D Model of Proposed Building

IV. STABILITY OF THE SUPERSTRUCTURE CHECKING

The design superstructure is checked for

(1) Overturning,

(2) Story Drift

(3) Torsional Irregularity

(4) P-Δ Effect

Table 4. Stability Checking

static load case Checking		X-Direc:	Y-Direc:	Limit
OTM	Static	20.08	14.39	>1.5
	Dynamics	33.91	33.92	>1.5
Story Drift	Static	0.59	0.7	<2.4
	Dynamics	0.92	1.2	<2.4
Torsion	Static	1	1	<1.2
	Dynamics	1	1	<1.2
P-Δ Effect	Static	0.002	0.031	>0.1
	Dynamics	0.025	0.035	>0.1

All checking for stability of superstructure are within the limits. The results of unfactored load are received by applying ETAB software. The base point levels of super structure are described in Figure2.

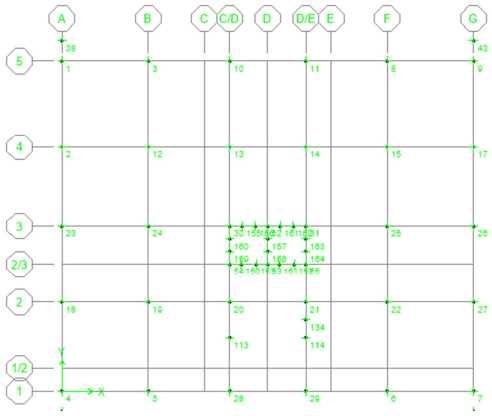

Figure2. Point Levels Layout Plan

V. PILE WORKING FROM MATERIAL

Shear reinforcing yield stress (fy) = 50000 psi

Concrete cylinder strength (f′c) = 3500 psi

Modulus of elasticity = 3.37 x10⁶

ϕPT = 0.7 (0.33 f′c Ac + 0.39 fyAst)(ACI318-99)

= 0.7 (0.33 × 3500 × 122+ 0.39 × 50000 × 10 × 0.31)

= 140952 lbs.

= 62 Tons

0.86ϕPT= 0.86 × 62

= 54.11 Tons (Use 54 Tons)

VI. CALCULATION ALLOWABLE BEARING CAPACITY

According to CQHP Guideline

Up to 10,000 ft² Area – one bore hole for 2,500 ft²(min)

≥ Two bore hole

For this project,

Project area = 81′-0″ × 65′-0″

= 5265 ft²

Three bore holes are adequate.

For the evaluation of bearing capacity of pile foundation, the formula for calculation of bearing capacity of two pile foundations, derived from “A modified version of the Terzaghi bearing capacity equation for pile design” would be applied for this analysis

Table6. Allowable Bearing Capacity

Name	Q_b (KN)	Q_s (KN)	Q_{all} (KN)	F.S	Q_{ult} (Ton)
BH1	146.9	1343.5	1490.4	3	49.7
BH2	154.7	1363.1	1517.7	3	50.6
BH3	193.4	1637.5	1830.9	3	61.0
Average Allowable Bearing Capacity					54

VII. ANALYSIS RESULTS OF SPUN PILE FOUNDATION

The used number of spun pile are described in the following by analyzing and design due to static and dynamics of ETABS

software. These numbers of spun pile are justified to resist the superstructure.

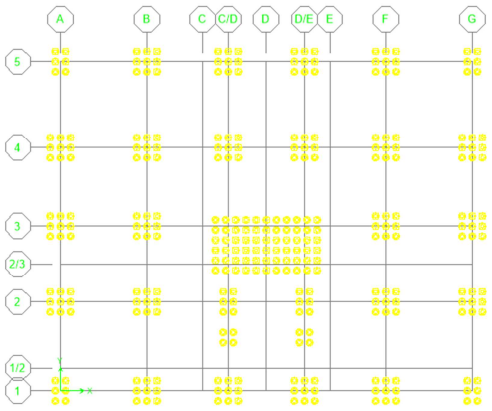

Figure 3. Spun Pile Layout Plan (Static Load Case)

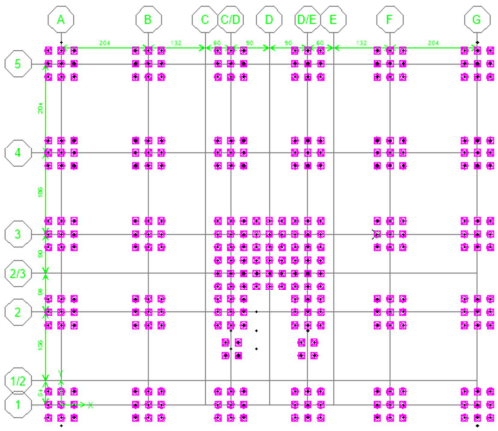

Figure4. Spun Pile Layout Plan (Dynamics Load Case)

The group 1,2,3 are considered from the total unfactored load of point 1, point 24 and Point 30+31+53+54+55 of shear wall loading because of applying the reaction of superstructure by two load cases. These groups are compared to study the behavior of spun pile due to apply the two types of load combinations. The used number of pile and the size of pile cap are described in table 6 and 7.

Table6. Required Number Pile Cap Size

Name	No of pile	L(m)	B(m)	H(m)
GP1	6	1.68	2.44	0.91
GP2	9	2.44	2.44	1.22
GP3	66	6.7	3.66	1.52

Table7. Required Number Pile Cap Size

Name	No of pile	L(m)	B(m)	H(m)
GP1	9	2.44	2.44	1.22
GP2	9	2.44	2.44	1.22
GP3	66	6.7	3.66	1.52

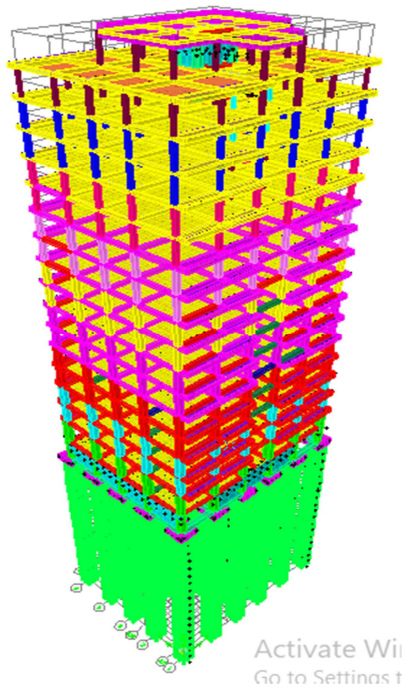

Figure5. 3D Modeling for Combination of Superstructure and Substructure

The results of spun pile foundation are described in figure 6, 7, 8, 9, 10 and 11 by applying two load cases.

Comparison of deflection due to seismic load in X-direction (For Group 1)

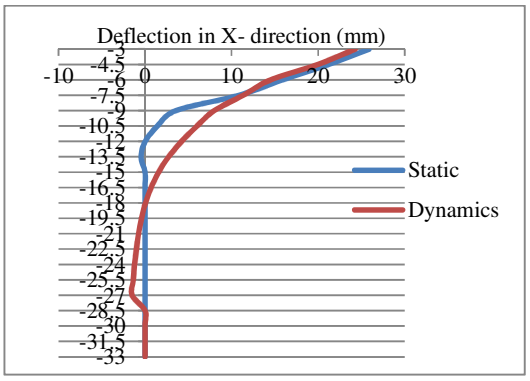

Figure 6. Deflectionalong Spun Pile

The results of deflection for group 1 of spun pile in X-direction by applying Dynamics load case are obviously no difference at top and bottom of the pile than by applying Static load case and are more than in the middle of the pile.

Comparison of deflection due to seismic load in X-direction (For Group 2)

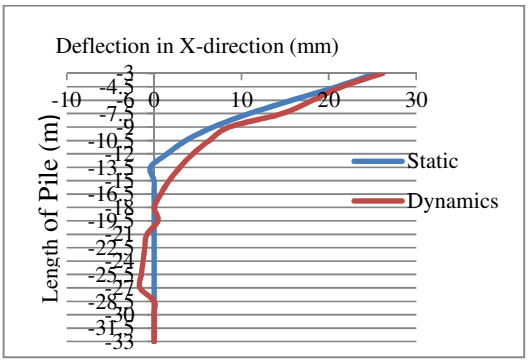

Figure 7. Deflection along Spun Pile

The deflections of group 2 for spun pile by applying Dynamics Loading are more than the Static Loading and then the deflection due to dynamics slowly reduce with depth more than static.

Comparison of deflection due to seismic load in X-direction (For Group 3)

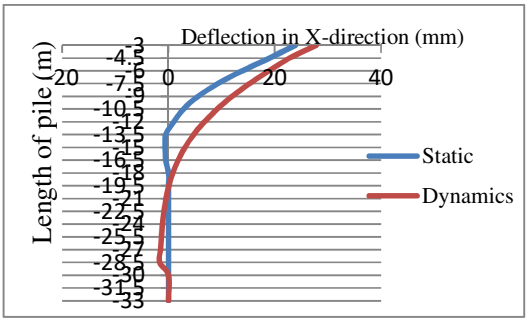

Figure 8. Deflection along Spun Pile

The deflections of group 3 for spun pile due to static load case are more reliable than ones due to dynamics. The maximum deflections of pile occur at the tip of the pile and then gradually decrease with the depth. The minimum deflections cause at the bottom of the pile.

Comparison of deflection due to seismic load in Y-direction (For Group 1)

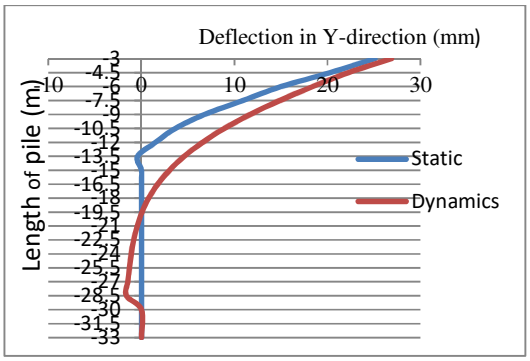

Figure 9. Deflection along Spun Pile

Comparison of deflection due to seismic load in Y-direction (For Group 2)

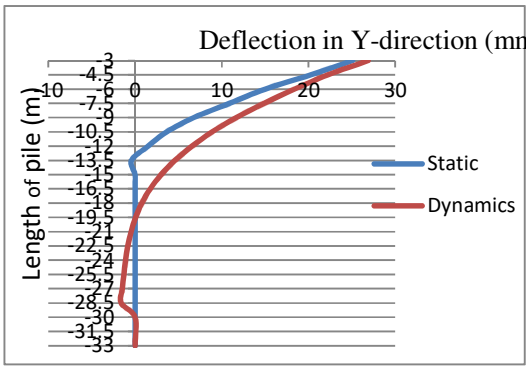

Figure 10. Deflection along Spun Pile

Comparison of deflection due to seismic load in Y-direction (For Group 3)

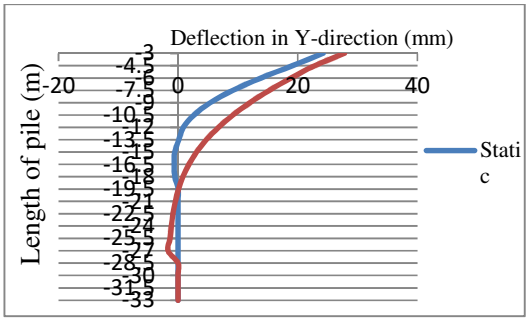

Figure 11. Deflection along Spun Pile

The deflections of spun pile in both directions by using static load combination are more reliable than ones by using dynamics load combination. The mass of the superstructure reduce by applying the two different load combinations.

Table8. Comparison of Settlement Values

Group	Static(mm)	Dynamics(mm)
1	26.54	61.5
2	28.25	60.35
3	29.32	61.5

Comparison of settlement due to seismic load

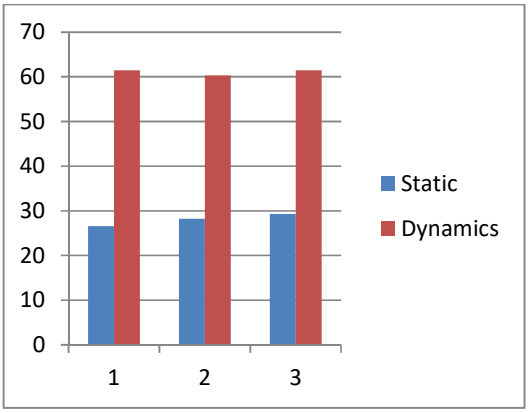

Figure 11. Results of Settlement

VII. DSICUSSION AND CONCLUSION

For the design of spun pile foundation, the required soil parameters are obtained from the soil report on, Yangon. The allowable bearing capacity of the soil is calculated by Terzaghi Equation based on Myerhof's method of Tomlinson. The soil condition of the proposed building at the base of mat foundation is soft soil and so the pile foundations are used. The proposed site is located on seismic zone 2A. The superstructure is analyzed and designed by using ETABS software and load combinations are considered by static load case and dynamics load case. The lateral load and gravity loads are considered and the design superstructure is checked for sliding resistance, overturning effect, story drift, and torsional irregularity. In design of spun pile foundation, the use of the same number of pile divided into three groups. The required pile length for four groups of spun pile foundations are 85 Ft. The deflection and settlement of spun pile foundations due to seismic loading is satisfied within the allowable limits. The number of spun concrete pile are used at the least to construct the 16th storeyed building because the skin friction of spun piles also increase due to two surfaces is created by the hollow section and so the bearing capacity of the pile just increase than similar size of square pile. The most common feature of spun concrete pile is the cylindrical hollow nature of the middle which makes the final product lighter. The number of spun pile can be reduced at least more than the precast concrete piles and occurred which these piles resist the effects due to the seismic loading. The number of pile is no difference by analyzing two load combinations. The deflection and settlements of spun pile due to the effects of static load combination are more reliable and the results of deflection and settlement due to two load combinations are within the allowable limits.

ACKNOWLEDGMENT

First of all, the author is thankful to Dr. Theingi, Rector of Technological University (Thanlyin), for her valuable management. The author would like to express my deepest thanks and gratitude to her supervisor Dr. Nyan Phone, Professor and Head of the Department of Civil Engineering of the Technological University (Thanlyin). The author special thanks go to her co-supervisor Daw Myat Thidar Tun, Lecturer of the Department of Civil Engineering of the Technological University (Thanlyin), for his invaluable advice and suggestion throughout the study. The author would like to express her thanks to her member Daw Wint Thandar Aye, Assistant Lecture of the Department of Civil Engineering of Technological University (Thanlyin), for her valuable comments and guidance during this study. Finally, her special thank goes to all who help her with necessary assistance for this study.

REFERENCES

[1]Foundation Design and Construction MJ Tomlinson (Seventh Edition) 3. Taranth Pile Design and Construction Practice –Tomlinson.

[2]Foundation Analysis and Design – Joseph E. Bowles (Fifth Edition

[3]Principles of Foundation Engineering – Braja M. Das (Adapted International Student Edition)

[4]Geotechnical Engineering Calculations and Rules of Thumb Nilson, A.H., and Winter, G.1991

[5]Das,BrajaM.1998.″Principles of Foundation Engineering″. Fourth Edition. United State of America.

[6]Day,R.W: Foundation Engineering Handbook, Design and Construction with the 2006 International Building Code, The McGraw- Hill Companies, Inc, (2006).

[7]FHWA HI 97-013,Design and Construction

Driven Pile Foundation.

Mathematical Analysis of Reservoir Flood Routing

Hla Tun

Myat Noe Yadana Engineering Company

Myatnoeyadanaco@gmail.com

INTRODUCTION- Many dams are situated in Myanmar . Most dams are used for irrigation and some dams are used for hydro power generation. Reservoir flood routing is required for design of dams, spillway and flood mitigation.

ABSTRACTS

Reservoir flood routing can be tabulated (calculated) by graphical method . Length of time interval is usually 6 hours or more . Duration of time interval can be reduced to a few hours by using mathematical analysis. Any combination of storm duration , intensity and surcharge , discharge rate of reservoir can be calculated(simulated) and it gives more accurate result.

KEYWORDS

Inflow-Storage- Discharge relation curves, Power series representation of curves, Unilateral and bilateral curve fittings.

Main Parameters of storm rainfall

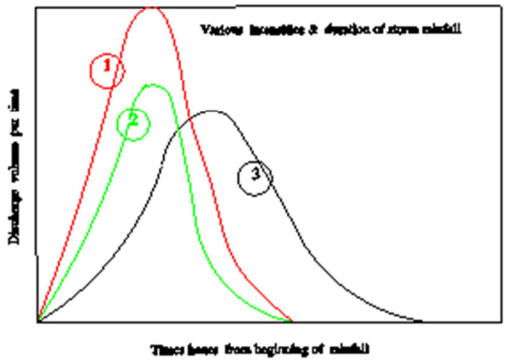

For steep crest of storm rainfall, it is advisable to use two curves from start to crest and another equation from crest to end.

Characteristics of various types & combination of spillway

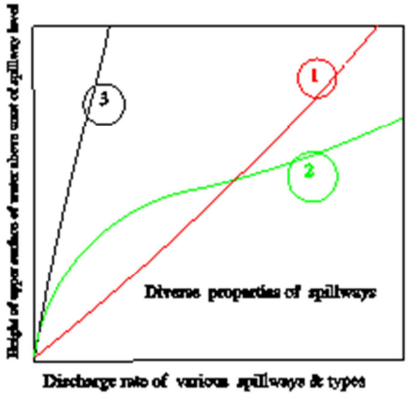

Serial (3) is ordinary spillway such as broad crest type .Discharge rate of serial (1) is more than (3). Serial (2) is combination of more types of spillway on the condition of upper surface of water is near the critical level of reservoir.

Different Characteristics of reservoirs

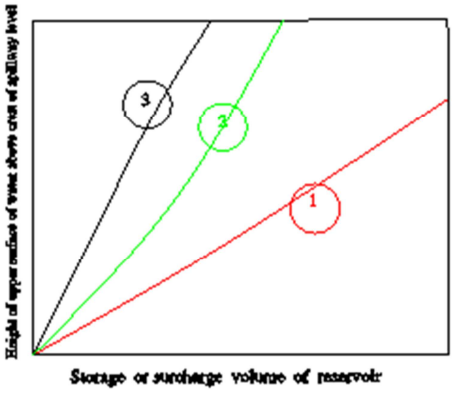

Serial (1) is for a little flat banks type reservoir, serial (2) is moderate slant bank reservoir and serial (3) is for reservoir with steep banks.

Representation of characteristic equations

Most of characteristic equation can be represented by power series equations , suchas:-

$$Y= \sum_1^N A_i * X^{i-1} \text{-----(1)}$$

Coefficients $A_1, A_2, -- A_N$ are to find .

In the above equation Y is dependent variable and X is independent variable. i = serial number of digit , N= Numbers of coefficients to calculate by the method of minimizing of errors of least square . N numbers must be less than corresponding pairs of points,

It can also be found to find X in terms of Y and unknown coefficients will be another sets such as B_1

$,B_2, - - -B_n,$ to find as above method.

$$X= \sum_1^N B_i * Y^{i-1} \text{-----(2)}$$

Shifting of one or both of two sets of data might be met to find coefficients. Change to logarithmic scale or other methods is possible Combination of unit steps function and other linear function might be occurred.

In finding each coefficients of above two sets equations two dimensional arrays DIM C(N.N+1) algebraic equation must be solved. N is numbers of unknown coefficients . LU Decomposition method is more preferable than Gauss Elimination method.

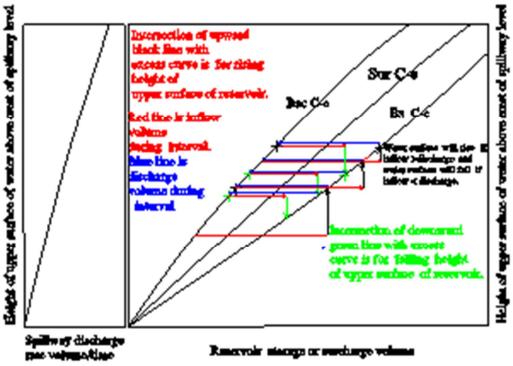

Horizontal length of the line between the B curve and E curve(blue colpur) is discharge volume per interval(time hour) at height of respective elevation.Red line start from B curve and it is average inflow to reservoir during time interval.

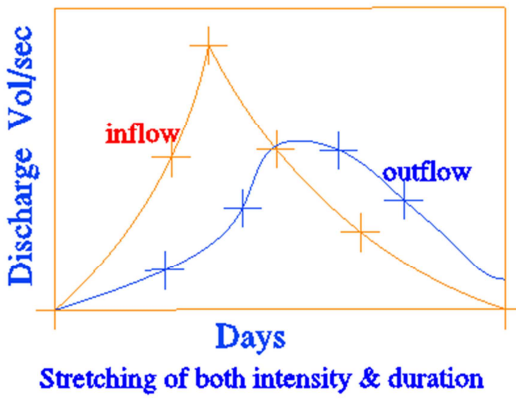

Stretching of both intensity & duration

Intensity of storm is mitigated and duration is stretched out by reservoir flood routing.

Above presentation is tabulated by taking appreciable amount of interval of time such as 6 to 12 hours, Mathematical analysis can be done by taking a few hours and gives more precise results. Mathematical method preceded by dint of flexibility of input characteristic curves,

ACKNOWLEDGEMENT

This paper is written to submit at **Federation of Myanmar Engineering Societies, Annual General Assembly ,National Conference on Engineering Research to promote harnessing methods of dams and affiliated structures.**

REFERENCES

[1] Creager W.P & Justin J D . Engineering for Dams Vol-1 John Wiley & Sons,Inc.1966.PP 195-202

[2]Creager W.P & Justin J D. Hydro Electric Handbook 2nd edition , John Wiley & Sons,Inc1950.

[3]Conte S D. Elementary Numerical Analysis Mc-Graw Hill Company

[4]Scarborough J B. Numerical Mathematical Analysis .Oxford Book Company.

Key Factors for the Successful Construction of Tunnels and Shafts

Tun Min Thein

Department Of Hydropower Implementation

Ministry Of Electricity And Energy, Myanmar

***Abstract* — In the Comparison of all the Construction works, underground construction works are very challenging and very expensive including many risks such as human lives. Nowadays tunnels and shafts play an important role for many hydropower projects. This paper emphasizes on key factors which should be kept in mind of planners and site engineers to evaluate successful excavation and construction of tunnel and shaft.**

Keywords: Hydropower projects, planners and site engineers, tunnels and shafts, underground.

I. ROLE OF INVESTIGATOR AND GEOLOGIST

The investigation Branch makes a reconnaissance survey in the project area. Multiple alternatives for tunnel alignment will be resulted after survey. Test drilling along the alignments of one or more proposed alternatives will be conducted. After required judgment, one alternative alignment will be selected as a final one. Those steps seem to be very easy and not so important for the project. But all the works conducted by investigators and geologists are very crucial and the information they have explored will be taking part from the beginning to the completion of the project. The tasks of Investigation Branch and Geologists are very precious and respectable because their information decides the type of a project, size of a project and cost of a project.

II. INFORMATION VERSUS TECHNOLOGY

I have already mentioned that the information provided by investigators and Geologists are very precious. They are also vital in deciding tunneling method and technique. The Design Branch has made a final selection of tunnel alignment depending upon the information provided by investigation branch and geology branch. Geologists have provided a geological profile along the tunnel alignment and in the shaft area by judging core sample from the drill-holes along the alignment.

Design Branch has predicted excavation technique and support system by using geological interpretation. Test drill holes tell the geological condition such as soft rock, hard rock, mudstone or fractured layer that exists along the course of the tunnel.

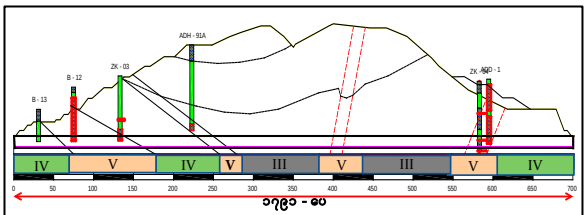

	Rock Properties	Rock Mass Rating	Remark
III	Fair	41 ~ 60	30 %
IV	Poor	21 ~ 40	34 %
V	Very Poor	< 20	36 %

Figure 1 Sample core drill holes.

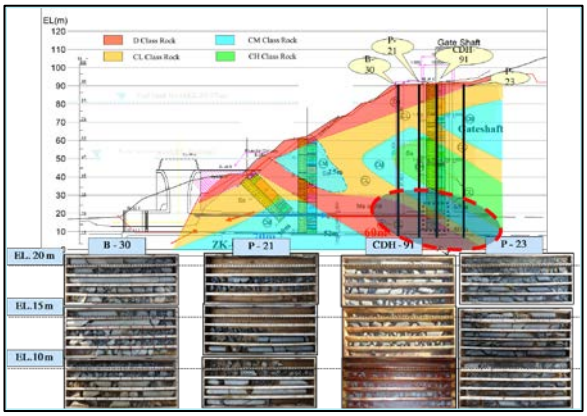

Figure 2 Core Sample.

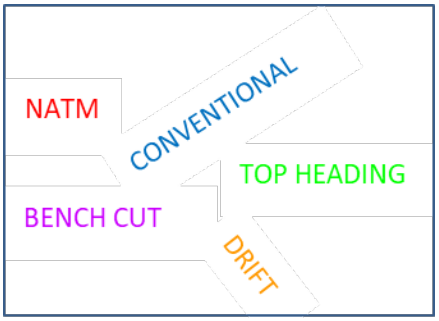

Figure 3 Excavation Methods.

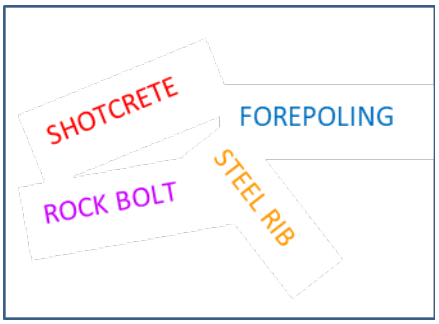

Figure 4 Support Systems.

III. TUNNELING KIT FOR SITE ENGINEERS

The most important fact for a tunnel or shaft engineer is to be very familiar with geological condition along the tunnel or shaft. Site engineers must study the geological profile thoroughly so that they can make necessary preparation for each sectional excavation.

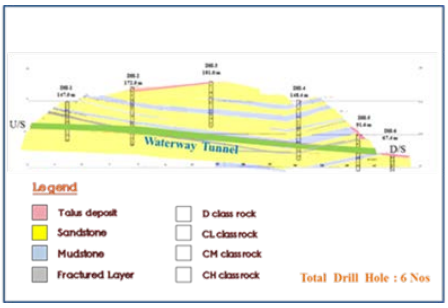

Figure 5 Geological Profile

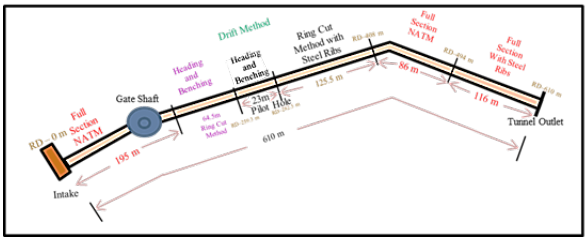

Figure 6 Tunneling Method Selection by geology.

Depending upon the excavation method, required machinery, material and equipment will be different. Tunnel engineers must study all the tunneling methods especially the most adaptable methods for each respective project. For soft rock tunneling, support systems are vital in addition to excavation method.

Figure 7 Tunneling Kit.

Water supply system, drainage and dewatering system, ventilation system and electricity supply system need to meet the necessary workability and safe standards. Tunnel engineers and workers must follow safety precaution and must wear the respective PPE for each construction site.

Figure 8 Power supply and ventilation system

Figure 9 Tunnel excavation and shotcret1ng

IV. TUNNELING METHODS APPLYING IN MYANMAR HYDROPOWER PROJECTS

NATM (New Austrian Tunneling Method) and conventional methods are generally applied for Myanmar Hydropower Projects. NATM is best suited for medium to hard rock excavation and combination of NATM and conventional method is applicable for soft rock and poor geological conditions. Depending upon the size of the tunnel and encountering geology, bench cut method or drift

method or other suitable methods can be applied.

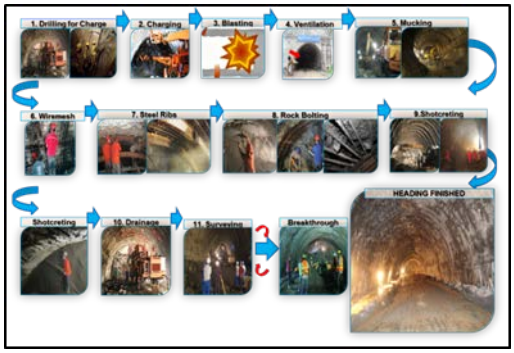

Figure 10 NATM procedures.

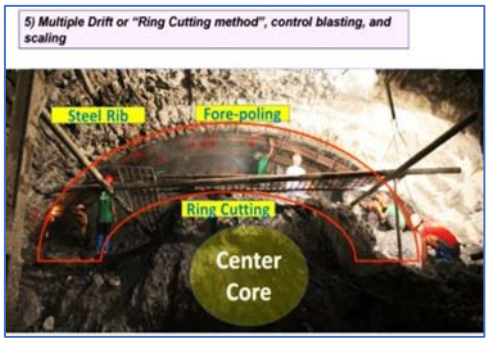

Figure 11 Ring cutting method.

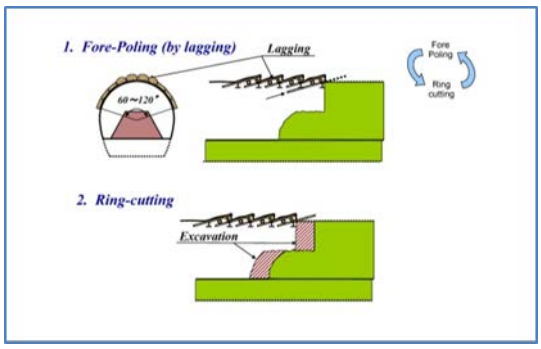

Figure 12 Ring cutting method.

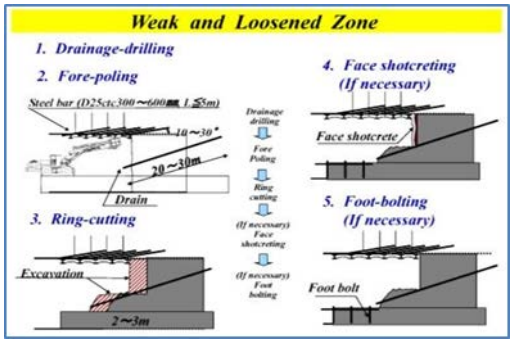

Figure 13 Supporting methods in weak and loosen zone.

Precision in survey is vital for hydropower tunnels because the hydropower tunnels include many turnings and difference in elevations. The tunnels are excavated from up-stream and down-stream in parallel. A small mistake in elevation reading may lead deviation of upstream and downstream tunnel excavations, resulting oversized breakthrough.

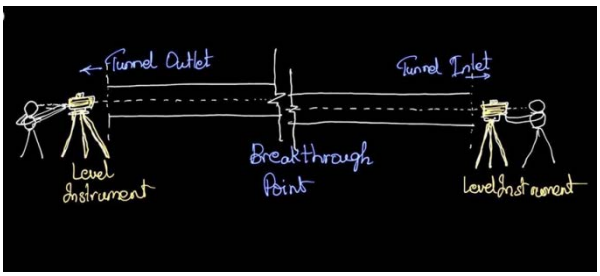

Figure 14 Missing at breakthrough by level error.

Angular and distance reading mistakes may lead deviation of excavation fronts resulting in two tunnels unfortunately.

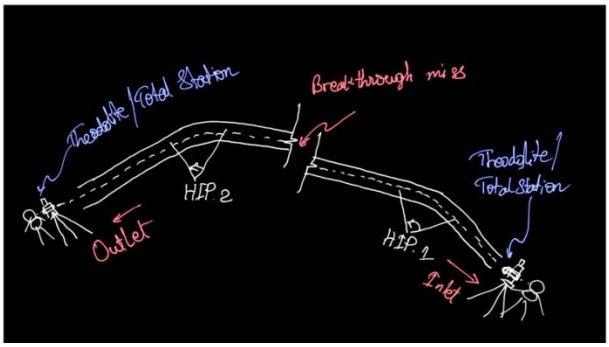

Figure 15 Missing at Breakthrough Because of Alignment Error

Therefore both skilled surveyor and modernized and précised survey equipment are very important for hydropower structures because their locations and elevations are linked with each other from upstream to very far downstream of the Project.

Figure 14 Measuring Instrument

Figure 16 Surveying

V. SUPPORT SYSTEMS FOR TUNNEL AND SHAFT

Flexible support system is the main concept of NATM. Excavated Surface is secured by Shotcrete first to prevent falling of Loosen stone and to reinforce weaken disturbed surface. Quick rock bolt system adds another dimension to the reinforcement purpose and maintains probable falling blocks of stone and fractured layer in their positions firmly. If more reinforcement is needed, steel rib supports may be applied.

Figure 17 Shotcreting, rockbolting, steel-rib supporting.

Fore poling is necessary for excavation through soft and fractured rock zone. For the shaft support system, ring grouting around the circumference of the shaft is recommendable.

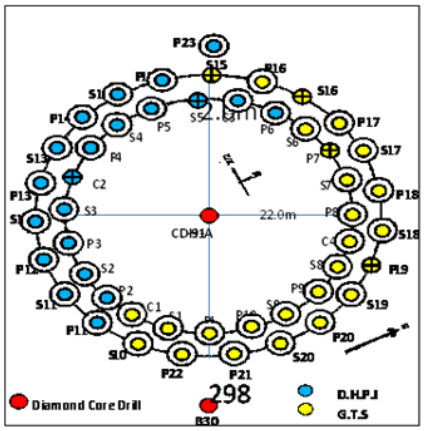

Figure 18 Ring grouting pattern.

Figure 19 Ring grout for Shaft

Shotcrete, wire-mesh and rock-bolts are normally applied in the shaft support system. When the excavation diameter is large and geology of the shaft is not very good, steel rib supports and primary RC concrete support work effectively in the support system.

Figure 20 Steel-ribs and primary lining supporting.

VI. ACCIDENTS IN TUNNELS AND SHAFTS

For a developing country like Myanmar, there are many challenges and risks in tunnel and shaft construction including risk of lives. Lives and property of tunnel workers and operators mainly depend upon the action and decision of tunneling Staff officers and SAEs (Sub Assistant Engineers) because they are always closely supervising and operating the tunneling 24/7. Efficient water supply system is very important to prevent much

water leakage and over feeding to the machines and equipment using in the tunnel. Systematic dewatering and drainage system is important to eliminate very muddy tunnel access and provide favourable work-way in the tunnel for promoting morale standards of the tunnel workers.

Figure 21 Muddy access and clean access in tunnels.

High voltage Cables must be installed high enough for the safety of the workers. Emergency breakers must be installed according to specified standards and no leakage in the cables and wire connections must be allowed. Most of the workers get electrified in the tunnel because of Leakage in the wire or they do not wear respective PPE such as gloves and safety shoes. Accidents concerning with heavy machine occur after blasting circle while there is still some dust in the tunnel and at night because the workers do not wear PPE such as safety vest with reflection or machine operators are drunk at night.

Figure 22 Night operations.

VI. CONCLUSION

Most of the tunnel collapse occurs during night time due to lack of supervision of night shift supervisor or not enough supervisors for the whole night shift. Recommendation is to locate the tunnel engineers' unit nearest to the tunnel. Site engineer need to know the respective roles of Investigation Branch. Site engineers must value the data and information provided by those branches and have to study them carefully and thoroughly. No perfect victory will be gained without considering key factors. Tunnel portal and slope collapse occurred twice at Thahtay Hydropower Project due to insufficient geological investigation and proper judgment of site engineer.

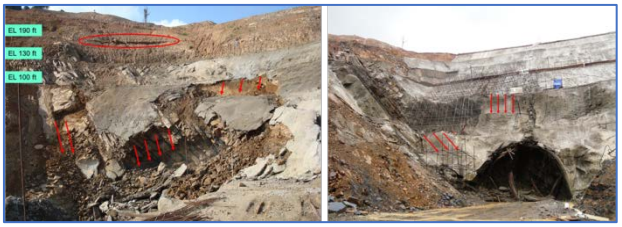

Figure 23 Tunnel portal and slope collapse occurred twice.

Tunnel collapse in the crown portion of Diversion Tunnel No.(2) outlet in Thahtay Hydropower Project occurred due to improper support system and lack of proper monitoring system.

Figure 24 Improper support system.

Adit-2 tunnel of Kun Hydropower Project was finally backfilled and closed because of wrong excavation technique and support system.

Figure 25 Collapse of wrong excavation technique.

There are many risks in tunneling work such as electric shock, machinery accidents, minor failure and major failure of tunnel and so on. Without considering key factors, we will experience loss of time, money, dignity and lives. That is why we need to emphasize on these key factors if we are going to dig a tunnel or shaft. Tunnel engineers have to compromise between safety and progress in balance. A tunnel engineer must be able to make quick and right decision when facing a problem with the tunnel. A lot of lives and property depend upon the action and decision of a tunnel engineer. This paper provides a helpful hand for all

the tunnel engineers so that they may become not only skillful but also accountable tunnel engineers of DHPI (Department of Hydropower Implementation).

ACKNOWLEDGEMENT

The author is grateful to Deputy Director General of Department of Hydropower Implementation for giving such opportunity to prepare this paper. Thanks are also due to Director of Construction No.(4) for his encouragement in preparing this paper.

REFERENCES;

Proceedings Papers

[1] Tun Min Thein. Problems and Solutions of Tunneling at PHYU Hydropower Project.

[2] Tun Min Thein. Big Shaft Excavation in Poor Geology.

[3] Tun Min Thein. Large Tunnels and Shaft Excavation in Geological Risky Region.

U Tun Min Thein, BE (Civil) is a Civil Engineer Graduated from Yangon Institute of Technology in 2002. He joined the Government service in 2004 as a Staff Officer in Ministry of Electric Power. He worked at Phyu Hydropower Project in Tunnel, Shaft, Penstock and Switchyard Constructions. In 2014, He was transferred to Tha-htay Hydropower Project as an Assistant Director responsible for Tunnels, Shaft and Power Station up to now. His Foreign experience includes training and study visits to China, Japan, Lao PDR, Sweden, Vietnam, Singapore and Indonesia.

Transition of Urban Sustainability Approach

Thi Thi Khaing[1]

Deputy Director, Department of Urban and Housing Development, Ministry of Construction, Office No.40, NayPyiTaw[1]

Email: *dawthithikhaing@gmail.com*

***Abstract* – One of the greatest challenges in our society is climate change as extremely going up temperature within a decade. In this paper, why innovative urban infrastructure should adopt designing focused on ecosystem and nature – based engineering solutions. This paper is composed of two parts, how the cities are facing the threat of socio-economic impacts due to vulnerable conventional infrastructure and ecosystem based nature solution could particularly keep to be urban sustainability. The current situation of water management in Yangon city, the more urbanization is faster, the more water demand is higher in future. The provision of surface water is very limited up to demand. The subsidence rate of Yangon city is getting worse due to extracting of underground water. Consequently, the salt water intrusion into the aquifer occurring can be noticed when the water table is getting low. This is leading to address not only water shortage happening but also flooding in vulnerable areas. Likewise, the solid waste management is needed a proper technology to dispose at the final dumping site to keep surface and ground water quality. There is no systematic way on disposal of solid waste like an opened final dumping site at surrounding of people living areas which cannot control a highly contaminated liquid called a leachate percolate into the aquifer. This is also potential to impact on ground and surface water contamination and make shorter life expectancy and the conventional drainage system is often flooded as well. Moreover, the innovative infrastructure adoption is very important to adapt the climate change and urban sustainability. This paper illustrates not only about the impacts of conventional infrastructure with low technology is highlighted but also will make effort to overcome these challenges adopting innovative infrastructure based on ecosystem function nature based solutions.**

***Keywords* – Conventional infrastructure, Sustainable Urban Drainage System(SUDS), Nature based solution(NBS).**

I. INTRODUCTION

Nowadays, the world is facing more challenges from urbanization and climate change due to increasing greenhouse gases which consequently happens the Global warming. A Half of the earth's population currently lives in Urban areas that is expected to be getting increased up to 66% in mid of this century. In Myanmar, 70% of people are living in Rural areas and the rest of the people in urban areas which is rapidly growing especially in Yangon city. Expansions of Urban area are getting increased size of the city which dramatically effects on destroying natural resources, open spaces and will have various impacts on ecosystem functioning. Consequently, the cities would be faced so many challenges that concerns climate change issues such as increasing temperatures, heat waves, heavy rain fall, Floods and droughts. This is potential to cause not only economic losses but also effect on social health and human well-being.

The objectives of the paper are as follow; (1) To provide urban policy making process (2) To adopt innovative urban infrastructure based on nature based solutions. (3) To address the socio-economic impacts upgrading technology (4) To keep the benefits of ecosystem functioning (5) To adapt climate change mitigation (6) To reduce the rehabilitation cost of capital (7) To enhance the public health and well-being.

II. CONVENTIONAL URBAN INFRASTRUCTURE

In the past, urban infrastructure ideas in land and resource management have relied on conventional engineering solutions but there is still necessary to include a holistic approach of ecosystem functioning to lead urban sustainability. Some infrastructures in Yangon city involving Housing, Road, Drainage system, parking and landscape, green space should be designed based on ecosystem and be created all inclusive ideas connecting each of its concepts.

1. The Water Management

In the current situation of water supply in Yangon city, the domestic water for a half of city population is supplied from reservoirs managed by the city Development Committee while the rest of water demand for people living in Yangon city is extracted from aquifers drilling tube wells nearby their houses where this is leading to occur a subsidence. Therefore, flooded events and seawater intrusion in Yangon areas are often occurring and vulnerable due to the effects of subsidence by extracting of underground water. Making assessment of surface deformation measurements were performed using Synthetic Aperture Radar interferometry (InSAR) with data from the recently launched Sentinel-1, the subsidence rate up to 9mm/y were found by a mapping through water extractions onto the Yangon City.

2. The Solid Waste Management

YCDC is responsible for managing "Municipal Waste" generated by residential and commercial areas which are known as a domestic waste. However, the other waste such as Electronic-wastes, Hospital wastes and Industrial wastes which are promptly needed to manage by respective authorities. In Yangon, there are 1690 tons of waste per day are normally generated from the households, commercial centres, institutions, and industries which sums up to 0.396 kg per capital per day. In case of recycled waste in Yangon, there is only 5% of the total waste could be recycled. There are six FDS (final Dumping Site) in Yangon City and they are opening dumping sites. Since the waste is not buried, there is high emission of SLCPs (short live pollutants) which would surely effect the health of the people living at surrounding area of the dumping sites. There are two obvious problems with the existing SWM practice in Yangon City if they cannot control the opened dumping site and landfill. Moreover, there is a highly contaminated liquid called leachate that is generated from decomposition of garbage and precipitation. It would be harmful to the public health and aquaculture when the leachate flows into the river or sea and it may also infiltrate and percolates downward through some aquifers. The serious environmental problems can be addressed, when the leachate reach the groundwater. There is still needed to do proper management to control the leachate from the waste so far. The relevant ministry and Department is urgently needed trying effort to enact making policy, rules and regulation regarding with solid waste management. The solid waste management at present stage is shown in figure1.

Figure 18: Hard surfaced, well-maintained access road to the disposal site

Figure 19: Flow of leachate, a major environmental issue of the disposal site

Figure 1. The present stage of the solid waste management

3. The Sewage and Sanitation Management

There is only a conventional sewage treatment plant which was constructed since 1888 and it can cover 7% of Yangon City population. The disposal of effluent Quality is facing challenges to meet with the environmental Conservation Law to conserve aquacultures in the Yangon river and diversity of species. The rest (97%) of people are using Septic tank and soak-pit system and pit latrine. However, if it is not properly built or maintained, the surface and groundwater would be contaminated which also leads to public health and pollution problems. There are so many risks to the public, especially, children and animals due to not only contact with surface water but also drink the ground water. The mosquitoes and flies can carry infectious diseases in breeding areas where liquid waste water reaches that place. It is a major issue that the greenhouse gas (Co_2) heavily reaches the atmosphere continuing impact on climate change where the proper technology could not be adopted. On the other hand, the effluent from conventional method could contaminate in ground and surface water that might affect the public health as well. Therefore, innovative Sewage management is needed to replace instead of non-functional septic tank & soak-pit in Yangon city. So, there is needed to build properly design with maintenance that is very important factor to make sure for function properly. The conventional treatment plant and Septic tank & Soak-pit at present stage is shown in figure2.

Figure 2. The present stage of conventional treatment plant

4. Conventional Drainage System

The drainage system of Yangon City was built since the colonial era. The storm water drainage system was designed by only gravity flow that the water was released to the river around the City. There is still needed to build a lot of sluice gates to control an affected tidal water to prevent floods. Making effort is still necessary to do the way like retention pond, detention pond to control the flood for a period when it is raining heavily. Proper arrangement for automatic drainage system is essential to release the water until designated level. The wet land area is still scared to land the diversity of species and to refill underground water enrichment. Even holistic concept is very crucial for ecosystem function, when the arrangement of conventional urban infrastructure have been made without connecting of each. So, the proper design for urban infrastructure is very important to do approaching ecosystem function.

The conventional drainage system at present stage is shown in figure3.

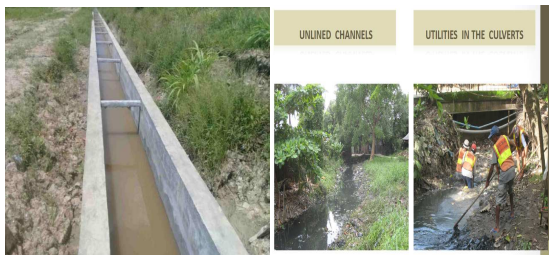

Figure 3. The present stage of conventional drainage system

III. ADOPT NATURE BASED SOLUTIONS FOR URBAN SUSTAINABILITY

Climate change is significantly impact on ecosystem functioning and people's health problems. In addition, this is leading to scare in the distribution of various native species, influencing society and socio-economic impacts. Moreover, urbanization on increasing size of the city and lack of the technology managing infrastructure are impacting ecosystem with a number of inter-linked pressure including loss and degradation of natural areas, soil sealing and the densification of built-up areas. The consequences of these pressures challenge to ecosystem functionality, the providing of ecosystem services and human well being. However, the action taken by adoption of an innovative infrastructure based solution (NBS) can typically counteract these pressures.

1. Sustainable Urban Drainage System

Flood Risk could be managed by sustainable urban drainage systems based on NBS that can minimize the potential impact of floods and save the money and time. The proper design is helpful to release not only the regular storm water by gravity flow but also the heavy flood controlling detention and retention pond by automatic system. The detention and retention pond can refill the underground water when it maintains the water for a period. Likewise, it is a kind of wet area to land the species. The landscape and road street are designed that the storm water through it before the drain. The storm water can be cleaned passing through the roots of trees and can control the flood by absorbing when it is rained. Therefore, the concept of sustainable drainage system including cleaned water, landscape and diversity of species landed on wet land areas are leading to bring cleaned environment, reduced global warming, climate change mitigation and benefits of public health. The interactive pressure of these features is resilient for ecosystem function. In particular, if sustainable urban drainage systems are cost effective, there is needed to consider for offering it instead of conventional drainage systems. The concept design depends on the strategies regarding with urban storm water management are as follows;

- On site infiltration (reduce volumes)
- On site detention (reduce top flow)
- Drain in preferably open systems
- Secure secondary drainage paths, and use multi-functional areas
- Treat the water that needs treatment

The sustainable urban drainage system can take many forms, both above and below ground. It can be used in even the smallest spaces. Good drainage design maximise the use of the available space by delivering efficient drainage together with other functions to meet the objective of the site. The drainage system should follow the guidance of provided in the sustainable urban drainage system manual, with due regard for any national or local regulatory requirements. The proper design related to storm water management including sustainable urban drainage system and wet land area for nature based solutions is shown in figure 4.

Figure 4. The sustainable urban drainage system and wet land area.

2. Green Walls and Roofs

The provision of urban green areas, street trees which may alleviate extreme temperature and uptake the nutrients while green roofs and walls installation of architectural solutions for building may reduce green-house gas and save energy. Therefore, the arrangement for proper design is needed to adopt the implementation on Nature Base Solution (NBS) that can adapt climate change and get co-benefits in urban areas such as acceleration of urban sustainability transitions and create additional multiple health and social benefits related to socio-economic equity, fairness and justice considerations. The green walls and roofs for nature based solutions is shown in figure5.

Figure 5. The green wall and green roof

3. Eco Friendly and Sustainable Sewage Management

Nowadays, there is increasingly becoming aware of how eco-friendly and sustainable options is very important to do that pollution is at a critical level and has become a serious worldwide concern. So, the people should choose ecofriendly and sustainable home sewage treatment options. The concept of modern sewage treatment technology is already based on ecofriendly process. It can reduce harmful compounds in sewage water that would otherwise cause damage to human health and natural eco systems. The technology is very essential to avoid the depletion of natural resources in order to maintain an ecological balance. A sustainable home sewage treatment system would have to operate without electricity using natural aeration to oxygenate the incoming wastewater. In addition, the NOWTR-Concept (Natural Oriented municipal Wastewater Treatment and Re-use concept) could be used to treat of municipal wastewater and sustainable re-use for natural eco-systems conserving by a low cost technology development in developing countries. It is environmentally sound and economical attractive solutions for wastewater treatment and re-use. The wastewater is anaerobically treated to gain a biogas as an alternative source of energy as well as less quantity of sludge with a very good stabilization status, and cost effective benefits as low capital, operation and maintenance cost. The treated wastewater will be naturally disinfected in polishing pond and re-used for agriculture purposes to recover the high valuable nutrients N (nitrogen), P (phosphorus) and K (potassium).

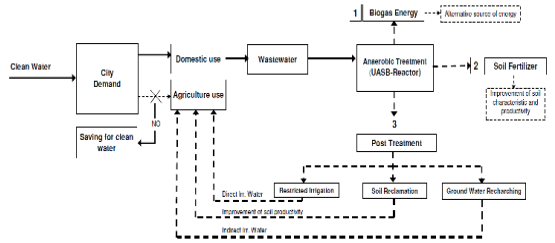

Figure 6. NOWTR Concept for Wastewater Treatment and Re-use

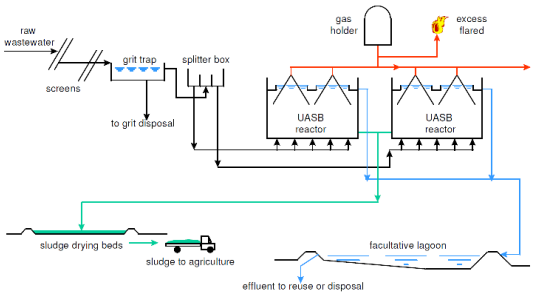

Figure 7. Flow diagram of a UASB (Up flow anaerobic sludge blanket) Treatment Plant

Successful approaches will provide a high removal-efficiency of pollutants and nutrient recovery while also reducing the carbon footprint, minimizing waste, and protecting human health and the environment. It considers various aspects of pollution prevention, control, remediation, and restoration. The applications of these technologies toward a sustainable society are considered.

4. Surface Water Treatment

Normally the surface water needs to be treated to meet the required water quality standard. Surface water typically contains a high suspended solids content, bacteria, algae, organic matter, creating bad taste and odour. There is very important to do disinfection since surface waters contain a wide range of coliforms (E.Coli), viruses and protozoa. Conventional treatment including clarification (coagulation/flocculation, sedimentation or dissolved air flotation), sand filtration, activated carbon adsorption and disinfection. Advanced treatment based on utrafiltration technology.

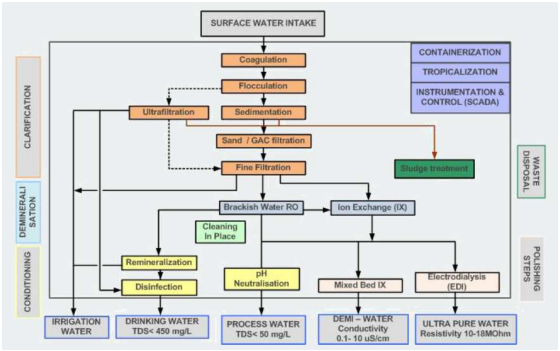

Figure 8. Surface Water Treatment Process

5. Smart City Approach

Sustainable smart city should set up managing the integration of technology and a strategic approach to sustainable development which is focused on energy efficiency, reducing pollution, keep good condition resources , citizen well-being (public safety, education, healthcare, social care) and economic development (investment, jobs, innovation).Smart city and sustainable development policies and goals must be based on smart industries and services (smart energy, water, transport, buildings and government) and supported by smart infrastructure (sensor networks, data analytics, intelligent devices, control systems, communication platforms, web services). In fact, this paper is emphasized the important of urban infrastructure to do based on ecosystem friendly to be a progressive urban sustainability. Therefore, this is very vital of basic thing to reach a designated smart level of city.

IV. CONCLUSIONS

In this paper, the concepts of conventional urban infrastructure and innovative infrastructure based on ecosystem friendly and nature based solutions are

highlighted in order to reduce greenhouse gas and get low impact development. The green spaces and sustainable urban drainage systems including detention ponds to prevent the floods that should be considered in making urban planning process in future. The sustainable waste water treatment systems should do consider the appropriate technology for the culture, land, and climate. In addition to cost and treatment performance energy aspects, recycling and social issues are important when evaluating sustainability of a wastewater treatment system in which the design criteria must be focused on environmentally friendly ecosystem. This requires a multidisciplinary approach where engineers cooperate with social scientists, economists, biologists, health officials and the public. In surface water treatment process, the sediment or sludge produced in this process could be used in agricultural fields after proper composting. The technology is very thoughtful to be simple, inexpensive and ecofriendly method could be used for urban sustainability. In particular, there is needed to create wet land areas to land diversity of species. The interaction of linkage between clean water, clean air and different species can occur an ecosystem function. Consequently, there are some benefits such as life expectancy, symbolic values, landscaping, increased bio-diversity and bio-resilience, drainage, resource-efficiency and cost efficiency by keeping ecosystem function. In addition, functioning ecosystem can ensure human societies against external disturbance and these habitats need to be resilient themselves in the face of future disturbances. Therefore, special attention is very crucial to do design urban infrastructure based on ecosystem friendly focusing nature based solution (NBS) have transformative social impact contributing to social innovation in cities. Particularly, the practices of urban infrastructure can be transition initiatives in cities can get scaled up and hence contributing to accelerating sustainability. To hope, the concept of this paper shows how to lead urban sustainability and a level of smart city.

ACKNOWLEDGEMENTS

The author wishes to express her deep gratitude to his Excellency, U Min Htein, Director General, Urban and Housing Development, Ministry of Construction, for valuable permission and kind support in carrying out this research work. The author wishes to record her thanks to Claus Pedersen, Programme Director for Urban WASH capacity building in Asia (SUWAS ITP Asia), for his guidance, suggestions and necessary advice. The author also wishes to thank all her friends for their helps and advices on her studying. Finally, the author would like to express grateful thanks to all teachers and parents for their supports, kindness and unconditional love.

REFERENCES

[1] Nadja Kabisch, Horst Korn, Jutta Stadler, Aletta Bonn "Nature-based Solutions to Climate Change Adaptation in Urban Areas"

[2] Henrik Alm, "Sustainable Stormwater Management", Stockholm Royal Seaport.

[3] Tim Van Der Horst, "Sinking Yangon; Detection of subsidence caused by groundwater extraction using SAR interferometry and PSI time-series analysis for Sentinel-1data"

Earthquake Safety Assessment of RC Buildings in Myanmar

Wai Yar Aung[1], Technical Research Engineer, Myanmar Earthquake Committee

INTRODUCTION

Before 1988, Yangon does not have many tall buildings. However, after 1988, due to economic changes, there was abrupt rise in housing demand and many mid-rise reinforced concrete buildings around six to eight storied reinforced concrete buildings were built concentrating in some crowed townships without considering earthquake risks until 2002. Therefore, it is necessary to investigate the actual condition of existing buildings. Therefore, this study focused on evaluating earthquake safety assessment of the existing buildings in Yangon, which buildings are located in high population density.

OBJECTIVES

For this study, 3 townships from urban areas and 1 township from sub-urban area of Yangon are selected to study. The main objectives of this study are:

- To assess the seismic risks of existing RC buildings.
- To calculate the structural capacity of the selected RC buildings.
- To evaluate the seismic performance and recommendation for further actions.

RESULTS

Generally, earthquake safety assessment of existing buildings is carried out in three steps as below.

- Step 1: Rapid Visual Screening
- Step 2: Numerical Evaluation
- Step 3: Detailed Analysis and Retrofitting Design

Step 3, Detailed analysis and retrofitting design, is not included in this study. Only Step 1 and Step 2 assessments were carried out based.

In addition to Step 1 and Step 2 assessments, Microtremor measurements were conducted to determine the dynamic response of the buildings and soil conditions.

Firstly, rapid visual assessment was conducted to identify the deficiencies of the building before conducting detailed analysis. Numerical evaluation was carried out for 12 buildings which having the score lower than the required cut-off score.

Step 1: Rapid Visual Screening

Rapid Visual Screening (RVS) is a rapid way of assessing the building vulnerability based on visual inspection, seismicity of the location, and vulnerable features of the building using standard survey form. Based on the RVS score, the vulnerability of the building can be estimated, and decisions can be made on whether further detail assessment is required or not. According to the RVS results, 56% of all buildings are reinforced concrete buildings without considering earthquake risks. Average storey number is between 4 to 8 stories. These buildings are built between 1984 to 2005. Average RVS Score of RC buildings in selected area is 1.67 and collapse probability is 2%.

Step 2: Numerical Evaluation

Seismic hazard level considered in this evaluation is 225-year return period with 20% of probability of exceedance in 50 years. “Life Safety” structural performance level is considered in this evaluation. Based on the initial RVS assessment and potential deficiencies, numerical evaluation was performed by calculating the internal forces of primary members and expected capacities according to the specified performance level and seismic input.

In this study, 10 Pre-Code RC Buildings and 2 Post Code Buildings are selected to evaluate Shear Stress in Concrete Columns, Overturning, Storey Drift are checked according to MNBC and ASCE 41-13. Rebound Hammer and Ultrasonic Pulse Velocity Test were conducted and Microtremor measurement was conducted and check to understand potential resonance effect according to Gosar, 2010.

This table and Chart Below shows the summary of earthquake safety of selected RC Buildings. Interpretation of table and chart is that the higher the index rate of particular section, the higher the vulnerability rate. PC means Pre-Code building and PB means Post Code Buildings. “F” means particular floor level.

Table (1) shows the summary of earthquake safety of selected RC Buildings

Building name	RVA	Shear	Overturning	Strength	Drift	Average
1BPC2F	0.41	0.11	0.07	0.11	0.13	0.82

2BPC5F	0.20	0.07	0.10	0.07	0.06	0.50
3BPC2F	0.30	0.08	0.08	0.13	0.05	0.63
4BPC2F	0.41	0.10	0.08	0.09	0.07	0.76
5BPC3F	0.30	0.13	0.08	0.11	0.10	0.72
6BPC6F	0.41	0.11	0.13	0.08	0.05	0.77
7BPC4F	0.20	0.10	0.10	0.08	0.06	0.54
8BPC2F	0.20	0.04	0.11	0.10	0.06	0.51
9BPC4F	0.21	0.09	0.10	0.07	0.06	0.53
10BPC2F	0.50	0.06	0.07	0.11	0.03	0.77
11BPB2F	0.20	0.06	0.06	0.09	0.02	0.43
12BPB6F	0.21	0.06	0.08	0.08	0.02	0.44

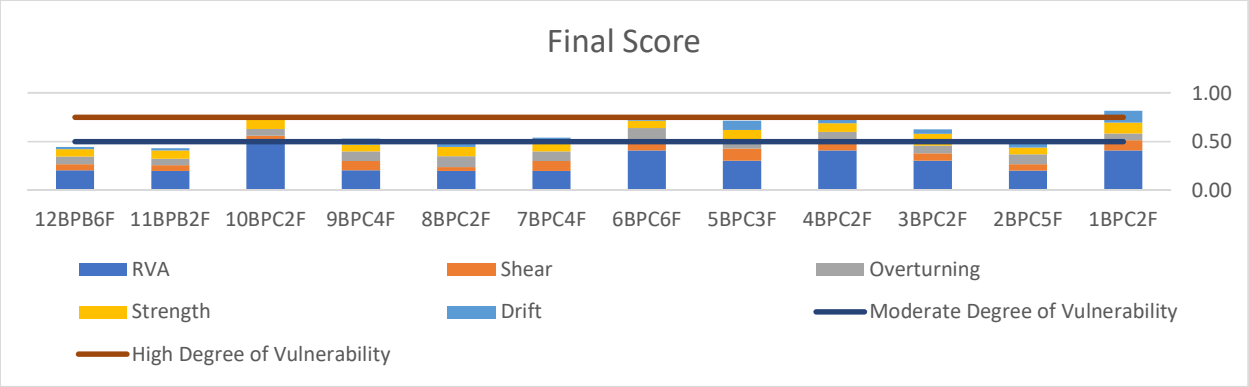

Figure (1) shows summary of earthquake safety of selected RC buildings accordance with recommended safety level

CONCLUSION

It could be clearly observed that seismic performance of pre-code RC buildings are lower than lower than Recommended Safety level because none of these buildings are designed for seismic resistance. At that time, construction technology is adequately low and quality control for construction materials were questionable. However, in Post code new buildings it could found that seismic demands were lower than Pre-Code buildings due to its good material strength and strong structural capacity of important members.

More importantly that there are a lot of RC buildings (56% of pre-code RC buildings as mentioned above) were built without considering earthquake risks. Therefore, the risks of Yangon of could be expected to high in the case of strong earthquake.

REFERENCES

Guidelines of Rapid Visual Screening of Buildings for Potential Seismic Hazards, FEMA-154P

Seismic Evaluation and Retrofi t of Existing Buildings, ASCE/SEI 41-13

Guidelines for seismic evaluation and retrofitting of existing buildings in Myanmar, Myanmar Earthquake Committee

2014-Myanmar Population and Housing Census, Yangon Region Report

Myanmar National Building Code (2016)

MARITIME EDUCATION,TRAINING AND CAPACITY BUILDING IN MYANMAR MERCANTILE MARINE COLLEGE

KHIN HNIN THANT

Marine Engineering Department,
Myanmar Mercantile Marine College (MMMC), Yangon, Myanmar
Email: khthant@gmail.com

Abstract — **In this paper, maritime education, training and capacity building process of Myanmar Mercantile Marine College at present time is introduced in specific details. The main theme of this paper is to present the effort how to improve the maritime capacity building and how to create a change in maritime education and training from skill based to education research based approach. MMMC is always finding the ways and means to deal with the change and progress of maritime education and training. Research and development is one of the central components and also the sustainable root cause for the improvement of every educational institution. The strategies and procedures to upgrade and enhance the maritime education research capacity building of MMMC are also discussed in this paper. Finally, the difficulties and challenges faced by MMMC to full-fill and align the demands from regional and international engineering accreditation bodies and awarding authorities. Thus, this paper intends to present the trend and progress of enhancing maritime education capacity building in MMMC.**

Keywords: Maritime Education and Training, Maritime Research Capacity Building, Engineering Accreditation

I. INTRODUCTION

Training and Development is the heart of a continuous effort designed to improve employee competency and organizational performance. Training provides learners with knowledge and skill needed for their present jobs. Myanmar seamen have enjoyed working in international maritime service with well-known attributes of competence, sense of responsibilities and discipline. Therefore, Myanmar needs to make endeavors in order to become a maritime nation that ensures the all-round development of maritime workers and that produced greater numbers of capable and competent seafarers, so that Myanmar will be competitive in maritime labor markets, not only in terms of quality but also in terms of quantity. For that reason, the government has upgraded with both the quality and quantity of the production of international level officers and engineers for maritime commerce through the development of human resources competent in maritime activities at the Maritime Institute.

Maritime Education and Training systems for seafarers in Myanmar includes maritime education and training units and maritime administration. Myanmar MET has a concrete foundation and has developed rapidly in these years.

Myanmar government has also encouraged of research study of Maritime Education. Maritime Education and Training (MET) System is actually needed for the

development of Myanmar economy because of the growth of working onboard ships in Myanmar has paralleled with the increase in seaborne trade.

1. Objective

The objective of this paper is to present Maritime Education, Training and Capacity Building process in MMMC.

2. Method and Scope of the Study

The method of this study is descriptive method. The information, facts and figures used in this study are secondary data obtained from the Department of Marine Administration, Myanmar Mercantile Marine College and Universities Research Capacity Building Committees.

II. MARITIME INSTITUTION TRAINING

Maritime Institutions in Myanmar can be classified into government owned and private owned institutions. The two major institutions; Myanmar Maritime University and Myanmar Mercantile Marine College are government owned institutions and are playing the vital role in the maritime education and training sectors in Myanmar. Myanmar Maritime University is mainly focus on maritime engineering education and Myanmar Mercantile Marine College is mainly for marine vocational training and education trend at present. They both are playing the vital role in the maritime education sectors in Myanmar. Moreover, there are also 10 private owned training institutions in maritime vocational training field. All maritime institutions are well organized and perform the requirements of Department of Marine Administration in Myanmar and International Maritime Organization (IMO).

III. MARITIME EDUCATION AND TRAINING IN MYANMAR MERCANTILE MARINE COLLEGE

Myanmar Mercantile Maritime College is well-known and well-organized government owned institution since 1974. MMMC mainly provides Teaching and Training Services for seafarers such as Ship Masters, Chief Engineers, Nautical and Marine Engineer Officers, Electro Technical Officers, Cadets and Ratings to serve on board Foreign-Going and Near Costal Voyage vessels and crafts. The training courses conducted in the MMMC are designed not only to provide training in relevant fields but also to give emphasizes on discipline and formation of responsible mariners to meet with the requirements of International Convention on Standard of Training, Certification and Watch keeping for Seafarers, 1978 as amended (SCTW Convention). MMMC selects and provides the trainings for seafarers in accordance to the requirements of the Department of Marine Administration (DMA) and the applicable STCW 95 requirements as amended.

Upon completion of Training and passing the relevant examination from the DMA they will possess certificates and qualifications that conform to the requirements of National and International Regulations or to the requirements stipulated by the Flag states; etc., and shall be eligible to service Worldwide.

1. Teaching and Training Aids

The Teaching and Training Services for ship's personnel, provided by MMMC do not use all their own designed syllabi, but uses syllabi that have been designed by an outside party such as International Maritime Organization (IMO) and approved by the department of Marine Administration. The teaching Aids and Simulators programs are provided by the manufacturers as software. All teaching and Training Requirements such as Teaching and Training syllabi and Training Course requirements and guides, to be in compliance with the SCTW 95 (requirements as amended). All the teaching syllabus in use by the MMMC are reviewed and approved by the Department of Marine Administration. The teaching and learning process, course conducted and training process are described in specific details MMMC website. Furthermore, we are trying our best to upgrade and full-fill with our MMMC diploma holders both COC requirements and engineering accreditation because the teaching hours, credit units and other academic requirements

of MMMC marine engineering cadet course and marine electro technology cadet course are full-fill and align with the requirements of higher education system and the demands from regional and international engineering accreditation bodies and awarding authorities.

2. Training of Trainers

It is the known fact the driving force of training activities is teaching staffs. Presently, the strength of academic staff including visiting lecturers is about 50 and 80 other staffs. To ensure the outcome of training courses meeting with SCTW requirements, strengthening of training for teaching staffs is essential. MMMC provides the teaching staffs from academic field to attend the Master Degree and Ph.D. courses related to their first degree. The teaching staffs of this institute consists mainly of professionals who have sea going experience as well as high academic and internationally recognized qualifications. Most of teachers and assessors are trained from the Maritime Universities from all over the world such as World Maritime University, Shanghai Maritime University, Korea Maritime University and Tokyo University of Marine Science and Technology. Furthermore, all academic teachers have successfully completed of the STCW Convention and based on the IMO Model Course 6.09, Training of Trainers (TOT Course) and Assessment, Examination and Certification of Seafarers in accordance with the requirements of the STCW Convention based on the IMO Model Course 3.12 (Administrators, Trainers and Assessors Course).

3. Quality Management System

MMMC has been accredited with certification by Lloyd's Register Quality Assurance (LRQA) and United Kingdom Accreditation Service (UKAS) from 6th July, 2007 to July, 2019. MMMC got its ISO certificate from Lloyd's for its well-habited Quality Management System. MMMC was intensively checked and inspected by Lloyd's within its certified period. Now MMMC got ABS Accreditation Service since August 1, 2019.

IV. MARITIME RESEARCH AND CAPACITY BUILDING IN MMMC

MMMC is always finding the ways and means to deal with the change and progress of maritime education and training. MMMC tries to improve the maritime capacity building and to create a change in maritime education and training from skill based to education research based approach. Research and development is one of the central components and also the sustainable root cause for the improvement of every educational institution.

1. Building Research Capacity

Vision of MMMC Research Building Capacity is to become the Vocational Training Centre of Excellence in Maritime Education, Training and Research field. Our mission is to produce ethically minded, and technically competent Marine officers and seafarers who have the will and ability for the maritime field. Moreover, MMMC intends to help conduct the National Maritime Education and Research and to collaborate with international Maritime Societies to share information and knowledge.

2. Ethics and Research Committee (ERC)

Ethics and Research Committee is formed in MMMC by Principal and Heads of Academic Departments. There are internal members and also external members in ERC. External members are visiting professors, lectures and experts from maritime field. The duties and responsibilities of ERC's is to enhance for the quality of research based on research ethic, scientific validity, impact on maritime industry and social contribution. As capacity assessment, identifying the main strengths and weakness of research and institutional framework at the individual, organizational level and institution level.

3. Research Training Activities

MMMC conduct Research Training Activities such as Research Ethics and Responsible conduct of Research Workshop, Short course on Research Methodology for teachers, Paper Writing

Workshop; etc. Besides, MMMC urge to do departmental research with international collaboration, maritime education research and students group term papers as the teaching & learning based research approach. Presently, we are strategic trying to prepare research oriented teaching, balancing teaching and research papers, creation of small research grants, creation of related research resources and creation of research database system. The challenges in building research capacity faced by MMMC are upgrading Research skill including language, Peer review and ISBN, ISSN recognition, internal and external funding, technological barriers, data collection, ICT infrastructure, online digital library, inadequate time for research, etc. We are trying to develop and reform from teaching to learning organization to create the progress of research capacity.

V. CONCLUSIONS

In this paper, we present the current situation of Maritime Education and Training Procedures and the functions of Building Research Capacity of MMMC. We also present how MMMC serves to stimulate improvement of MET standards. The goals and aims of the Maritime Education and Training in Myanmar need to be modified to meet with the challenges and opportunities in the international shipping world. Furthermore, we discuss the difficulties and challenges faced by MMMC to full-fill and align the demands from regional and international engineering accreditation bodies and awarding authorities. We try our best to upgrade and full-fill with our MMMC diploma holders both COC requirements and engineering accreditation. Finally, we illustrate the strategies and procedures of building research capacity in MMMC.

ACKNOWLEDGMENT(S)

This research was financially supported by the Myanmar Mercantile Marine College Research and Academic Fund.

REFERENCES

[1]. Tin Oo, The Asia Maritime & Fisheries Universities Forum 2013. Proceedings 12th The Asia Maritime & Fisheries Universities Forum 2013, Far Eastern State Technical Fisheries University, Russia, 2013. pp. 170-177.

[2]. Dr.G.Thiruvasagam, Maritime Education on India, A Study on Productivity Enhancement, The Asia Maritime & Fisheries Universities Forum 2017. Proceedings 16th The Asia Maritime & Fisheries Universities Forum 2017, Ho Chi Minh University of Transport, Vietnam, 2013. pp. 19-25.

[3]. Guideline for Establishing Research Centers at the University of Malaya.

[4]. Peter Sigmund, Good and Bad Scientific Practice, Department of Physic and Chemistry, University of Southern Denmark, Odense, June 5, 2011

[5]. Policies and Guidelines for Establishment of Research Center, Hindustan Institute of Technology and Science.

[6] Available online at http://www.mmmc.edu.mm

[7]. Building Research Capacity in Education, Evidence from recent initiatives in England, Scotland and Wales https://www.researchgate.net/publication

CAPACITY BUILDING FOR FUTURE-ORIENTED EDUCATION IN MYANMAR

Thu Thu Aung

Department of Computer Engineering and Information Technology ,
Yangon Technological University, Yangon, 11012, Myanmar

mamagyi.thu@gmail.com

Abstract— **Capacity building is the phenomenon by which individuals and organizations obtain, improve and retain the skills, knowledge and other resources needed to do their jobs competently. Capacity building in the context of developing function, solving problems within a sustainable manner involves awareness, skills, knowledge, motivation, commitment and confidence. Capacity building framework is not only for teachers but also for students. In this framework, there is a need to be synchronized with system policies and performance management. Moreover teacher improvement is based on student improvement and student outcomes. This paper aims to focus on improving effective teaching and professional learning. Professional learning without depth in evidence or theories or feedback does not enable effective growth or change that, in turn, builds capacity and develops quality in achieving student learning outcomes. Future-oriented education is important for all teachers and instructors. In addition, future-oriented education system of a country is needed to plan and to be higher education system. Because helping students developed a future-oriented perspective allows them to manage the uncertainly of the future logically in academic settings. In this paper, it intends to explore the perception of teachers and students for future-oriented education. Surveys and assessments are used as research tool from one Myanmar University included as population for future-oriented education. Some attributes such as learning outcomes and assessments include in this paper. In this study, achievements of students are mainly analyzed on two academic years. According to the basis of findings, the conclusions can be drawn. So it is very important to prepare for future needs and challenges of higher education. Capacity building and planning should be carried out better future-oriented education.**

Keywords: Capacity building, future-oriented education, learning outcomes, professional learning

I. INTRODUCTION

Higher education system of a country depends on the history, the culture, the economics and the growth potential of that country. There can measure whether a country develops or not with an effective education system. Education system is a lead role in the development of a country. In 21st century, the challenges become more and more. The influencing of universities will also have the impact of education. Higher education reflects directly with the development of economic, human beings and modern societies.

Higher education is very important for a developing country as Myanmar. Higher education promotes the economic knowledge, richer culture and intellectualism in a country. Some developed countries already planned for future perspectives of higher education and attained the futurology. A country with sustainable higher education enhances over the world.

Now a day, the progress level of a country cannot assure without training and research on higher education. The new touchstones of quality of a higher education are not only its human resource development, but also its moral commitment to society for desirable social change or progress through modernization, even strategic factorization [1].

Today, higher education is the important role of developing country like Myanmar to manage the demands and to solve the challenges of present time. So, we have to prepare ourselves for future needs, demands and challenges of higher effective education. Preparation for the future has been a primary function of education. Planning should be made about what may be expected future of higher education and how may be constructed the capacity buildings for teachers and students of effective professional

teaching and learning.

II. CAPACITY BUILDING

Ensuring capacity for lasting improvement is critical to address challenges of quality and equality [2]. The general orientation is towards addressing sets of improvement-related capacities. Especially the changing teaching and learning is absolutely needed fundamental to improvement.

Capacity building is an extremely complex endeavor. In capacity building for future-oriented education, the sustainable teaching and learning is the core for school, college and universities. Life-long learning based on higher effective education of a country, continuous learning of teachers and institutions itself for the purpose of enhancing students learning, influenced by individual teachers within an institution of that country.

So today building capacity for future-oriented education is facing on as a challenge of country improvement. Capacity building also needs to provide support for and development of a wider workforce. Several countries have adapted to this agenda by developing integrated community schools and services [2].

In a rapidly changing world, capacity building needs to address both the present and the future. A recent widening of the educational agenda to include, among important outcomes, involving both internally and supporting them externally of teachers and students.

A large body of education improvement literature highlights generic features of improvement, frequently citing the following: a focus on learning and teaching; using data to help guide improvement efforts; high quality professional development, embedded within professional learning communities [2].

In this paper, framework is provided by analysis of improvement and effectiveness based on research, practice and strategies as evaluation tools worked with university to support and quality assure self evaluation efforts.

Capacity building for future-oriented education approaches different countries strategies of education. There are also efforts in several other countries to find ways to help build capacity in universities facing significant challenges where student achievement is poor, including government initiatives in their own system.

Improving what goes on in the classroom was synonymous with instructional improvement; finding out what instructional strategies were linked with better student outcomes and thinking of ways to build teachers‟ capacity to use these strategies [2].

In many cases, curriculum, learning and teaching strategies can offer to success the future-oriented education. So learning outcomes and assessments of teachers and students are analyzed to forecast and prepare for future education in this paper.

III. OBJECTIVES OF THE STUDY

The major objectives of the study are the following:

- To focus on improving and effective teaching and professional learning in Myanmar,
- To intend to perception of teachers and students for future-oriented education in Myanmar,
- To prepare achievement on teachers and students capacity needing for future higher education,
- To fill the demands based on teachers and students suitable on education environment and society in Myanmar country.

IV. DATA COLLECTION

In this study, some course information, learning outcomes and assessments of teachers and students from Computer Engineering and Information Technology Department on Yangon Technological University in Myanmar were collected as input data. Out of the whole population, students' achievement and assessments on each subject and individual teachers included on academic year. In compliance with the university's guidelines regarding classroom research, all the study materials were reviewed to the implementation of the study. Data were collected in a class which had the second, third, fourth and fifth year students on CEIT 2nd batch course files.

V. METHODS AND PROCEDURES

This paper was descriptive research in nature. A class which a subject on one academic year consists of course information and mapping. According to relevant subjects, different course information and mapping. But a class met fifty minutes per session, at least three days a week. This survey based on different subjects in one academic year. Assessment is a process of measuring and collecting the data (mark/score) in a manner that enable to analyze the achievement of the intended learning outcomes and the effectiveness of the learning activities.

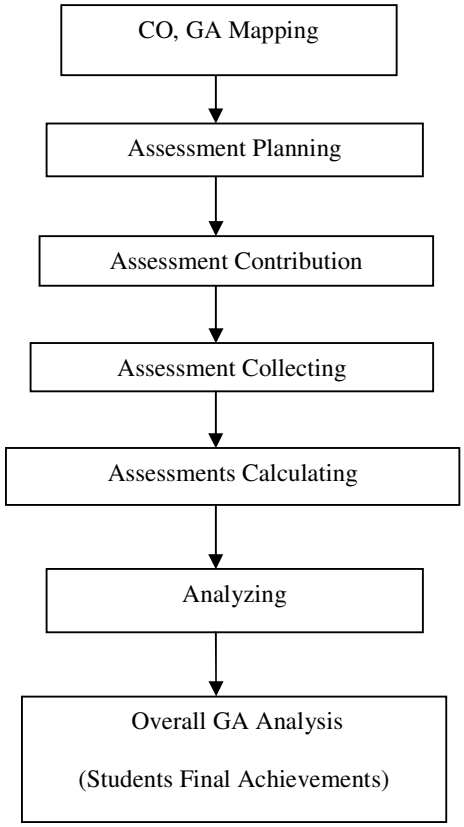

Figure 1 The steps of assessment plan

In step 1, course outcomes (CO) description was mainly based on syllabus; topics and level of difficulty and graduate attributes (GA) have twelve types of assessments such as engineering knowledge, problem analysis and life-long learning etc. CO description and GA are connected as a mapping.

In step 2, assessment planning, course works marks such as assignments, tutorial, practical and exam marks are connected with GA.

In assessment contribution, CO distributions and GA distributions are calculated based on assessment items such as course work and final exam.

In assessment collecting, the percentage of course work and exam for each student is calculated based on CO and GA distributions.

In assessment calculating, the achievements of each student are calculated based on CO and GA distributions. Then grading of each student is got and the numbers of students got different grading are calculated.

In step 6, course outcomes achieved by students with KPI (Key Performance Indicator). In KPI, excellent is noted by pass 100% with minimum 20% A, good is more than 80% pass, fair is more than 60% pass and bad is more than 40% fail.

In finally, overall GA analysis included GA mapping, GA marks distribution and student achievements with KPI are achieved for each course/subject on one academic year.

VI. EXPERIMENTS

According to assessments, the achievements of students on each course for each year in one academic year can be calculated.

For example, the student achievement of one subject for second year student in one academic year can be found in Table 1.

Table 1 The sample of student achievement

Subject- Introduction to Computer System		
Overall GA Analysis		
	Engineering Knowledge	Modern Tool Usage
	GA 1	GA 5
GA- Mapping	CO (1,2,4)	CO 3
GA- Mark Distribution	71.0	29.0
GA- Student Achievement	69	66

KPI : above 60% GA Achievement

Student Achievement : GA 1 and 5 above 60%

In Table 2, the achievement of third year student can be found on one subject in one academic year.

The student achievements of fourth and fifth year on one course can also be found in one academic year in Table 3 and 4.

The following Table can also describe the KPI based on the GA achievement. Therefore, according to the KPI and student achievement, it can know and study how the capacity building is raised for the next academic year. So assessment calculating, CLO and PLO mapping, KPI and achievements support to improve for future education.

Table 2 The sample of achievement for third year student on one course

Subject – Operating System I			
Overall GA Analysis			
	Engineering Knowledge	Problem Analysis	Investigation
	GA 1	GA 2	GA 4
GA-Mapping	CO 1	CO 2	CO (3,4)
GA-Mark Distribution	30.0	12.0	58.0
GA-Student Achievement	72	78	58

KPI : above 60% GA Achievement

Student Achievement : GA 1 and 2 above 60% ,

GA 4 under 60%

Table 3 The sample of achievement for fourth year student on one subject

Subject – Software Engineering		
Overall GA Analysis		
	Engineering Knowledge	Problem Analysis
	GA 1	GA 2
GA- Mapping	CO 1	CO (2,3,4)
GA-Mark Distribution	27.0	73.0
GA-Student Achievement	73	80

KPI : above 60% GA Achievement

Student Achievement : GA 1 and 2 above 60% ,

Table 4 The sample of achievement for fifth year student on one course

Subject – Artificial Intelligent			
Overall GA Analysis			
	Engineering Knowledge	Problem Analysis	Investigation
	GA 1	GA 3	GA 4
GA-Mapping	CO 1	CO (3,4)	CO 2
GA-Mark Distribution	33.0	42.0	25.0
GA-Student Achievement	85	78	79

KPI : above 60% GA Achievement

Student Achievement : GA 1, 3 and 4 above 60%

VII. CONCLUSIONS

According to the final achievement results, teachers can prepare their course and teaching techniques for next academic year. In addition, planning can draw the better teaching and learning strategies and then their capacity can also be built on future-oriented education for their students and learners to improve.

ACKNOWLEDGMENT(S)

The author would like to acknowledge the support of Myanmar Engineering Council and Society. And then I would like to thank the Rector and the teachers from Yangon Technological University.

REFERENCES

Journal Papers

[1] Saima Rasul, Qadir Bukhsh, Muzamilla Akram, Opnion of Teachers and Students about Futurology of Higher Education in Pakistan, International Journal for Cross-Disciplinary Subjects in Education (IJCDSE), 1(4), 2010.

[2] Louise Stoll, Capacity Building for School Improvement or Creating Capacity for Learning? A changing landscape, Journal of Educational Change, 10(2):115-127.

[3] Skylar Davidson, Futurology in the College Classroom, https://www.researchgate.net/publication/304353984.

Books

[4] Abasyn University Ring Road Peshawar Subject: Trend & Issues in Education: Unit 01, Futurology and Education, pp. 1-31.

[5] Hopkins, D, Every School a Great School. Maidenhead: Open University, press, 2007, McGraw-Hill.

IMPLEMENTATION OF SCADA SYSTEM FOR HYDROPOWER STATION

Aung Kyaw Myint[(1)], Kyaw Zin Latt[(2)], Tin Tin Hla[(3)], Nay Min Tun[(4)]
Department of Electric Power Generation Enterprise, Branch of Renewable Energy and Hydropower Plant

aungkyawmyint84@gmail.com[(1)], kyawzinlattsbo@gmail.com[(2)], tintinhla99@gmail.com[(3)], naymintun.ec2@gmail.com[(4)]

ABSTRACT

This paper presents an efficient and automatic data monitoring IoT based SCADA system which is capable of monitoring the hydropower station with electronic devices in real time operation mode. The system has been utilized the IoT based platform and ESP 8266 Node MCU wireless communication modules to transfer the data on watching the IoT cloud on anywhere with internet acceptance. There are two hardware modules namely RTU (Remote Terminal Unit) and MTU (Main Terminal Unit). ESP 8266Wi-Fi modules are used to configure in master and slave mode for SCADA system. Microcontroller is used to set out the command to PLC for driving the generator status (on/off). Crucial histogram data such as active power, current, voltage, frequency, power factors, temperature, pressure, vibration will be taken into accounts with respective sensors which have been configured into the several components of the power station. The IoT platform is used to design the user interface to display the real time operation and information of hydropower station being monitored the authorized personal on anywhere assessments via the internet.

KEYWORDS: *SCADA, IoT, ESP8266, IoT Platform, Microcontroller*

1. INTRODUCTION

SCADA is acronym from "Supervisory Control And Data Acquisition" which refers to the combination of telemetry and data acquisition and encompasses the data collection, transferring it back to the central site, carrying out any necessary analysis and control anyhow displaying the collected data on PC or any detected embedded devices that are specialized to operate in hydropower station. SCADA system that is implemented in every hydropower plants rather than all in plants are automatically performed by the RTU with PLC. To execute a feasibility study for data monitoring and control system of hydropower plant, it is necessary to control model design to implement the data collection and control system in hydropower plants. Simulation and emulation system for hydropower station use MATLAB and SCADA to process information and make it available to the operator in real time operation [1]. However, in this paper, control system design is proposed for SCADA system of hydropower plants to create the data acquisition and control in the generator side. The OPC (Object linking and embedding for Process Control) is used for communication system to improve the integration between all devices without requirement for specific drivers for each pair of devices [2]. Wireless communication interface is used to transfer the collected data from hydropower station's components such as power line, transformers, generators, thrust bearing, upper guide bearing, lower guide bearing, turbine guide bearing, stator coil, water inlet and outlet system, condition of upstream and downstream level, rotor and cooling water system in this paper. Practical implementation of SCADA system for Falluja substation is made up of 3RTU devices that are used to collect data from 10N 6200 devices installed inside incoming and outgoing panels for 11kV and 33kV. The collected data is then sent to main terminal unit control operator via rotor for power monitoring, control and energy management functions [3]. The main objective of SCADA system is to supervise, control, optimize, and manage the generation system and transmission system. The main components of this system are RTUs that collect data automatically and are directly connected to sensors, meters, loggers or process equipment. RTUs contain all of the transceivers, encoders and processors needed for proper functioning in the event that a primary RTU stop working. Report status of components can be performed by Programming Logic Controller (PLCs) [4]. In the paper of SCADA on Hydropower Plant Cascade Case Study, Network Architecture SCADA System are DCS (Distributed Control System) using TCP/IP

protocol and an internet network and communication network is the fix and mobile telephone network to communicate with remote devices operators [5]. The purpose of smart transformer using PLC and SCADA says that the various parameters monitoring system design to optimize the system operation, system reliability, moreover, to integrate protection control system and monitoring system of electrical parameter together for optimum condition [6].

2. METHODOLOGY

Software and hardware implementation of SCADA system is demonstrated and proposed for monitoring the information of hydropower station from various sensors at Remote Terminal Unit (RTU) and Master Terminal Unit (MTU). Wireless communication interface is used between the RTU and MTU.

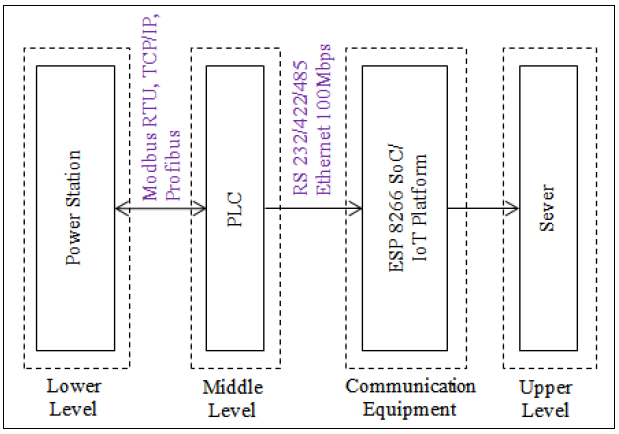

Fig 1. System Block Diagram

Fig 1 demonstrates the implementation of a SCADA system for a power plant, meant to supervise and control field electrical devices, motor and generator using Mitsubishi PLC software and equipment. At the lower level of power station measuring transducers are located. The most common protocols are Modbus RTU, Modbus TCP/IP, and ProfiBus. At the middle level, PLC is used to act as the device of collection, processing and data transmission to the upper level. PLC is installed for a modulator structure that includes modules: digital input, digital output, analog input, and analog output, the interface modules (VF, RS-232/422/485, and Ethernet). Different technologies can be used as communication equipment for experimental studies. In this research work, ESP 8266 SoC is as the communication equipment to monitor the data on IoT platform from any location using Internet Service Provider (ISP).All the information about the power system must be processed and used to optimize the operation [7].

2.1. Hardware Implementation Design

Fig 2 demonstrates the design of SCADA-based hydropower control system. The design of hardware was to implement a schematic diagram to find out the connection of electronic components in these SCADA systems. The main components are

(1) ESP 8266 Wi-Fi Module
(2) AT Mega 328 microcontroller
(3) Programmable Logic Controller
(4) PZEM-014/ 016 AC Communication module and sensors

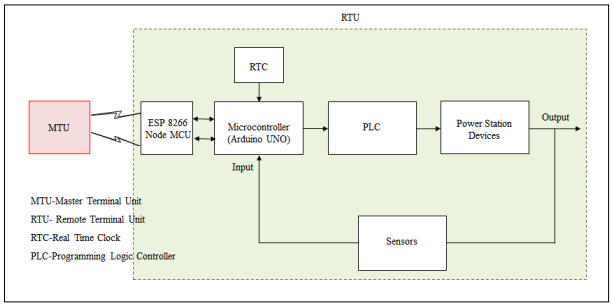

Fig 2. Design of SCADA-Based Hydropower Control System

2.1.1. ESP 8266 Wi-Fi Module

ESP 8266 Wi-Fi Module is a self-contained SoC (System-on Chip) with integrated TCP/ IP protocol stack that can give any microcontroller access to Wi-Fi network. It is capable of either hosting an application or offloading all Wi-Fi networking functions from another application processor. This module is an extremely cost effective board with a huge and ever growing community. It has a powerful enough onboard processing and the storage capacity that allows it to be integrated with the sensors and other application specific devices through its GPIO pins with minimal development up-front and minimal loading during run time. ESP 8266 supports APSD for VOIP applications and Bluetooth co-existence interfaces and contains a self-calibrated RF allowing it to work under all operating conditions and requires no external RF parts. It can be imply into an IoT. Flash memory size of ESP 8266 new version has increased from 512 kB to 1MB. [8]

2.1.2. AT Mega 328 microcontroller

AT Mega 328 microcontroller is a single-chip microcontroller that is commonly used in many projects and autonomous system. This chip is implemented on the Arduino Uno and Arduino Nano models. AT Mega 328 is basically an Advance Virtual RISC (AVR) microcontroller and supports the data up to eight bits and has 32kB internal built in memory and 1kB Electrically Erasable Programmable Read Only Memory (EEPROM). Moreover, it has 2kB Static Random Access Memory

(SRAM) and has several different features that consist of advanced RISC architecture, good performance, low power consumption, real timer, counter having separate oscillator, 6PWM pins, programmable serial USART, programming lock for software security, throughput up to 20 MIPS. It is the heart of Arduino Uno and operates the ranging from 3.3V to 5.5Vhowever; normally operation is 5V as a standard usage in embedded systems applications. [9]

2.1.3. Programmable Logic Controller (PLC)

PLC is a special form of microprocessor based controller that uses programmable memory to store instructions and specific functions that include On/ Off control and to implement functions such as logic, sequencing, timing, counting and arithmetic in order to control machines and process. Advances of PLC control systems are flexible, faster time response, less and simpler wiring, solid-state (no moving parts), modulator design (easy to repair and expand), handles much more complicated systems, sophisticated instruction sets available, allows for diagnostics (easy to troubleshoot) and less expensive. PLC is used with the input and output sections that are where the processor receives information from external devices and communicates information to external devices to acquire the data and control the machine. [10]

2.1.4. PZEM-016 AC Communication Module and Sensors

PZEM is mainly used for measuring AC voltage, current, active power, frequency, power factor and active energy. The module is without display function but the data is read through the RS485 interface. This data is primary data of hydropower station such as power line, transformers and generators. [12].

Temperature sensor, PT 100 is used as industrial temperature sensor to measure high range temperature (200°C). DHT11 is a basic, ultra-low-cost digital temperature and humidity sensor that is used to measure the surrounding air and spits out a digital signal on the data pin. Temperature is essential information of transformers, thrust bearing, upper guide bearing, lower guide bearing, turbine guide bearing and stator coil of hydropower plant. Moreover, pressure sensor is used for water inlet (penstock) and outlet (draft tube), water level sensor is needed for upstream and downstream of hydropower plant and vibration sensor is mainly used for rotor (rotating for turbine).

2.2. Software Implementation

The main focus of Industrial Internet of Things (IoT) is to enable communication across a range of devices and IoT uses protocols such as MQTT (Message Query Telemetry Transport) to make it possible to communicate across different devices throughout the entire system for acquiring the data from sensors. Two program codes are developed to program the microcontroller (Arduino UNO) and ESP 8266 Node MCU Wi-Fi Module. These microcontrollers are used to receive the data from sensors by using the C language code. Moreover, Ladder program is used on Programming Logic Controller (PLC) to control the ON/OFF state such as the generator control system of hydropower station. SCADA system lacks the much needed interoperability, which is a mandate for developing seamless programmability for devices and sensors. The IoT can reduce the hardware devices, while also eliminating the need for software licensing and upgrading by using the cloud services. [11]

No.	Collection Data	For Objective Items
1	Active Power (W)	Power Line, Transformers and Generators
2	Current (A)	
3	Voltage (V)	
4	Frequency (Hz)	
5	Power Factor	
6	Temperature (^{o}C)	Transformers, Thrust Bearing, Upper guide Bearing, Lower guide Bearing, Turbine Guide Bearing, Stator Coil
7	Pressure (Pa)	Water Inlet (Penstock), Water Outlet (Draft Tube)
8	Water Level (m)	Up Stream and Down Stream
9	Vibration (m/s^2)	Rotor
10	Flow of Water (m/s^2)	Cooling Water System for all Bearing, Shaft Seal

Table 1. Important data of hydropower station

Table 1 expresses the essential data that is concerned with the sensors of hydropower station's components. In this paper, the information of hydropower station has already been collected by using the sensors. However, the information such as active power, current, voltage, frequency, power factor and temperature on the above mentioned data will be found out.

3. Experimental Results

SCADA system is used Open Platform Communications (OPC) for collecting data and IoT Standards that like it are used to enable real-time device communication within plant floors that use different devices and sensors from different manufactures. IoT Standard is often known as Industry 4.0. [13] In this section, the operation of data acquisition and control system for some essential data of hydropower station on

SCADA system is demonstrated. Fig 3 indicates the hardware implementation of electricity monitoring system.

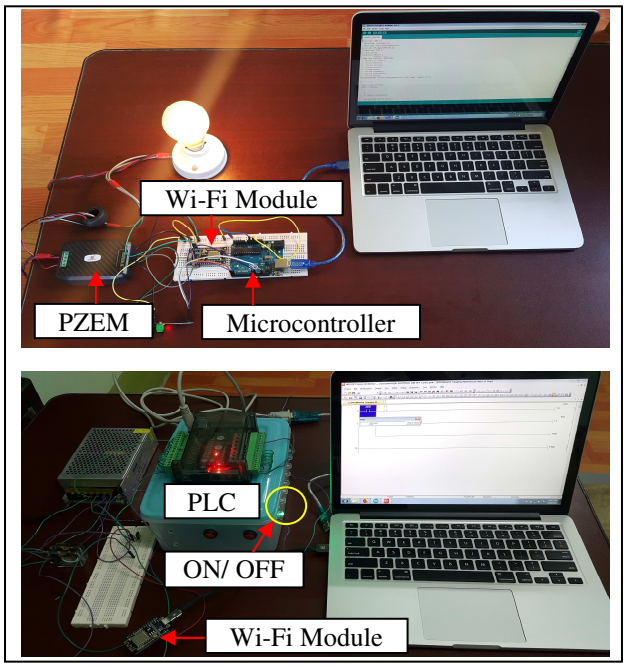

Fig 3. Hardware Implementation of SCADA System

Fig 4 points out the collected data from the sensor to post on IoT cloud. The interface between hardware and software implementation for SCADA system was based on the IoT cloud.

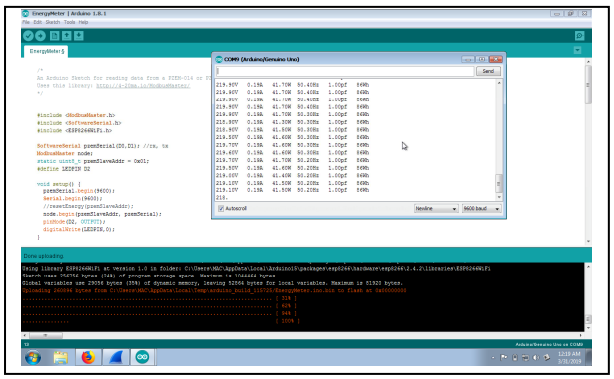

Fig 4. Sending the collected data to IoT Cloud

Fig 5 expresses the Monitoring System using IoT Platform. There have been several conditions for various kinds of control purposes. The top level control could be accomplished with the control panel on the monitoring windows of SCADA system of hydro power station in real situation.

Fig 5. Energy Data for Monitoring System Using IoT Platform

Fig 6 shows the Temperature Data for Monitoring System Using IoT Platform. It is only considered on the monitoring of temperature values for that station.

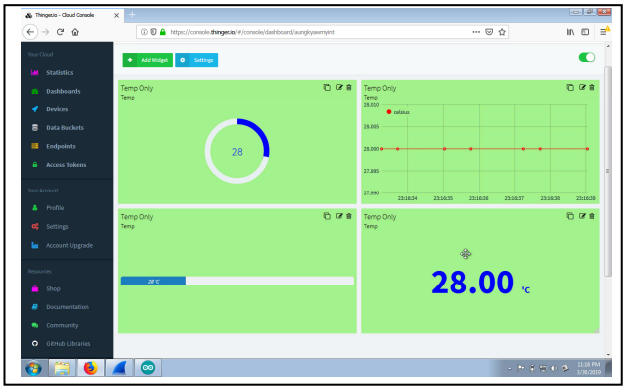

Fig 6. Temperature Data for Monitoring System Using IoT Platform

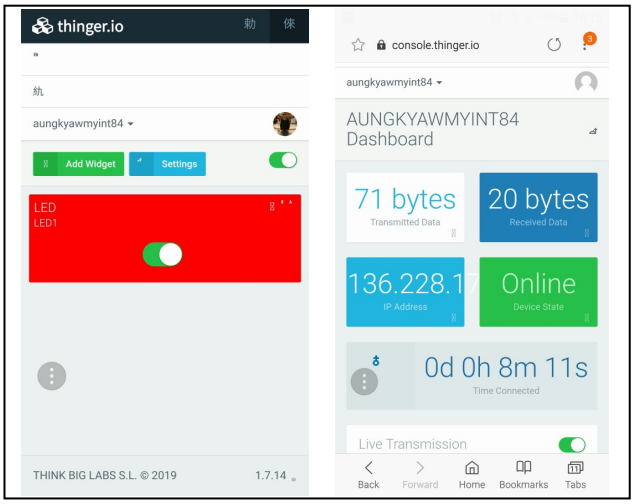

Fig 7. Master Terminal Control over Remote Terminal Unit

Normally, the temperature control system could be maintained the stable condition of the station in real world. Fig 7 illustrates the Master Terminal Control over Remote Terminal Unit into the cloud based system. Fig 8 mentions the comparison between experimental results and calculated results from power equations (P=VI). Table 2 shows that the tolerance between actual values

and calculated values is ±3% over specific values of the devices.

Time	Volt-age	Curr-ent	Power from Modbus	Calcu-lated Power	Accur-acy Rate	Tole-rance
6:00:00	186.5	0.17	32.5	31.7	98%	2%
6:04:00	183.6	0.17	31.7	31.2	98%	2%
6:08:00	181.8	0.17	31.3	30.9	99%	1%
6:12:00	188.8	0.17	33.1	32.1	97%	3%
6:16:00	189.7	0.18	33.4	34.1	102%	-2%
6:20:00	191.2	0.18	33.8	34.4	102%	-2%
6:24:00	186.4	0.17	32.6	31.7	97%	3%
6:28:00	188.3	0.18	33.1	33.9	102%	-2%
6:32:00	189.7	0.18	33.5	34.1	102%	-2%
6:36:00	188.1	0.18	33.1	33.9	102%	-2%
6:40:00	193.9	0.18	34.6	34.9	101%	-1%
6:44:00	191.6	0.18	34.0	34.5	101%	-1%
6:48:00	194.9	0.18	35.0	35.1	100%	0%
6:52:00	202.6	0.18	37.0	36.5	99%	1%
6:56:00	200.3	0.18	36.4	36.1	99%	1%
7:00:00	200.2	0.18	36.4	36.0	99%	1%

Table 2. Calculated Data for Power Accuracy Rate

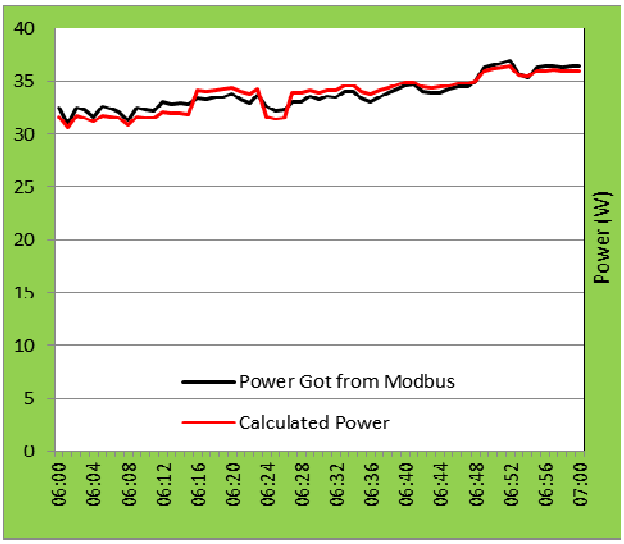

Fig 8. Comparison between Experimental Results and Calculated Results

4. CONCLUSION

The implementation of SCADA system on IoT Cloud is a low-cost technology at power plants. This implemented system can be assisted the industrial control system such as energy monitoring and control algorithm, distribution of electricity on open source protocols. The experimental results were proved that the supervisory control and data acquisition system have to successfully monitor voltage, current, frequency, energy, active power, power factor and temperature and control the on/off state of PLC. For future scenario implementation, it could be modified the system by creating own website with database for saving the data, electrical parameters of hydropower plant and then can control from it.

ACKNOWLEDMENT

The author would like to express heartfelt thanks research supervisor for enthusiastic guidance on shortfall this paper. The author absolutely gratitude to his teachers and many colleagues from the control engineering research group under the Department of Electronic Engineering of Mandalay Technological University.

REFERENCES

[1] Gilberto Schneider, Vanessa F. de Lima, Lucas G. Scherer, Robinson F.de Camargo and Claiton M. Franchi, Power Electronics and Control Group "SCADA System Applied to Micro Hydropower Plant" in Federal University of Santa Maria, 2013 IEEE.

[2] D.Wei and Q. Chen, "The technology of OPC and its application in Supervisory information system of hydropower plant," in Computing, Communication, Control and Management, 2009. CCCM 2009. ISECS International Colloquium on, vol. 2, pp. 237-240

[3] D Mohamed, "Practical Implementation of SCADA System for Fallujah Substation", Research Gate, 2009

[4] Mackay, S., Wright, E., Reynders, D. "Practical Industrial Data Network : Design, Installation and Troubleshooting" Newnes, 2004

[5] Ioan Stoian, Eugen Stancel, Dorina Capatina, Ovidiu Ghiran, Istvan Kovacs, Teodora Sanislav "SCADA on Hydropower Plant CASCADE CASE STUDY" in Cluj-Napoca, Romina, 2007 IFAC Workshop ICPS'07

[6] Neethu Nm, Anil Das, Sarath S, NithinPremsy, Anagha, "Smart Transformer using PLC and SCADA" in International Journal of Multidisciplinary Research and Development, 2016

[7] Industrial Control for SCADA System

[8] www.udemy.com : IoT Automation with ESP8266

[9] www.alliedelec.com; Arduino UNO

[10] www.mitsubishielectric.com FX PLC Main Unit MELSEC-F Series

[11] www.arduino.cc Arduino IoT Cloud

[12] https://community.openenergymonitor.org

[13] https://www.softwebsolutions.com Comparative analysis of SCADA system vs industrial IoT

Simulation and Analysis on Power Factor Improvement and Harmonic Reduction of High-voltage, High-frequency Power Supply for Ozone Generator

Nwe Ni Win[1], Yin Yin Pyone[2], Mai Kai Suan Tial [3]
Department of Electrical Power Engineering, Technological University (Taunggyi)
The Republic of the Union of Myanmar
[1]nweniwin150044@gmail.com, [2]yinyin260380@gmail.com, [3]maikaisuantial21@gmail.com

Abstract- **Ozone generating system needs High Voltage, High Frequency (HV-HF) power supply. The ozonizer distorts the supply currents and henceforth affects the supply power factor. This paper presents the application of active power filter (APF) for power factor improvement and harmonic reduction in power supply of ozone generation system. The conventional inverter has front end bridge rectifier with smoothing inductor/capacitor. It draws non-sinusoidal current from AC mains; as a result input supply has more harmonics and poor power factor. Hence, there is a continuous need for power factor improvement and reduction of line current harmonics. The proposed system has active power factor which is used to achieve sinusoidal current and improve the supply power factor. The active power factor correction (PFC) converter with pulse width modulation (PWM) inverter fed ozone generator generates more ozone output compared to the conventional inverter. Thus the proposed system has less current harmonics and better input power factor compared to the conventional system. The performance of active power factor (APF) applications are compared and analyzed with the help of simulation results using Matlab/Simulink.**

Keywords: Active power filter, Harmonic reduction, High voltage, High frequency power supply, Ozone generator, Power factor improvement

I. INTRODUCTION

Ozone (O_3) is considered as an excellent powerful oxidizer and germicide. Its disinfection potential is significantly higher than chlorine and other disinfectants. Nowadays, ozone is widely used for disinfecting and oxidizing in substitution of chlorine, due to the latter's by products such as smell, bad taste and carcinogenic agents resulting from it. Indeed, ozone produces much less byproducts and ozone itself is transformed into oxygen within a few hours. Applications of ozone technology are various and could be found in disinfection, water and air purification, medicine and so on.

The use of high frequency power supplies increases the power density applied to the ozonizer electrode surface which in turn enhances the ozone production for a given surface area, with reduced peak voltage requirement. By increasing the operating frequency the ozone production can easily be controlled. Many compact converter topologies have been proposed in order to improve efficiency of the ozonizer. Some power supply derived from AC main supply. In this case the front end has uncontrolled rectifier with a large DC link capacitor. This rectifier is widely used because of its simplicity and robustness but with the distorted line currents. As a result, the input power factor is poor. Various power factor correction (PFC) techniques are employed in converters to overcome these power quality problems out of which the basic boost converter topology has been extensively used in various power supply conversion applications. Implementing power factor correction (PFC) into low frequency to high frequency power supplies will maximize the power handling capability of the power supply and current handling capacities of power distribution networks.

With conventional high voltage high frequency power supply, the poor power factor and harmonic distortions are the main problem for Ozone generator. This type of utility interface draws excessive peak input currents; it produces a high level of harmonics, and both the input power factor (PF) and total harmonic distortion (THD) are poor. The low PF makes the efficiency of the electrical power grid to be very low. Regulatory standards with origins in Europe (EN 61000-3-2) and North America (IEC 1000-3) have been established that aim at protecting the utility grid from excessive harmonics [1]. Currently, IEEE 519 is used for harmonic regulations. In order to meet the harmonics limits imposed by these standards, new active power filters (APF) are used.

The aim of the present work is the development of an efficient active power filter (APF) for high voltage, high frequency (HV-HF) power supply of a ozone generator, consisting in power stage, filters and control circuit. The modeling and simulations are executed using Matlab/Simulink software.

II. OZONE GENERATOR

The configuration of the ozonizer used in this work is shown in Figure 1. This type of ozonizer is designed for operation at high frequencies (up to 15 kHz) and ozone is generated by means of a silent

discharge, also known as dielectric barrier discharge (DBD). In this type of discharge a high AC voltage is applied between two electrodes one of which is covered with a thin dielectric layer, such as glass, ceramic material, etc. The dielectric barrier prevents from spark generation between the two electrodes [2].

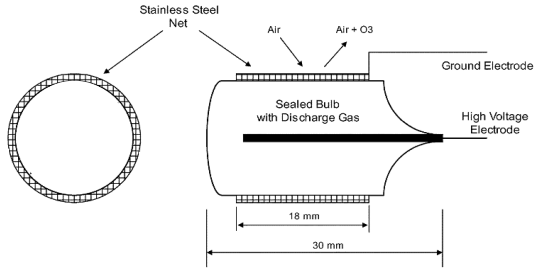

Figure 1 Configuration of ozonizer

Thus, the plasma that takes place in a silent discharge self-extinguishes when the charge built up on the surface of the dielectric layer reduces the local field. In the ozonizer shown in Figure 1, one of the electrodes is formed by a stainless steel net and the other is implemented by means of plasma inside a sealed bulb. The dielectric used is borosilicate glass, which exhibits a high electric strength. The surrounding stainless steel net provides also the necessary air gap inside which the oxygen in the air is partially converted to ozone by the action of the silent discharge.

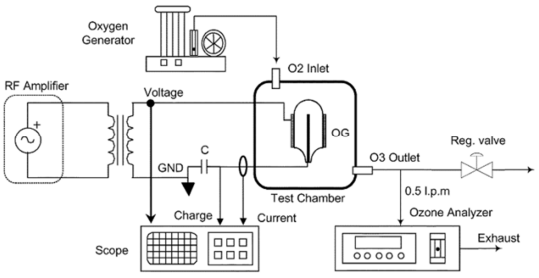

Figure 2 Power supply arrangement for ozonizer [2]

The ozonizer has been supplied electricity using the arrangement shown in Figure 2. The ozonizer is supplied with a sinusoidal waveform from a radio-frequency amplifier by means of a step-up transformer.

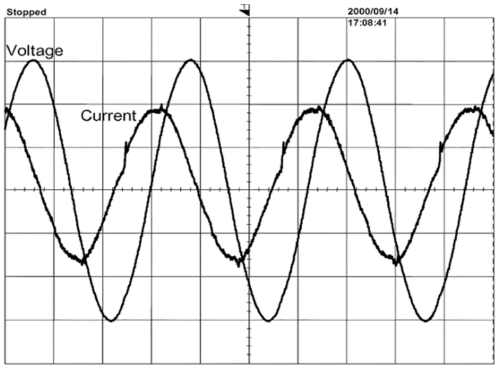

Figure 3 Voltage and current waveforms of power supply used with ozonizer [2]

The selected supply frequency is 6 kHz in this research. Figure 3 illustrates the voltage and current waveforms in the ozone generator. Some current ripple can be observed near the positive and negative peaks of the current waveform, due to the micro discharges generated by the applied voltage. By varying the gain of the RF amplifier the ozone generator was supplied with different voltage amplitudes. The nominal rms voltage of the ozone reactor is 5 kV in this research. The supply voltage ranges from approximately 1 kV to several kV [2].

III. HIGH VOLTAGE, HIGH FREQUENCY POWER SUPPLY FOR OZONIZER

Since ozone cannot be stored, it must be generated on site. High voltage electric discharges are widely used in industry and the dielectric barrier discharge (DBD) method is considered as the most efficient way to produce ozone as shown in Figure 4. Oxygen is injected to pass through a small discharge gap between two high voltage electrodes, one of them or both being covered by a dielectric layer in order to avoid sparks taking place. The reason for the different configurations of dielectric is due to the multiple applications of the DBD. For example, in the case of waste gases sterilization and ozone generation, at least one electrode is covered by a dielectric. While for DBD new generation lamps, the gas in the lamps is completely isolated from the metallic electrodes, which are covered with a dielectric layer. In this way, gas contamination is prevented and the lifetime of the lamps is enhanced [3].

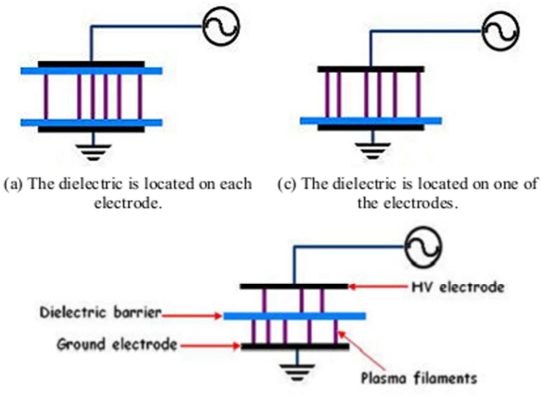

Figure 4 Dielectric barrier discharges with a gas gap [3]

These devices are usually supplied by a high voltage, high frequency (HV-HF) power supply, since high frequency decreases the necessary power to be used and increase the ozone production rate. Thus, the power density applied to the discharge surface is increased as well as the ozone generation rate, for a given surface area, while the necessary voltage is decreased. The increase in the frequencies up to several kilohertz is now

feasible using power electronic switching devices, such as MOSFETs and IGBTs [3].

The HV-HF power supply comprises a control circuit stage for generating a high frequency square signal and a power block composed of four MOSFETs/IGBTs controlled by the square signal. At the same time, a rectified and adjustable voltage, that feeds the primary of a step up high frequency ferrite transformer, is transformed in a high frequency signal by the MOSFETs controlled by the square signal, thereby obtaining an adjustable high voltage output. The main circuit of the ozone generation HV-HF power supply is shown in Figure5. The switches used are MOSFETs/IGBTs, in parallel with diodes necessary to prevent from conducting a reverse current.

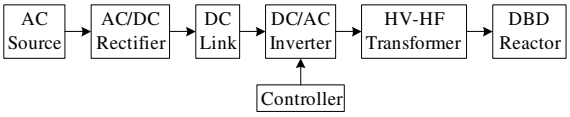

Figure 5 System block diagram of high voltage high frequency power supply for ozonizer

IV. POWER FACTOR IMPROVEMENT AND HARMONIC REDUCTION BY ACTIVE POWER FILTER

The use of high frequency power supplies increases the power density applied to the ozonizer electrode surface which in turn enhances the ozone production for a given surface area, with reduced peak voltage requirement. By increasing the operating frequency the ozone production can easily be controlled. Many compact converter topologies have been proposed in order to improve efficiency of the ozonizer. Some power supply derived from AC main supply. In this case the front end has uncontrolled rectifier with a large DC link capacitor. This rectifier is widely used because of its simplicity and robustness but with the distorted line currents. As a result, the input power factor is poor. Various power factor correction (PFC) techniques are employed in converters to overcome these power quality problems out of which the basic boost converter topology has been extensively used in various power supply conversion applications. Implementing power factor correction (PFC) into low frequency to high frequency power supplies will maximize the power handling capability of the power supply and current handling capacities of power distribution networks [4].

The low frequency to high frequency high voltage power supply system has more input current distortion and poor power factor. It affects the system performance and life time. These harmonics can be reduced by active power factor correction (PFC) converter. The power factor correction (PFC) converter is used to improve the input power factor, reduce cable and device rating and reduce the current harmonics. This paper proposes power factor correction (PFC) high voltage high frequency power supply for ozonizer.

Power factor is a measure of the displacement between the input voltage and current waveforms to an electrical load that is powered from an AC source.

1. Power Factor of a Linear Load

The linear loads like lamp, cooking stoves draw sinusoidal currents. The voltage and current waveforms for a linear load are shown in Figure 6.

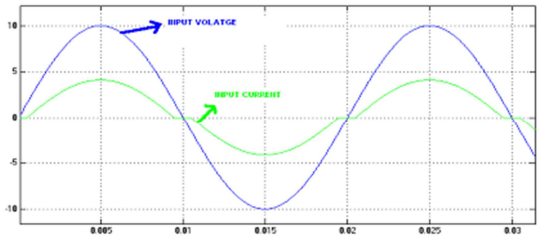

Figure 6 AC input voltage and current waveform for linear load [4]

2. Power Factor of a Non Linear load

A non-linear load on a power system is typically a rectifier, fluorescent lamp, welding machine etc. These loads draw the non-sinusoidal current. This current also has more distortion and the supply power factor is poor. Figure 7 shows the relation between current and voltage for nonlinear load. For sinusoidal voltage and non- sinusoidal current the input power factor can be expressed as

$$PF = \frac{V_{rms}\, I_{1rms} \cos\varphi}{V_{rms}\, I_{rms}} = K_p \cos\varphi \qquad (1)$$

Where $K_p = \frac{I_{1rms}}{I_{rms}}$ and K_p range is $[0,1]$

cos ϕ is the displacement factor of the voltage and current. K_P is the purity factor or the distortion factor.

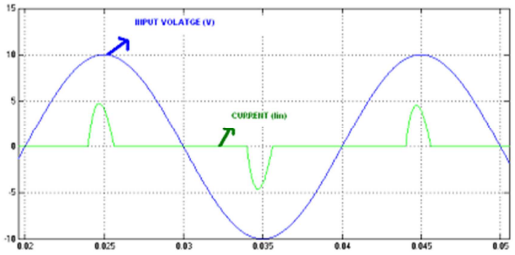

Figure 7 AC input voltage and current waveform for nonlinear load [4]

Another important parameter that measures the percentage of distortion is known as the current THD which is defined as follows:

$$K_p = \frac{1}{\sqrt{1 + THD_i^2}}$$

$$\text{where } THD_i = \frac{\sqrt{\sum_{n=1}^{\infty} I_{hrms}^2}}{I_{1rms}}$$

Conventional AC to DC conversion is a very inefficient process, resulting in waveform distortion

of the current drawn from the AC main supply. At higher power levels severe interference with other electrical and electronic equipment may become apparent since harmonics are injected to the power utility line. Another problem is that the power utility line cabling, the installation and the distribution transformer, must all be designed to withstand these peak current values resulting in higher electricity costs for any electricity utility company. This problem can be addresses using power factor correctors. Power factor correctors are of two type's viz. Passive and Active. The passive power factor correction (PFC) is made of passive components and is normally bulky and operates at power frequency. Active power factor correction (PFC) offers better THD and is significantly smaller and lighter than a passive PFC circuit. To reduce the size and cost of passive filter elements, an active PFC operates at a higher switching frequency. The active PFC shapes the input current and there will be feedback control to regulate the output voltage. Buck, boost, fly back and other converter topologies are used in active PFC circuits. The basic boost converter topology has been extensively used in various power supply conversion applications [4]. Therefore a boost converter is used along with the inverter as a supply unit for an Ozonizer. In this research, active power filter (APF) is employed for power factor improvement and harmonic reduction.

V. MODELING AND SIMULATION FOR HIGH-VOLTAGE, HIGH-FREQUENCY POWER SUPPLY OF OZONE GENERATOR

For modeling of HV-HF power supply for Ozone generator, Matlab/Simulink software is used. Formerly the modeling for power supply without active power filter (APF) is carried out. The important parameters used with simulation model are shown in Table 1.

Table 1 Simulink model parameters for HV-HF power supply

SN	Parameter	Rating/Value
1	Source	230 V, 50 Hz
2	Source Impedance	0.05 Ω, 0.25 mH
3	Input Inductance	10 µH
4	Input Capacitance	100 mF
5	Output Capacitance	1 µF
6	Transformer	500 VA, 6 kHz 230/5000 V
7	Load	200 W, 10 µF
8	Inverter Output Frequency	6 kHz
9	Inverter Modulation Index	0.7
10	Inverter Switching Frequency	20 kHz

The model consists of five sections as source, rectifier, inverter, high frequency transformer and load. The model consists of two subsystems as inverter control and measurement system. The simulation models without active power filter (APF) are shown in Figure 8 through Figure 10.

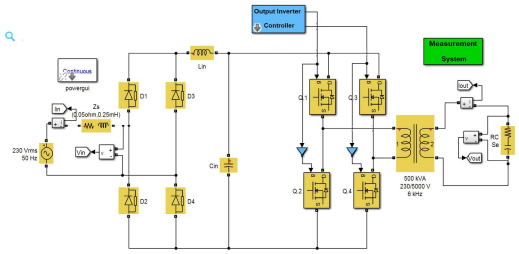

Figure 8 Simulink model for HV-HF power supply without active power filter (APF)

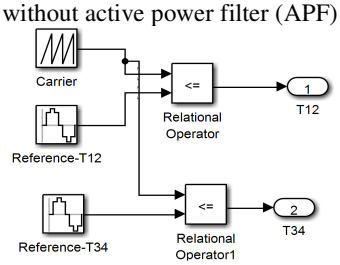

Figure 9 Simulink model for inverter control

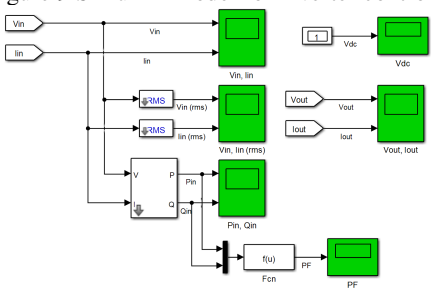

Figure 10 Simulink model for measurement system

The simulation results for without active power filter (APF) are shown in Figure 11 through Figure 16. As shown in Figure 11, the input voltage and current waveforms are harmonic polluted.

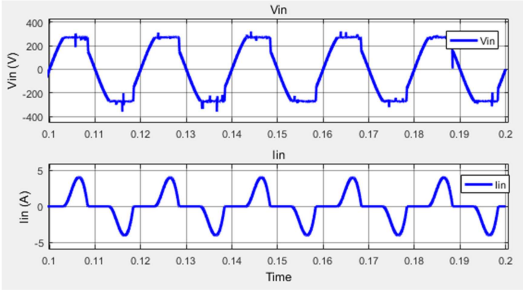

Figure 11 Simulation results for input voltage and current without APF

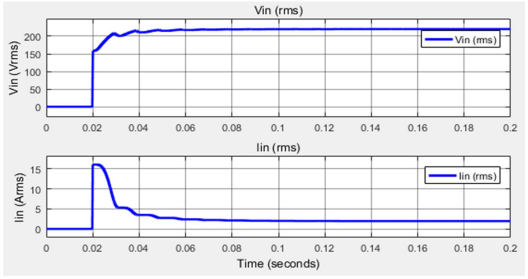

Figure 12 Simulation results for RMS values of input voltage and current without APF

The active and reactive power at input is shown in Figure 13. With these powers, the power factor is calculated and obtained as shown in Figure 14. Due to high frequency transformer and harmonic distortions, the power factor is very poor and about 0.705.

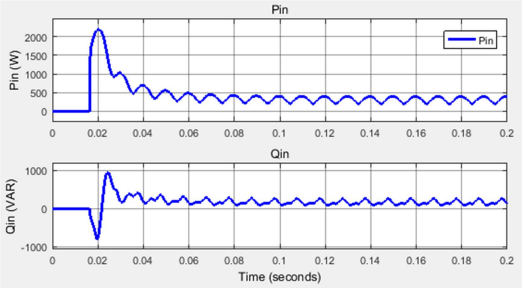

Figure 13 Simulation results for input real and reactive powers without APF

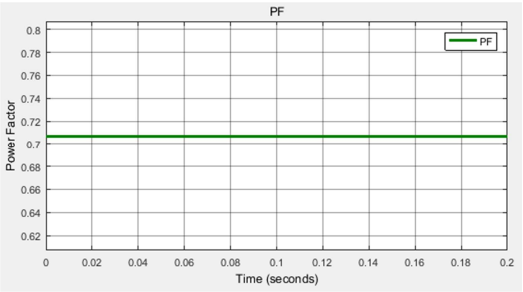

Figure 14 Simulation results for input power factor without APF

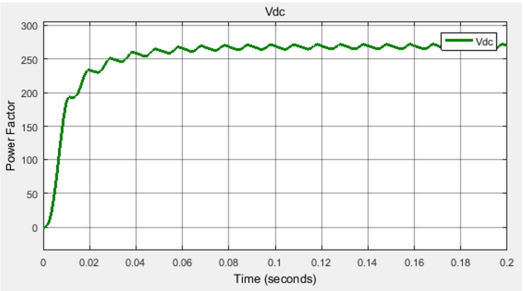

Figure 15 Simulation results for DC link voltage without APF

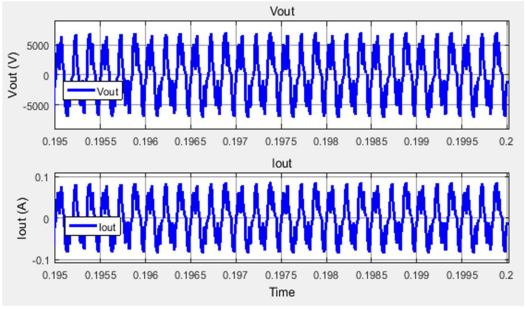

Figure 16 Simulation results for HV-HF output voltage and current without APF

Figure 16 simulation results for HV-HF output voltage and current without APF. The output voltage magnitude is about 5000 V and frequency is about 6 kHz. Figure 17 and Figure 18 show the FFT analysis results for input voltage and current.

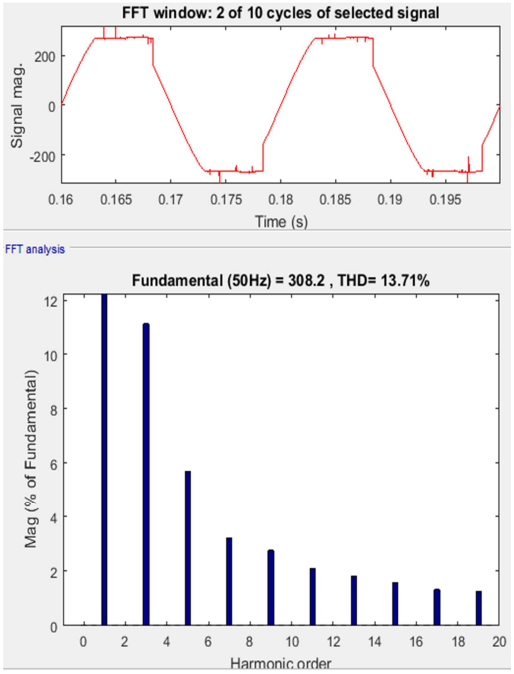

Figure 17 FFT analysis for input voltage without APF

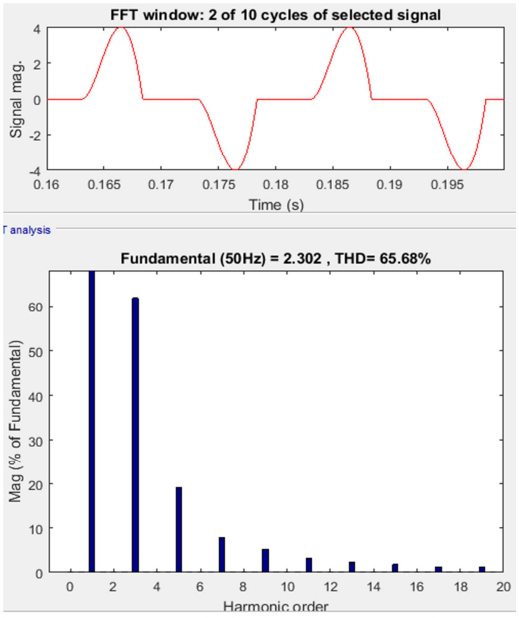

Figure 18 FFT analysis for input current without APF

According to the simulation results, total harmonic distortion (THD) voltage is about 13.71 % and THD current is about 65.68 %. These THD values are much larger than IEEE regulation of 5 %. Thus, the efficient active power filter is needed for power factor improvement and harmonic reduction of high voltage, high frequency power supply used in Ozone generation.

VI. MODELING AND SIMULATION FOR POWER FACTOR IMPROVEMENT AND HARMONIC REDUCTION

For power factor improvement and harmonic reduction, the design calculation for APF is executed and connected at the common coupling point (PCC) of HV-HF power supply. The complete simulation model with APF is shown in Figure 19 and the control system of APF is shown in Figure 20.

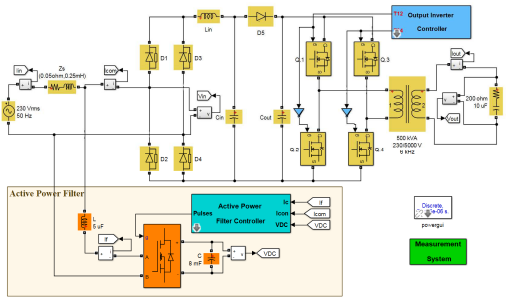

Figure 19 Simulink model for HV-HF power supply with APF

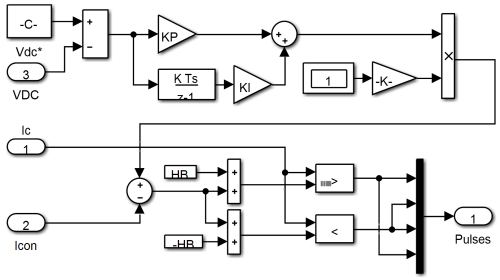

Figure 20 Simulink model for control of APF

For the control of APF, the proportional-integral controller is employed. The important parameters for APF are described in Table 2.

Table 2 Simulink Model Parameters for APF of HV-HF Power Supply

SN	Parameter	Rating/Value
1	Reference DC Voltage	650 V
2	Hysteresis Band Current	1.0 A
3	Inductance of APF	5 µH
4	Capacitance of APF	8 mF
5	PI Controller Proportional Gain Integral Gain	 0.1 0.01

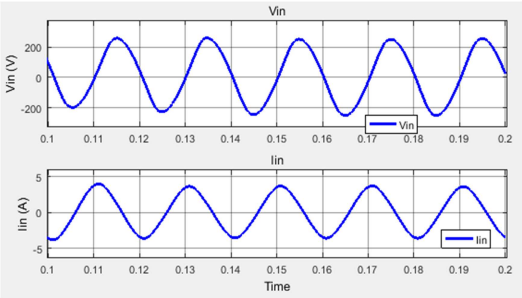

Figure 21 Simulation results for input voltage and current with APF

The simulation results for HV-HF power supply with active power filter (APF) are shown in Figure 21 through Figure 24. As shown in Figure 20, the harmonic distortion at input voltage and current are negligible. The rms voltage and current as well as real and reactive power are nearly the same as the without APF case. The power factor at PCC is increased and is about 0.98 which is much better compared to without active power filter (APF) case.

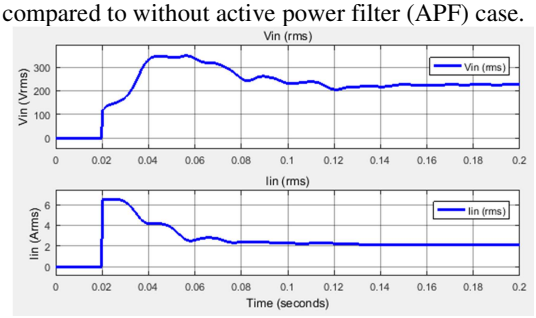

Figure 22 Simulation results for RMS values of input voltage and current with active power filter (APF)

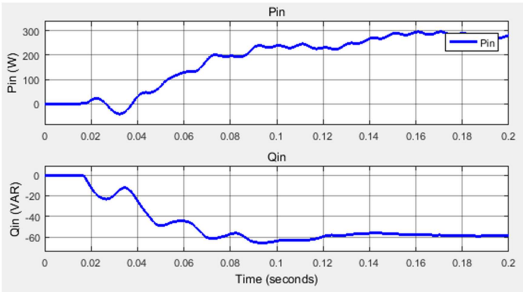

Figure 23 Simulation results for input real and reactive powers with (APF)

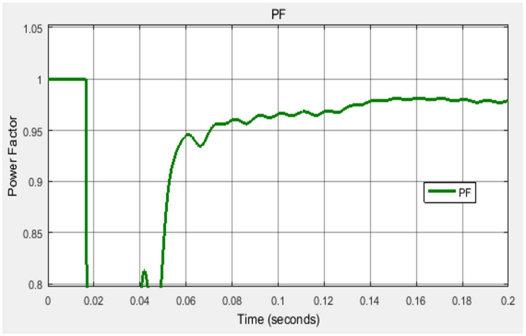

Figure 24 Simulation results for input power factor with APF

With the application of active power filter (APF), the THD of input voltage and current are significantly reduced. According to the simulation results, THD voltage is about 3.36 % and THD current is about 2.86 %. These THD values are within the IEEE regulation of 5 %. Thus, the active power filter can reduce the harmonic distortion effectively. Thus, the application of APF can reduce system cost and improve system power quality.

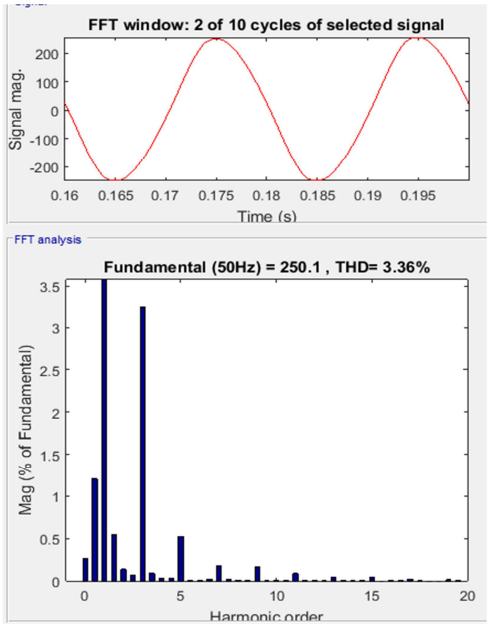

Figure 25 FFT analysis for input voltage with APF

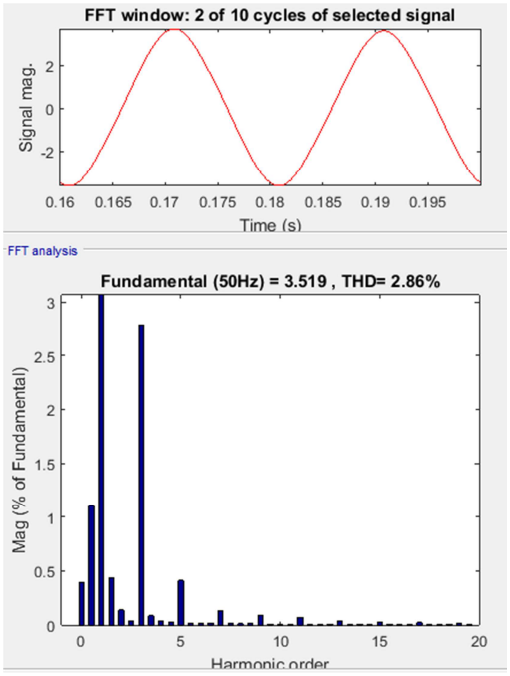

Figure 26 FFT analysis for input current with APF

VII. ANALYSIS ON RESULTS

The use of HV-HF power supply for Ozone generator causes low power factor and large harmonic distortion. The active power filter can improve these weaknesses. Thus, the two main problems i.e. power factor and harmonic are emphasized in this research. Table 3 shows performance comparison for HV-HF power supply using APF. As shown in table, the power factor and harmonics conditions are improved by active power filter (APF).

Table 3 Performance comparison using APF

SN	Parameter	Without APF	With APF
1	Power Factor	0.705	0.98
2	Current THD	13.71%	2.86%
3	Voltage THD	65.68%	3.36%

VIII. CONCLUSION

An active power factor for high voltage, high-frequency power supply for ozone generation has been presented in this paper. The whole design has been tested by means of simulation using Matlab/Simulink software. From the simulation results, the power factor with APF is 98 % and that of without APF is 71%. It is observed that the proposed configuration offer better power factor compared to without APF case. The voltage and current harmonics are also significantly reduced and can maintain within the regulation limits of IEEE 519. Even though the simulator restricted the implementation of the control law, the results are encouraging. There is indication that if a practical system is realized with the presented technique, excellent results will be achieved.

ACKNOWLEDGEMENTS

The author would like to thank Dr. Yin Yin Pyone, Processor and Head, Department of Electrical Power Engineering, Technological University (Lashio) for her helpful and valuable guidance. The author also has to say thank Dr. Mai Kai Suan Tial, Department of Electrical Power Engineering, Yangon Technological University and all the teachers from Department of Electrical Power Engineering, Technological University (Taunggyi) for their support and guidance.

REFERENCES

[1] Ekemezie, P.N., Design of A Power Factor Correction AC-DC Converter, IEEE Transactions On Industry Applications, 2007

[2] Alonso, J.M., Low-Power High-Voltage High-Frequency Power Supply for Ozone Generation, IEEE Transactions On Industry Applications, Vol. 40, No. 2, March/April 2004

[3] Hammadi, N., Development of High-Voltage High-Frequency Power Supply for Ozone Generation, Journal of Engineering Science and Technology, Vol. 11, No. 5 (2016) 755 - 767

[4] Udhayakumar, G., Supply Power Factor Improvement in Ozone Generator System Using Active Power Factor Correction Converter, International Journal of Power Electronics and Drive System (IJPEDS), Vol. 6, No. 2, June 2015, pp. 326~336

[5] Udhayakumar, G., Implementation of High-frequency High-voltage Power Supply for Ozone Generator System Using Embedded Controller, 2016 International Conference on Circuit, Power and Computing Technologies [ICCPCT]

Microtremor Measurement at Some Sites in Mandalay City, Myanmar, for Earthquake Disaster Mitigation

Yu Nandar Hlaing[1], Ichii Koji[1]

[1] Myanmar Earthquake Committee
Myanmar Engineering Society,Yangon,Myanmar

[2] Faculty of Social Science
Kansai University, Osaka, Japan

*yunandar.tgyi@gmail.com, ichiik@kansai-u.ac.jp

Abstract — Estimation of earthquake motion is important for sustainability of a city. It is well known that the characteristics of earthquake motion relates to the geological condition of the site (i.e., Idriss and Seed,1968). Microtremor is quite small vibration can be measured at anywhere, and the measurement of microtremor gives some amount of geological information.

In this study, microtremor measurement was done for 10 points with different geological profile in Mandalay, Myanmar. The difference of the local site conditions can be found in the difference of microtremor measurement results. Then it can be used for the evaluation of important characteristics of strong earthquake motions such as frequency content. Assuming H/V spectra as the natural frequency of the site, there is a clear tendency of variation of the natural frequency in the measured results in Mandalay. The results show that the microtremor observations are acceptable method for assessing dynamic characteristics of soil and site effect in Mandalay City with ease of measurement and analysis.

Keywords: microtremor, H/V spectra, Mandalay, Earthquake.

I. INTRODUCTION

Ground response may be used for prediction of ground motion and development of design response spectrum in order to determine the dynamic stress and strains assessment. The study of distribution of damages caused by various earthquakes indicates the significant site effects on earthquake characteristics (Idriss and Seed,1970)[3] .Local site conditions can influence on all of the important characteristics such as amplitude, frequency content and duration of strong ground motion. As an earthquake prone area such as Mandalay in Myanmar, several studies on site response analysis were carried out. Myo Thant et.al [1] proceeded 43 microtremor measurements to analyse seismic hazard maps by using PSHA, and Pyi Soe Thein et.al [4] conducted seismic microzonation mapping through 50 soil columns by using multiple reflection analysis and Yu Nandar Hlaing and Ichii [2] conducted one dimensional site response analysis at several sites in Mandalay. However, these studies have mostly focused on seismic vulnerability and micro-zonation of Mandalay city, the comparison of characteristics of observed microtremor and the results from geological profile will be helpful for the complete study for Mandalay city where earthquake prone area with dense population..

II. MICROTREMOR MEASUREMENT

Microtremor is a very convenient tool to estimate the effect of surface geology on seismic motion without other geological information. The dynamics characteristics of soil can be stated by microtremor measurement. Microtremors are ground vibrations with displacement amplitude about 1-10 micron, and velocity amplitude is 0.001-0.01cm/s that can be detected by seismograph with high magnification (Rezaei and Choobasti 2014) [5]. One of the most popular techniques for estimation of site effects in the region with low seismicity is microtremor measurements by Nakamura method [6] (H/V). Regarding H/V spectral ratio method, peak frequency and amplification factor were calculated for all microtremor sites. Geonet 2-2S3D is used for measurement shown in Fig 1.

Geonet is three component velocity sensor unit; two in two orthogonal horizontal directions and one in vertical direction), GPS, laptop and 12V battery are used.

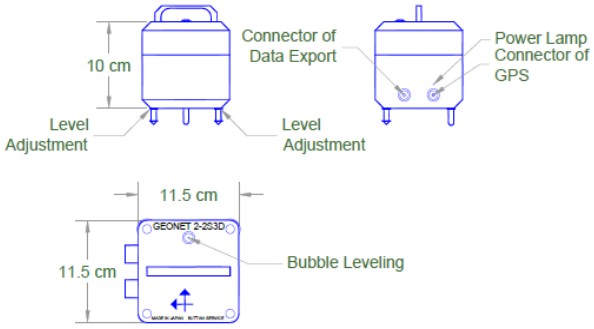

Figure 1. Geonet 2-2S3D

The arrangement of measurement is shown in Fig 2. Micro tremor measurement was carried out from Feb 26th to Feb 30th in 2018, in Mandalay City. 12 locations were proposed for the 6 soil classifications, alluvial, clay with minor sand layer, clayey silt, dark clay, silt with gravel and clay and slope wash deposit according to geological map of Mandalay.For each site, measurements were carried out three time in three days. Each time, the data was collected 3 or more times. Fig 3 shows the locations of measured sites on six soil classifications.

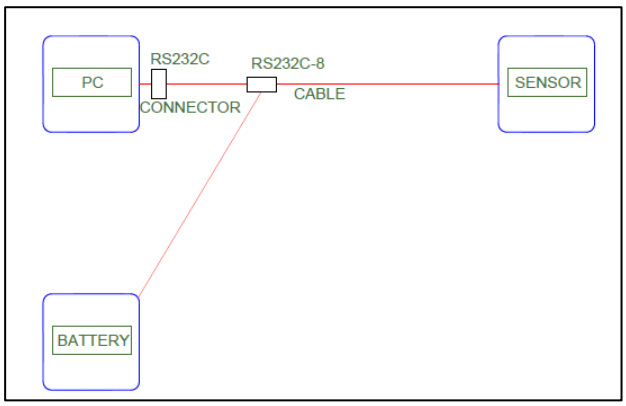

Figure 2. The arrangement of measurement

III. MEASUREMENT

The measured sites were determined by soil site location. Time of measuring (morning or evening) was determined by the passing of cars and distance from the downtown. FID 1, 7, 8, and 10 were firstly measured because they are far away from the downtown and cannot be measured at night time. For example, FID 7 and FID 8 are on the way of Yangon -Mandalay Highway. FID 10 is on the river bank. FID 1 is the in the downtown. Note: FID 9 is not measured. As an example, FID 1 measured on 26th January is presented in this report. The soil class belongs to slope wash deposit. When conducting measurement, the weather was fine and sunny. The measurement was from 15:35:00 to 16:00:00. the Geo net is set up 50HZ A/D converter frequency and measured for 1200 sec (20min) with digitized with equal-interval of 0.02s. Since the environment of site was in the centre of Mandalay city, there were passing motor vehicles during measuring. The output data set of measurement was given in three directions, East -West, North-South and Up-down directions. Fig 4 shows the microtremor measurement in sites.

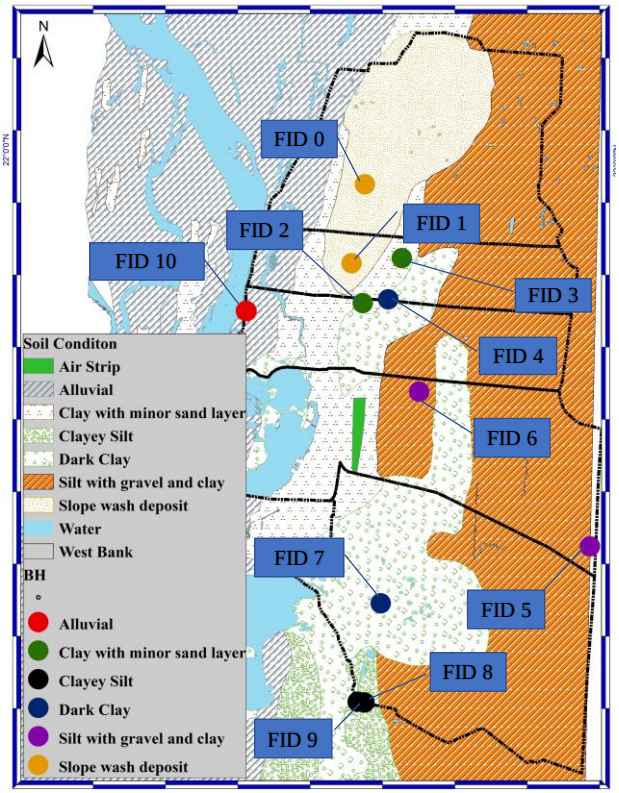

Figure 3. Location of measurement, FID

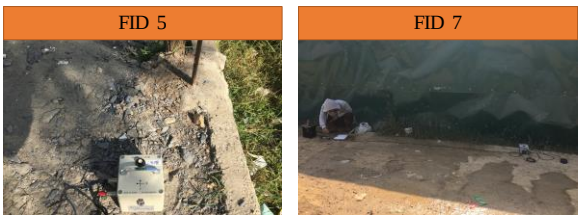

Figure 4. Showing the microtremor measurment in site

IV. ANALYSIS

The FFT calculation was done in excel. Since the sample was collected 0.02 sec interval for 20 min measuring, the sample size becomes 60,000. Sometimes measurements were interrupted by some disturbance, and the data was less than 60000. Following example is sample size 52000. FFT calculation was done in EXCEL, but the maximum sample size in EXCEL FFT is 2_n = 4096. Thus the data sample has to be subdivided into 13 windows with 8sec interval. Tremor measured in N-S and

E-W are shown in Fig 5 (a) and (b). By Fig 5(b), the data set in portions 4 and 6 cannot be chosen because of noise of motor vehicle passing in these data set. The respective spectral for FID 0~12 are summarized in Fig 6 (a) and Fig 6 (b).

V. ON H/V SPECTRUM

In order to evaluate site amplification characteristics during earthquakes, Nakamura [6] proposed a method to estimate the horizontal -to - vertical (H/V) Fourier spectrum ratio of microtremor. This is one of the most popular techniques for estimation of site effects in the region with low seismicity. In the method, a predominant period is given by a peak period in the H/V ratio, while an amplification factor at the periods is roughly assessed by the ratio itself.

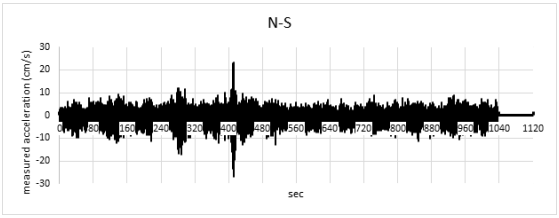

Figure 5(a) Measured motion in North-south direction

On the H/V spectrum, the horizontal motion is larger than vertical motion on the soft ground while the horizontal and vertical motions are similar on the hard ground.

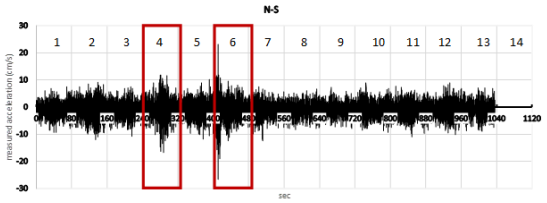

Figure 5(b) Showing noise in portion 4 and 6 (240-320 sec and 400-480 sec)

The confirmed of H/V ratio is applicable for the practical disaster prevention with easily handling measurement. Moreover, it is able to estimate the predominant frequency f(peak) . H/V components for X-direction and Y-direction are illustrated and then the average spectral ratio of H/V components at each frequency can de expressed as

$$\frac{H_{avg}}{V} = \frac{\sqrt{\frac{H_X + H_Y}{2}}}{V} \quad (1)$$

Where H and V are the spectra of horizontal (northsouth and east-west direction) and vertical components respectively. After obtaining the H/V spectra, the average of the spectra was obtained as the H/V spectrum for a particular site. The peak frequency of H/V spectrum plots show the resonance frequency and amplification factor of the site. The H/V spectra for each FID is shown in the following Fig 7.

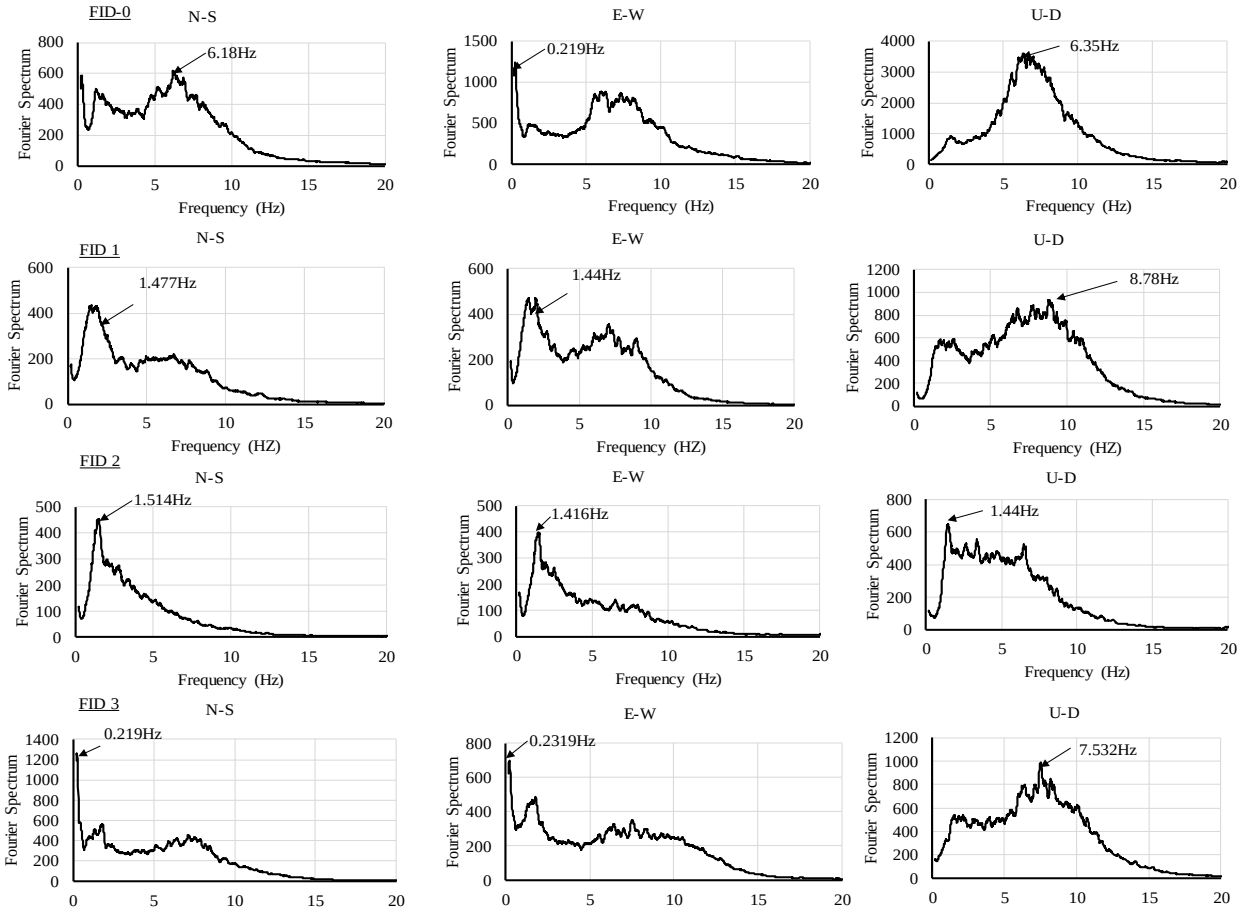

Figure 6 (a) Respective fourier spectra for FID 0-3

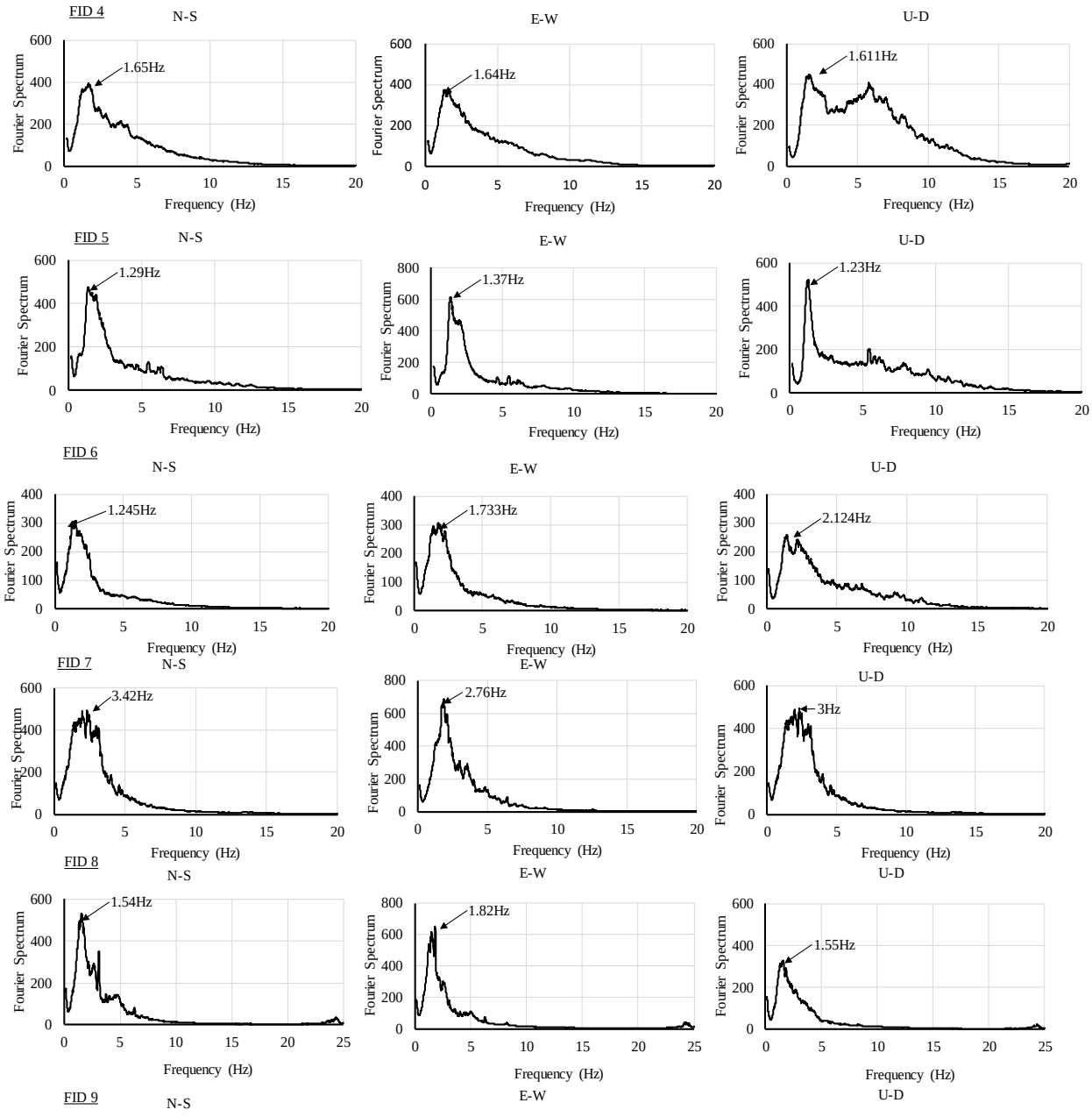

Figure 6 (b) Respective fourier spectra for FID 4-10 (FID 9 is not exist)

VI. DISCUSSION

H/V Spectrums in Fig.7 can be categorized into 4 groups. First group is FID 0 and FID 3. There is not clear peak in the spectrum. Their geological profile is different: slope was deposit and clay with minor sand. But these sites locate in the northern part of Mandalay as shown in Fig. 8. Thus, the observation of the similarity in these close sites is reasonable. The second group is FID 1, 2, 4, 6, and 7. Peak value of H/V spectrum is about 1.5 to 2.0. And the corresponding frequency is 0.5 to 0.7 Hz.The location of the sites in the second group is the center of Mandalay city, as shown in Fig. 8. Again, it is reasonable to see the sites nearby show similar results.

The third group is FID 5, and 10. Peak value of H/V spectrum is larger than that of group 2, in the rage of 2.2 to 2.8. The corresponding frequency is about 0.5 Hz, and it is same with that of group 2. The location of these sites are far east and far west of the Mandalay city. These site are not nearby, and their geological profile is also quite different (west bank / silt with gravel and clay). The fourth group is FID 8. It locate in the south of Mandalay. The frequency of the peak in H/V spectrum is about 5 hz. This peak may be corresponding to the second peak of H/V spectrum in FID 5 and 7, which locate to the south of the Mandalay city. Thus, the observed results relates to their location, and it is quite resonable. However, these results also implies that the geological profile shown in Fig.3 is not good information for the evaluation of site response characteristics.

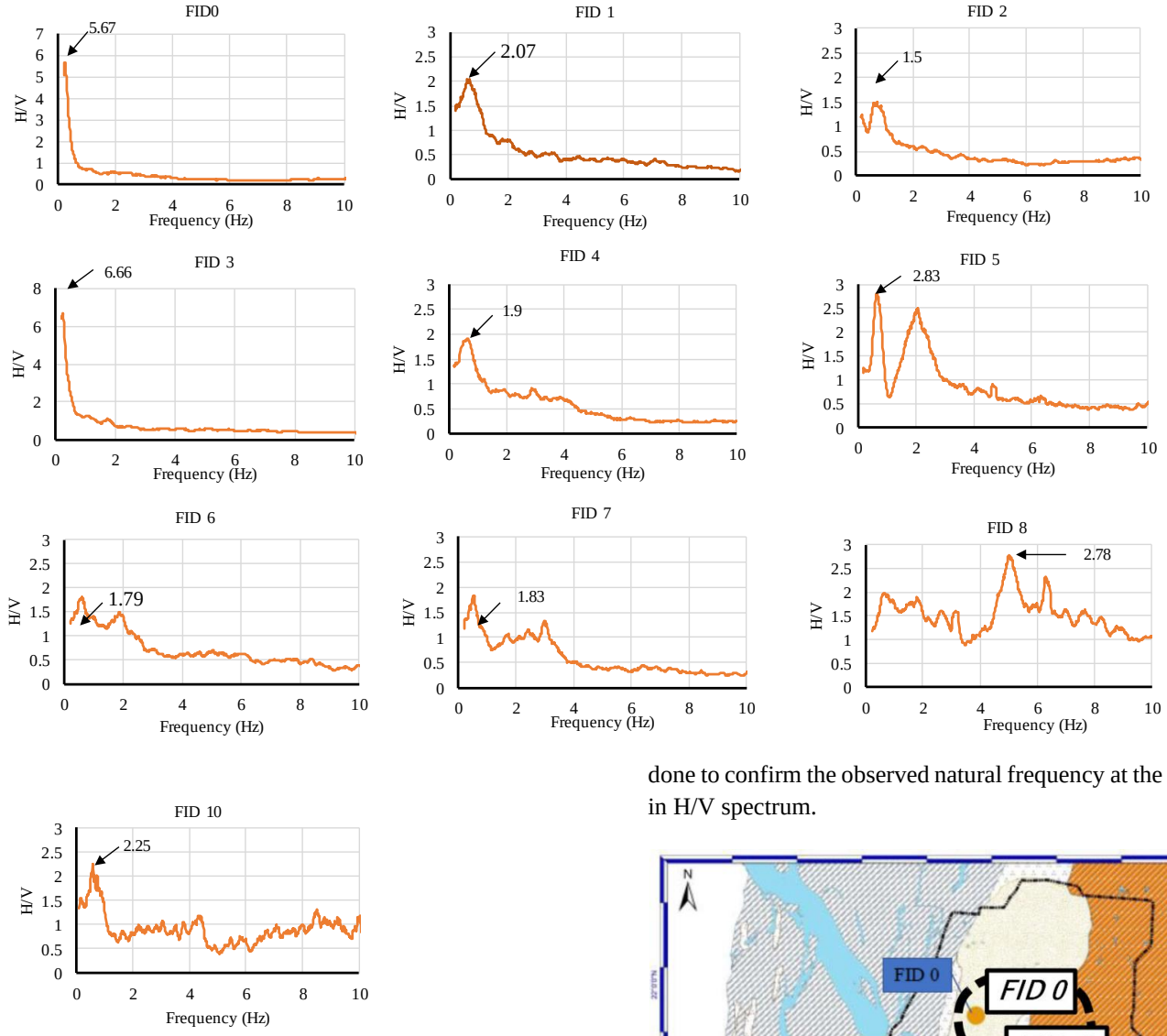

Figure 7 H/V spectra for FID (FID 9 is not exist)

VII. CONCLUSION

In this study, microtremor measurement was conducted 10 places in Earthquake prone area, Mandalay, Myanmar. The observed microtremor were analyzed by H/V spectrum. The H/V spectrum were categorized into 4 groups. Basically, sites nearby showed similar results, and it was confirmed that the observation is reasonable. However, existing information of the geological profile did not much to the grouping. Thus, these results implied that the geological profile is not good enough for the evaluation of site response characteristics, and observation of microtremor at the sites will give more reasonable information. As the next step, computation of site response analysis using the geological profile (boring logs) at each site should be done to confirm the observed natural frequency at the site in H/V spectrum.

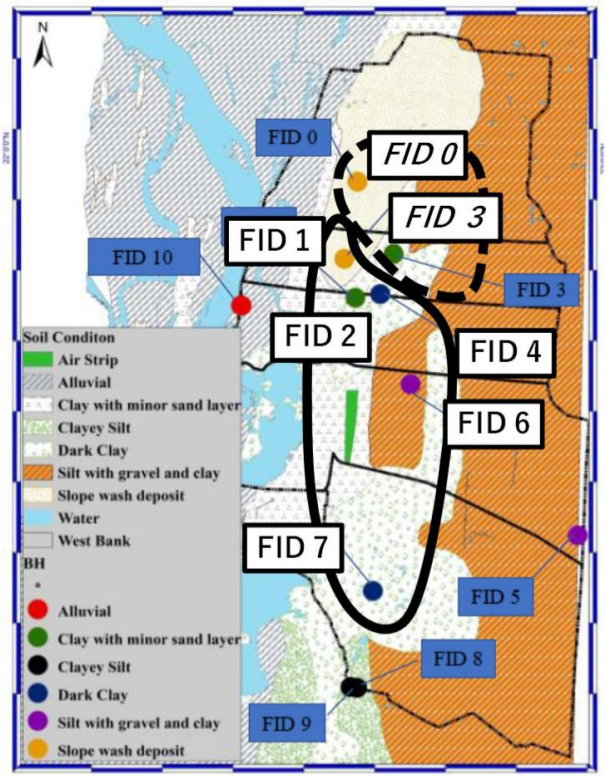

Figure 8 Grouping of FID by H/V spectra

ACKNOWLEDGEMENT

This research was financially supported by JICA (JDA program) and Japanese people.

REFERENCES

Proceeding Papers

[1] Myo Thant et. Al . Development of seismic hazard maps for Mandalay, Mandalay Region. International conference on geological engineering, Jakarta, Indonesia. December 11-12, 2013

[2] Y.N. Hlaing, Koji Ichii, [2018] Ground Response Analysis and Site characterization of Mandalay City, Conference on Myanmar Engineering Society, Annual General Meeting, Jan 19-20,2018.

Journal Papers

[3] Seed, H.B & Idriss, I.M 1970. Soil Moduli and Damping Factor for Dynamic Response Analysis. Report No. EERC 75-29, Earthquake Eng. Research Center, University of California at Berkeley, California.

[4] P.S. Thein, Kiyono J, T.T. Win, T.T. Nu and Aung D.W. Seismic Microzonation of Mandalay City, Myanmar. Journal of Geological Resource and Engineering (2018) 1-13.

[5] Rezaei S, Choobbasti AJ [2014] Liquefaction assessment using microtremor measurement, conventional method and artificial neural network (Case study: Babol, Iran). Front Struct Civ Eng 8(3):292–307

[6] Nakamura Y (1989) A method for dynamic characteristics estimation of subsurface using microtremor on the ground surface. Q Rep RTRI 30:25–33

Secure and Authenticated Data Hiding using Edge Detection

Zin Mar Htun [1], Aye Zarchi Minn [2], Aung Kyaw Oo [3]

[1] *Information Technology, Technological University (Taunggyi)*
Taunggyi, Myanmar
[2] *Information Technology, Technological University (Taunggu)*
Taunggu, Myanmar
[3]*Information Technology, Technological University (Taunggyi)*
Taunggyi, Myanmar

zinmarhtun.myanmar@gmail.com, ayemin.rose@gmail.com, aung15kyaw.ak@gmail.com

ABSTRACT

Data hiding is a great trade-mark in information security. For information security and intellectual property, effective methods are required. Steganography is the art of hiding information which no one can detect its presence except sender and receiver. The major characteristics of data hiding are less perception of data existence and hiding capacity. Formerly, the most important technique is Least Significant Bit (LSB) and the users only use it to hide information. However it has major weak point that information hides serially and so it causes high perception of data existence. Recently, many edge detection established steganography approaches have been developed to provide high imperceptibility of the stego image. However, the embedding capacity of these approaches can be limited. This paper presents an improved method that uses Canny Edge detection and chooses non-edges as LSB embedding area to give high embedding capacity and security. Moreover, it produces position file to authenticate the fact that the stego image is ensure that it comes from original image by comparing the position file and edges of stego image. It declares that it gives high payload, security, less perception and image checking to authenticate the sender.

Keywords: Data Hiding, LSB, Edge Detection, Sobel or Canny

1. INTRODUCTION

Steganography comes from the Greek Words: Steganos-"Covered", Graphe-"Writing". The central objective of steganography is to offer security for most important data of a user by beating it into an image and it keeps data existence from attackers. Image steganography is very popular in these days that can provide high embedding capacity. Many steganography applications for digital image, include copyright defence, feature classification, and secret communication [1,2]. Unfortunately the associates of terrorist groups are using steganography as a techniques to attack against the western interests [3, 4].

The traditional image Steganography algorithm is based upon the LSB bits but it can simply perceive by enemies because the data is hidden in all pixels. If the enemy identifies at least one pixels location, easily they hack the original entire message. Instead of sequentially beating the data in all pixels some of the algorithms are to hide the data in selected pixels, but it causes speckles in an image. Moreover embedding in edges gives less capacity.

So we proposed a novel image steganography algorithm integrating Canny Edge Detection algorithms for hiding secret message. The Organization of the paper is as follows. In section 2 the related work is discussed. Section 3 describes our proposed method. Finally the results are presented in section 4.

2. RELATED WORKS

The least significant bit (LSB) technology is the blandest method to be applied in steganography. Steganography is a method to hide secret data in a meaningful image. The highest priority is to maintain the quality of the stego image.

Consequently, steganography is used to embed secret information in the least significant bit of every pixel. However, Fridrich [5] asserts that this technique cannot resist statistical attacks. A few years later, some works of research [5, 6, 7, 8, 9, 10] proposed that under the condition which isn't detectable, more information can be embedded in sharp areas than in smooth areas.

Youssef Bassil proposed an Image Steganography based on a Parameterized Canny Edge Detection Algorithm [11]. It was intended to hide top-secret data into pixels of the image that were chosen the boundaries of objects detected in the image. More specifically, bits of the secret data replace the three LSBs of every colour channel of the pixels detected by the Canny Edge Detection

algorithm as part of the edges in the carrier image. It gave high imperceptibility but low capacity.

R. Wazirali presented that a new edge detection method based on gradient, 9x9 mask of LOG and zero crossing [12]. It combines with clustering to classify the image to edge and non-edge regions. Different amount of secret message will be embedded in each cluster after the finding of the edge regions. It gained the stability between stego image imperceptibility and high payload capacity.

3. BACKGROUND THEORY

In this paper, two methods are utilized to hide the data in images. The main method for hiding is LSB. To hide the data, firstly we find non-edges in cover image using canny edge detection algorithms.

3.1 Least significant bit (lSB)

Least Significant Bits substitution is one of the most public hiding method due to its easiness. The secret message is considered as bit stream and will be concealed into cover image by varying the LSBs of the cover image with the boot stream of the secret file.

With only 1 bit substitution, the change between the cover and stego image is scarcely obvious by human visual system. However, when the extent of secret message is great, the hiding capacity will increase. Therefore, more bits will be used to cover the large secret message and consequently, more degradation may announce to the stego image and hence effects its imperceptibility.

3.2 Canny Edge Detection

Fundamentally, edge detection is the process of identifying points in a computer image at which the image brightness changes abruptly, for instance, pixels difference from low intensities to high intensities or vice versa, exhibiting some discontinuities. The goal of edge detection is to detect and capture important events and changes in the properties of the image.

The advantage of edge detection is that it decreases the amount of data to be analysed and processed by image processing algorithms. It in fact eliminates the less significant information while maintaining the more significant structural features of the image. In practice, many edge detection algorithms have been used, however, one of the most capable and widely known algorithm is the Canny edge detection which was developed by John Canny in 1986 [12]. In essence, it is a multi-stage algorithm that can extract a wide range of edges in images regardless of the noise present in them. The algorithm has the following five stages are grayscale conversion, Gaussian blur, determine the intensity gradient,non-maximum suppression and double threadsholding.

Moreover, it has two basic adjustable parameters, the size of the Gaussian filter and the threshold.

As Gaussian filter is used in the first stage to smooth the image and reduce the noise and unwanted details, declining its size would result in fuzzy image that permits the finding of smaller details. In contrast, increasing its size would result in even more blurry images, spreading the value of a given pixel over a greater area of the image and permitting the detection of bigger edges.

The Canny algorithm uses two thresholds which agree more flexibility for edge detection. Often, a threshold set too high can miss important information; whereas, a threshold set too low can extract irrelevant information such as noise.

4. PROPOSED SYSTEM

System design of the proposed system is as shown in Fig. 1.

In embedding of proposed system shown in Fig. 1(a), an original image is converted to as grayscale image to find edges. And then the binary data converted from message is embedded in non-edges and the system is put edges data into position file.

The extracting process in Fig. 1(b) is reversed from embedding. The stego image is transformed to grayscale image and the system detect edges. The user can get original message from non-edges and check edge data. If the position of the edges are the same between the edges from images and the position file, the original message verify the real image form the real sender.

4.1 Algorithm for the Proposed System

The algorithm for the proposed system is divided to two subsection. Embedding algorithm is as follows.

- Input cover image and secret message(data).
- Transform cover image to grayscale image.
- Detect Edges using canny edge detection techniuques.
- Embed message in non-edges of using least significant bit (LSB).
- Output stego image and position file that contains edges points
- Measure MSE, PSNR, embedding capacity of image.

Extracting algorithm is as follows.

- Input stego image and position file
- Transform the stego image to grayscale image and detect edges using canny edge detection techniques
- Check whether the edges points are the same of the points in position file.

- If equal, extract message of using least significant bit (LSB).
- Output original message.

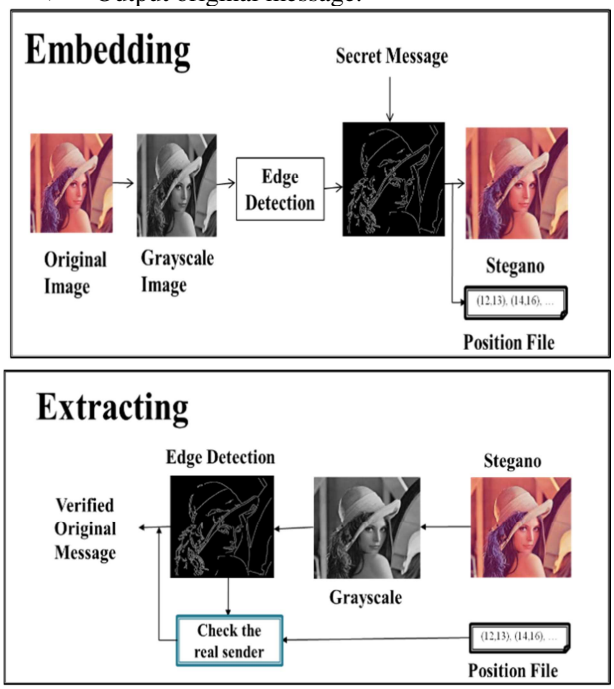

Figure 1. Proposed System Design

4.2 Steps of the System

There are two main steps in proposed system. The first step is canny edge detection and the second step is LSB algorithm.

The main steps of canny edge detection are

Step 1 : Grayscale Conversion
Step 2 : Gaussian Blur
Step 3 : Determine the intensity Gradient
Step 4 : Non maximum suppression
Step 5 : Double thresholding

According to Step 1, the system converts the cover image to grayscale image. The intensity values of the pixels are 8 bit and range from 0 to 255. After converting the grayscale image, the user can seen in Fig. 2.

Figure 2. After converting to Grayscale Image

In step 2, the system performs a Gaussian blur on the image. The blur eliminates some of the noise before further processing the image. It aims to decrease the level of noise of in image. The equation of this function is shown in Fig 3.

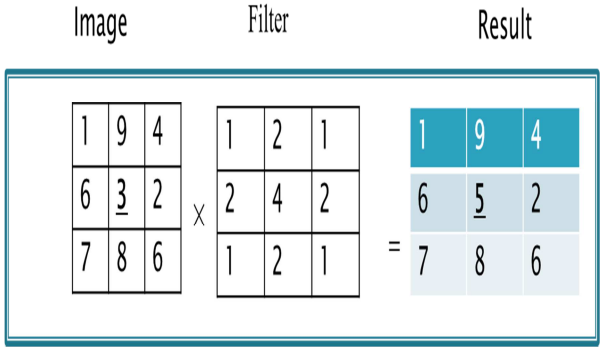

Figure 3. Guassian Blur Function

In Step 3, the gradients can be determined by using sobel filter .An edge occurs when the color of an image changes, hence the intensity of the pixel changes as well.

$$G_x = \begin{matrix} -1 & 0 & 1 \\ -1 & 0 & 1 \\ -1 & 0 & 1 \end{matrix}, \quad G_y = \begin{matrix} -1 & -2 & -1 \\ 0 & 0 & 0 \\ -1 & 2 & 1 \end{matrix}$$

Taking the derivatives will output as Fig. 4.

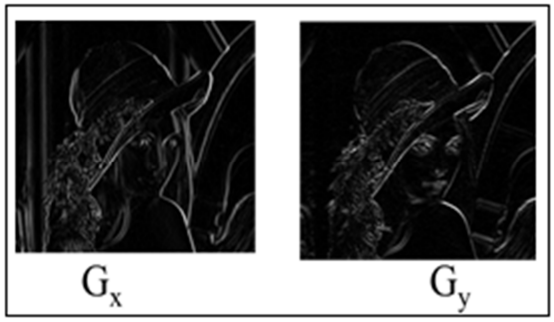

Figure 4. Gradient Images

Then, it calculates the magnitude and angle of the directional gradients:

$|G| = \sqrt{(Gx2+Gy2)}$ (1)

$\angle G = \arctan(Gy/Gx)$ (2)

(or) Angle (ɵ) = tan-1(Gy/Gx)

The magnitude of the image results in the following output in Fig. 5.

In Step 4, non-maximum suppression methods can reduce thick edges. Thus, we must perform non maximum suppression to thin out the edges. Non maximum suppression works by finding the pixel with the maximum value in an edge.

In the above image, it occurs when pixel q has an intensity that is larger than both p and r where pixels p and r are the pixels in the gradient direction of q.

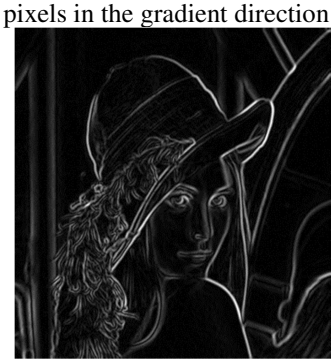

Figure 5. Gradient Magnitude

If this condition is true, then we keep the pixel, otherwise we set the pixel to zero (make it a black pixel).

Non maximum suppression can be achieved by interpolating the pixels for greater accuracy.

$$r=\alpha b+(1-\alpha)a \quad (3)$$

The result of this step is as Fig. 6.

Figure 6. NON MAXIMUM SUPPRESSION WITH INTERPOLATION

The final step is double thresholding. The result from non-maximum suppression is not perfect, some edges may not actually be edges and there is some noise in the image.

Double thresholding takes care of this. It sets two thresholds, a high and a low threshold. In this algorithm, I normalized all the values such that they will only range from 0 to 1.

Pixels with a high value are most likely to be edges. For example, you might choose the high threshold to be 0.7, this means that all pixels with a value larger than 0.7 will be a strong edge. You might also choose a low threshold of 0.3, this means that all pixels less than it is not an edge and you would set it to 0. The values in between 0.3 and 0.7 would be weak edges, in other words, we do not know if these are actual edges or not edges at all.

This threshold is different per image so I had to vary the values. In my implementation I found it helpful to choose a threshold ratio instead of a specific value and multiple that by the max pixel value in the image.

As for the low threshold, I chose a low threshold ratio and multiplied it by the high threshold value:

4.3 Consideration of Edge Detection

The system considers and confuses whether it can get the same edge points from stego images as original images. LSB can produce the same edge points. However the other methods can cause the error in edge detection.

4.4 Disadvantages of the proposed system

The system considers and confuses whether it can get the same edge points from stego images as original images. LSB can produce the same edge points, However the other methods can cause the error in edge detection.

5. TEST AND RESULT

Performance parameters for this system is embedding capacity, more security and authenticate the real sender.

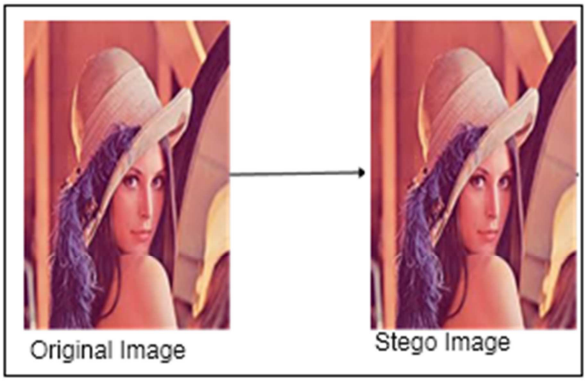

Figure 7. ORIGINAL IMAGE AND STEGO IMAGE

According to Fig. 7, there are no more difference between original image and stego image using both edge detection and LSB than only LSB.

5.1 Embedding Capacity

The system embeds the data in non-edge pixels and so it only get less amount to omit edge pixels. It can give high embedding capacity other data hiding method using edge detection. It can easily be seen in Fig. 7.

In Fig. 8, tests use five 256×256 images. All image has more non-edge pixels. Therefore the proposed system is higher embedding capacity than edges embedding.

The red line shows the less embedding capacity for data hiding method using edge detection.

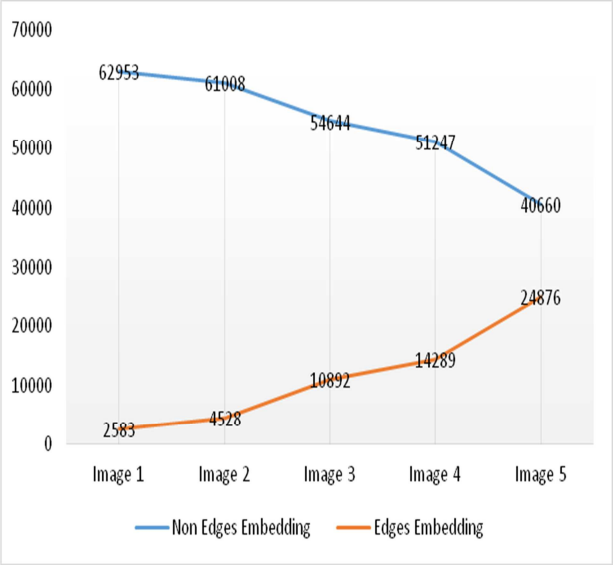

Figure.8 . Embedding Capacity between Non-edge embedding and edge embedding

5.2 Security

Original LSB has less security because it embeds the data serially. So the attacker can easily get the secret message. The proposed system can give higher security than original LSB because to extract the original message the attacker needs to know the position of edges. So the proposed system has higher security than original LSB.

5.3 Authentication

The system can check whether the stego image comes from original user by comparing the non-edge pixel position from stego image and the position file. This detection takes small time as shown in Table 1.

Table 1. Time Duration for Checking

No. of edge pixels	Time Duration (milli second)
2583	0.001
4528	0.012
10892	0.068
14289	0.081
24876	0.12

6. CONCLUSION

The main aim of the proposed system gets high embedding capacity and security. Moreover the receiver checks the real sender. The disadvantages of the system is that it is suitable only for LSB method.

7. REFERENCES

[1] N.F. Johnson, S. Jajodia, “Stag analysis: The Investigation of Hiding Information”, IEEE, pp. 113-116, 1998.

[2] D. Artz, “Digital Steganography: Hiding Data within Data”, IEEE Internet Computing, pp. 75-80, May-Jun 2001.

[3] D. Verton, "Expert Debate Biggest Network Security Threats", USA Today, 12 April, 2002.

[4] K. Maney, "Bin Laden's Messages could be Hiding in Plain Sight", USA Today 19 December, 2001.

[5] W. J. Chen, C. C. Chang and T. H. N. Te, High payload steganography mechanism using hybrid edge detector, Expert System with Applications, vol. 37, no. 4, pp. 3292-3301, 2010.

[6] A. Ioannidou, S. T. Halkidis and G. Stephanides, A novel technique for image steganography based on a high payload method and edge detection, Expert System with Applications, vol. 39, no. 14, pp. 11517-11524, 2012.

[7] C. C. Chang and H. W. Tseng, A steganographic method for digital images using side match, Pattern Recognition Letters, vol. 25, no. 12, pp. 1431-1437, 2004.

[8] D. C. Wu and W. H. Tsai, A steganographic method for images by pixel-value differencing, Pattern Recognition Letters, vol. 25, no. 9-10, pp. 1613-1626, 2003.

[9] C. M. Wang, N. I. Wu, C. S. Tsai and M. S. Hwang, A high quality steganographic method with pixel-value dierencing and modulus function, Journal of Systems and Software, vol. 81, no. 1, pp. 150-158, 2008.

[10] C. C. Thien and J. C. Lin, A simple and high-hiding capacity method for hiding digit-by-digit data in images based on modulus function, Pattern Recognition, vol. 36, no. 12, pp. 2875-2881, 2003.

[11] Y. Bassil, “Image Steganography based on a Parameterized Canny Edge Detection Algorithm,” vol. 60, no. 4, pp. 35–40, 2012.

[12] R. Wazirali and Z. Chaczko, “Hyper Edge Detection with Clustering for Data Hiding,” vol. 7, no. 1, pp. 1–10, 2016.

Mathematical Approach to Stable Hip Trajectory for Ascending Stairs Biped Robot

Aye Aye Thant, Khaing Khaing Aye[1]
Faculty of Computing
Myanmar Institute of Information Technology, Mandalay, Myanmar
Department of Engineering Mathematics
Yangon Technological University, Yangon, Myanmar
Aye_Aye_Thant@miit.edu.mm

Abstract ---- The key contribution of this paper is to generate the stable hip trajectory for ascending stairs of the biped robot from the mathematical point of view. To approach this goal, we first construct the mathematical model for kinematics constraints of k^{th}step of ascending stairs and discuss the concept of hip trajectory relative to stability. From this, the stable hip trajectory for one cycle of ascending stairs step is derived by interpolation polynomial. Finally, the numerical result of the proposed trajectory is verified with Matlab figures. The present algorithm is also applicable for descending stairs of the biped robot.

Keywords: Ascending stairs, Biped Robot, Hip trajectory, Stable motion, Trajectory planning

I. INTRODUCTION

Biped robots have higher mobility than conventional wheeled robots, especially when moving on rough terrain, steep stairs, and in environments with obstacles [1]. Since a biped robot tends to tip over easily, it is necessary to take stability into account when determining a walking pattern. To walk stably in various environments, stability is the most important topic in bipedal robot walking. The zero moment point, (ZMP) is the point on the ground around which the sum of all the moments of the active force equals zero, has been widely used as a criterion to assure stability of bipedal walking in many studies [1].

The walk of biped robot can be determined by foot and hip trajectory. Zhang et al [2] have used the cubic polynomial for motion planning of biped robot for climbing stairs. However, in these methods do not ensure continuity of acceleration at the path points. So, generation of a smooth and continuous motion has not been guaranteed as cubic spline interpolation method. To alleviate this problem, foot and hip trajectory for level ground are generated by cubic spline interpolation in my previous research [6]. And then, generation of foot trajectory for ascending stairs by applying cubic spline interpolation has been derived [11]. Now, stable hip trajectory for ascending stairs of biped robot has been generated. To be able to get stable hip trajectory, either generates the smooth trajectory or points the two hip parameters for stability. From this concept, we formulate the problem of smooth hip motion with the largest stability margin using two parameters, and derived the hip trajectory. Also, both foot trajectories and the hip trajectory are smooth, and the ZMP trajectory is always near the center of the stability region, that is the robot has a large stability margin [1].

The structure of the paper is as follows: Section 2 describes theoretical element for ascending stairs cycle of biped robot. . Section 3 represents kinematic constraints for hip trajectory. Section 4 includes stable hip trajectory planning of biped robot. Section 5 demonstrates of the resulting hip trajectory by applying Matlab.

II. THEORETICAL ELEMENT FOR ASCENDING STAIRS OF BIPED ROBOT

A biped robot is two-legged robot and is expected to eventually evolve into with a human-like body. Each leg of an anthropomorphic biped robot consists of a thigh, a shank, foot and has six degrees of freedom (DOF); three DOF in the hip joint, one in the knee joint and two in the ankle joint [1].

Biped walking is a periodic phenomenon. A complete climbing upstairs cycle is composed of two phases. These are single support phase and double support phase as shown in Figure 1.

Double support phase: During the double support phase, both feet are in contact with the stairs.

Single support phase: During the single support phase, while one foot is stationary with the stair, the other foot swings from the rear foot to the font.

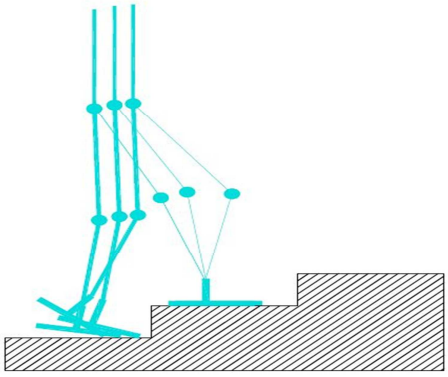

Figure 1(a)

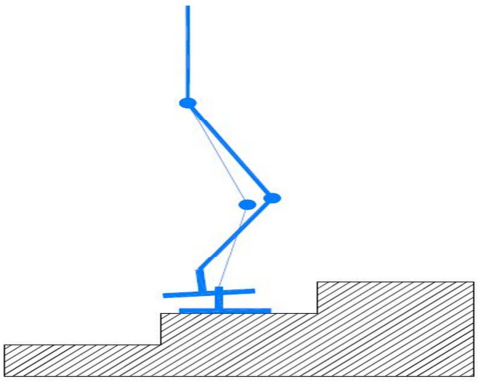

Figure 1(b)

Figure 1(a) double-support phase (b) single-support phase

To enable the robot to adapt to ascend stairs, first foot trajectories and then hip trajectory must be specified. If both foot and hip trajectories are known, all joint trajectories of the biped robot will be determined by kinematic constraints [1]. The walking pattern can therefore be denoted uniquely by both foot and hip trajectories. Biped robot motion in 3D space, x axis point to the forward direction, and z axis points upward, and y axis is cross product of z and x axis. The x-z plane is the sagittal plane (lateral plane), x-y plane is the transverse plane and y-z plane is frontal plane. In this paper, trajectories are discussed only in the sagittal plane.

III.KINEMATICS CONSTRAINTS FOR HIP TRAJECTORY

The kinematic constraints were also taken into consideration during the ascending stairs of the biped robot. In this section, kinematic constraints for k^{th} ascending step of hip trajectory are formulated.

1. Hip Trajectory

Each hip trajectory can be denoted by a vector

$$X_h = [x_h(t), z_h(t), \theta_h(t)]^T,$$

where $(x_h(t), z_h(t))$ is the coordinate of the hip position, and $\theta_h(t)$ denotes the ankle of the hip as shown in Figure 2.

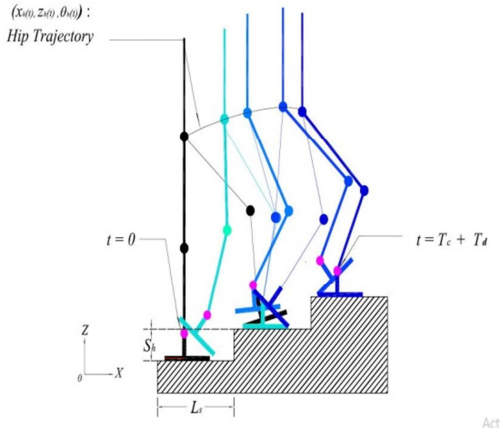

Figure 2 Hip trajectory of biped robot

The time intervals for one cycle of ascending stairs are denoted as following:

Place (entire sole contact) $(t = 0)$

Deploy (heel off) $(t = T_d)$

Deploy (heel contact) $(t = T_c)$

Place (entire sole contact) $(t = T_c + T_d)$ as shown in Figure 3.

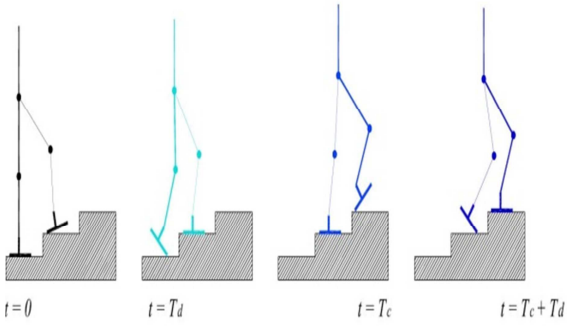

Figure 3 Time interval for one cycle of ascending stairs

The other hip parameters are listed as following:

x_{sd}	distances along x axis from the hip to the ankle of the support foot at the start of the single- support phase
x_{ed}	distances along x axis from the hip to the ankle of the support foot at the end of the single- support phase as shown in Figure 4.
H_{hmax}	the hip highest position at the middle of single support phase during one ascending cycle
H_{hmin}	the hip lowest position at the middle of double support phase during one ascending cycle
D_s	step` length
L_s	stair length
S_h	stair height
ZMP	zero moment point

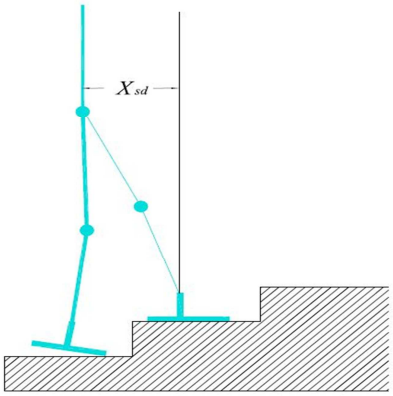

Figure 4(a)

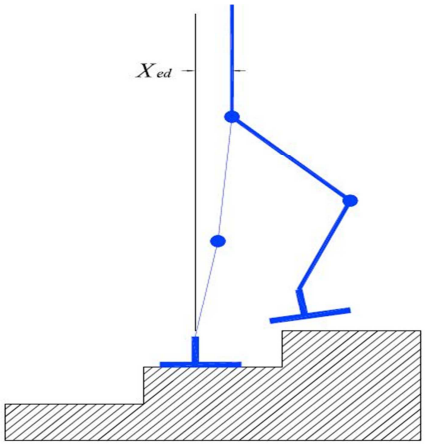

Figure 4(b)

Figure 4 Hip parameters (a) x_{sd} and (b) x_{ed}

For the hip trajectory for one cycle of ascending stairs, three phases are composed.: a starting phase in which the ascending speed varies from zero to a desired constant velocity, a steady phase with a desired constant velocity and an ending phase in which the speed varies from a desired constant velocity to zero.

The time intervals for k^{th} ascending step are as follows:

i. Starting position $(t = kT_c)$

ii. Steady position $(t = kT_c + T_d)$

iii. Ending position $(t = (k+1)T_c)$

The hip trajectory on k[th] walking step is as follows:

$$x_h(t) = \begin{cases} kD_s + x_{ed}, & t = kT_c \\ (k+1)L_s - x_{sd}, & t = kT_c + T_d \\ (k+1)L_s + x_{ed} & t = (k+1)T_c \end{cases} \quad (1)$$

$$z_h(t) = \begin{cases} H_{hmin}, & t = kT_c + 0.5T_d \\ s_h + H_{hmax}, & t = kT_c + 0.5(T_c - T_d) \\ 2s_h + H_{hmin}, & t = (k+1)T_c + 0.5T_d \end{cases} \quad (2)$$

To be able to get stability motion, the hip motion parameter $\theta_h(t)$ is constant.

1.1 The Concept of Ascending Trajectory Relative to Stability

Hip motion $x_h(t)$ hardly affects the position of the zero moment point. x_{sd} and x_{ed} to vary within a fixed range is specified [1], in particular

$$\begin{cases} 0.0 < x_{sd} < 0.5D_s \\ 0.0 < x_{ed} < 0.5D_s \end{cases} \quad (3)$$

To obtain a smooth periodic $x_h(t)$ of the steady phase, the following constraints must be specified.

$$\begin{cases} \dot{x}_h(kT_c) = \dot{x}_h(kT_c + T_c) \\ \ddot{x}_h(kT_c) = \ddot{x}_h(kT_c + T_c) \end{cases} \quad (4)$$

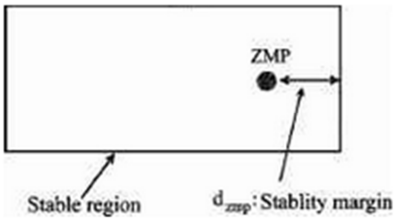

Figure 5 Zero Moment Point

Based on the whole smooth trajectory $x_h(t)$ and (4) and condition for stability (ZMP) as shown in Figure 5, a smooth trajectory with the largest stability margin can be formulated as follows:

$$\text{Max} \quad d_{zmp}(x_{sd}, x_{ed}) \qquad (5)$$
$$x_{sd}\epsilon(0.0.5D_s), x_{ed}\epsilon(0.0.5D_s)$$

where $d_{zmp}(x_{sd}, x_{ed})$ denotes the stability margin.

If the ZMP is within the convex hull of all contact points_(stable region) between the feet and the ground, the biped robot is possible to walk.

IV. TRAJECTORY PLANNING OF BIPED ROBOT

In this section, the trajectory planning of ascending stairs of biped robot is introduced. Trajectory planning is crucial for stable motion of biped robot [5]. A trajectory is the path followed by the manipulator, plus the time profile along the path. A not trivial problem in bipedal robot ascending stairs is instability produced by the violent transition between the different dynamic walk phases. The mathematical interpolation is one of the simplest methods used for providing the suitable curves with respect to the given break points that the system must undergo. Considering a single higher order polynomial for the whole trajectory has many disadvantages. To avoid them, lower order interpolating polynomials are considered in place of single higher polynomial. These are cubic polynomial and cubic spline interpolation.

The cubic spline interpolation method (see Appendix) is applied to find the trajectory planning of biped walking. The result for applying this interpolation method is that the resulting trajectory be smooth and continuous. So, the ascending of biped robot can get high path curvature. Cubic spline interpolation guarantees velocity and acceleration continuous in control trajectories.

In biped ascending phase, there are always start condition and end condition. So, the starting and ending accelerations of walking are always zero. This start and end points condition is correspond to natural spline interpolation. So, cubic natural spline is applied to generate trajectory planning of biped robot.

1. Kinematics Constraints for one cycle of ascending stairs

In this study the complete one cycle of ascending stairs stable hip trajectory will be generated. The definition of one ascending step is now given as follows:

One cycle of Ascending Stairs: The one cycle of ascending stairs of the biped robot is defined as to begin with the heel of the right foot leaving the stair and with the heel of the right foot making first contact with the next up stair.

The hip trajectory for one cycle of ascending stairs of the biped robot can be easily followed from (1) and (2).

$$x_h(t) = \begin{cases} x_{ed,} & t = 0 \\ L_s - x_{sd}, & t = T_d \\ L_s + x_{ed} & t = T_c \end{cases} \qquad (6)$$

$$z_h(t) = \begin{cases} H_{hmin,} & t = 0.5T_d \\ s_h + H_{hmax}, & t = 0.5(T_c - T_d) \\ 2s_h + H_{hmin,} & t = T_c + 0.5T_d \end{cases} \qquad (7)$$

The parameter $\theta_h(t)$ can be determined as a constant. And then, parameters of hip trajectory are defined as follows:

Table 1 Parameters for the one cycle of ascending stairs

parameter	value
T_d	0.18 s
T_m	0.4 s
T_c	0.9 s
x_{sd}	19.39 cm
x_{ed}	10.31 cm
H_{hmin}	86.75 cm
H_{hmax}	87.8 cm
D_s	50 cm
L_s	39 cm
S_h	13 cm

In order to achieve stable motion, the two hip parameters are satisfied (3).

$$\begin{cases} 0.0 < x_{sd} < 25 \\ 0.0 < x_{ed} < 25 \end{cases} \qquad (8)$$

By substituting the values of hip parameters to the one ascending step constraints (6) and (7), we get

$$x_h(t) = \begin{cases} 10.31, & ,t = 0 \\ 19.61, & ,t = 0.18, \\ 49.31, & ,t = 0.9 \end{cases} \qquad (9)$$

$$z_h(t) = \begin{cases} 86.75, & t = 0.09 \\ 100.8, & t = 0.36 \\ 112.75 & t = 0.99 \end{cases} \qquad (10)$$

The ascending of biped robot's velocity and acceleration are always zero at the initial and final positions of one cycle of ascending stairs. From this concept, natural spline condition

$m_1 = m_3 = 0$ will be used according to its initial and final position.

By using (13), the values of time interval can be determined and these values are as follows:

$$h_1 = 0.18 - 0 = 0.18$$

$$h_2 = 0.9 - 0.18 = 0.72$$

From this, d_1 and d_2 can be calculated by using (14),

$$d_1 = \frac{19.61 - 10.31}{0.18} = 51.667$$

$$d_2 = \frac{49.31 - 19.61}{0.72} = 41.25$$

For natural spline condition, the value of u_2 is determined by using (14),

$$u_2 = 6(41.25 - 51.667) = -62.52$$

Now the value of acceleration m_2 is obtained as follows from (14):

$$2(h_1 + h_2)m_2 + h_2 m_3 = u_2$$

$$2(0.18 + 0.72)m_2 = -62.52$$

$$m_2 = -34.733$$

For the pre-swing hip trajectory $t\epsilon(0.0.18)$, cubic spline interpolation can be expressed as

$$x_h(t) = a_{1,0}t^3 + a_{1,1}t^2 + a_{1,2}t + a_{1,3} \qquad (15)$$

Use (12) for the values of coefficients,

$$a_{1,0} = \frac{m_2 - m_1}{6h_1} = \frac{-34.733 - 0}{6(0.18)} = -32.16$$

$$a_{1,1} = \frac{m_1}{2} = 0$$

$$a_{1,2} = d_1 - \frac{h_1(2m_1 + m_2)}{6}$$

$$= 51.667 - \frac{(0.18)(-34.733)}{6} = 52.709$$

$$a_{1,3} = f_1 = 10.31$$

Substitute the values of coefficients in (15),

$$x_h(t) = -32.160t^3 + 52.709t + 10.31.$$

For the hip trajectory $t\epsilon(0.18.0.9)$, cubic spline interpolation can be expressed as

$$x_h(t) = a_{2,0}(t - 0.18)^3 + a_{2,1}(t - 0.18)^2 + a_{2,2}(t - 0.18) + a_{2,3}. \qquad (16)$$

Similarly for the pre-swing phase, the values of the coefficients $a_{2,0}, a_{2,1}, a_{2,2}$ and $a_{2,3}$ can be determined.

By substituting the values of $a_{2,0}, a_{2,1}, a_{2,2}$ and $a_{2,3}$ to (16),

$$x_h(t) = 8.04(t - 0.18)^3 - 17.37(t - 0.18)^2 + 49.59(t - 0.18) + 19.61.$$

Finally the complete one cycle of standing stairs hip trajectory $x_h(t)$ is obtained as follows:

$$x_h(t) = \begin{cases} -32.16t^3 + 52.71t + 10.31 & , t \in (0,0.18) \\ 8.04(t - 0.18)^3 - 17.37(t - 0.18)^2 + 49.59(t - 0.18) + 19.61 & t \in (0.18,0.9) \end{cases}.$$

Similarly, the hip trajectory $z_h(t)$ can be derived as follows:

$$z_h(t) = \begin{cases} -68.043(t - 0.09)^3 + 57(t - 0.09) + 86.75 & , t \in (0.09,0.36) \\ 29.16(t - 0.36)^3 - 55.115(t - 0.36)^2 + 42.116(t - 0.36) + 100.8 & , t \in (0.36,0.99) \end{cases}.$$

V. DEMONSTRATION OF HIP TRAJECTORY BY APPLYING MATLAB

In this section, the numerical results of hip trajectory along x-axis and z axis are demonstrated as shown in Figure 6 and 7.

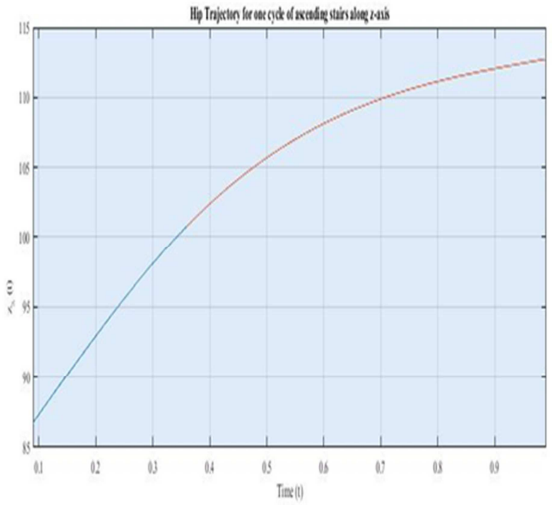

Figure 6 one-cycle of ascending stairs along x-axis

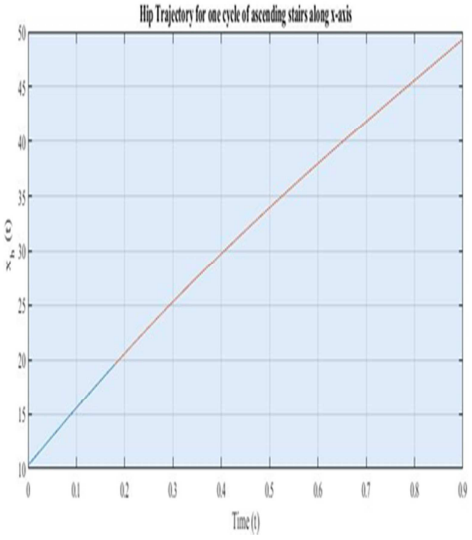

Figure 7 one cycle of ascending stairs along z-axis

VI. CONCLUSION

In this paper, mathematical modeling to stable hip trajectory for ascending stairs of a biped robot has been generated. As theoretical background of ascending stairs hip trajectory has been discussed. And then, kinematics constraints for k^{th} ascending stairs have been described. Finally, the goal of this research, the one cycle of ascending stairs hip trajectory has been generated by cubic spline interpolation. The resulting trajectories for applying this interpolation method are stable, smooth and continuous has been verified by Matlab figures.

APPENDIX

Cubic Spline Interpolation

Suppose that $\{(t_j, f_j)\}_{j=1}^{n}$ are n points, where $t_1 < t_2 < \cdots < t_n$. The function $S(t)$ is called cubic spline if there exist $n-1$ cubic polynomials $S_j(t)$ with coefficients $a_{j,0}, a_{j,1}, a_{j,2}$ and $a_{j,3}$ that satisfies the following properties [4]:

I. $S(t) = S_j(t) = a_{j,0}(t-t_j)^3 + a_{j,1}(t-t_j)^2 + a_{j,2}(t-t_j) + a_{j,3}$ for $t \in [t_j, t_{j+1}]$ and $j = 1,2,\cdots,n-1$

II. $S(t_j) = f_j$ for $j = 1,2,\cdots,n$.

III. $S_j(t_{j+1}) = S_{j+1}(t_{j+1})$ for $j = 1,2,\cdots,n-2$.

IV. $S_j'(t_{j+1}) = S_{j+1}'(t_{j+1})$ for $j = 1,2,\cdots,n-2$.

V. $S_j''(t_{j+1}) = S_{j+1}''(t_{j+1})$ for $j = 1,2,\cdots,n-2$.

Property I states that $S(t)$ consists of piecewise cubies. Property II states that piecewise cubies interpolate the given sets of data points. Property III and IV require that the piecewise cubies represent a smooth continuous function. Property IV states that the second derivatives of the resulting function are also continuous.

A piecewise function is constructed as follows [4]:

$$S(t) = \begin{cases} S_1(t) & if \quad t_1 \le t \le t_2 \\ S_2(t) & if \quad t_2 \le t \le t_3 \\ \vdots & \\ S_{n-1}(t) & if \quad t_{n-1} \le t \le t_n \end{cases}$$

where $S_j(t)$ is a cubic polynomial defined by

$$S_j(t) = a_{j,0}(t-t_j)^3 + a_{j,1}(t-t_j)^2 + a_{j,2}(t-t_j) + a_{j,3}, j = 1,2,\cdots,n-1. \quad (11)$$

By using the properties, I, II, III and IV, we can get the coefficients of cubic spline interpolation as follow:

$$\begin{aligned} a_{j,0} &= \frac{m_{j+1}-m_j}{6h_j}, \\ a_{j,1} &= \frac{m_j}{2}, \\ a_{j,2} &= a_{j,3} - \frac{h_j(2m_j+m_{j+1})}{6}, \\ a_{j,3} &= f_j \end{aligned} \quad (12)$$

where $m_j = S_j''(t_j)$ and $h_j = t_{j+1} - t_j$. (13)

Construction of natural spline interpolation

There exists a unique cubic spline with the free boundary conditions $m_1 = m_n = 0$ Mathews& Fink [3]. The linear system equations for finding $m_2, m_3, \ldots, m_{n-1}$ connected with natural spline condition are

$$2(h_1+h_2)m_2 + h_2m_3 = u_2$$

$$h_{j-1}m_{j-1} + 2(h_{j-1}+h_j)m_j + h_jm_{j+1} = u_j$$

for $j = 3,4,\ldots,N-2$

$$h_{n-2}m_{n-2} + 2(h_{n-2}+h_{n-1})m_{n-1} = u_{n-1}$$

where $u_j = 6(d_j - d_{j-1}), j = 2,3,\ldots,n-1$ and $d_j = \frac{f_{j+1}-f_j}{h_j}$. (14)

ACKNOWLEDGEMENT

I am also grateful to my respectable teachers, Dr.Khaing Khaing Aye and Dr, Ni Ni Win, Heads of Department of Engineering Mathematics at YTU, Faculty of computing at MIIT who provided

a support and encouragement. I also wish to express gratitude to my adorable benefactor parents for their encouragement and support and my husband for his AutoCAD drafting for this paper.

REFERENCES

[1] Huang, Qiang, Kazuhito Yokoi, Shuuji Kajita, Kenji Kaneko, Hirohiko Arai, Noriho Koyachi, Kazuo Tanie.: Planning walking patterns for a biped robot. IEEE Trans. Robot. Auto vol.17, no.3 2001 pp.280-284.

[2] Zhang, R. and Vadakkepet, P. Motion Planning of Biped Robot Climbing Stairs. Department of Electrical and Computer Engineering, National University of Singapore at 4 Engineering Drive 3, Singapore 117576 pp. 1.

[3] Mathews, J.H. and Fink, K.K. 2004, Numerical Methods Using Matlab. 4th ed. U.S.A: Prentice-Hall pp. 281-284.

[4] Mckinley, S. and Levine, M. Cubic Spline Interpolation Math45: Linear Algebra. Niku, S.B,2001 pp. 1-9.

[5] Tang, Z., Zhou, C, and Sun, Z, "Trajectory planning for smooth transition of a Biped Robot". Proceedings of IEEE, International Conference on Robotics and Automation Taipei, Taiwan, 2003, pp.1, September.

[6] Thant, A. and Aye, K. Application of Cubic spline interpolation to walking patterns of biped robot. Proceedings of World Academy of Science, Engineering and Technology, 2009, pp. 1.

[7] Bagheri, A., Minpour, B. and Naseradinmousavi, P. Mathematical Modelling and Simulation of Combined Trajectory paths of a Seven Link Biped Robot The University of Guilan, Faculty of Engineering, Iran, March 2010 pp.2.

[8] Ranjbar, M., and Mayorga, R. A Seven Link Biped Robot Walking Pattern Generation on Various Surface Wise& Intelligent Systems& Entities (WISE) Lab, Faculty of Engineering and Applied Science, University of Regina, CANADA. Vol 16, 2017 pp.305.

[9] Bachor, Y. Developing Controllers for Biped Humanoid Locomotion School of Informatics, University of Edinburgh, 2004 pp.24-26.

[10] Cuevas, E., Zaldivar, D., Perez-Cisneros, M. and Ramirez-Ortegon, M. Polynomial Trajectory Algorithm for a Biped Robot International Journal of Robotics and Automation 25 (4), 2010 pp.7-9.

[11] Thant, A.. and Khaing, M. Foot Trajectory Generation for Climbing Upstairs of a Biped Robot 10th international Conference on Science and Engineering 2019 pp.15-18.

Modeling Information Security System using Huffman Coding

Khaing Thanda Swe
Mandalay Technological University, Lecturer
khaingthandasweutycc@gmail.com

Abstract- Information security is the protection of information and minimizes the risk of exposing information to unauthorized third parties. Information security's primary focus is a balanced protection of the confidentiality, integrity and availability of data (also known as the CIA triad) while maintaining a focus on efficient policy implementation, all without hampering organization productivity. The proposed system mainly intends to get the data integrity while compressing the data when embedding the data into the image. The system uses the Huffman coding theory for data compression and binary symmetric channel for sharing data. The system fits the compressed data into the image using the K-means clustering. The system aims to maintain the data confidentiality and integrity while the increasing embedded capacity because of the use of variable length Huffman coding.

Key Words- CIA, Huffman coding, K-means

I. INTRODUCTION

Information security is not all about securing information from unauthorized access. Information security is basically the practice of preventing unauthorized access, use, disclosure, disruption, modification, inspection, recording or destruction of information. Information can be physical or electrical one. Thus Information Security spans so many research areas like Cryptography, Mobile Computing, Cyber Forensics, Online Social Media etc. Thus, the field of information security has grown and evolved significantly in recent years. It offers many areas for specialization, including securing networks and allied infrastructure, securing applications and databases, security testing, information systems auditing, business continuity planning etc.

There are so many cryptography techniques such DSA, DES, RSA and so on. The main aim of the cryptography is to increase the embedding capacity. But in the information security considers the data integrity and confidentiality. All of the above problems including embedding capacity, getting data integrity and confidentiality are solved by the Huffman coding theory.

In computer science and information theory, a Huffman code is a particular type of optimal prefix code that is commonly used for lossless data compression. The process of finding is using such a code proceeds by means of Huffman coding, an algorithm for developed by David A. Huffman while he was a student at MIT and published in the 1952 paper "A Method for the Construction of Minimum-Redundancy Codes".

II. LITERATURE REVIEW

In 2008, the authors in [1] commonly implemented the technical measures (security policy, procedure and methods) in Information security management measurement.

In 2003, the authors in [2] developed an integrative model of Information security effectiveness and empirically tested the model.

Suchi Goyal et al [3] in their paper proposed an enhanced detection of the 1-2-4 LSB steganography and RSA cryptography in Gray Scale and Color images. For color images, they apply 1-2-4 LSB on component of the RGB, then encrypt information applying RSA technique. For Gray Images, they use LSB to encrypt information and also detect edges. In the experimental outcomes, calculates PSNR and MSE. This method makes sure that the information has been encrypted before hiding it into an input image.

Zinia Sultana et al. [4] proposed a technique which adds double layer security to hide data in image using LSB algorithm, AES-128 encryption and a new approach of choosing index of image pixel. Secondly, they developed a steganography tool using proposed technique and evaluated the performance of the proposed technique using MSE, PSNR and by payload capacity which measures how much data can be hidden in an image using the steganography tool. The drawback of proposed method is during implementation a warning is given requesting to increase the image size or decrease the secret text size, if the payload capacity ratio is not maintained and the tool designed is not updated for compressed images.

Sherin Sugathan et al [5] proposed a new algorithm for LSB replacement based image steganography for RGB color images. The directional aspects of embedding data are explored to develop an improved LSB embedding technique. The results report an improvement in image quality measured by means of PSNR and MSE. The paper reported a simple LSB replacement approach that can

improve the quality of a stego image. The results indicate that the proposed method performs well especially when embedding secret data at higher LSB bit positions. The data parallel nature of the problem makes it suitable for implementation in parallel hardware. The position of the direction bit can also be shifted and the position can even act as part of a key for extracting the secret data.

III. METHODOLOGY

This section discusses the background theories used in the proposed system. These are principles of information theory C-I-A traid, working flow of Huffman coding and K-means clustering system.

3.1. Principles of Information Theory C-I-A traid

Information security policy is a well-written and clearly defined strategy towards protecting information systems security and maintaining secure practices to the resources and network of organization (SANS, security policy, 2007). A general content of information security policy includes password policy, risk assessment, user responsibilities, policies of using Internet, policies of using emails, disaster recovery and incidence detection (SANS, security policy, 2007) [6].

There are three characteristics that constitute the principle of information security: confidentiality, identity and availability; which are commonly called C-I-A traid. These three characteristics are not necessarily connected or dependent on each other, however, if there is problem occurring in any part of this traid, the others are consequentially affected. Confidentiality guarantees that only authorized parties or processes with sufficient privileges could access to the information. Integrity ensures that information is only created, modified or deleted by authorized parties. Availability ensures that the information can be accessed in a timely and reliable way when people or applications need it. These three characteristics can also be goals or objectives of information security since they together represent three very desirable properties of information system [6].

3.2. Working Flow of Huffman Coding

An optimal (shortest expected length) prefix code for a given distribution can be constructed by a simple algorithm discovered by Huffman. Their technique works by creating a binary tree of nodes. Initially, all nodes are leaf nodes, which contain the symbol itself, the weight (frequency of appearance) of the symbol and optionally, a link to a parent node which makes it easy to read the code (in reverse) starting from a leaf node. Internal nodes contain a weight, links to two child nodes and an optional link to a parent node.

The process begins with the leaf nodes containing the probabilities of the symbol they represent. Then, the process takes the two nodes with smallest probability, and creates a new internal node having these two nodes as children. The weight of the new node is set to the sum of the weight of the children. We then apply the process again, on the new internal node and on the remaining nodes.

The simplest construction algorithm uses a priority queue where the node with lowest probability is given highest priority:

1. Start with as many leaves as there are symbols.
2. Enqueue all leaf nodes into the first queue (by probability in increasing order so that the least likely item is in the head of the queue).
3. While there is more than one node in the queues:
    1. Dequeue the two nodes with the lowest weight by examining the fronts of both queues.
    2. Create a new internal node, with the two just-removed nodes as children (either node can be either child) and the sum of their weights as the new weight.
    3. Enqueue the new node into the rear of the second queue.
4. The remaining node is the root node; the tree has now been generated [7].

3.2.1. Modeling of Huffman Coding

The example we're going to use throughout this paper is encoding the particular string "happy". Using the standard ASCII encoding, this 5- character string requires 5*8 = 40 bits total. The table below shows the relevant subset of the standard ASCII table.

Table1. ASCII character conversion

Char	ASCII	Bit Pattern (binary)
h	104	01101000
a	97	01100001
p	112	01110000
y	121	01111001

The string "happy" would be encoded in ASCII as 104 97 112 112 121. Although not easily readable by humans, it would be written as the following stream of bits (each byte is boxed to show the boundaries):

0110 1000	0110 0001	0111 0000	0111 0000	01111 001

Creating such an encoding is trivial: the systems creates a list of the unique characters, and then goes through and assign each a distinct encoded number from 0 to N-1. For example, here is one possible 3-bit encoding (of the 7! possible permutations):

Table2. 3-bit Pattern Conversion

Char	Number	Bit pattern
h	0	000
a	1	001
p	2	010
y	3	011

Using this table, "happy" is encoded as 0 1 2 2 3, or in binary:

000	001	010	010	011

Then the optimal Huffman encoding for variable length is as follows:

Table3. Variable Length Huffman Coding

Char	Bit pattern
h	01
a	000
p	10
y	1111

Each character has a unique bit pattern encoding, but not all characters use the same number of bits. The string "happy" encoded using the above variable-length code table is:

01	000	10	10	1111

One way to visualize any particular encoding is to diagram it as a binary tree. Each character is stored at a leaf node. Any particular character encoding is obtained by tracing the path from the root to its node. Each left-going edge represents a 0, each right-going edge a 1. For example, this tree diagrams the compact variable-length encoding we developed previously:

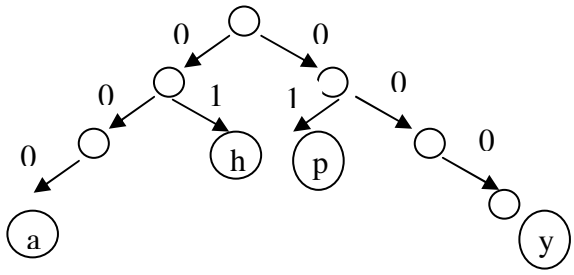

Figure 1. Binary Tree for Optimal Huffman Coding

The general approach is as follows: 1. Create a collection of singleton trees, one for each character, with weight equal to the character frequency. 2. From the collection, pick out the two trees with the smallest weights and remove them. Combine them into a new tree whose root has a weight equal to the sum of the weights of the two trees and with the two trees as its left and right sub trees. 3. Add the new combined tree back into the collection. 4. Repeat steps 2 and 3 until there is only one tree left. 5. The remaining node is the root of the optimal encoding tree [8].

3.3. Implementing K-means Clustering Algorithm

K-means clustering is one of the simplest algorithms. It works well for all distance metrics (where mean is defined) such as Euclidean distance. It takes the partitions N observations into K clusters (K<N).

Observation	X	Y
1	1	1
2	1.5	1.5
3	1	0.5
4	0.8	1.2
5	3.3	3.1
6	2.58	3.68
7	3.5	2.8
8	3	3

Step1: Randomly choose two points as the cluster centers.

	Individual	Mean x	Mean y
Group 1	1	1	1
Group 2	8	3	3

Step2: Compute the distances and group the closest ones (x_2, y_2)

Observation	Distance 1	Distance 2	Group
1	0	2.8284271	1
2	0.7071068	2.123203	1
3	0.5	3.2015621	1
4	0.2828427	2.8425341	1
5	3.1144823	0.3162278	2

6	3.111077	0.7992496	2
7	3.0805844	0.5385165	2
8	2.8284271	0	2

Step 3: Compute the new mean and repeat step 2.

Step 4: If change in mean is negligible or no reassignment then stops the process.

IV. PROPOSED SYSTEM DESIGN

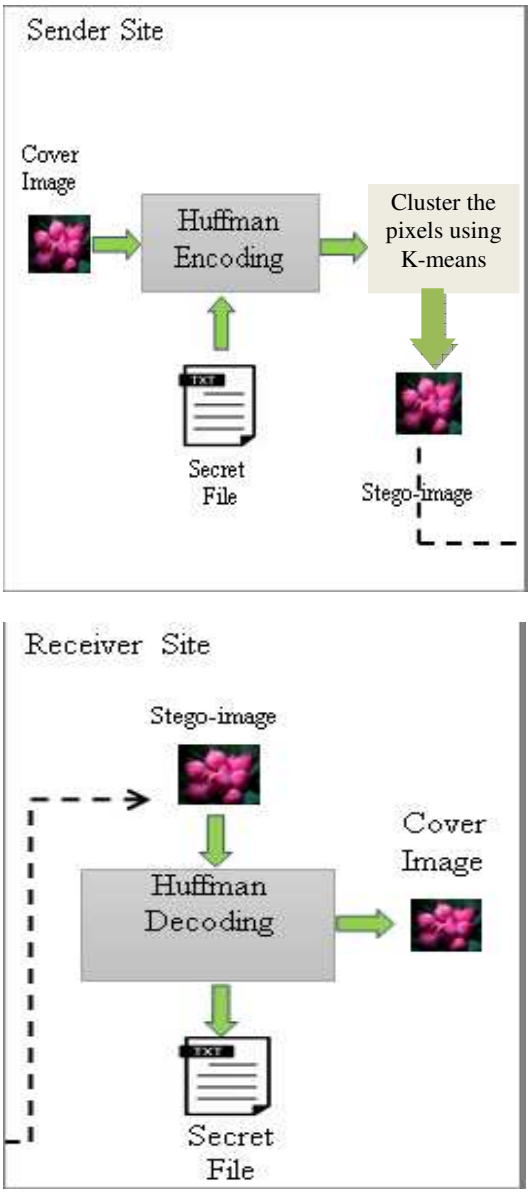

Figure 2. Proposed System Flow

When the sender sends the message to the destination, but the sender doesn't want to pay knowing the contents of the message to other party between their communications. So, the proposed system implements the data security system in communications. When designing and implementing the system, the system uses the Huffman Code for getting data integrity.

In the proposed system, first the sender sends the message to the receiver. At that time, the system encrypts the message using Huffman Code. And then the system finds the location of the encrypted message using K-means clustering. After that, the system places the encrypted message using Huffman Coding to the right location according to the cluster pixels of K-means clustering. This is so called the generation of Stego-image.

After receiving the message from the sender, the receiver decrypts the encrypted message to get the original message without degrading the contents of the message. Firsts the receiver finds the location of the cluster pixel. Then the receiver decrypts the message using the Huffman decoding scheme for achieving the data integrity.

V. PERFORMANCE ANALYSIS

The system proves by induction that the binary Huffman code is optimal. It is important to remember that there are many optimal codes: inverting all the bits or exchanging two code words of the same length will give another optimal code. The Huffman procedure constructs one such optimal code.

To prove the optimality of Huffman codes, we first prove some properties of a particular optimal code. Without loss of generality, we will assume that the probability masses are ordered, so _ that p1 ≥ p2 ≥ · · · ≥ pm. Recall that a code is optimal if pi li is minimal.

Calculation of the average length_

$L(p) = L^*(p') + p_{m-1} + p_m$

Huffman coding is optimal; that is, if C* is a Huffman code and C_ is any other uniquely decodable code,

$L(C^*) \leq L(C)$.

Compression Ratio: It is the ratio between the size of the compressed file and the size of the source file.

Compression ratio = Size after compression/ Size before compression

Compression factor: It is the inverse of the compression ratio.

Compression factor = (Size before compression)/(Size after compression)

Saving percentage: it calculates the shrinkage of the source file.

Saving percentage = (Size before compression-Size after compression)/ (Size before compression) [9]

Image Size	Arithmetic Coding	Huffman Coding
Compression ratio	Very good	Poor
Compression factor	Fixed	Variable
Saving Percentage	No	Yes
Embedding capacity	Mega Byte	Gega Byte

VI. CONCLUSION

The proposed system mainly aims to increase the embedding capacity and able to get the data integrity and confidentiality. The system embeds the data into the image. In this system, jpeg file only uses. First the system encodes the secret data using Huffman Encoding. Then the system clusters the pixels of the image using K-means clustering algorithm. After finishing all, the encoded secret data are embedded into the image according to the cluster values. This is the sender site.

And the other site, the receiver site, the receiver decodes the secrete data using Huffman Decoding according to the cluster values. In this way, it is more difficult to attack in Huffman Coding than the arithmetic Coding because Huffman uses variable-length encoding.

As the further extension, the system can give data confidentiality and integrity. But there is no evidence for this statement is true. The other researchers can check the security privacy using AVISPA and other network security tools.

VII. REFERENCES

[1] Dave Kaveri Atulbhai and Shilpa Serasiya, "A Survey: Prediction & Detection of Dengue – Mining Methods & Techniques, IJAR-IIE–ISSN (O)-2395-4396, Vol-3, Issue-2, 2O17.

[2] Xavier-CarvalhoC, Cezar RDDS, Freire NM, Vasconcelos CMM, Solorzano VEF, de Toledo-Pinto TG, Fialho LG, do Carmo RF, Vasconcelos LRS, Cordeiro MT,

[3] Suchi Goyal, Manoj Ramaiya, Deepika Dubey "Improved Detection of 1-2-4 LSB Steganography and RSA cryptography in color and Grayscale Images", International Conference on Computational Intelligence and Communication Networks,201

[4] Zinia Sultana , Fatima Jannat , Muhammad Nazrul Islam " A New Approach to Hide Data in Color Image Using LSB Steganography Technique",3rd International Conference on Electrical Information and Communication Technology (EICT), 7-9 December 2017, Khulna, Bangladesh

[5] Sherin Sugathan "An Improved LSB Embedding Technique for Image Steganography", 2016 IEEE

[6] Yang Yaping, "Literature review on Information Security Practice Survey Reports", Service Innovation and Management, Master's Thesis, 2018

[7] https://en.wikipedia.org/wiki/Huffman_coding

[8] Julie Zelenski, " Huffman Encoding and Data Compression", Spring , May 23 2012

[9] Hyderabad Jyot Maan, "Analysis Comparison of Algorithms for Lossless Data Compression", International Journal of Information and Computation Technology, ISSN 0974-2239, Volume 3, pp. 139-146, 2013.

PERFORMANCE EVALUATION FOR CLASSIFICATION ON DENGUE FEVER

Phyo Thu Zar Tun
Mandalay Technological University
dr.phyothuzartun@gmail.com

Abstract **- Dengue Fever is one of the most dangerous mosquito-brone viral diseases in the world and it is also a real problem in Myanmar. According to the statistics in the previous year, 2018, there have a total of 3649 dengue cases and 187 deaths. The total dengue cases were reported in 2018 is about 86%. The weather in Myanmar has three seasons and the transmission of the disease takes place during the rainy season which it from May to October. There have four types in dengue fever namely DENV-1, DENV-2, DENV-3 and DENV-4. The Infection may be asymptomatic in some people but in other people will develop between 4 to 7 days after bitten by mosquito. The proposed system is to classify the dengue fever dataset based on their symptoms using machine learning algorithms such as Support Vector Machine (SVM) and K-Nearest Neighbors (KNN). The symptoms in dataset are based on the dengue and severe dengue from World Health Organization (WHO). The total of 70 patients is listed in dengue fever dataset. In classification tasks, Dengue with no warning signs, Dengue with warning signs or severe dengue will give as results.**

Key Words- Dengue, classification, fever, symptoms

I. INTRODUCTION

Dengue fever may progress to a fatal complication known as Dengue Hemorrhagic Fever (DHF). The symptoms are abdominal pain, diarrhea, vomiting, convulsions, bruising and continual bleeding and the fever duration will be from 2 days to 7 days and circulatory collapse known as Dengue Shock Syndrome. In the transmission of dengue fever, there are mainly three ways and they are virus, human and mosquito. The Aedes aegypti and Aedes albopictus are able to transmit not only dengue fever but also yellow fever, chikungunya and Zika fever. The dengue fever can transmit to human by human when the female Aedes mosquito bites a person infected with dengue virus. The duration of pick up virus by mosquito is 4 to 10 days before the transmission virus for the rest of its life by being to humans. Aedes mosquitoes can be found in the tropical and subtropical regions which cover the America, Europe, Africa, Asia and India. The female Aedes lays about 100 eggs each time and these eggs are laid in clean water found in both natural and man-made containers. Then the eggs are able to resist desiccation for more than six months and will hatch in one day as soon as they are submerged in water. After hatching the mosquito larva will develop into pupa in as little as 5 days. Then spending 2 to 3 days as a pupa, a flying adult mosquito will emerge after completes in approximately 8 to 10 days. The female mosquitoes bite as they need blood for the development of eggs and they usually bite during the day. The control measures for mosquitoes can be divided into three types: biological, physical and chemical. The biological control involves the use of biological agents such as predators and pathogens to suppress the population of pests. The physical control of mosquitoes involves source removal, exclusion and trapping. Mosquito control is the most conventionally done using chemical methods that are used to control the larvae and adults. Mosquitoes are present everywhere so controlling them can be a challenge. Therefore dengue fever is a major problem and most dangerous disease by mosquitoes. In this proposed system, Matlab programming is used to implement the classification on dataset using machine learning algorithms. Finally this system is analyzed which machine learning algorithms between SVM and KNN can give the better classification.

II. RELATED WORKS

[1] Akash C. Jamgade, Prof. S. D. Zade published the disease prediction using machine learning in International Research Journal of Engineering and Technology (IRJET). In that paper, the dataset were collected based on symptoms from multisensory devices and other medical data and then analyzed the dataset using K-mean clustering machine learning algorithm. The structured data and text data of patient used to achieve higher accuracy. [2] C.V. Subbulakshmi and S.N. Deepa published in the Scientific World Journal with the article of medical dataset classification. This paper was proposed the hybrid methodology based on machine learning paradigm and then experimented on five datasets of UCI Machine learning Repository for classification. [3] The author

Md.Fazle published performance evaluation of data mining classification techniques for heart disease prediction in American Journal of Engineering Research (AJER). In this paper, classification on heart disease using Support Vector Machine (SVM), Artificial Neural Network (ANN) and K-Nearest Neighbor (KNN) and then analyzed the accuracy. According to their results SVM can outperform (85.1852%) that of ANN (73.3333%) and KNN(82.963%).

III. METHODOLOGY

The considering symptoms in dengue dataset are Fever, Headache, Vomiting, Rash, Sever Abdomin, Continued Bleeding, Irritable, Mucosal Bleeding and Diagnosis. The machine learning uses the two types of techniques: supervised and unsupervised learning. In supervised learning, it trains the model based on known input and output therefore it can predict the future output. On the other hand, the unsupervised learning group and interpret data based on only input data. In this paper supervised learning such as SVM and KNN algorithms are used to classify the dengue fever dataset. The dengue dataset, there are totally 70 data according to the symptoms of dengue fever in Myanmar.

1. Support Vector Machine

Support Vector Machine (SVM) is a method for classification of both linear and nonlinear data. It uses a nonlinear mapping to transform the training data into a higher dimension [4]. Within this new dimension, it searches for the linear optimal separating hyperplane. With an appropriate nonlinear mapping to a sufficiently high dimension, data from two classes can always be separated by a hyperplane. On the other hand, the label of training data and the output from algorithm are categorized by separating hyperplane. The hyperplane is just like a line dividing a plane into two parts for the label classes. A separating hyperplane can be written as

$$W.X+b=0$$

Where W is a weight vector, W={w1,w2,…,wn}, b is a scalar, referred to as bias and X is the value of attributes in training data.

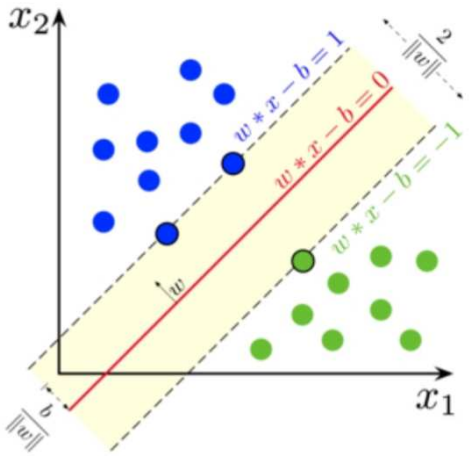

Figure 1. Samples on Maximum-margin hyperplane [5]

2. K-Nearest Neighbors

Nearest-neighbor classifiers are based on learning by comparing a given test tuple with training tuples that are similar to it. The training tuples are described by n attributes and each tuple represents a point in an n-dimensional space. K-Nearest Neighbors classifier find the pattern space in k training tuples that are closet to the unknown tuple when given an unknown tuple. k training tuples are the k "nearest neighbors" of the unknown tuple. The closet between training and unknown tuples, the Euclidean distance is used. The formula of Euclidean distance between two points or tuples X1=(x11,x12,x13,…,x1n) and X2=(x21,x22,x23,…,x2n) is described in the following.

$$EuDis=\sqrt{\sum_{i=1}^{n}(X_{1i}-X_{2i})^2}$$

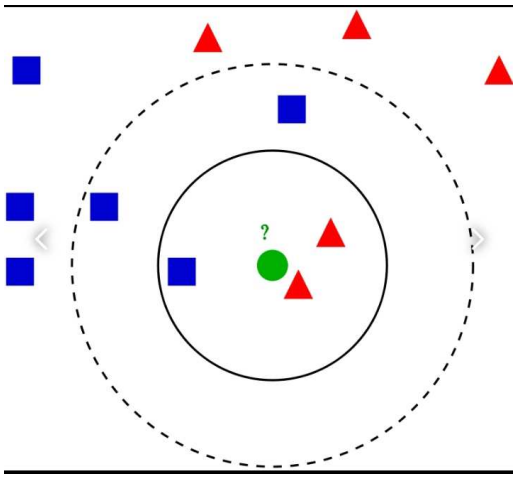

Figure 2. Sample of K-NN Classification [6]

IV. IMPLEMENTATION AND RESULTS

In the implementation of proposed system, firstly create the dataset based on the real symptoms related to the dengue fever. The attributes or symptoms for this dataset are totally nine namely Fever, Headache, Vomiting, Rash, Sever Abdomin, Continued Bleeding, Irritable, Mucosal Bleeding and Diagnosis All of symptoms in dataset are recognized by World Health Organization (WHO) for dengue fever. This system is intended to classify the dengue fever with warning signs, no warning signs or severe dengue. The ground truth data from patients are collected from Mandalay Children's Hospital. There are total of 70 patients data are recorded in dengue fever dataset. And then upload the dataset for classification in Matlab's classification learner using SVM and KNN machine learning algorithms. Finally analyzed the accuracy from classification results and which algorithms can give the better accuracy on dengue fever dataset.

The figure 3 is showed the classification results on dengue dataset using SVM and the correct classification data is described with full line and incorrect data showed with dashed line and asterisk.

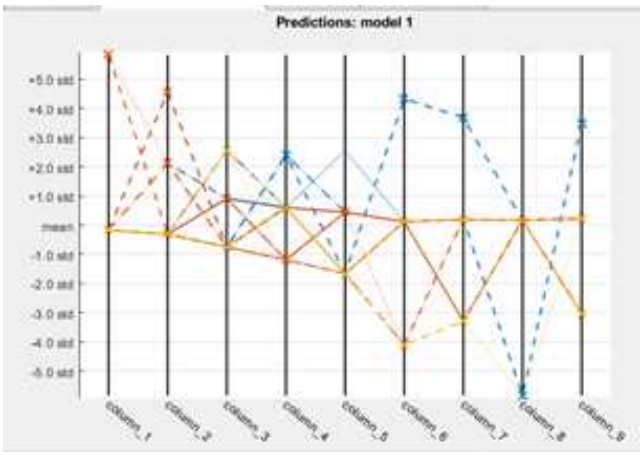

Figure 3. Classification results with SVM

The confusion matrix is used to plot in understanding how the currently selected classifier performed in each class. In this matrix, the rows show the true class and the columns show the predicted class. The confusion matrix can identify the areas where the classifier performed poorly. Its matrix is calculated using the predictions on the held-out observations. The confusion matrix for classification with SVM is shown in the following figure 4.

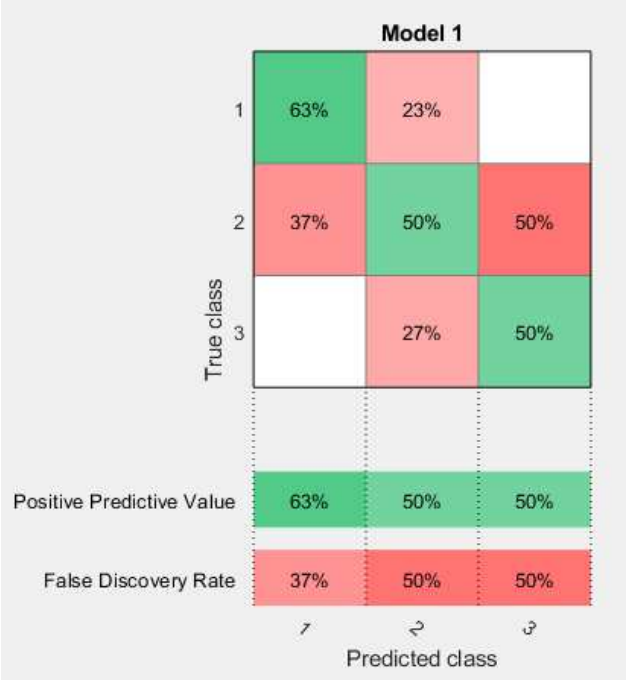

Figure 4. Confusion Matrix of SVM on Dengue

In the above confusion matrix, the green cells are described the classifier has performed well and classified observations of true class correctly. The classification resuts using KNN is shown in figure 5.

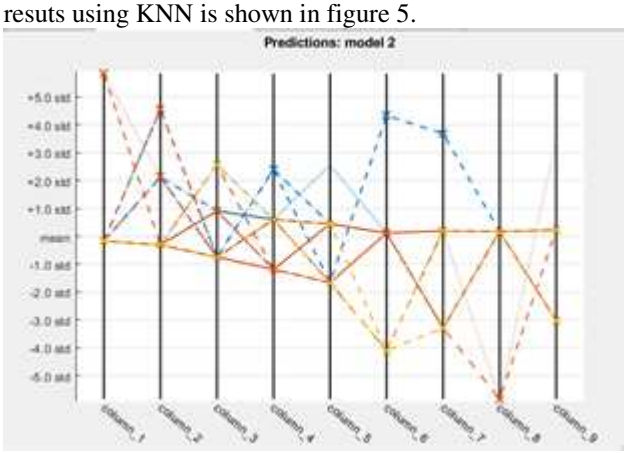

Figure 5. Classification results with KNN

The figure 6 is about the confusion matrix for KNN and the performance for this classifier is more better than the previous SVM classifier when the KNN is 69% in class one whereas SVM is only 63%. Similarly the difference between two machine learning algorithms can be seen in figure 4 and 6.

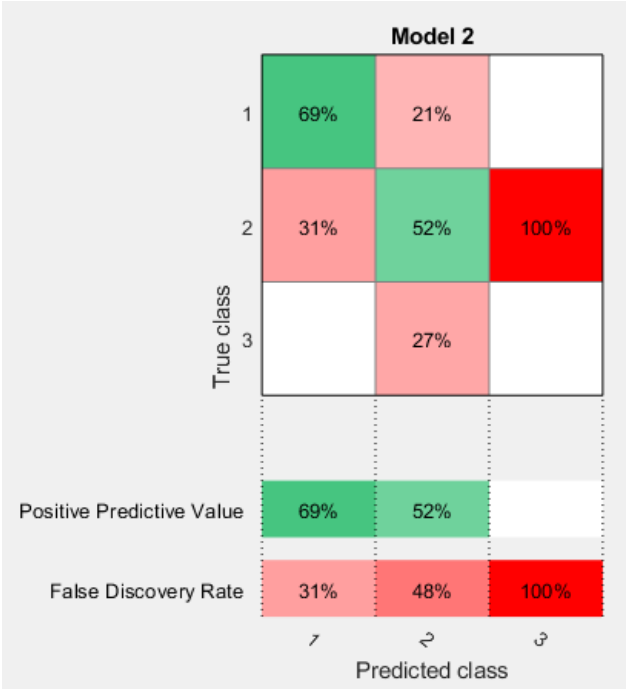

Figure 6. Confusion Matrix of KNN on Dengue

The receiver operating characteristic (ROC) curve shows the true positive rates versus false positive rates for the currently selected trained classifier. The marker on the in ROC plot shows the performance of classifier with the value of false positive rate (FPR) and true positive rate (TPR).

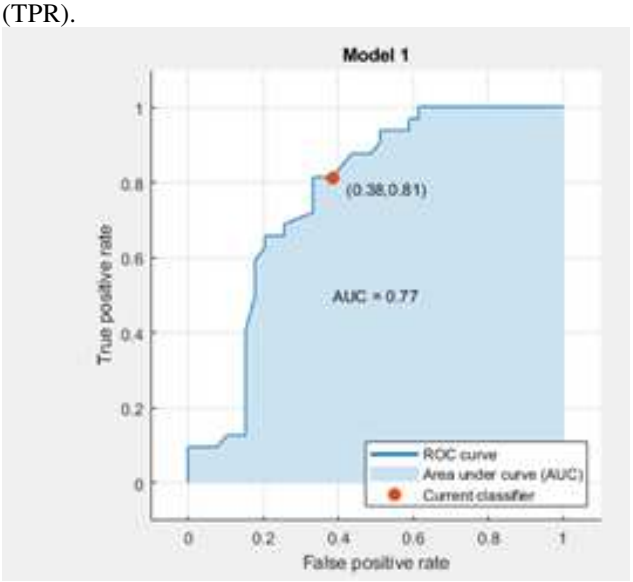

Figure 7. ROC Curve for SVM

In above ROC figure for SVM, the marker value 0.38 indicates the classifier assigns 38% of the observations incorrectly to the positive class and 81% assigns for true positive class or correctly positive class.

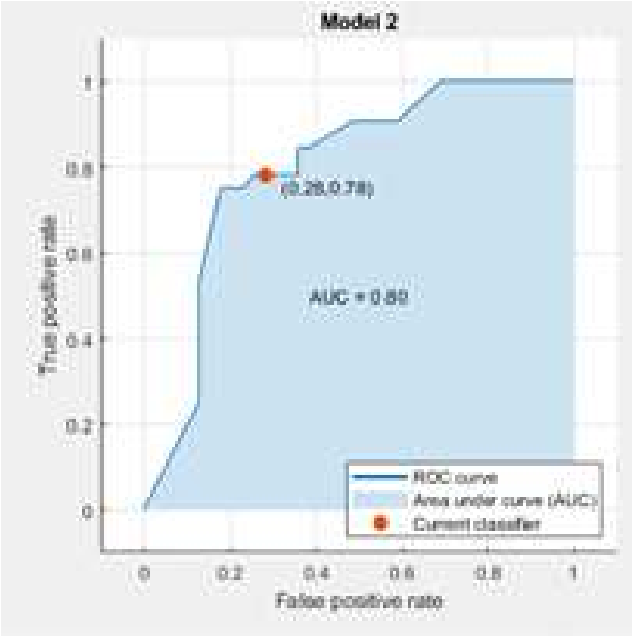

Figure 8. ROC Curve for KNN

According to the ROC curve of KNN, the false positive rate assign value is 28% while the 78% is the true positive class.

V. CONCLUSIONS

The total number of symptoms in dengue dataset is 9 namely Fever, Headache, Vomiting, Rash, Sever Abdomin, Continued Bleeding, Irritable, Mucosal Bleeding and Diagnosis for 70 patients. Then classify this dataset to analyze the dengue fever with warning signs, without warning signs or severe dengue. According to the results, the accuracy of classification with Support Vector Machine (SVM) is 57.7% whereas the K-Nearest Neighbors (KNN) is 59.2%. Therefore the K-Nearest Neighbors can give the better classification accuracy on dengue dataset in Myanmar. Moreover the other supervised or unsupervised method can also use to classify on this dataset.

REFERENCES

[1] Akash C. Jamgade, Prof. S. D. Zade, “Disease Prediction Using Machine Learning”, International Research Journal of Engineering and Technology (IRJET)
[2] C.V. Subbulakshmi and S.N. Deep
[3] Md.Fazle Rabbi, Md.Palash Uddin, Md.Arshad Ali, “Performance Evaluation of Data Mining Classification

Techniques for Heart Disease Prediction", American Journal of Engineering Research (AJER) 2018, Volume-7, Issue-2, pp-278,283.
[4] Chapter2: SVM (Support Vector Machine)-Theory, Machine Learning 101, http://medium.com/machine-learning-101/chapter-2-svm-support-vector-machine-theory-f0812effc72
[5] https://en.m.wikipedia.org/wiki/Support-vector-machine

[6] https://en.m.wikipedia.org/wiki/K-nearest_neighbors-algorithm

Implementation of Sliding Mode Controller for Mobile Robot System

Zin Thuzar Naing[#1],
Yangon Region, Republic of the Union of Myanmar
[1] zinthuzarnaingzin@gmail.com

Abstract-The development of a Sliding Mode controller has been done to be compared with the conventional controller that is being used in a direct current (DC) motor. Simulation study was used to overcome the appearance of nonlinearities and uncertainties in the system with the proposed controller for the armature voltage controlled DC motors. The results are shown that the outputs changes have very little impact on each other, and controller is robust against input disturbances. The proposed model for control system design is implemented using MATLAB/SIMULINK.

Keywords: DC Motor Speed Control System, Mobile Robot, Sliding Mode Controller, SIMULINK, Stability Analysis.

I. INTRODUCTION

Normally, good dynamics of speed command tracking and load regulating response is required in a high performance motor drive system in order to perform task. The simplicity of DC drives is used because of its favorable cost, ease of application, high reliabilities, and flexibilities which is importantly being used in industrial applications, robot manipulators and home appliances which speed and position control of motor are required. Even though the DC motors have several weaknesses, DC motors have been used immensely nowadays in various applications where variable speed was needed due to DC motors flux and torque can be controlled separately by means of controlling the field and armature currents respectively [1].The less complex DC drives uses a single power conversion from AC to DC where DC motors tend to have speed torque characteristics which are better than AC motors. DC drives are also conventionally cheaper for most horsepower ratings which it can also give exceptional speed control in terms of acceleration and deceleration. Normally, the precise model of a nonlinear system in a definite DC motor is problematic to be obtained and parameters acquired from system identifications are possibly be only approximated values.

When there are disturbances and uncertainties in a system, an appropriate control should be designed so that the system stability and desired system responses are achieved. Sliding mode control (SMC) is insensitive in the presence of external disturbances and uncertainties. The robustness properties of SMC have led this approach to be an intensive, popular and suitable method for the control of wide classes of linear and nonlinear systems. PI controllers are not perfectly able to stabilize the system, particularly, when the nonlinearity is very high or the bound of uncertainty is large. In many practical problems, almost perfect disturbance rejection or control performance is required. Sliding mode control (SMC) may be applied to the system to obtain these performances [2].

The objectives of this work are to control the shaft speed and armature current of DC motor and check the stability analysis with the advanced controller system.

Reducing the peak overshot and steady-state error of the DC motor is candidate for controlling the DC motor in Mobile Robot. Therefore, to control the shaft speed and armature current as output variables, armature and field voltages are manipulating variables of a separately excited DC motor using sliding mode controller is the main research problem for the control engineering area.

A SMC could be designed such as to force the system trajectories to move onto a predefined surface within finite time and approaches to an equilibrium point all along this surface. The closed-loop dynamics of the system could be absolutely controlled through the switching function equations provided the system trajectories remain on this surface.

At first, the mathematical model of proposed DC motor has to be derived according to the physical parameters of that motor. And then the theoretical analysis could be carried out with the help of MATLAB/SIMULINK. After that the conventional controller system could be utilized for stability analysis. And the weakness point of conventional controller has to be specified by using the software method like SIMULINK. Finally, the sliding mode control system could be applied to that model for speed control of DC motor.

The rest of the paper is organized as follows. Section II presents the mathematical model of the DC motor which used in mobile robot system. Section III mentions the implementation of sliding mode controller design. Section IV discusses on the results

of the proposed system. Section V concludes the analyses.

II. MATHEMATICA MODEL OF DC MOTOR

The state space model of DC motor is

$$\dot{x}=Ax+Bu=\begin{bmatrix} -\frac{b}{J} & \frac{k_m}{J} \\ -\frac{k_e}{L} & -\frac{R}{L} \end{bmatrix} x+\begin{bmatrix} 0 \\ \frac{1}{L} \end{bmatrix} u$$

x is two dimensional vector x = [x1, x2] where x1 and x2 are angular velocity of shaft and armature current, respectively.

u is the armature voltage.

R and L are the resistance and inductance of the armature coil.

k_e , b , J , and k_m are velocity constant, viscous friction, moment inertia and torque constant.

$$\frac{W(s)}{U(s)}=\frac{\frac{k_m}{JL}}{s^2+\left(\frac{R}{L}+\frac{b}{J}\right)s+\left(\frac{Rb+k_ek_m}{JL}\right)}$$

$$\frac{d^2\omega}{dt^2}+\left(\frac{R}{L}+\frac{b}{J}\right)\frac{d\omega}{dt}+\left(\frac{Rb+k_ek_m}{JL}\right)\omega=\frac{k_m}{JL}u$$

$$\dot{\bar{x}}=\begin{bmatrix} 0 & 1 \\ A_1 & A_2 \end{bmatrix}\bar{x}+\begin{bmatrix} 0 \\ \frac{k_m}{JL} \end{bmatrix} u$$

$$A_1=-\left(\frac{Rb+k_ek_m}{JL}\right)$$

$$A_2=-\left(\frac{R}{L}+\frac{b}{J}\right)$$

Figure.1 shows the SIMULINK Model for DC Motor used in Mobile Robot. The parameters which used in this SIMULINK model is given in Table. I.

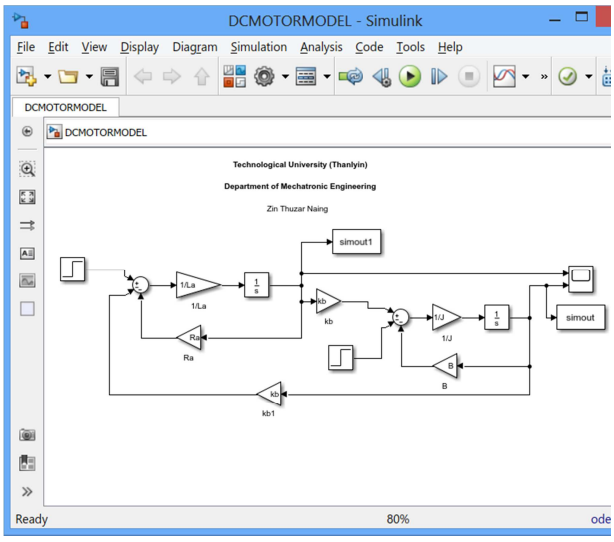

Figure.1. SIMULINK Model for DC Motor used in Mobile Robot

Table1 Parameters of DC Motor

Parameter	Value
R	7.17 Ω
L	0.953×10^{-3}H
k_e	0.29 Vs
k_m	46×10^{-3}NmA^{-1}
J	4.42×10^{-6}Kgm^2
b	2.99×10^{-4}Nms
λ	-100
K_s	1
K_p	0

III. IMPLEMENTATION OF SLIDING MODE CONTROLLER DESIGN

Sliding mode techniques are one approach to solving control problems and are an area of increasing interest.SMC has been applied including nonlinear system, multi-input multi-output (MIMO) systems, discrete-time models, large-scale and infinite-dimension systems, and stochastic systems. The most eminent feature of SMC is it is completely insensitive to parametric uncertainty and external disturbances during sliding mode. In SMC, the system is designed to drive and then constrain the system state to lie within a neighborhood of the switching function. Its two main advantages are (1) the dynamic behavior of the system may be tailored by the particular choice of switching function, and (2) the closed-loop response becomes totally insensitive to a particular class of uncertainty. Trajectory of a system can be stabilized by a sliding mode controller. After the initial reaching phase, the system states "slides" along the line s=0. The particular s=0 surface is chosen because it has desirable reduced-order dynamics when constrained to it. In this case, the $s=cx_1+x^\circ_1$; c>0. Surface corresponds to the first-order LTI system $x^\circ_1=-cx_1$, which has an exponentially stable origin.

The system block diagram for sliding mode

controller design for mobile robot system is shown in Figure.2.

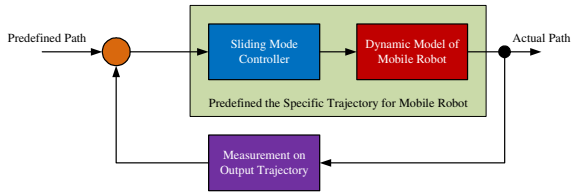

Figure.2. Overall System Block Diagram

IV. RESULTS AND DISCUSSIONS

The error between the reference and motor speed output is used as trajectory function to adapting the primes part and the consequences part of the sliding mode control and Conventional controller so that the error goes towards zero.Figure.3 illustrates the comparison results of SMC controller output signal (upper) and actual output signal from the DC motor (lower) based on simulation time. The results say that the selected motor is appropriate for designing the motor in mobile robot system.Figure.4 demonstrates the Step Response for SMC Gain at 1000. Figure.5 presents the Control Input Response for SMC Gain at 1000. Figure.6 mentions the Trajectory Accuracy Responses for SMC Gain at 1000. There have been many analyses for various kinds of SMC gain. We could easily find the higher gain of SMC for lower error between the real and actual results of tracking.

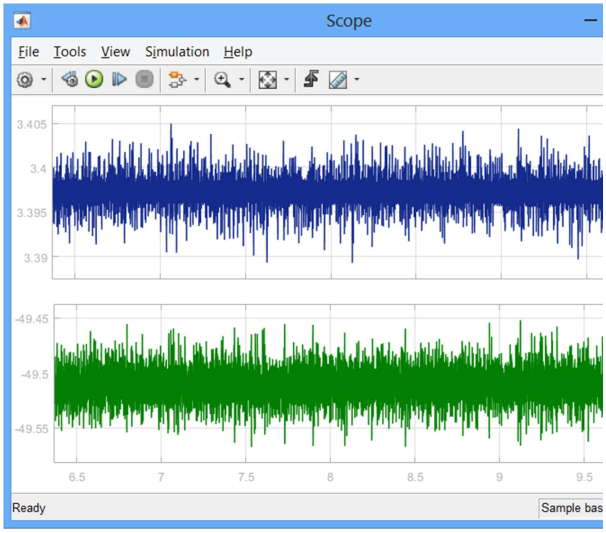

Figure.3. Comparison Results of SMC Controller Output Signal (Upper) and Actual Output Signal from the DC Motor (Lower) based on simulation time

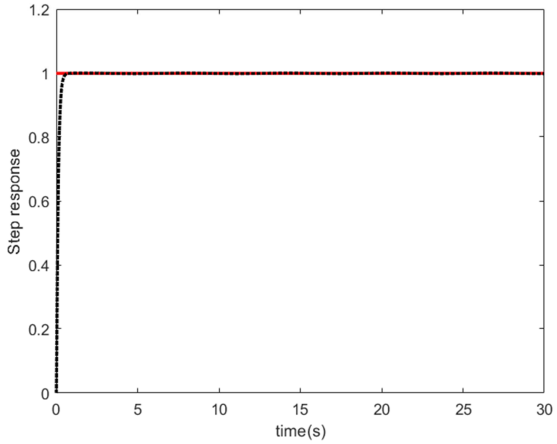

Figure.4. Step Response for SMC Gain at 1000

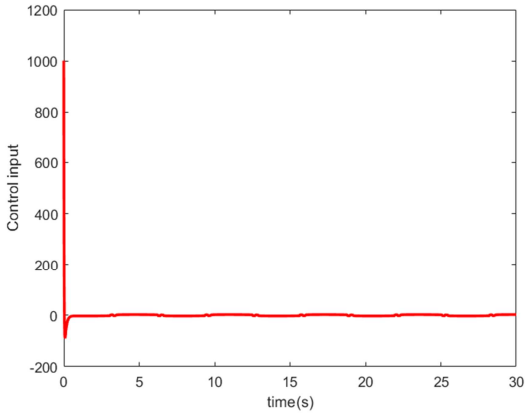

Figure.5. Control Input Response for SMC Gain at 1000

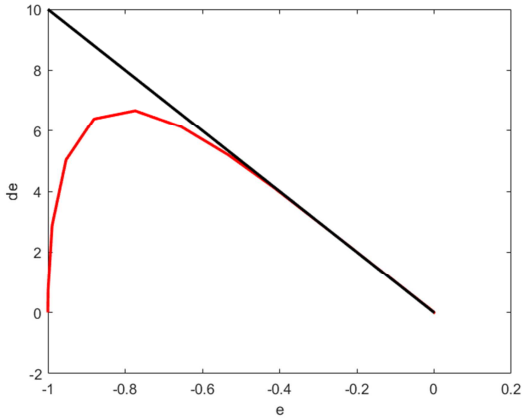

Figure.6. Trajectory Accuracy Responses for SMC Gain at 1000

V. CONCLUSION

A mathematical modeling was done on the DC motor. The step by step procedures for DC motor

analysis according to the various kinds of controller system are completed by theoretical approaches. The SMC gain is very important for analyzing the accuracy of the response for mobile robot. If the higher SMC gain is used in this system, the higher accuracy results of mobile robot system will be obtained. Overall, it is concluded that the sliding mode controller is found to be superior, more robust, faster andflexible and is insensitive to the parameter variation as compared with conventional controller. The research work is provided the obvious features of sliding mode controller are robustness in uncertain and input disturbance.

ACKNOWLEDGMENTS

I greatly appreciate to all teachers from the Yangon Region of the Union of Myanmar who work in Research.

I would like to give great thanks to the Yangon Region of the Union of Myanmar who work in Research for kind permission to study related on-going research projects.

REFERENCES

[1] J. J. E. Slotine, "sliding controller design for nonlinear systems", international journal of control, vol. 40, no.2, (1984), pp. 421-434.

[2] Vadim I. Utkin, "Sliding Mode Control Design Principles and Applications to Electric Drives", IEEE Transactions on Industrial Electronics, February 1993.

[3] K. David Young, Vadim I. Utkin and U mit 0 zguner, "A Control Engineer,s Guide to Sliding Mode Control", IEEE Transactions on Control Systems Technology, Vol.7, No.3, May 1999.

[4] S. J. Chapman, "Electric Machinery Fundamentals," the Mcgraw-hill companies, 1999.

[5] Utkin, V.I., Guldner, J., Shi, J. (1999). "Sliding mode control in electromechanical Systems" CRC Press.

[6] K. D. Young, V. Utkin and U. Ozguner, "A control engineer's guide to sliding mode control", IEEE conference(2002), pp. 1-14.

[7] Mohammed GodamSarwer, Md. Abdur Rafiq and B.C.Gosh, "Sliding Mode Speed Controller of a D.C. Motor Drive", Journal of Electrical Engineer-ing, The Institution of Engineers, Bangladesh, Dec 2004.

[8] Uma Maheshwararao, Y.S.KishoreBabu, K.Arnaresh, "Sliding Mode Speed Control of a DC Motor", 2011 International Conference on Communication Systems and Network Technologies.

[9] Ned Mohan, "Electric Drives: An Integtalive Approach", MNPERE Minneapolis, 2001.

[10] K.H. Ang, G.c.y. Chong, and Y. Li, "PID Control System Analysis, Design, and Technology," IEEE Transactions on Control Systems Technology., Vol. 13, No. 4, pp. 559-576, July.2005.

[11] J. K. Liu and F. C. Sun, "Research and development on theory and algorithms of sliding mode control", Journal of Control Theory and Applications, vol. 24, no. 3, 2007.

[12] Transl. J. Magn. Japan, vol. 2, pp. 740-741, August 1987 [Digests 9th Annual Conf. Magnetics Japan, p. 301, 1982].

[13] Edward C. and Spurgeon, S. K., "Sliding mode control: theory and application,", Taylor and Francis, London,1998.

[14] M. Young, The Technical Writer's Handbook. Mill Valley, CA: University Science, 1989.

[15] Herlino, A.L.; Jidin, A.; Faizal, C.W.; Zalani, C.W.M.; Sanusi, S.; Jopri, M.H.; Manap, M. "Comparative study of current control strategy for DC motors", Power Engineering and Optimization Conference (PEOCO), 2013 IEEE 7th International, On page(s): 588 - 593.

THEORETICAL AND NUMERICAL MODAL ANALYSIS OF SIX SPOKES WHEEL'S RIM USING ANSYS

Dr Htay Htay Win[1], May Zon Than Oo[2]

[1]Mechanical Engineering Department,
Mandalay Technological University, Mandalay, 05072, Myanmar
[2]Mechanical Engineering Department,
Mandalay Technological University,Mandalay, 05072, Myanmar

*htayhtayw@gmail.com,mayzonthanoo@mtu.edu.mm

***Abstract*—*This paper presents the frequency analysis of 6 spokes wheel's rim under the value of speed 100km/h. Modal analysis is to determine the vibration characteristics (natural frequencies and mode shapes) of a structure or machine component while it is being designed. Modal analysis is a way to calculate the working frequencies of system in structural mechanics. It is to determine the natural mode shapes and frequencies of an object or structure during free vibration. The natural frequencies and mode shapes are important parameters in the design of a structure for dynamic loading conditions. The numerical results of natural frequencies for global mode shapes were compared with working frequency of car's wheel's rim.The model of wheel's rim is drawn by using SolidWorks 2014 and analysed by ANSYS 14.5. The investigation is made on wheel's rim model of station wagon, Toyota's Kluger. The tyre sidewall marking is P225/65R*17. There are many forces acting on the wheel. Inflation pressure acts on the wheel's rim with magnitude of 241kPa. Principal stress theory, von-Mises stress theory, total deformation and natural frequency equations are applied by theoretically and numerically. The results from theoretical and numerical approaches of frequencies of wheel's rim are compared.The materials of wheel's rim are aluminum alloy, alloy steel and magnesium alloy. Among them, alloy steel is the suitable material for wheel's rim because it has the minimum values of natural frequency. Working frequency of wheel's rim is 41.6Hz.The pitch (angular motion) and the bounce (up and down linear motion) frequencies are 5 and 6.41rad/s. The numerical result of frequency for alloy steel are first mode shape 351Hz, second mode shape 353Hz, third mode shape431Hz, fourth mode shape 432Hz, fifth mode shape 552Hz, sixth mode shape 578Hz, seventh mode shape 592Hz, eighth mode shape762Hz,ninth mode shape 925Hz and tenth mode shape 927Hz.Working frequency does not match with natural frequencies of car's wheel's rim at all mode shapes. This gives clear indication that wheel's rim is safe against resonance phenomenon.*

Keywords: Car's Tyre, Deformation, Frequency, Speed, Von-Mises Stress

I. INTRODUCTION

The wheel is a device that there are forces acting on the car. Early wheels were simple wooden disks with a hole for the axle. The spoke wheel was invented more recently, and allowed the construction of lighter and swifter vehicles. Alloy Steel wheels are automotive wheels which are made from an alloy of aluminium or magnesium or sometimes alloy steel.

Alloy Steel wheels differ from normal steel wheels because of their lighter weight, which improves the steering and the speed of the vehicle. Spoked wheels of car are efficient, highly evolved, structural systems.

To install the wheel, the holes in the center section of the rim are placed over the studs and lug nuts are threaded onto the studs. The lug nuts can be tightened in across or star pattern. The tapered end of each lug nut matches a tapered area in the wheel mounting hole. The matching tapers help center the wheel.

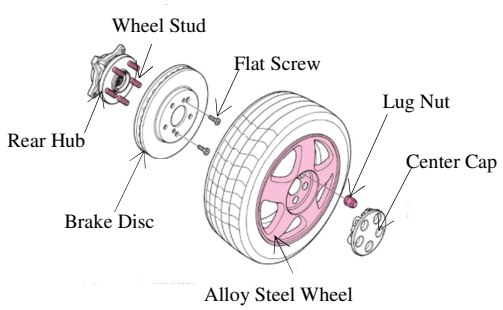

Figure1 Alloy Steel Wheel is fastened to the Rear Hub with Steel Studs and Lug Nuts [16]

Figure 1 illustrates Alloy Steel wheel is fastened to the rear hub with steel studs and lug nuts.

II. FORCES ACTING ON THE CAR'S TYRE

Braking force, aerodynamic drag force, centrifugal force, friction force and tangential force act as x direction of car's wheel. Bump force, aerodynamic lift force and radial force act in the vertical direction as y axis of car's wheel. Lateral force and axial force act in the direction as z of car's wheel.

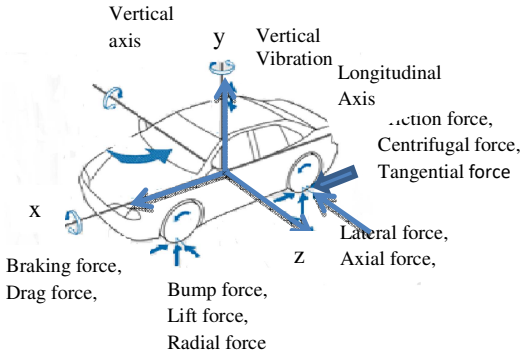

Figure 2 Forces Acting on the Car [1]

(i) Vertical Weight, W_V

The total vertical weight is determined by the sum of the vehicle weight, passenger weight and extra weight.

Vertical weight=vehicle weight+ passenger weight+ extra weight

(ii) Lateral Force, F_L

Lateral force acts upon the wheel when steering or when there is a crosswind. They cause the vehicle to change direction.

$$F_L = [(C_f+C_r)\beta] + \frac{1}{v}(aC_f - bC_r)\omega - (C_f\delta) \quad (1)$$

(iii) Braking Force, F_B

While the car is running with a constant speed, brake can be used to stop suddenly. Braking force appears at the time of one second and final speed is zero.

The braking time is the total time required to stop the vehicle absolutely.

$$F_B = ma = m\left(\frac{v_f - v_0}{t}\right) \quad (2)$$

(iv) Friction Force, F_R

When braking force is applied to the wheel, frictional force is generated between the tire and the road surface. Coefficient of friction value depends upon the road condition and the weather conditions.

$$F_R = \mu F_N \quad (3)$$

(v) Aerodynamic Drag Force, F_D

The aerodynamic drag force is the product of the density of air, the drag coefficient, frontal cross-sectional area of car and the car's speed. The value of lift coefficient (C_L) and drag coefficient (C_D) depend upon styles of car such as sedan, coupe, fastback and station wagon. The value of C_L and C_D is chosen for station wagon.

$$F_D = \frac{1}{2}\rho A C_D v^2 \quad (4)$$

(vi) Aerodynamic Lift Force, F_L

The aerodynamic lift force is the product of the density of air, the lift coefficient, bottom cross-sectional area of car and the car's speed.

$$F_L = \frac{1}{2}\rho A C_L v^2 \quad (5)$$

(vii) Radial Force, F_R

When the car is in motion, the radial load becomes cyclic in nature with a continuous rotation of the wheel. Radial load depends upon rim's radius, the width of the bead seat, the angle of loading and the inflation pressure in tire.

$$F_R = 8 b r_{rim} \theta_0 \quad (6)$$

(viii) Axial Force, F_a

The air pressure, acting against the sidewall of the Kluger's tire, generates a load, which is in the axial direction.

$$F_a = (r_t^2 - r_{rim}^2)\frac{P_0}{4 r_{rim}} \quad (7)$$

(ix) Bump Force, F_m

Bump force is the force between the passenger and passenger's seat of car.

$$F_m = \frac{mv^2}{r_{rim}} + mg \quad (8)$$

(x) Tangential Force, F_T

Tangential force is a force that acts on a moving body in the direction of a tangent to the curved path of the body.

$$F_T = \frac{mv^2}{r}\sin\theta \quad (9)$$

(xi) Centrifugal Force, F_c

A centrifugal force is a force , arising from the body's inertia, which appears to act on a body moving in a circular path and is directed away from the centre around which the body is moving. Table 1 shows the specification data for the tyre of P225/65R*17. Table 2 showsproperties of aluminum alloy.

$$F_c = \frac{mv^2}{r_{rim}} \quad (10)$$

Table 1. Specification Data of wheel's rim

Design Parameter	symbol	value	Unit
Aspect Ratio	AR	75	-
Diameter of rim	D_{rim}	381	mm
Tyre Diameter	D_t	688.5	mm
Overall width	w	80	mm
Inflation Pressure	P_o	241	kPa

The specification data for the tyre of P225/65R*17 is shown in Table 1. Aspect ratio is 75, diameter of rim is 381mm and tyre diameter is 688.5mm respectively. Overall width is 80mm and inflation pressure is 241kPa.

Table 2. Properties of Materials [1]

Properties	Aluminum Alloy	Magnesium Alloy	Alloy Steel
Density (kg/m^3)	2810	1800	7700
Young Modulus (GPa)	72	45	210
Poisson Ratio	0.33	0.35	0.28
Yield Stress(MPa)	483	250	552

Properties of materialsare shown in Table 2. The density of rubber is $1.1Mg/m^3$, young modulus is 0.05GPa, Poisson ration is 0.49 and yield stress is 5.5MPa respectively.

III. THEORETICAL MODAL ANALYSIS OF WHEEL'S RIM

The x-axis is the intersection of the wheel plane and the road plane with positive direction forward. The y-axis perpendicular to the road plane with positive direction upward. The z-axis in the road plane, its direction being chosen to make the axis system orthogonal and right hand.

There are vertical component acting in the y direction, longitudinal component acting in the x direction, and lateral component acting in the z direction.The force exerted in the x direction is the sum of friction force, braking force, aerodynamic drag force and tangential force. The force exerted in the y direction is the sum of bump force, lift force and radial force. The force exerted in the z direction is the sum of lateral force, axial force and centrifugal force.

Figure 2 shows the forces acting on car direction of x, y and z.

$$\text{Stress in x direction, } \sigma_x = \frac{F_x}{A_x} \quad (11)$$

$$\text{Stress in y direction, } \sigma_y = \frac{F_y}{A_y} \quad (12)$$

$$\text{Stress in z direction, } \sigma_z = \frac{F_z}{A_z} \quad (13)$$

By using von-Mises Criterion equation,

$$\bar{\sigma} = \frac{1}{\sqrt{2}}\left[(\sigma_1-\sigma_2)^2+(\sigma_2-\sigma_3)^2+(\sigma_3-\sigma_1)^2\right]^{\frac{1}{2}} \quad (14)$$

$$\text{Deformation, } \delta = \frac{Pl}{AE} = \frac{\sigma l}{E} \quad (15)$$

$$\text{Natural Frequency, } F(Hz) = \frac{1}{2\pi}\sqrt{\frac{g}{\delta}} \quad (16)$$

Effective stress, total deformation and natural frequency can be calculated by using the equation 14, 15 and 16.

IV. MODAL ANALYSIS OF WHEEL'S RIM

The modal of the wheel's rim was drawn in Solid work 2014 and added in ANSYS 14.5. This geometry model was meshed with high smoothing. This meshed model was imported to static structural analysis. Figure 3 shows design procedure for modal analysis using ANSYS.In modal analysis of car's wheel's rim, only fixed support is provided at the bolt hole circle location of car's wheel as shown in Figure 4. ANSYS 14.5 software is used to analyze the mode shapes of car's wheel's rim.

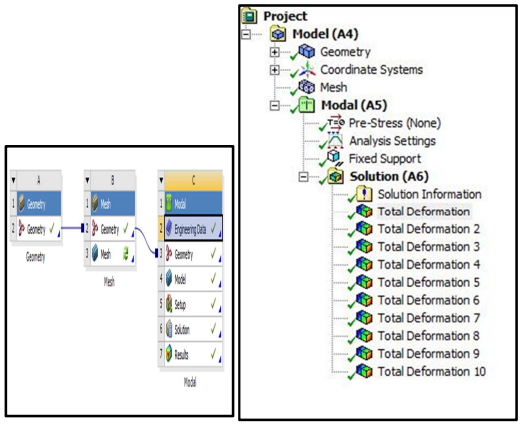

Figure 3 Design procedure for modal analysis using ANSYS

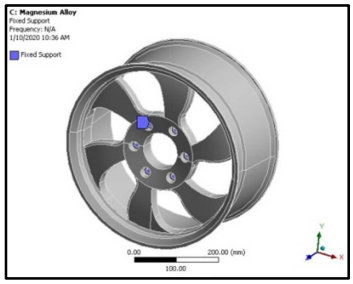

Figure 4 Fixed Support of 6 Spokes Wheel's Rim

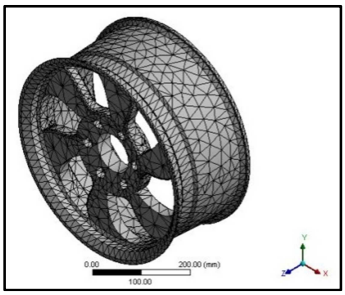

Figure 5 Meshing of 6 Spokes Wheel's Rim

This geometry model was meshed with high smoothing of 11230 nodes and 15120 elements as shown in Figure 5.

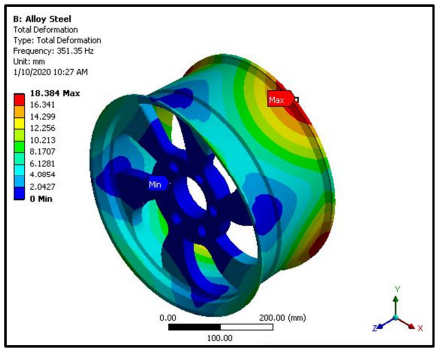

Figure 6 Natural Frequency of Mode Shape 1 at Total Deformation

If the wheel is being forced to vibrate at its natural frequency, resonance and large amplitude vibrations will occur. When designing objects, the mechanical natural or resonance frequencies of the component parts do not match vibration frequencies of oscillating parts. The numerical results of natural frequencies for global mode shapes were compared with working frequency of tyre.

In mode shape 1, the working frequency is 41.6 Hz. Figure 6 shows the natural frequency of mode shape 1 at total deformation. From obtained results, the natural frequency of the tyre at mode shape 1 is 351 Hz. As the operating frequency of wheel's rim and natural frequency of wheel's rim do not match so the wheel's rim structural has no tendency of resonance.

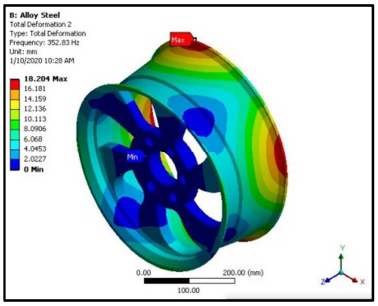

Figure 7 Natural Frequency of Mode Shape 2 at Total Deformation

A mode shape is a specific pattern of vibration executed by a mechanical system at a specific frequency. Different mode shapes will be associated with different frequencies. Figure 7 shows the natural frequency of mode shape 2 at total deformation. For global mode shape 2, the natural frequency is 353 Hz while operating frequency is 41.6 Hz. As both the frequencies do not match so the car's wheel rim has no tendency of resonance.

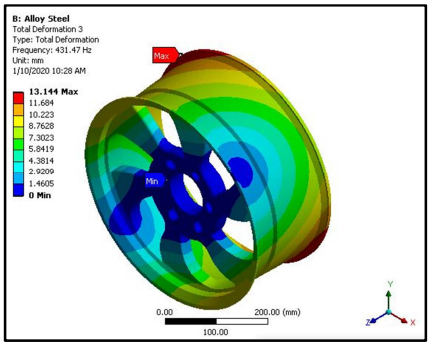

Figure 8 Natural Frequency of Mode Shape 3 at Total Deformation

For global mode shape 3, the natural frequency is 431 Hz while operating frequency is 41.6 Hz. As both the frequencies do not match so the wheel's rim has no tendency of resonance. Figure 8 shows the natural frequency of mode shape 3 at total deformation.

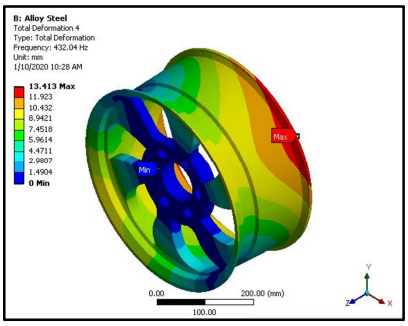

Figure 9 Natural Frequency of Mode Shape 4 at Total Deformation

For global mode shape 4, the natural frequency is 432 Hz while operating frequency is 41.6 Hz. As both the frequencies do not match so the wheel's rim has no tendency of resonance. Figure 9 shows the natural frequency of mode shape 4 at total deformation.

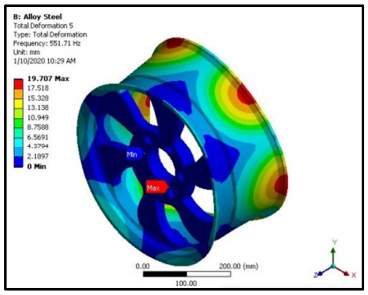

Figure 10 Natural Frequency of Mode Shape 5 at Total Deformation

For global mode shape 5, the natural frequency is 552 Hz while operating frequency is 41.6 Hz. As both the frequencies do not match so the wheel's rim has no tendency of resonance. Figure 10 shows the natural frequency of mode shape 5 at total deformation.

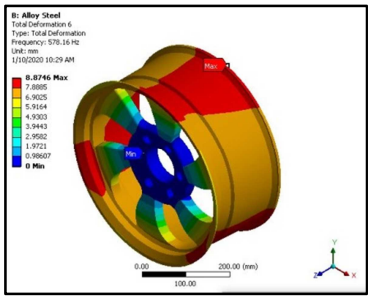

Figure 11 Natural Frequency of Mode Shape 6 at Total Deformation

For global mode shape 6, the natural frequency is 578 Hz while tyre operating frequency is 41.6 Hz. As both the frequencies do not match so the wheel's rim has no tendency of resonance. Figure 11 shows the natural frequency of mode shape 6 at total deformation.

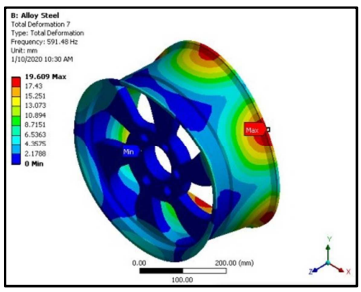

Figure 12 Natural Frequency of Mode Shape 7 at Total Deformation

For global mode shape 7, the natural frequency is 591 Hz while operating frequency is 41.6 Hz. As both the frequencies do not match so the wheel's rim has no tendency of resonance. Figure 12 shows the natural frequency of mode shape 7 at total deformation.

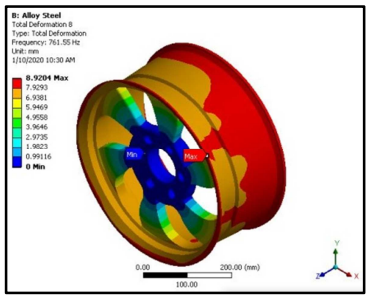

Figure 13 Natural Frequency of Mode Shape 8 at Total Deformation

For global mode shape 8, the natural frequency is 762 Hz while operating frequency is 41.6 Hz. As both the frequencies do not match so the car's wheel's rim has no tendency of resonance. Figure 13 shows the natural frequency of mode shape 8 at total deformation.

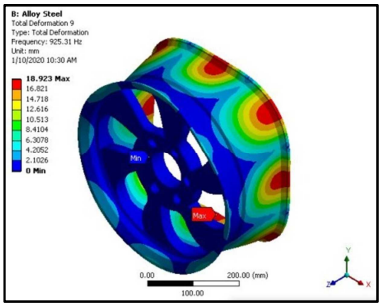

Figure 14 Natural Frequency of Mode Shape 9 at Total Deformation

For global mode shape 9, the natural frequency is 925Hz while working frequency is 41.6 Hz. As both the frequencies do not match so the wheel's rim has no tendency of resonance. Figure 14 shows the natural frequency of mode shape 9 at total deformation.

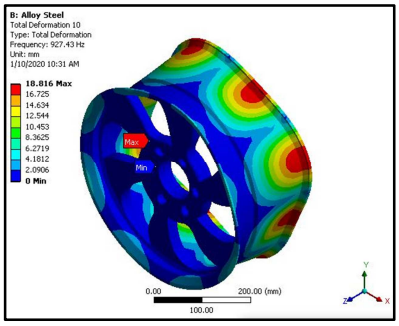

Figure 15 Natural Frequency of Mode Shape 10 at Total Deformation

For global mode shape 10, the natural frequency is 927Hz while operating frequency is 41.6 Hz. As both the frequencies do not match so the wheel's rim has no tendency of resonance. Figure 15 shows the natural frequency of mode shape 10 at total deformation.

The natural frequencies and mode shapes are important parameters in the design of a structure. The numerical results of natural frequencies for global mode shapes were compared with working frequency of wheel's rim. The natural frequencies at mode shapes of wheel's rim are shown in Table 3.

Table 3. Natural frequencies of mode shapes of car' wheel's rim for different materials

Mode	1	2	3	4	5
Natural Frequency, Aluminium Alloy (Hz)	144	278	344	459	529
Natural Frequency, Alloy Steel(Hz)	351	353	431	432	552
Natural Frequency, Magnesium Alloy (Hz)	347	349	429	480	550
WorkingFrequency (Hz)					41.6
The Pitch(angular motion) frequency,rad/s					5
The Bounce (up and down linear motion) frequency,rad/s					6.41

Mode	6	7	8	9	10
Natural Frequency Aluminium Alloy (Hz)	570	597	917	928	1117
Natural Frequency, Alloy Steel(Hz)	578	591	762	925	927
Natural Frequency, Magnesium Alloy (Hz)	576	589	755	925	928
Working Frequency (Hz)					41.6
The Pitch(angular motion) frequency,rad/s					5
The Bounce (up and down linear motion) frequency,rad/s					6.41

Table 4. Result Values of Working Frequency of Rim at Various Speeds

Velocity, km/h	Alloy Steel δ, mm	Working Frequency, Hz
20	0.00287	294.3
40	0.05752	65.73
60	0.08629	53.66
80	0.11505	46.5
100	0.14381	41.6
120	0.17257	38
140	0.20133	35
160	0.23008	32
180	0.25886	31

Natural frequencies of mode shapes of wheel's rim are shown in Table 3. Working frequency of car's wheel's rim is 41.6Hz.The natural frequencies are 351Hz for first mode shape, 353Hz for second mode shape, 431Hz for third mode shape, 483Hz for fourth mode shape, 552Hz for fifth mode shape, 578Hz for sixth mode shape, 594Hz for seventh mode shape, 762Hz for eighth mode shape, 925Hz for ninth mode shape and 927Hz for tenth mode shape respectively.

V. CONCLUSIONS

In this research, forces acting on the wheel's rim are calculated in the direction of x, y and z. Then, the von-Mises stresses, total deformation and working frequency of the wheel's rim are calculated for materials alloy steel at speed 100km/h. And working frequency and natural frequency are compared. From result, working frequency of car's wheel's rim is 41.6 Hz. Working frequency does not match with natural frequencies of wheel's rim with all mode shapes. Therefore, the car's wheel's rim has no tendency of resonance. The first natural frequency is far higher than maximum operating frequency. This gives clear indication that wheel's rim is safe against resonance phenomenon. Similarities, in second, third, fourth, fifth, six, eighth, ninth and tenth mode shape the designed wheel's rim working frequency and natural frequencies do not match. In all global mode shapes, the wheel's rim have no tendency of resonance so designed wheel's rim is safe. Working frequency changes according to car's speed. But the working frequency does not exceed at speed 20 to 180km/h. A real model has an infinite number of natural frequencies. However, a finite element model has a finite number of natural frequencies. Only the first few modes

are needed.

ACKNOWLEDGMENT(S)
The first author wishes to acknowledge her deepest gratitude to her parents, professors, relatives and friends to carry out this paper.

NOMENCLATURE

v -speed of car
β -slip angle of car
δ -steering angle
μ -coefficient of friction
C_D , C_L-Drag Coefficient and Lift Coefficient
r_{rim} -the radius of rim
r_t -radius of tire
P_0 -inflation pressure in tire
$\bar{\sigma}$ -von-Mises stress
$\bar{\varepsilon}$ -equivalent elastic strain
δ -deformation
E - Modulus of elasticit

REFERENCES

[1] D. Santhosh Kumar, "Modal Analysis and Design Optimization of Automotive Wheel Rim",2017.
[2] ShwetabhSuman. "Impact and modal analysis for different alloy wheel compositions",2017.
[3] Prof.Sharad, D.Kachave, "Experimental and Finite Element Analysis of Automobile Wheel Disc",2016.
[4] K. Reif (Ed.), "Basic principles of vehicle dynamics," *Brakes, Brake Control and Driver Assistance Systems*, 2014.
[5] Sourav Dos, "Design and Weight Optimization of Aluminum Alloy Wheel",2014.
[6] S.Ganesh, "Design and Analysis of Spiral Wheel Rim for Four Wheeler",2014.
[7] Nicholas Spagnol, "The Influence of the Disc Manufacturing Process on the Fatigue Life of Commercial Vehicle Wheels Manufactured By S55JR Steel",2014.
[8] Saran theja, Vamsi Krishna Mamidi, "Structural and Fatigue Analysis of Two Wheeler Lighter Weight Alloy Wheel", 2013.
[9] Mr Sunil, "Analyze the Effect of Slip Angle on Fatigue Life of Wheel Rim of Passenger Car by Using Radial Fatigue Testing",2013.
[10] P.Meghashyam, "Design and Analysis of Wheel Rim using Analysis",2013.
[11] Ch.P.V.Ravi Kumar, "Topology Optimization Of Aluminum Alloy Wheel",2013.
[12] S Vikranth Deepak, "Modelling and Analysis of Alloy Wheel for Four Wheeler Vehicle",2012.
[13] J. Stearns, T. S. Srivatsan, X. Gao, and P. C. Lam, "Understanding the Influence of Pressure and Radial Loadson Stress andDisplacement Response of a Rotating Body:The Automobile Wheel",2005.
[14] N.Kovunovic, M.Trajanovis and M.Stojkovic, " FEA of tyres subjected to static loading", 2007.
[15] Keller, T.A., "Model for the Prediction of the Contact Area and the Distribution of Vertical Stress below Agricultural Tyres from Readily Available Tyre Parameters", Biosystems Engineering, Vol.92, 2005, pp.85-96.
[16] Tonuk,E., " Prediction of Automobile Tyre Cornering Forces Characteristics by Finite Element Modeling and Analysis", Computer &Struct, Vol.79,N0.13, 2001,pp.1219-1232.
[17] Willcox, "Driveline and Wheel Components", 2000.

Synthesis, Characterization and Application of Carbon Nanotubes for Conductive Ink Application

Htein Win[*], Hsu Pyae Sone Lwin[**]

[*]*Faculty of Advanced Materials Engineering, University of Technology (Yatanarpon Cyber City), Pyin Oo Lwin, 05087, Myanmar*
[**]*Faculty of Advanced Materials Engineering, University of Technology (Yatanarpon Cyber City), Pyin Oo Lwin, 05087, Myanmar*

[*]kohtein@gmail.com, [**]hsupyaesonelwin.ycc@gmail.com

ABSTRACT

Chemical synthesis method is a kind of method in which carbon nanotubes were prepared from graphite powder by using a new chemical route of oxidation method in a mixed solution of nitric acid and sulfuric acid with potassium chlorate. After heating the solution up to 70°C for 24 hours and leaving them in the air for 3 days, nearly 0.02 g carbon nanotube bundles were obtained. Carbon nanotubes were characterized by X-ray diffraction (XRD) and Scanning Electron Microscope (SEM). The resultant carbon materials can be confirmed as carbon nanotubes which have hair- like structure and their diameter is 20~40 nm approximately. Carbon Nanotubes are remarkable electrical conductivity because of their structure. Multi-walled carbon nanotubes obtained by chemical synthesis method for conductive ink application. Resistance of carbon nanotubes in conductive ink is ~ 4 Ω and conductance is 0.25 siemens approximately.

Key Words- ***Carbon Nanotubes (CNTs), Conductive Ink, Scanning Electron Microscope (SEM), X-ray Diffraction (XRD).***

I. INTRODUCTION

Carbon nanotubes are graphite sheets rolled up into cylinders with diameters of the order of a few nanometers and up to some millimeters in length with at least one end capped with a hemisphere of the fullerene structure [1]. Nanotubes are members of the fullerene structural family. Their name is derived from their long, hollow structure with the walls formed by one-atom-thick sheets of carbon, called grapheme [2]. Carbon nanotubes were discovered by Sumio Iijima by arc evaporation method in 1991[3]. There are two main types of nanotubes: the single-walled carbon nanotubes (SWCNTs or SWNTs) and the multi-walled carbon nanotubes (MWCNTs or MWNTs), in particular the double walled carbon nanotubes (DWCNTs or DWNTs) [1].

CNTs have captured the intensive attention of researchers worldwide due to the combination of their expected structural perfection, small size, low density, high stiffness, high strength, and excellent electronic properties [4]. They feature extraordinary strength, show efficient conductivity of heat, and unique electrical properties (metallic conductivity and semi-conductivity). Many potential applications have been proposed for carbon nanotubes, including conductive and high-strength composites; energy storage and energy conversion devices; sensors; field emission displays and radiation sources; hydrogen storage media; and nanometer-sized semiconductor devices, probes, and interconnect [5].

II. SYNTHESIS OF CARBON NANOTUBES

The three commonly-used methods for production of CNTs are arc-discharge method, laser ablation method and chemical vapor deposition method which require high temperature and high pressure. Therefore, these methods cannot be performed easily and inexpensively. Synthesizing CNTs remains costly and difficult. After studying the literature, it was discovered that carbon nanotubes can be synthesized

by chemical method at low temperature without applying pressure.

1. Materials

Graphite was used as starting materials. Potassium chlorate ($KClO_3$) was used as catalyst and a mixture of nitric acid (HNO_3) and sulfuric acid (H_2SO_4) was used for oxidation.

2. Instruments

Some instruments were utilized for synthesis of carbon nanotubes. Glassware was washed by using ultrasonic cleaner. Digital balance was utilized for weighting graphite and potassium chlorate and measuring cylinder was for measuring acids. Magnetic stirrer, overhead stirrer, hotplate and oven were used for the purpose of stirring and heating. Fume hood was the most important ventilation device to limit exposure to hazardous of toxic fumes during the process.

3. Safety Tips

Safety rules are important in laboratory. Concentrated sulfuric acid and concentrated nitric acid are strongly corrosive to all body tissue, especially eyes and skin. These concentrated acids are highly toxic due to their extreme corrosiveness [6]. Potassium chlorate appears as a white crystalline solid. Forms a very flammable mixture with combustible materials. Contact with strong sulfuric acid may cause fires or explosions [7]. This method included concentrated acids and a lot of heat was produced when potassium chlorate was added. For safety reasons, this chemical synthesis process was operated by using fume hood. All protective clothing, coat, masks, chemical splash goggles, chemical-resistant gloves, and a chemical-resistant apron whenever using concentrated acids or acid, were put on before research work.

4. Experiment

The flow chart for experimental procedure of carbon nanotubes preparation is shown in Fig.1 and the resultant carbon nanotube bundles are shown in Fig. 2.

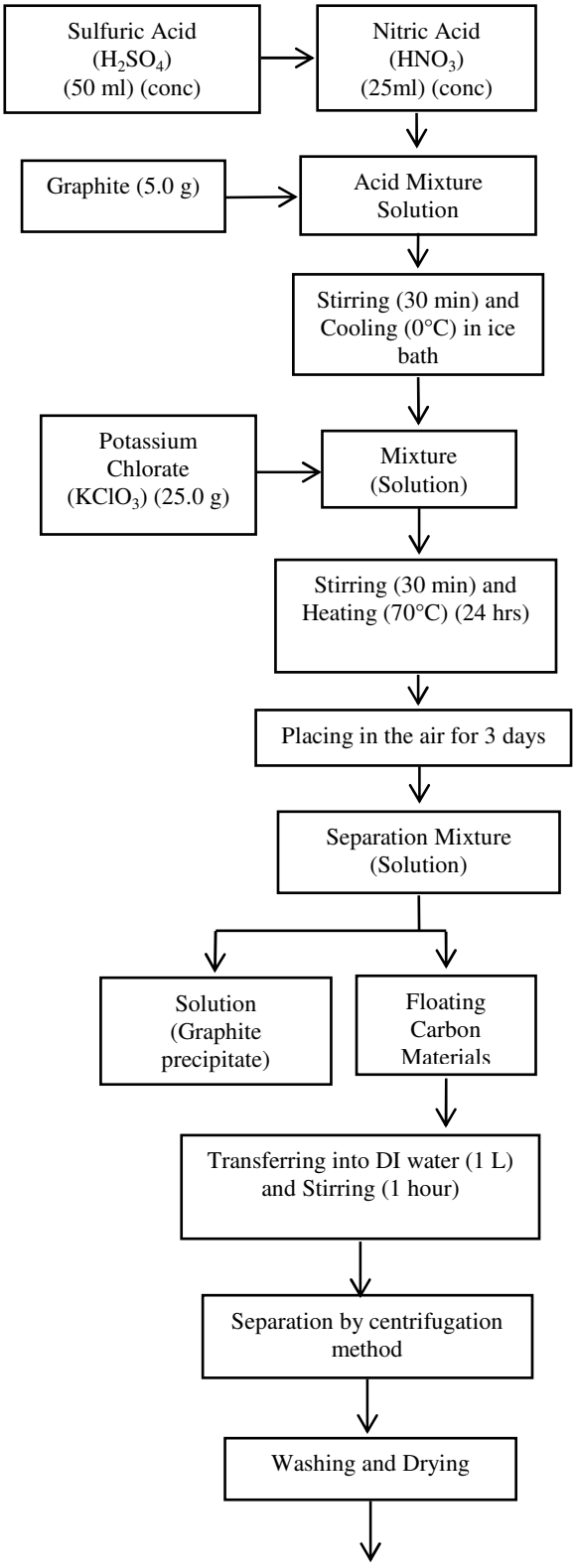

Carbon Nanotubes
(CNTs)

Figure 1 Flow Sheet for Chemical Synthesis of Carbon Nanotubes.

In chemical synthesis method, graphite powder was used as the main raw material to prepare carbon nanotubes. At first, 5.0 g of graphite was weighted. Then, 50 ml of concentrated sulfuric acid was slowly added into 25 ml nitric acid and the mixture was stirred to mix homogeneously. For safety, sulfuric acid should slowly be added with special care.

As the next step, 5.0 g weighted graphite was added to a mixture of acid solution and that mixture solution was stirred for 30 minutes with 300 rpm by using magnetic stirrer. After adding graphite, the mixture was cooled down to 0°C in an ice bath. While adding potassium chlorate, a lot of heat was produced. Therefore, the mixture was cooled down firstly. When the temperature of solution had reached to 0°C, 25.0 g of potassium chlorate was slowly added into the solution. Since a lot of heat was produced, this step was taken with special care.

The mixture was stirred for 30 minutes with 300 rpm. A lot of heat was produced. After stirring, the solution was heated up to 70°C for 24 hours. Hot plate was used to heat the solution. Since the temperature do not affect homogeneously, thermometer was used to know the actual temperature of solution. Therefore, the beaker was heated up to 120°C to reach the actual solution temperature up to 70°C. Some reacted carbon materials were floated during processing.

After heating for 24 hours, the solution was placed in the air for 3 days. Then, the solution was separated. Some carbon reacted with potassium chlorate and floated but most graphite was precipitated on the bottom. These reacted carbon materials were transferred into deionized water (1L) by pipette. It was stirred for 1 hour and the required carbon nanotube bundles were separated by centrifugation with 2000 rpm for 2 hours.

After stirring for 1 hour, these carbon materials were washed three times repeatedly by using centrifuge and were then dried in oven (~50°C). Carbon nanotubes obtained by chemical synthesis method could be seen as shown in Fig.2. Nearly 0.2 g of carbon nanotube was obtained. Final product, carbon nanotubes bundles were characterized by X-Ray Diffraction (XRD) and Scanning Electron Microscope (SEM) analysis and the results were studied.

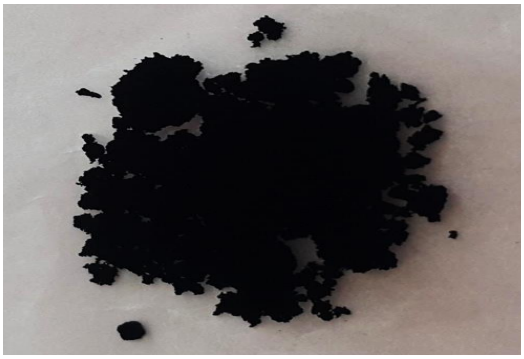

Figure 2 The Resultant Carbon Nanotubes Bundles.

III. CHARACTERIZATION OF CARBON NANOTUBES

Resultant carbon nanotubes bundles were analyzed by X-Ray Diffraction (XRD) to determine whether they were carbon nanotubes or not and to calculate the crystalline size of carbon nanotubes. Scanning Electron Microscope (SEM) analysis was applied to study the morphology of resultant carbon nanotubes and to determine the diameter of carbon nanotubes.

1. X-Ray Diffraction Analysis

Carbon Nanotubes obtained by chemical synthesis method was analyzed by Rigaku, Cu K_{α} X-ray Diffractometer.

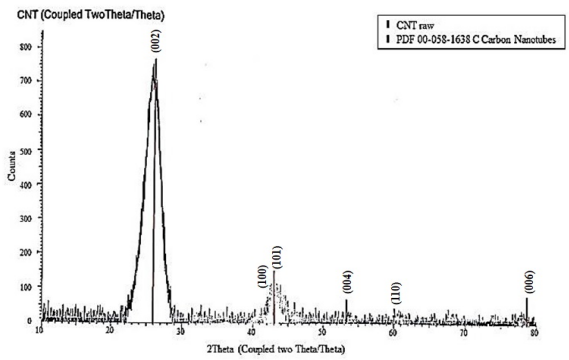

Figure 3 X-Ray Diffraction (XRD) Pattern of Carbon Nanotubes.

As shown in Fig.3, the location of the peaks with the standard characteristics of carbon nanotubes. There is no (0 0 2) peak can be measured by X-ray diffraction with well-aligned straight nanotubes on the substrate surface. In the case of carbon nanotubes with tube axis perpendicular to the substrate surface, the X-ray incident beam is scattered inside the sample and is not collected. Consequently, the intensity of the (0 0 2) peak decreases monotonically as CNTs are better aligned. The standard MWCNT line and the resultant CNT line are same at values of highest intensity (002), (101), (004), (110) and (006)

Peaks. Therefore, the resultant carbon materials were confirmed as multi-walled carbon nanotubes.

Debye-Scherrer equation is;

$$D = k\lambda / \beta\cos\theta$$

By using Debye-Scherrer equation, the crystallite size of carbon nanotubes was calculated. The values of highest intensity (002) peak (2-Theta = 25.8, FWHM = 1.95) are used and the calculated particle size by Scherrer equation is 4.18 nm.

2. Scanning Electron Microscope Analysis

To study the morphology of carbon nanotubes, resultant carbon nanotubes were analyzed by EVO 60 (ZEISS, Germany) Scanning Electron Microscope operated at 20 kV. SEM images of carbon nanotubes analyzed with different magnifications can be seen as shown in Fig. 4 and Fig. 5.

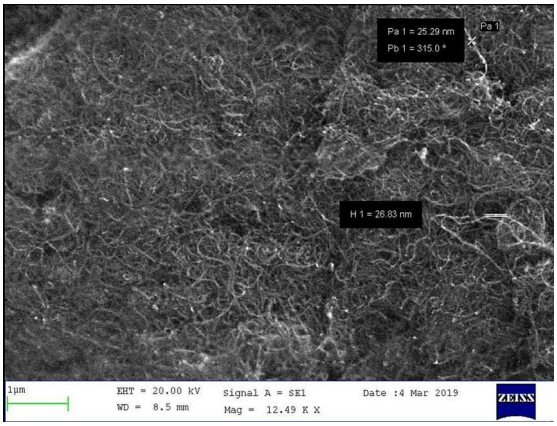

Figure 4 SEM Image of Carbon Nanotubes (Mag = 12.49 K X).

As shown in above SEM images, carbon nanotubes can be seen as hair-like structure. According to SEM images, the average diameter of carbon nanotubes is 20~40 nm approximately. SWCNT have a typical diameter of 0.5–1.5 nm, while those of MWCNT are typically above 100 nm. MWCNT consist of 2 or more layers of carbon average diamter 20 nm. Hence the resultant carbon nanotubes can be confirmed as multi-walled carbon nanotubes.

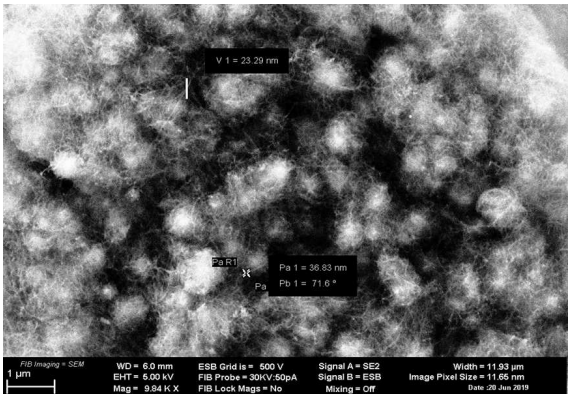

Figure 5 SEM Image of Carbon Nanotubes (Mag = 9.84 K X).

IV. APPLICATION OF CARBON NANOTUBES IN CONDUCTIVE INK

Electrical properties are the superior properties of carbon nanotubes because of their structure. Carbon nanotubes obtained by chemical synthesis method was applied to prepare conductive ink.

1. Conductive Ink Preparation

An ink composition contains three main elements: acetone as a solvent, MWCNT as a filler and cigarette filter as a binder (glue). 0.005 g of cigarette filter was dissolved in 5 ml of acetone and then 0.1 g of carbon nanotubes (MWCNTs) were added into this solution. The solution was stirred to mix homogeneously and then conductive ink was obtained. Flow sheet for carbon nanotubes conductive ink preparation is as shown in Fig. 6.

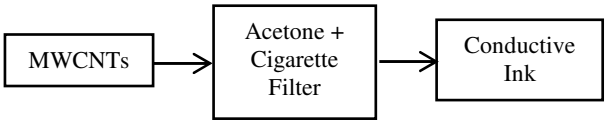

Figure 6 Flow Sheet for CNT Conductive Ink Preparation.

Table 1. Conductive ink composition

	Experiment	MWCNT, g	Graphite, g	Acetone, ml	Cigarette Filter, g	Sodium Silicate, ml
	1	0.1	-	5	0.005	-
	2	0.01	-	5	0.005	-
	3	-	3 g	20	0.1	-
	4	-	3 g	-	-	20

2. Measurement of Resistance

The experiment of carbon nanotubes application in conductive can be discussed based on the results determined by using digital multi-meter. The resistivity of resultant conductive inks was measured by digital multi-meter. The electrical resistance of an object is a measure of its opposition to the flow of electric current. The inverse quantity is electrical conductance and is the ease with which an electric current passes. Resistance and conductance are constants but they also depend on the size and shape of the object and so when measuring resistance and conductance, the length of the conductive inks was kept constant (length = 2 cm). Experimental measurements are shown in Fig.7. Four types of inks were prepared and results were studied.

Experiment 1 Experiment 2

Experiment 3 Experiment 4

Figure 7 Experimental Measurement of Resistance

As shown in Fig. 7. the resistances of experiment 1, 2, 3 and 4 are 4 Ω, 14.5 Ω, 76.7 Ω and 124.7 Ω respectively. Conductance is the inverse quantity of resistance and its unit is siemens (S). Therefore, the conductance of experiments 1, 2, 3 and 4 are 0.25 S, 0.069 S, 0.013 S and 0.008 S respectively.

Experiment 1 which is conductive ink made with 0.1 g carbon nanotubes has better conductance. Sample 2 which is conductive ink made with 0.01 g of carbon nanotubes has lower conductance than experiment 1 and so greater amount of carbon nanotubes, lower surface resistance and greater conductivity can give. On the other hand, experiment 3 and 4, which are conductive ink made with 3 g graphite, have lower conductance than experiment 1 and 2. Although greater amount of graphite is contained in experiment 3 and 4, it has lower conductivity. As a result, carbon nanotubes are better than graphite in conductive ink.

The resistance of resultant conductive inks was measured by digital multi-meter to compare wire and resistor.

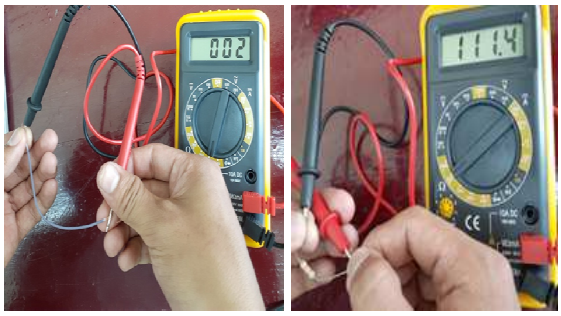

(a) Wire (b) Resistor

Figure 8 Measurement of Resistance

The resistance of a wire has nearly 2 Ω in Fig.8 (a) and in Fig. 8 (b) the resistors have nearly 100 Ω in resistance. As shown in Fig.7, resistance of carbon nanotubes conductive ink is ~ 4 Ω and conductance is 0.25 siemens approximately. Resistance of experiment 1 has similar amount of resistance like wire. The resistance of experiment 2 is slightly greater than that of wire and experiment 3 and 4 were more likely to be resistors. Therefore, conductive ink made with carbon nanotubes can be used like wire in electronic device as conductor.

3. Measurement of Current Flowing Through Conductive Ink

Conductive ink made with 0.1 g carbon nanotubes was tested with LED and 9 V battery and current was measurement by using multi-meter.

As can be seen in Fig.9, current flowing without conductive ink was 2 mA. Then, current flowing through conductive ink was measured and the resultant current was 2mA. Conductive ink did not significantly reduce current.

Conductive inks are widely used in solar cells, digital circuits, sensors and antennas. According to the results discussed in this experiment, conductive ink made with carbon nanotubes was suitable for applying in micro and nano electronics.

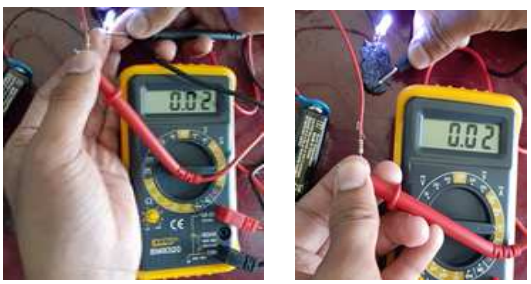

(a) (b)

Figure 9 Experimental Measurement of Current (a) without conductive ink, (b) with conductive ink.

V. CONCLUSION

Nearly 0.2 g carbon nanotubes were obtained by chemical synthesis method which is a simple chemical method for producing CNTs in liquid solution at 70 °C without any pressure treatment. Moreover, XRD and SEM analysis of carbon nanotubes prove that the resultant carbon materials obtained from this chemical synthesis method can be confirmed as multi-walled carbon nanotube bundles which have 20~ 40 nm diameter. According to the results discussed in applications of carbon nanotubes, multi-walled carbon nanotubes are suitable conductive materials to prepare conductive ink. Resistivity of conductive ink depends on length and wide and amount of conductive materials. Resistance of carbon nanotubes based conductive ink is ~ 4 Ω and so conductance is 0.25 siemens approximately.

6. References

[1] Werner M. and Andreas B. Carbon Nanotubes – A scientometric study, Carbon Nanotube, Jose Mauricio Marulanda (Ed.), ISBN: 978-953-054-4, 2010.

[2] Bornmann L. & Werner M. & Hermann S. Hirsch – Type Index Values for Organic Chemistry Journals: A Comparison of New Metrics with the Journal Impact Factor. European Journal of Organic Chemistry. 1471- 1476, 2009.

[3] Sumio I. Helical microtubules of graphitic carbon. Nature, 354, 56-58, 1991.

[4] Chang I. L. Structural Instability of Carbon Nanotube, Synthesis, Characterization, Applications, ISBN: 978-953-307-497-9, 2011.

[5] Ray H. B. Anvar A. Z. Walt A. D. H., Carbon Nanotubes- the Route Toward Applications. Science. Vol 297, Issue 5582, 787-792, 2002.

[6] https://www.blueridge.edu/sites/default/files/pdf/ehsi/Acid%20Safety.pdf

[7] https://pubchem.ncbi.nlm.nih.gov/compound/Potassium-chlorate

[8] T. Belin. F. Epron. Characterization methods of carbon nanotubes: a review. Materials Sci. & Engr: B119, 105–118, 2005.

[9] Bansi D. Malhotra. Saurabh Srivastava. Shine Augustine. Biosensors for food toxin detection: Carbon Nanotubes and Graphene. Mater. Res. Soc. Proc. Vol. 1725, 2015.

Effect of Sintering Time on Properties and Shape Memory Behavior of Cu-Zn-Al Shape Memory Alloy

Saw Mya Ni[1], Htet Soe Aung [2]

Faculty of Advanced Materials Engineering, University of Technology

(Yatanarpon Cyber City), Pyin Oo Lwin, Myanmar

[1]sawmyani2017@gmail.com, [2]koreaame@gmail.com

Abstract

A shape-memory alloy (SMA) is an alloy that remembers its original shape and that returns to its original shape when heated. They are strong, lightweight alloys (generally, mixtures of two or more metals). The combination of Cu, Zn and Al by using powder metallurgy can also produce shape-memory alloys. The microstructural, physical and mechanical properties of CuZnAl alloys are studied by using different sintering times and temperatures. Porosity, density and hardness tests were measured to know the physical and mechanical properties of CuZnAl alloys. The best properties are obtained at sintering time (2h) and temperature (900°C).

Key Words- ***Shape memory alloy, X-ray diffraction (XRD), X-ray fluorescence (XRF), Microstructure, Hardness***

1. INTRODUCTION

Shape memory alloys (SMAs) are groups of alloys which can recover their shape when they are heated above a certain temperature. The shape memory effect is based on martensitic transformation (MT) which is a reversible phase transformation. It occurs between the high-temperature austenite temperature and the low-temperature martensite phase. It is well known that many copper alloys such as Cu-Al, Cu-Zn-Al, Cu-Al-Ni and Cu-Al-Mn exhibit shape memory properties. Cu-based SMAs have attracted attention due to their good shape memory capacity, narrow temperature region of transformation, ease of fabrication and low production cost. CuZnAl SMAs have the advantage that they are made from relatively cheap metals using conventional metallurgical processes. These reasons make them amongst the cheapest of the commercial SMAs. [1][2]

Powder metallurgy (PM) is a term covering a wide range of ways in which materials or components are made from metal powders. PM processes can avoid, or greatly reduce, the need to use metal removal processes, thereby drastically reducing yield losses in manufacture and often resulting in lower costs. Powder metallurgy can produce products of materials that are very difficult to manufacture. Powder metallurgy products can be designed to provide the targeted properties. Variations in product size, production rate, quantity, mechanical properties, and cost can be change in powder metallurgy [3][6]

The powder metallurgy process is neither energy nor labor intensive, it conserves material, it is ecologically clean, and it produces components of high quality and with homogeneous and reproducible properties. In more recent years, these attributes have attracted studies into the application of the technique to the development of materials for high technology uses. [9]

2. THEORETICAL BACKGROUND

Only three alloy systems, namely NiTi-based, Cu-based and Fe-based, are presently more of commercial importance. NiTi SMAs have high performance and good biocompability, which is crucial in biomedical applications. Cu-based SMAs have the advantages of low material cost and good workability. Fe-based SMAs are relatively weaker and they are most likely used only as fastener due to the extremely low cost. All these SMAs are thermos-responsive, i.e; the stimulus required to trigger shape memory is heat. Shape-memory alloys are widely used in aircraft and spacecraft (wing, propeller, rudder, elevator), automotive, robotics, civil structures, telecommunication and medicine (fixation devices for osteotomies in orthopedic surgery, in dental braces to exert constant tooth-moving forces on the teeth). [10][11]

CuZnAl SMAs usually contains 15-30 % Zn and 3-7% Al, with the balancing copper. The addition of small quantities (usually less than 1%) of boron, cobalt, iron, titanium, vanadium and zirconium) are commonly added to control the grain size. However, additions should be made carefully as they can upset

the stability of the structure, thus affecting the shape memory characteristics. CuZnAl SMAs have the advantage that they are made from relatively cheap metals using conventional metallurgical processes. [8][9]

CuZnAl alloys can be produced using conventional processes such as vacuum arc melting or induction melting. Nitrogen or other gases must be used for shielding purposes over the melt and during pouring to prevent zinc evaporation. Powder metallurgy processes can be used to produce fine grained structures. [5][12]

3. EXPERIMENTAL PROCEDURE

The experimental procedure of CuZnAl shape memory alloy is shown with the schematic flow diagram as follows:

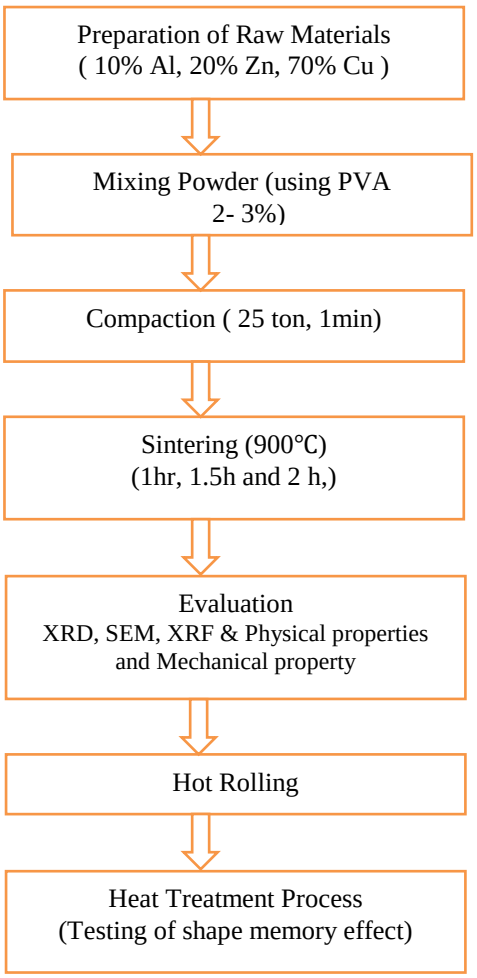

Figure 1. Flow diagram of Experimental Procedure

3.1. Raw Materials

Copper powder, zinc powder, aluminium powder and poly vinyl alcohol from Academy Chemical Group and Golden Lady (Yangon, Burma). All glassware are washed with distilled water and dried in oven before use.

3.2. Production of CuZnAl Shape-Memory Alloy

In this research, powder metallurgy method is used to get the CuZnAl shape-memory alloy. Copper powder (75%), zinc powder (20%) and aluminium powder (5%) are weighed according to their respective compositions. After weighing, the powders were mixed by using mixer. The particle sizes of powders were approximately 200 mesh and the raw powders are uniformly blended with PVA (2-3%). Then, the powders are compacted in the hydraulic press machine with a pressure of 25 tons. The shape of die is cylinder and size is 1 inch diameter. For one sample billet, 10 g of powder alloy is used. After compaction, the green compacts are sintered in the muffle furnace by varying temperature and time. For this research, the sintering temperatures used at 800 ºC and 900ºC. The sintering times are 1h, 1.5h and 2 h. The sintered samples were characterized by X-ray diffraction analysis, X-ray fluorescence and microstructure analysis. The physical properties; the density and porosity were measured by boiling water method. The mechanical property of harness was measured. Furthermore, hot rolling and heat treatment process followed by this technique, homogeneous CuZnAl alloys exhibit shape memory behaviour could be produced.

3.3. Hot Rolling of CuZnAl Shape-Memory Alloy

Firstly, the pellets are deformed into rectangular shape by heating. Then, these are hot rolled in the roller machine to the required shape by reducing the diameter step by step. Finally, sintered pellets are transformed into 0.75mm diameter wire. There is important to be rolled at sufficient temperature because it can cause break down during rolling.

3.4. Heat Treatment of CuZnAl Shape-Memory Alloy

The CuZnAl wires are heated at 800 ℃ for about 1 hour and they are slow-cooled in the furnace. Then, these wires are heated by 825 ℃ for about 1 hour, 850 ℃ for about 1 hour , 875 ℃ for about 1 hour and 900 ℃ for about 1 hour step by step. After reaching at 900 ℃, the wires are taken from the furnace and cooled rapidly by quenching in water or by cooling with air.

4. RESULTS AND DISCUSSION

4.1. Density, Hardness and Porosity Results of Samples

The results of the measurement of physical properties and mechanical property of CuZnAL shape memory alloy are presented in Figure 2, 3 and 4.

The graphs shown in Figure 2 indicate the increasing of the density of the sintered pellets with increasing of the sintering conditions; times and temperatures.

The hardness increases with increasing sintering temperature and time as shown in Figure 3.

But the porosity decreases as the sintering condition increases as shown in Figure 4. All these graphs confirm that the physical properties increase with increasing of the sintering time and temperature.

The hardness increases with increasing sintering temperature and time

The maximum sintering condition was obtained at 900°C and 2hr.

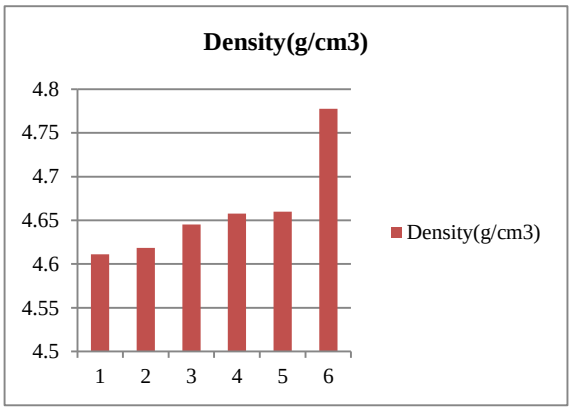

Figure 2. Density Results of Sintered Samples

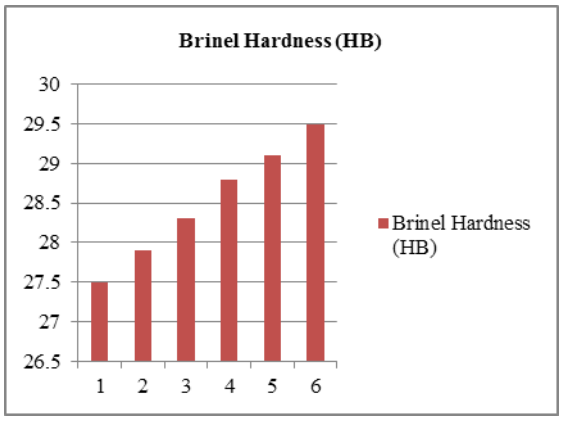

Figure 3. Brinel Hardness Results of Sintered Samples

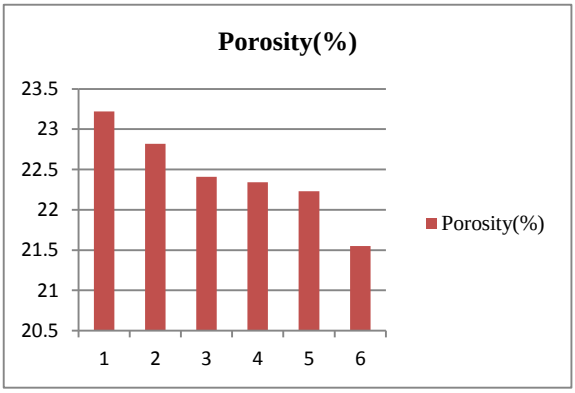

Figure 4. Porosity Results of Sintered Samples

4.2. XRD Analysis of 900°C, 2h Sample

From this result, the diffraction peaks for CuZnAl shape-memory sample at (2Θ = 14º, 42º, 48º and 73º) are occurred. It is mainly important to combine the powder particles of Cu, Zn, and Al particles because it can effect on the XRD analysis of sample and shape memory characteristics of sample. The CuZnAl alloy peak can be occurred at 42º and the remainings are the peaks of major constituent, Cu. The other major constituents of alloy sample can be occurred in low angles. The XRD patterns of CuZnAl samples show dominant (111) diffraction peak along with the low intensity (200) diffraction peak. A reduction in particle size with increase of milling time can be found. The XRD analysis of standard sample is shown in Figure 5.

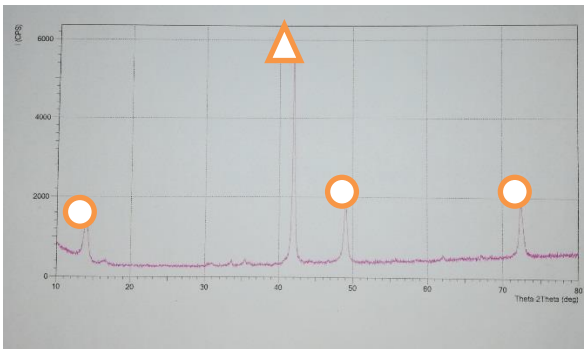

-Copper-zinc-aluminium, CuZnAl
- Copper, Cu

Figure 5. XRD result for the sample (900ºC, 2h)

4.3. XRF Analysis Results

From the X-ray fluorescence analysis, the sample sintered at 800ºC for 1h contained about 74.54% Cu, 19.45% Zn, 5.03% Al and traces of other elements. The sample sintered at 800ºC for 2h contained about 74.12% Cu, 19.13% Zn, 4.96% Al and traces of other elements. The sample sintered at 900ºC for 1h contained about 73.84% Cu, 18.87% Zn, 4.87% Al and traces of other elements. The sample sintered at 900ºC for 2h contained about 73.81% Cu, 19.22% Zn, 4.54% Al and traces of other elements.

Table 1. XRF Analysis of Samples

Type	Cu %	Zn%	Al%	Si%
1	74.54	19.45	5.03	0.34
2	74.22	19.32	5.12	0.21
3	74.12	19.13	4.96	0.33
4	73.84	18.87	4.87	0.42
5	73.78	19.13	4.92	0.48
6	73.81	19.22	4.54	0.53

4.4. Microstructure Analysis Result

Figure 6 shows the microstructure analysis result for CuZnAl alloy sintered at 900ºC for holding 1h. Figure 7 shows the microstructure analysis results of sample 5 at 900°C, 1.5h and Figure 8 shows the microstructure analysis result of sample 6 at 900°C, 2h. Some pores (impurities) are occurred between the grains and grain boundaries. Most of the pores exhibit in different structures. The occurrence of pores can depend on the alloy composition, compaction pressure, sintering temperature and sintering time.

Figure 9 is the microstructure analysis of Sample- 3 at 900°C for 2h after heat treatment process. Figure 5 have shown in the martensitic phase.

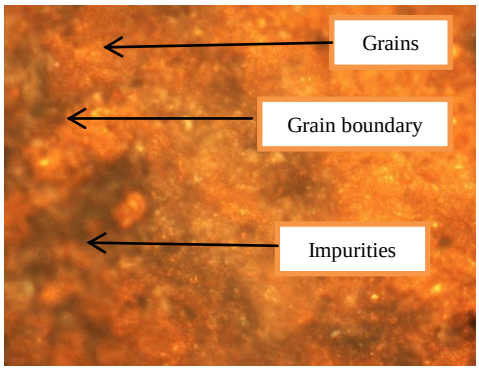

Fig. 2 Microstructure analysis results of sample 4 at 900°C, 1h (1000x magnification)

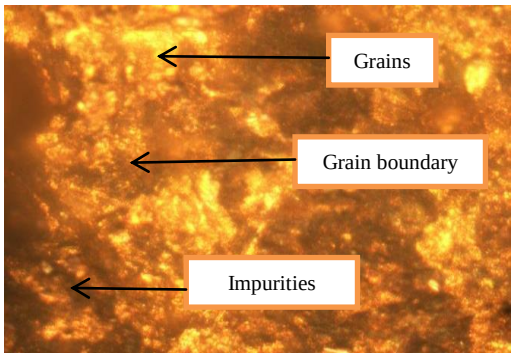

Figure. 7 Microstructure analysis results of sample 5 at 900°C, 1.5h (1000x magnification)

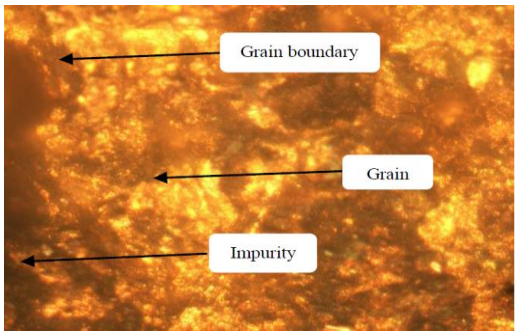

Figure 8. Microstructure analysis result of sample 6 at 900°C, 2h (1000x magnification)

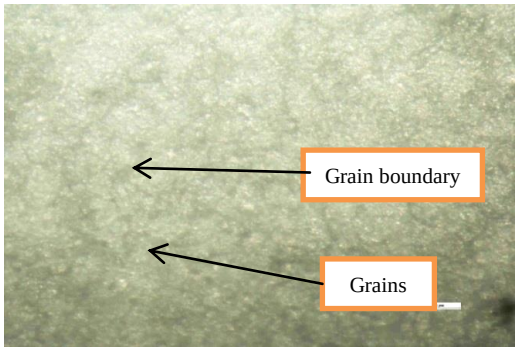

Figure 9. Microstructure Analysis of Sample 6 at 900°C for 2h after heat treatment process (1000x magnification)

4.5. Testing of Shape Memory Effect

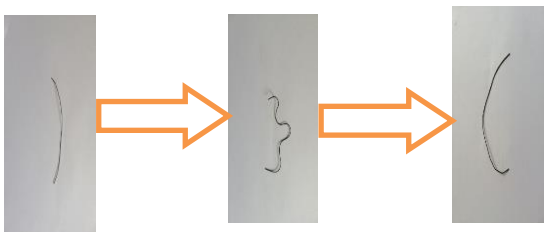

(a) (b) (c)

Figure 10. Shape Memory Effect Analysis Results (a) CuZnAl Wire in Original Form, (b) CuZnAl Wire in Bending Form, (c) CuZnAl Wire after Adding in Boiling Water Form

Figure 10. can be seen that to get the shape memory effect, the sintered pellets are deformed into the hot-rolled machine and transformed into the wire shape. The wires are heated into the muffle furnace step by step according to the diameter of wire. In this research, 0.75mm diameter of wire is used. For this research, the shape memory effect is firstly occurred at 875°C of sintering temperature and 1 hr of sintering time. The shape-memory wire is deformed from the original straight shape. In this deforming the shape, it is not recommended for twisting. Then, the wire is added into the boiling water, the wire returned into the original straight line shape. This is called the shape-memory effect. For larger diameter shape-memory wire, more heat is needed to get into the original form.

5. CONCLUSION

The CuZnAl shape memory alloys with different sintering temperature and time are studied. The sintering characteristics, mechanical property, physical properties, X ray diffraction analysis and microstructure were studied. The density and hardness of the sintered samples are increased with the increasing sintering time and temperature. The porosity was decreased with increasing sintering time and temperature. The optimum sintering condition was obtained at 900ºC and 2h. In this research, the shape memory effect was occurred as shown in Figure 10. Powder composition, powder size, sintering temperature, sintering time, hot rolling and heat treatment process are important to get shape-memory effect.

RECOVERY OF COBALT METAL FROM SPENT LI-ION BATTERY BY COMBINATION METHOD OF PRECIPITATION AND REDUCTION

Dr. MyatMyatSoe[1], Dr. Nay Myo Htike[2]

[1] Metallurgical Research Division, Department of Research and Innovation, Ministry of Education, MYANMAR
[2]Metallurgical Research Division,Department of Research and Innovation, Ministry of Education, MYANMAR

* E-mail:dr.myatmyatsoe99@gmail.com,naymyohtike007@gmail.com

Abstract—**Now a day, recycling of valuable metals from spent li-ion battery has being increased. When it may be taken to landfills, the toxic metals may be leached into the underground and then contamination of underground water or contamination of crop. In this research, recovery of cobalt metal from spent li-ion battery was extracted by metallurgical method. There were two steps in this research; first step, cobalt oxalate was extracted from li-ion batteries by precipitation method and second step, cobalt oxalate was decomposed at high temperature to get cobalt metal.**

Keywords: (Battery, Cobalt, , Gases, Metal, Metallurgical Method)

I. INTRODUCTION

Cobalt is a chemical element with symbol Co and atomic number 27 like nickel. Cobalt is found in the Earth's crust only in chemically combined form, save for small deposits found in alloys of natural meteoric iron. The free element, produced by reductive smelting, is a hard, lustrous, silver gray metal.

Lithium-ion batteries are essential to modern technology, powering smartphones, laptops, medical devices and even electric vehicles. There are many different types of li ion batteries; lithium cobalt oxide battery, Lithium manganese battery, lithium nickel manganese battery and more. Lithium cobalt oxide battery is a high specific energy as compared to the other batteries.

Improper disposal of these batteries becomes seriousenvironmental problems due to their hazardous constituents which include heavy metals and electrolytes. That leads toaffect the human health and environmental pollution. There are three ways to prevent environmental damage are conservation of water, cleaning air and reducing waste. One way of preventing environmental damage is recycling or reducing waste. Cobalt is animportant basic material for industrial application; however, it is difficult to recover cobalt from minerals since there is a lack of independent deposits in nature.

Cobalt is a shiny, brittle metal that is used to produce strong and heat resistant alloys,permanent magnet and hard metals. Cobalt is also used to;make alloys for jet engines and gas turbines, magnetic steels and some types of stainless steel. Cobalt 60, a radioactive isotope of cobalt, is an important source of gamma rays and has been used to treat some forms of cancer and as a medical tracer. In addition to the metal itself, cobalt compounds for instance, cobalt oxalate, cobalt oxide, cobalt chloride, and cobalt sulfate also have extensive industrial applications.

II. MATERIALS AND METHOD.

To provide a process to recover cobalt from spent lithium-ion battery, many methods have been developed including mechanical process, thermal process, acid or base leaching, bioleaching, solvent extraction, chemical precipitation and electrochemical process. Hydro-metallurgical method is the main method to recycle valuable

materials from lithium ion batteries. Cobalt from lithium-ion battery was leached with sulphuric acid or nitric acid and then precipitated with ammonium oxalate.

Cobalt oxalate is used in the preparation of cobalt catalyst, to cobalt metal powder for metallurgical applications.Cobalt oxalate is an inorganic compound with a formula of CoC_2O4. Process for extraction of cobalt oxalate from lithium-ion battery consist sample preparation, leaching with sulphuric acid, adding with hydrogen peroxide and precipitation with ammonium oxalate. Oxalic acid or ammonium oxalate was used for recovering cobalt from leaching solution of spent lithium ion battery by precipitation method. Crushed powders containing $LiCoO_2$ of spent lithium ion battery were obtained by crushing, magnetic separation and screening process. These powders were dissolved in 2 M H_2SO_4 solution with H_2O_2 as a reducing agent. After dissolving Co and Li components, ammonium oxalate solution was added. Co (II) in leaching solution could be removed in the form of insoluble oxalates. The precipitate formed was crystalline, compact and easily filtered. When cobalt ion was precipitated into cobalt oxalate, nickel and copper ions were also co-precipitated but there were no co-precipitates of Li, Al and Fe. The amounts of Ni and Cu in the solutions were below 1%. After drying of precipitates at 100°C for 1 hour, cobalt oxalate was obtained. If heating above 200°C cobalt oxalate hanged into cobalt oxide. [2][3]

The leaching process of $LiCoO_2$ in H_2SO_4 solution could be represented as follows;

$$2LiCoO_2(S) + 3\ H_2SO_4\,(aq) + H_2O_2\ (aq) \longrightarrow$$

$$2CoSO_4(aq) + Li_2SO_4(aq) + 4H_2O(g) + O_2(g) \quad (1)$$

And then cobalt ion was precipitated into cobalt oxalate by adding ammonium oxalate.

$$CoSO_4\ (aq) + (NH_4)_2C_2O_4\ (aq) \longrightarrow$$

$$CoC_2O_4(s) + (NH4)_2\ SO_4\ (aq) \quad (2)$$

Solvent extraction process, reduction process and precipitation process were used for recovering cobalt from spent lithium ion battery. More over cobalt oxalate is also used as a starting compound for cobalt extraction. At very high temperatures cobalt oxalate was heated to remove carbon and oxygen and to get cobalt powder.[2][3]

III. EXPERIMENTAL PROCEDURE

In this study, cobalt oxalate was extracted from spent lithium cobalt oxide ion batteries. Samples were collected from spent li cobalt oxide batteries manually. Next, samples were analyzed to quantitative determinations of elements, by using Atomic Absorption Spectroscopy. The figures of collection of samples from batteries and sample assay determinations by Atomic Absorption Spectroscopywere shown in figure 1 and 2.

In each experiment, ten grams of sample was taken to extract cobalt oxalate from batteries. It contained 23% of cobalt. Samples were dissolved into H_2SO_4-H_2O_2 solution in beaker. Then samples were leached at 70˚C for 1 hour. After complete leaching, solutions were filtered off to remove residue, and then pH 5 was adjusted by adding NaOH solution. Then 5 ml of H_2O_2 was added to the solution and agitated at the speed of 300 rpm for 1 hour. After 1 hour, the pink color crystalline precipitate was formed. The precipitate was filtered anddried, CoC_2O_4 powder was obtained. Processes for preparation of CoC_2O_4 were illustrated in figures 3, 4, 5 and 6.

To obtain the optimum conditions, experiments were should be madeby the variation of sulphuric acid concentration, temperature, reaction time and the amount of hydrogen peroxide. In this research, the effect of sulphuric acid concentration on the leaching efficiency and purity of Co% in CoC_2O_4 precipitate were determined.In these experiments, leaching temperature and leaching time were kept constant at 70˚C and 1 hour. Leaching temperature 70˚Cand leachingtime1hourwere chosenaccording to references. Concentration of H_2SO_4 varied from 0.5 moles / lit to 2.5 moles / lit with reluctant amount of 2.0% H_2O_2.[3]

The precipitate obtained from optimum conditions were heated with oxyacetylene torch at 3000˚C. The powder was obtained after removing carbon and oxygen from cobalt oxalate at high temperature. The powder was preliminary examined with magnetic pieces. Then it was analyzed by X-ray Diffraction Spectrometer. Results showed that the powder was cobalt powder. Flow sheet for extraction of cobalt from li-ion batteries is shown in figure 7.

Figure1 Collecting Samples

Figure 2 Assay Analysis by Atomic Absorption Spectroscopy

Figure 3 Leaching test for 1 hour

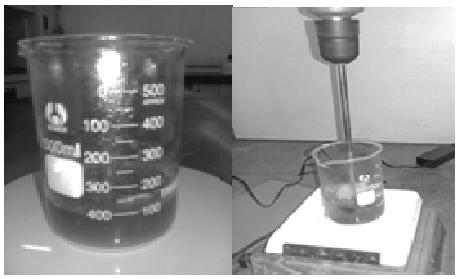

Figure 4 Adding with $(NH4)_2C_2O_4$ in Cobalt

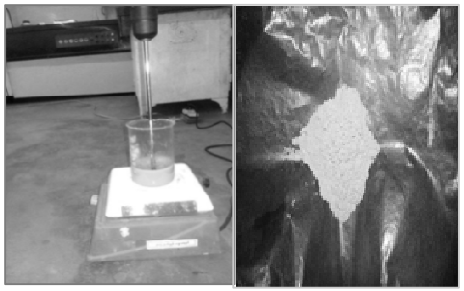

Figure 5 Cobalt Oxalate Precipitations

Figure 6 Cobalt Powder after Heating with Oxyacetylene Torch

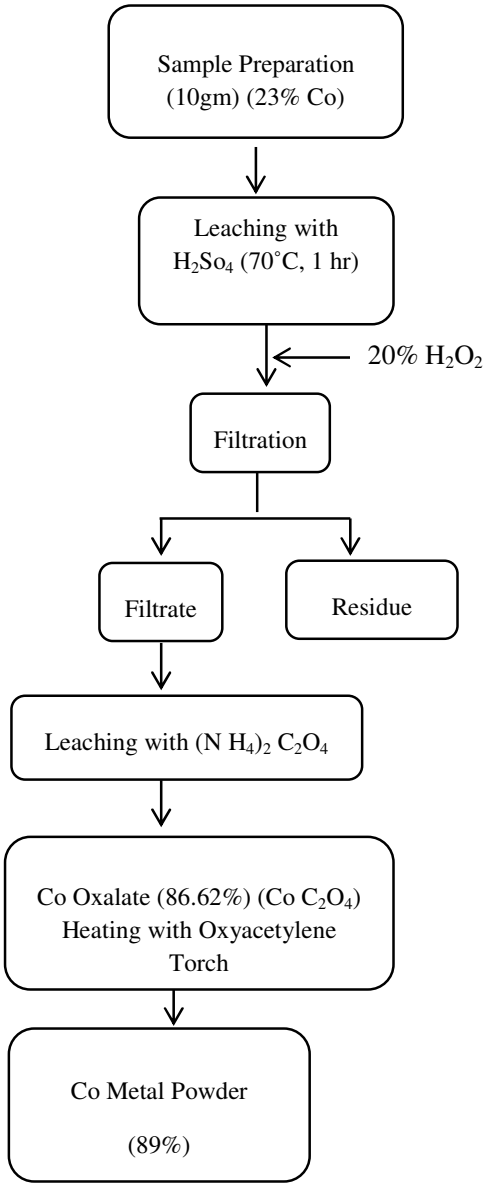

Figure 7 Flow sheet for Extraction of Cobalt from li-ion Battery

V. RESULTS AND DISCUSSION

In this paper, the effect of H_2SO_4 concentration on the leaching efficiency and purity of Co% in cobalt oxalate precipitate were investigated. During the leaching process, leaching temperature and reaction time were kept constant. The results showed that the leaching efficiencies and the purity of cobalt in cobalt oxalate were increased when the concentration of H_2SO_4increased up to 2 moles/lit. Increasing the concentration of H_2SO_4 from 0.5 to 2 moles/lit, leaching efficiencies increased from 29% to 83.33% and purity of cobalt in cobalt oxalate also increased from 28% to 86.62%. But the concentration of H_2SO_4above 2 moles / lit, the leaching efficiency and the purity of cobalt in cobalt oxalate decreased significantly. Effects of H_2SO_4 concentration on leaching efficiency and on purity of Co % were shown in figure 8 and 9. XRD pattern for cobalt powder was shown in figure. 10.

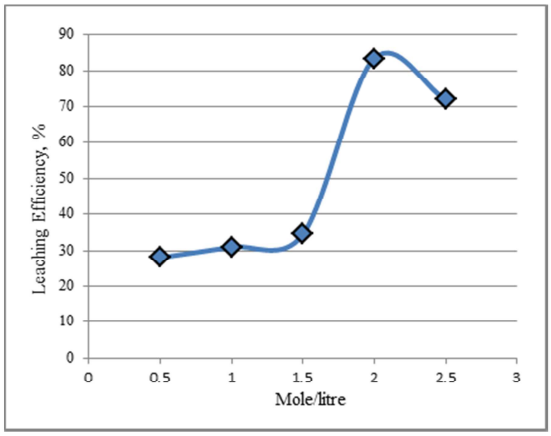

Figure 8 Effect of H_2SO_4 concentrations on leaching Efficiency

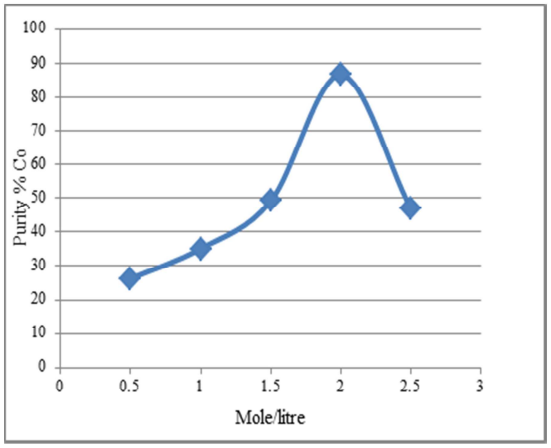

Figure 9 Effect of H_2SO_4 concentrations on Co% in CoC_2O_4

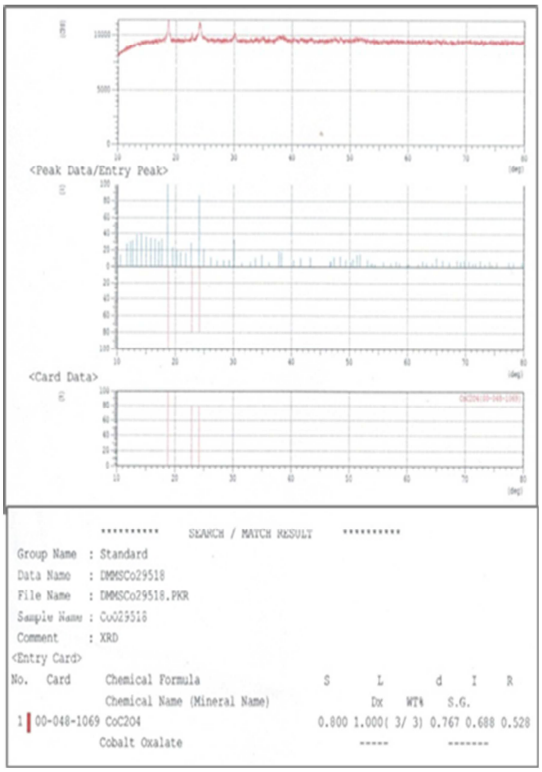

Figure 10 X.R.D pattern for CoC_2O_4 precipitate

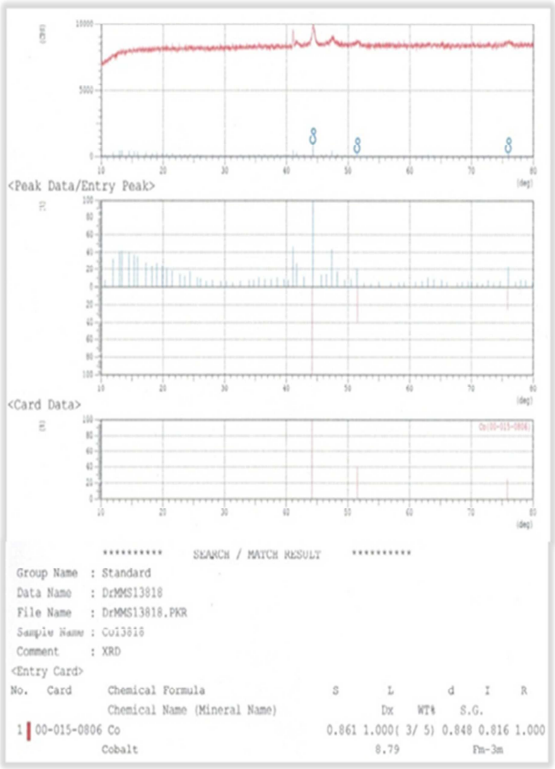

Figure 11 X.R.D pattern for Co metal powder Extraction

V. CONCLUSIONS

The leaching efficiency 83.33% and cobalt purity 86.62%were observed at the H_2SO_4 concentration of 2 moles /lit. The purity of 89 % cobalt powder was obtained. In this research, the variations of H_2SO_4 solution concentration were studied for cobalt oxalate extraction. CoC_2O_4 can be used as a starting compound to recover cobalt from spent lithium ion battery.

ACKNOWLEDGMENT(S)

I would like to express my thanks of gratitude to all staff from Metallurgical Research Division. I want to express specialthanks to our Director General and Deputy Director General who gave me the golden opportunity to do this project.

REFERENCES

[1] MiamariAaliton, Chao Peng, Benjamin P. Wilson:Leachingof Metals from Spent Lithium-Ion Battery, www.mdpi.com/journal/recycling.

[2] L W Ma, X L Xi, Z ZZaung, Z Q HAUNG, J P Chen: Hydrometallurgical Treatment for Mixed Waste Battery Materials, 3rd International conference on Advanced Materials Science and application (AMRA2016).

[3] ZHU Shu-guang, HE Wen-zhi: Recovery of Co and Li from spent lithium ion batteries by combination method of acid leaching and chemical precipitation, School of Environmental Science and Engineering, Tongji University, Shanghai 200092, China.

[4] ELSEVIER, Separation and Purification Technology Volume 186, 2 October 2017, Pages 318-32

Assessment of Surface and Ground Water Quality around the Kyinsintaung Mine, Myanmar

Myint Aung [1], Dr. Aung Lay Tin[2]

[1]Associate Professor, Department of Mining Engineering
Yangon Technological University
Insein Road, Gyogone, Yangon, 11011, Myanmar

[2] Professor and Head, Department of Mining Engineering
Yangon Technological University
Insein Road, Gyogone, Yangon, 11011, Myanmar

*Corresponding author: myintag25@gamail.com

Abstract—**This study carried out at the Kyisintaung copper (Cu) mine, located in Monywa District, Sagaing Region. The mine is on the west bank of Chindwin River and on the east side of Monywa, the capital of Sagaing Region. Chindwin is the biggest tributary of Ayeyarwaddy river and the longest navigable one in Myanmar flowing from north south. Acid mine drainage of Kyisintaung minecan be a multi-factor pollutant unless the proper mine drainage system is conducted. It can affect surface and underground water quality by a number of direct and indirect pathways which lead to destruction of aquatic ecosystems. Potential impact area includes rivers, lakes, estuaries and coastal waters especially at the downstream area of mine. Due to its complexity, the impact of acid mine drainage is difficult to quantify and predict, especially in riverine systems. Pollution effects of acid mine drainage are complex but can be categorized as (a) sedimentation processes, (b) acidity, (c) metal toxicity and (d) salinization. Thus this study points out the water quality including surface and ground water in the vicinity of Kyisintaung Mine to help minimize the water quality impacts by the mine in near future. The impacts of surface and ground water quality are discussed in this study.**

Keywords: Environmental Impact, Management Systems Mine, Water Quality,Surface Water, Ground Water

I. INTRODUCTION

The Kyisintaung mine is located at the coordinates of 22° 7' 21.56" N and 95° 1' 58.27" E, Monywa District, Sagaing Region in Myanmar. This is an open-pit mine and Copper ore is being extracted since early 17th century. Many international companies have been involved in the development of this mine under several eras of ownership. In the 1950's the Sebaltaung and Kyisintaung deposits began to be explored on a much larger scale and have developed into a mining enterprise today. Currently, the mining is operated by Wanbao Mining Limited with the name of Myanmar Yang Tse Copper Limited (MYTCL) at an annual production rate of 50,000 tonnes of copper ore with the average content of 0.31%. The Yama stream which is the tributary of Chindwin river is located at the northern part of the mine. The Chindwin river which is the largest tributary of the country's chief river of the Ayeyarwady river located at the eastern part of mine. This river plays vital role in movement of small and medium vessels for transportation of goods and materials. It also serves as portable water resources for the residences and agricultural farms existed along the river. It has been said that mining activities cause water pollution. Thus, this study focused on monitoring of water quality in the vicinity of Kyisintaung mine. Location of Kyisintaung mine is shown in Figure 1.

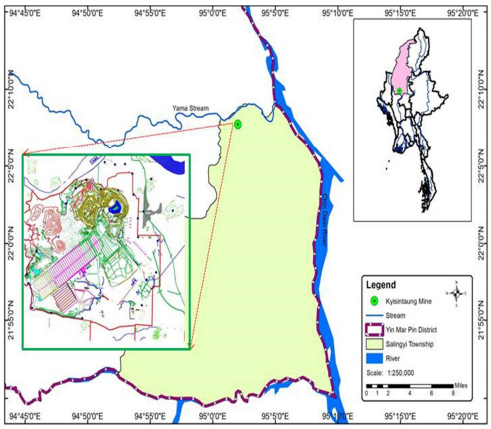

Figure 1 Location of Kyisintaung mine

This paper is organized as the following: Section II describes the methodology of this study. Results and discussions are presented in Section III and Section IV shows the conclusions.

II. METHODOLOGY

Field study was conducted at the mine site to understand the current mining practice of MYTCL and help identify the water pollution sources, sampling locations and parameters to be monitored. Accordingly, the total of 21 water samples that comprises 12 surface water samples and 9 ground water samples around the mining area were collected in June 2018. Figure 2 shows the surface water sampling locations along the Yama stream and ground water sampling locations in Kyisintaug mine. In-situ measurements were carried out for the physical parameter-temperature-and some chemical parameters, pH, conductivity and dissolved oxygen using HI 98194 Multi-parameter probe. The other parameters such as TSS, TDS, Cu, Fe, Pb, Mn, SO4, Ca, Ma and total hardness were taken into consider for laboratory analysis. To collect the water samples, sterilized plastic bottles were used. The bottles were rinsed three times with the water to be sampled before being filled. Then the samples chilled and transported to laboratory. The laboratory analysis was carried out at the certified laboratories in Myanmar.

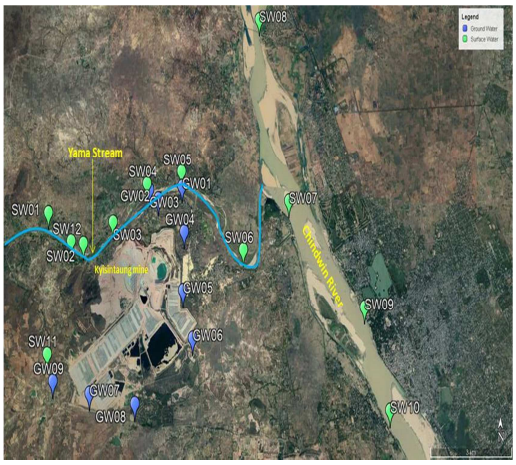

Figure 2 Sampling locations of surface water and ground water

III. RESULTS AND DISCUSSIONS

The results of surface water samples compared with National Emission Quality Guidelines (NEQG) are presented in Table 1 whereas ground water samples' results are illustrated in Table 2.

For the surface water quality (Figure 3), the concentrations of TSS of all samples expect SW11 and SW12, significantly exceed the NEQG value at 50 mg/l while the results of remaining parameters are within the guidelines limits. Regarding with the results of ground water samples (Figure 4), all the concentration of monitored parameters are within the acceptable limit of NEQG values. However, the TSS values appear to be higher than in GW 07 and 08 at 110 mg/l and 99 mg/l respectively while the other points are lower than NEQG limit. The concentrations of total hardness values are also appeared 2-3 times higher than the guidelines values. It was found that the concentration of sulfate in GW08 and GW09 are higher than the guidelines values and the remaining points are within the guidelines values.

Table 1 Results of surface water

Analysis	NEQG/ Composite Guide-line	SW 01	SW 02	SW 03	SW 04	SW 05	SW 06	SW 07	SW 08	SW 09	SW 10	SW 11	SW 12
pH	6-9	7.8	7.6	7.3	8.1	7.7	8.1	7.9	7.9	8.0	8.1	7.8	8
Temperature	-	29.1	28.6	29.3	28.1	28.9	27.1	28.2	30.3	25.7	26.5	31.4	28.6
Dissolved Oxygen	-	3.71	4.71	5.02	4.79	5.17	5.14	4.36	5.05	4.91	4.04	4.32	6.28
Conductivity @24.5C	-	106	103	108	521	109	106	521	102	123	169	1054	628
Total Suspended Solids	50 mg/l	687	892	608	233	788	750	292	763	86	63	29	19
Total Dissolved Solids	1500mg/l	533.27	523.37	536.93	746.91	547.30	504.11	738.13	517.44	525.14	558.20	1071.19	846.21
Cu (dissolved)	0.30 mg/l	<0.01	0.01	<0.01	<0.01	<0.01	<0.01	<0.01	<0.01	<0.01	<0.01	0.01	<0.01
Fe (dissolved)	3.5 mg/l	2.10	1.39	0.77	<0.01	0.73	0.47	<0.01	0.90	<0.01	<0.01	<0.01	<0.01
Lead	0.10 mg/l	<0.01	<0.01	<0.01	<0.01	<0.01	<0.01	<0.01	<0.01	<0.01	<0.01	<0.01	<0.01
Sulphate	400 mg/l	14	13	16	68	15	15	66	14	14	17	154	79
Calcium	200 mg/l	13	11	9	31	10	9	31	16	15	18	21	26
Magnesium	150 mg/l	5	5	5	17	5	4	17	5	5	6	28	21
Total Hardness	180 mg/l	51	47	41	146	44	40	145	61	57	70	167	150
Acid	0.50 mg/l	Nil	Nil	Nil	Nil	Nil	Nil	Nil	Nil	Nil	Nil	Nil	Nil

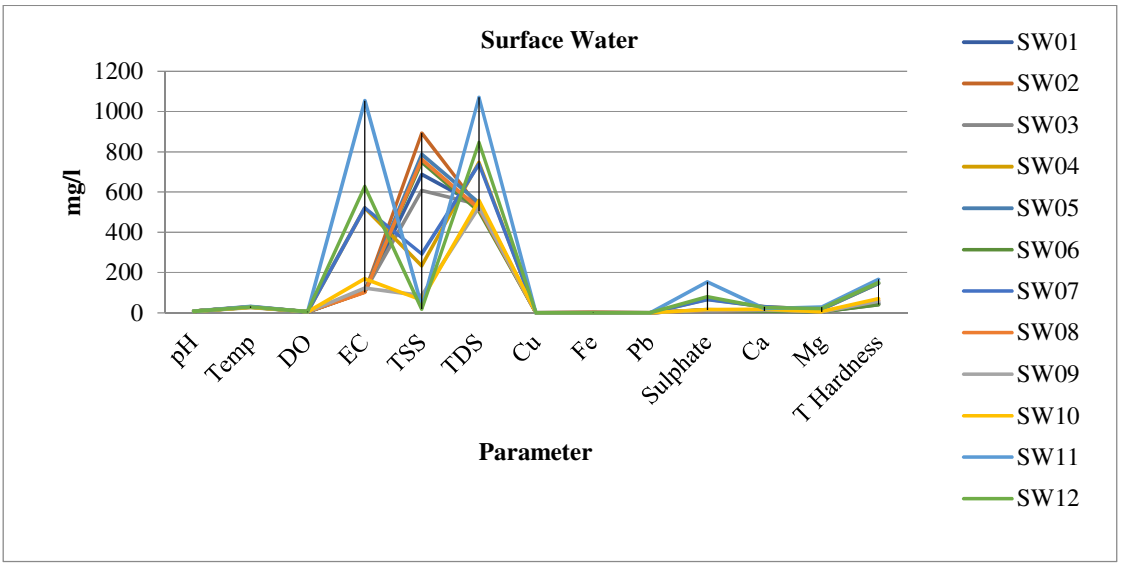

Figure 3 Analysis of surface water quality nearby Kyisintaung mine

Table 2 Results of ground water

Analysis	NEQG/ Composite Guideline	GW 01	GW 02	GW 03	GW 04	GW 05	GW 06	GW 07	GW 08	GW 09
pH	6-9.	7.2	7.6	7.7	7.5	7.6	7.6	7.2	7.2	7.5
Temperature	-	30.3	30.5	30.4	31	27.8	30.6	28.3	30.7	28.3
Dissolved Oxygen	-	1.54	2.24	3.06	0.87	2.13	2.23	1.04	1.42	2.77
Total Suspended Solids	50 mg/l	52	14	15	92	50	10	110	99	19
Total Dissolved Solids	1500mg/l	573	534	645	618	3165	781	1543	3807	2557
Cu (dissolved)	0.30 mg/l	<0.01	<0.01	<0.01	<0.01	0.04	0.01	0.01	0.02	0.01
Fe (dissolved)	3.5 mg/l	<0.01	<0.01	<0.01	<0.01	0.01	<0.01	0.01	0.01	<0.01
Lead	0.10 mg/l	<0.01	0.01	<0.01	<0.01	0.03	<0.01	0.01	0.05	0.03
Manganese	0.1mg/l	<0.01	<0.01	<0.01	<0.01	<0.01	<0.01	<0.01	<0.01	0.02
Sulphate	400 mg/l	146	122	196	182	910	194	234	1000	1280
Calcium	200 mg/l	111	96	81	116	7	54	11	67	24
Magnesium	150 mg/l	43	40	38	52	90	54	142	106	116
Total Hardness	180 mg/l	454	404	359	504	387	356	613	604	538
Acid	0.50 mg/l	Nil	Nil	Nil	Nil	Nil	Nil	Nil	Nil	Nil

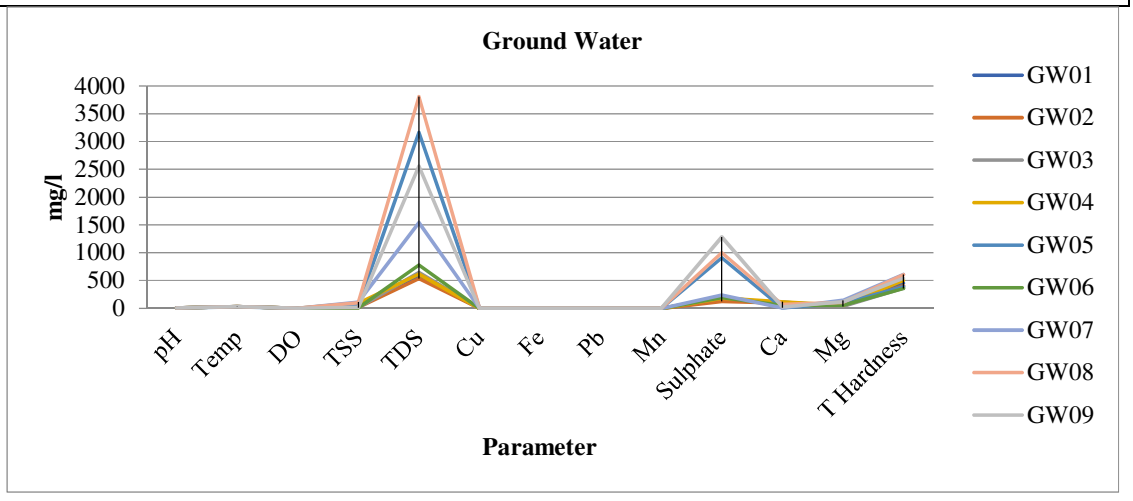

Figure 4 Analysis of ground water quality nearby Kyisintaung mine

IV. CONCLUSIONS

According to the results discussed above, the concentrations of monitored pollutants are within the acceptable limit of guideline values. However, the concentration of sulphate at GW08 and GW09 are higher as these sampling points are located very close to the heap leaching area. In addition, the concentrations of TSS values are notably exceeded the guidelines limits because the water samples were collected in the rainy season, June 2018 which increase the TSS level. On the other hand, the concentration of monitored pollutants in the nearby water resources are not considerably polluted since MYTCL adopts responsible mining methods, environmental friendly and zero discharge copper extraction during the mining operation (Figure 5).

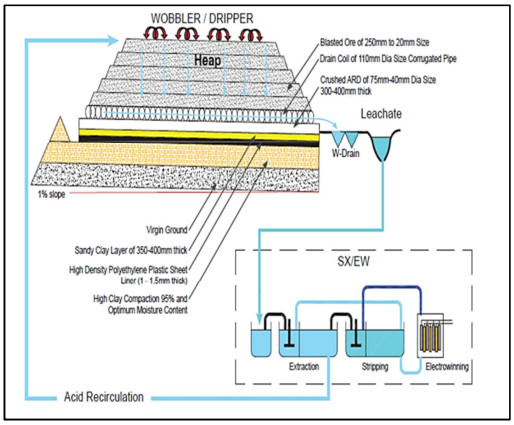

Figure 5 MYTCL's environmentally friendly and zero discharge copper extraction

ACKNOWLEDGMENT

The authors would like to express their appreciation to Myanmar Yang Tse Copper Limited, (MYTCL) for data provided of this study.

REFERENCES

[1] Barnes HL and Romberger SB. The chemical aspects of acid mine drainage. J. Water Pollut. Control Fed. 40, 1968, 371–384.

[2] Doyle TM and Gray NF. Protocol for monitoring andpredicting the impact of acid mine drainage: Designing and setting up a geographical information system (GIS). Technical Report: 25, Water Technology Research, Trinity College, University of Dublin, Dublin, 1995, pp 38.

[3] Gothschlich DE, Bell PRF and Greenfield PF. Estimating the rate of generation of acid drainage products" in coal storage heaps. Environ. Technol. Lett. 7, 1986, 1–12.

[4] Gray NF. Biorehabilitation of the acid mine drainage phenomenon by accelerated bioleaching of mine waste: Executive summary of the work done at Trinity College, Dublin. Technical Report: 33, Water Technology Research, Trinity College, University of Dublin, Dublin, 1995 a, pp 45.

[5] Gray NF.Procedure for the estimation of the impact of acid mine drainage to surface waters. Technical Report: 29, Water Technology Research, Trinity College, University of Dublin, Dublin, 1995b, pp 26.

[6] Gray NF. A substrate classification index for the visual assessment of the impact of acid mine drainage in lotic systems. Water Res. 30, 1996, 1551–4

[7] Gray NF and Doyle TM. Characterization of acid mine drainage generating sites". Technical Report: 11, Water Technology Research, Trinity College, University of Dublin, Dublin, 1994, pp 38.

[8] Kelly MG. Mining and the freshwater environment. London. Elsevier Applied Science, 1988, pp 213.

[9] Riley CV. The ecology of water areas associated with coal strip-mined lands in Ohio. Ohio J. Sci. 60 :106–21 Singer PC and Strumm W (1970) Acidic mine drainage: the rate determining step. Science (New York), 167, 1960, 1121–3.

[10] Sullivan M, Gray NF and O'Neill C.Synoptic overview of "the Avoca-Avonmore catchment and the Avoca Mines". Technical Report: 26, Water Technology Research, Trinity College, University of Dublin, Dublin, 1995, pp 43.

[11] Joh Muir Natural and Preservationlist , Glenn R. Wallis Enviroment& Operational Development Manager, "Sustainability Report, 2014-15.

[12] Hill, Loren G. Handbook of variables for environmental impact assessment. Ann Arbor Science, 1979.

[13] Myanmar Yang Tse Copper Limited. The Sustainability Report (2016-2017), 2017.

Water Management for Waterflooding in Mature Field

Thaw Zin[1], Naing Lynn[2,*]

[1] Department of Petroleum Engineering, Yangon Technological University,
Yangon, Republic of the Union of Myanmar
[1]thawzin.petroleum@gmail.com
[*]nainglynn.pe@gmail.com

***Abstract* – Increasing produced water is a one of the problems for oil and gas field. Therefore, water management is a crucial role especially in mature field where water production rate is more increasing than used to be and a knowledge of the properties of this formation water is important to petroleum engineers. During the oil production in mature fields, the implementation of waterflooding project also plays an important role for increasing the oil production and the recovery factor of the reservoir. In this paper, the analysis of dissolved solids of connate water, description of the amount of injection and disposal of produced water, and then, management plan for waterflooding in the field.**

Keywords: connate water, water management, waterflooding, mature field.

I. INTRODUCTION

Extraction of oil and gas from underground reservoirs often is accompanied by water or brine, which is referred to as produced water. As reservoirs mature, especially if secondary or tertiary recovery methods are used, the quantity of water climbs and often exceeds the volume of the hydrocarbons before the reservoir is exhausted. Traditionally, water extracted together with crude oil production is routed for sedimentation at the treatment pits before being discharged into the river. Water sources and treatment processes needed to produce acceptable water quality for waterflooding.

II. OIL FIELD WATER

1. Ideal water

Oilfield waters contain much higher concentrations of solids than seawater. All formation water contains dissolved solids, primarily sodium chloride. There are many applications of the pattern method of presentation of water-analysis data. Figure (1) shows one of the more commonly used methods of presenting water-analysis data.

The variations in concentrations and ionic compositions of formation water may be due to many factors:

- Nonmarine origin of some sediments
- Dilution by ground water
- Concentration through evaporation by migrating gas
- Sulfate reduction by anaerobic bacteria or petroleum constituents
- Absorption and base exchange of cations with clay minerals
- Dissolution of mineral salts by migrating formation water
- Exchange of magnesium and calcium ions during dolomitization
- Salt sieving by shales
- Precipitation of magnesium and calcium sulfates and carbonates
- Chemical reaction with constituents of the confining sediments

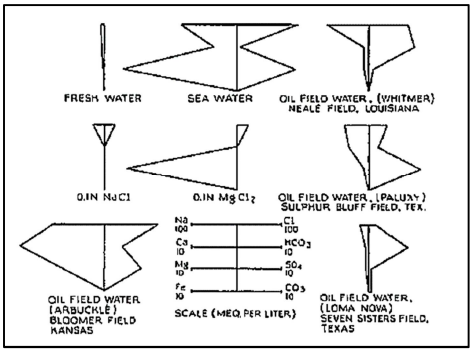

Figure 1 Common water pattern [2].

2. Water production and management

The objective is to maximize the value of the assest by increasing oil production, the reserve recovery factor, and reducing the production cost and practically canceling the environment impact figure (3).

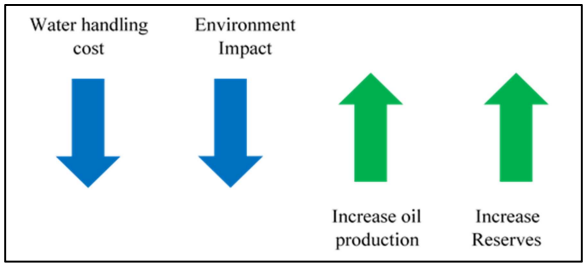

Figure 2 Objectives of water management [3].

3. Treatment and distribution

Difference types of treatment and distribution system are used in the field depend on water properties, the amount of water to be handle, etc. Typical water production and distribution scheme describes in figure (3). Managing production water involves different activities which are mentioned below:

- Production
- Treatment, distribution and injection
- Subsurface distribution
- Integrity control of the injector wells as well as surface installations

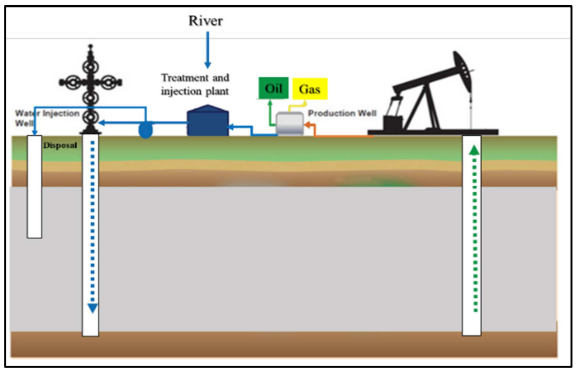

Figure 3 Typical water production and distribution scheme [3].

III. RESEARCH AREA DESCRIPTION

1. Geology background

This is the case of the Chauk-Lanywa Field that is located in the central Myanmar is one of the oldest productive basin of Myanmar with 113 active wells (Oct 2018). The depth of the oil and gas reservoirs range from 1,500 ft up to about 8,000 ft. Oil encountered in the field is a light crude oil (38° - 41° API Gravity). Gas cap occurs almost throughout the field. The first economic discovery took place in 1901 and reached peak production over 10,000 bbl/d. The structure is a narrow elongated asymmetrical anticline with the crest trending north-west direction as shown in figure (3). The oil, gas and water production rate and percent of water cut describe in figure (4) and (5) respectively.

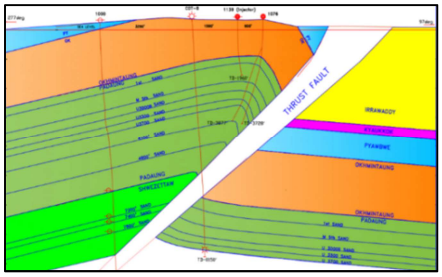

Figure 3 Stratigraphy of Chauk-Lanywa field.

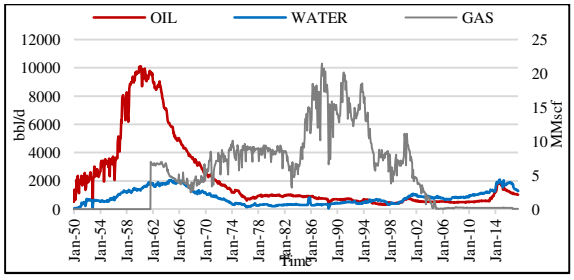

Figure 4 Oil, water and gas production history.

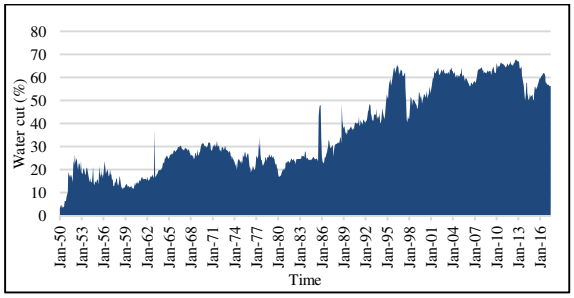

Figure 5 Water cut percentage.

2. Disposal water

Most of the oil field, produced water was reinjected into the formation because of environment impact and reduce the water handling cost to CHK-703 and CHK-753 that is converted from production wells to disposal wells because of original high rate of water production. Therefore, water production rate is high near adjacent wells of these two disposal wells.

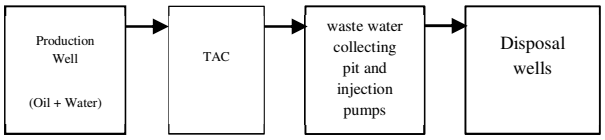

Figure 6 Disposal process flow diagram.

3. Waterflooding

Several waterflood projects have been conducted in the Chauk Field over the years. These are being reviewed to help determine if a moveable oil saturation by water injection existed at the time and to help assess the merits of initiating a waterflood project in the future.

A waterflood was initiated in 1963 in the North Central Fault Block (NCFB), Middle Fifth Sand. Performance data for the waterflood project was derived, in part by digitizing a performance plot provided by MOGE. Six new wells were drilled as water downdip (1074 and 1080) and four updip at the apparent gas-oil contact (1081,1083,1085 and 1086). While some respone to the waterflood is indicaed by the perforamce data, it was below expections.

The South Central waterflood was initiated in 1967. Additional waterfloods were conducted in the South Stray Sand and other areas. None of these projects have demonstrated the movement of oil by the injection of water. Waterflooding is now implected in C-B block beside the Aywewaddy River.

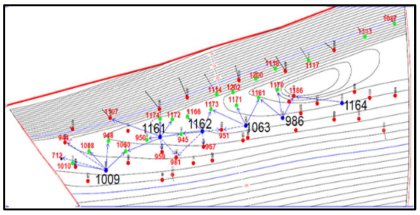

Figure 7 Injection and producting wells of C-B block.

3. Water Treatment system

Treatment processes needed to produce acceptable water quality. A lack of available water could prevent effective waterflooding, and poor water quality may result in a water flood failure. Improper or inadequate water treatment can also lead to problems that cause economic failure. There are two scenarios of water source is produced and river water. If the water source wells cannot meet the volume requirement, river water can be used as the source as illustrate in figure (8).

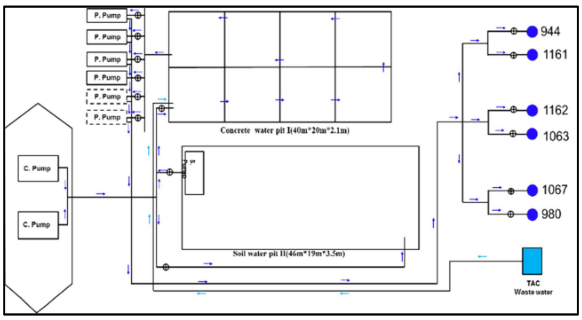

Figure 8 Surface process flow diagram of injection plant.

IV. RESULT AND DISCUSSION

The water sample was taken from ten wells. The type of water is sucker rod pumping unit. Sampling point is flow line at well site tank. According to the sample results, the dissolved cations found in water are Na (86.41 meq/L), Ca (0.97 meq/L) and Mg (1.46 meq/L) and the amount of dissolved anions are Cl (78.77 meq/L), SO_4 (0.52 meq/L), CO_3 (1.24 meq/L) and HCO_3 (8.26 meq/L) at CHK-1161. Difference dissolved solids at different wells are shown in figure (9 and 10). Therefore, the concentrations of the total solid is 5385.31 ppm (part per million). The density of water at reservoir condition is 62.87 lb/ft^3 and formation volume factor of water is 1.01. Stiff

diagram of CHK-1161 and LYA-147 are also shown in figure (11).

In figure (12), total volume for disposal is 398,243 bbl from March to December 2018. The amount of disposal water is generally increased due to the various reasons.

Total water injected volume was 2,180,285 bbl from March to December 2018 in figure (13). Among them, 514,986 bbl of formation water and 1,655,299 bbl of river were used respectively. The amount of water was dramatically increase during the first two months of water injection and then, the injection rate was fluctuated between May and December 2018. The amount of total water intake (disposal + injection) is described as show in figure (14).

The percentage of water used in the field is illustrated in figure (15). In waterflooding project, used of formation water was about 20%, river water was almost 64% and disposed into the formation approximately 15%.

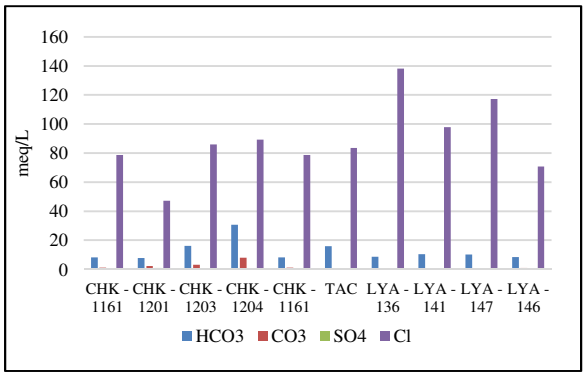

Figure 9 Dissolved solids (Anions).

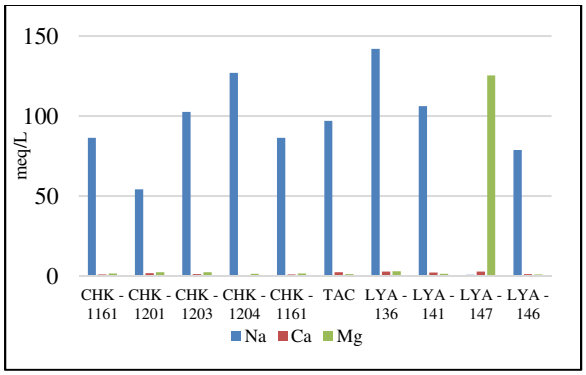

Figure 10 Dissolved solids (Cations).

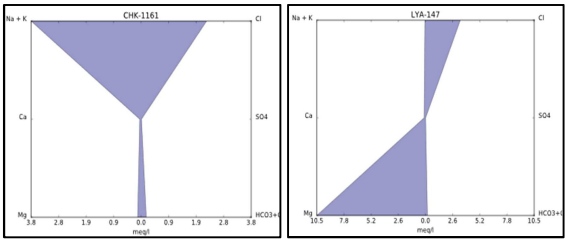

Figure 11 Stiff diagram of CHK-1161 and LYA - 147.

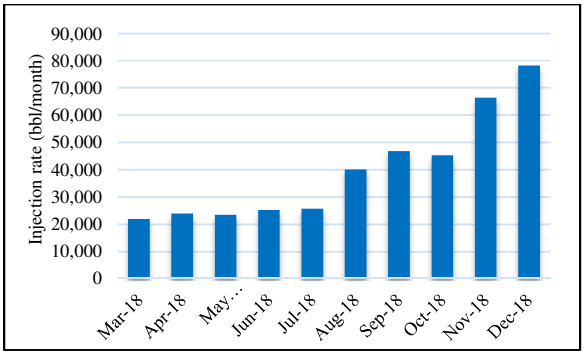

Figure 12 Injection rates of disposal water.

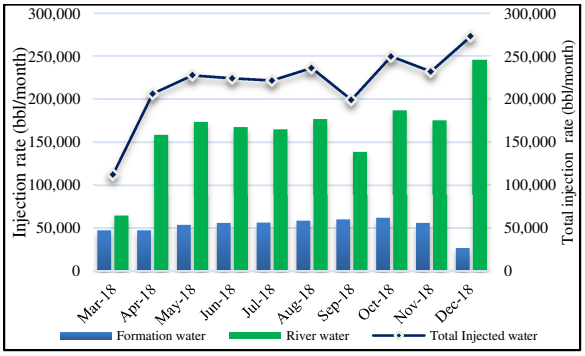

Figure 13 Injection rates of waterflood.

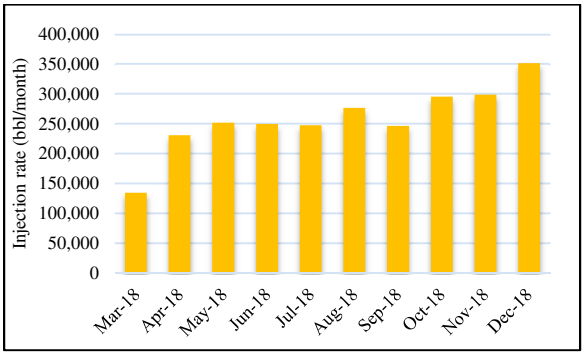

Figure 14 The amount of total water intake.

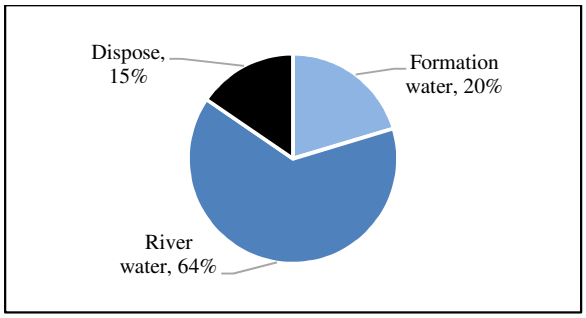

Figure 15 Percentage of injection rates.

VII CONCLUSION

The variations in concentrations and ionic composition of formation water may be due to many factors (precipitation of mangnesium and calcium sulfates and carbonate, and chemical reaction with constituents of the confining sediments, etc.).

The injection of water in oil fields to increase oil production in certain wells. As far as practicable, produced water will be used for gravity injection purposes, in order to reduce the discharge of water to the environment (i.e river, lake, etc). During the waterflood project, the amount of injected water will be increased. Therefore, more water will be needed to supplement from the other source, for example, river water. Most of the formation water is injected into the disposal well, therefore, water production rate is completely increase around of these disposal wells. All of these formation water should be used as injection water in C-B waterflooding project to reduce of river water up to 49%.

In mature fields, sometimes the water control is not an option, and it's necessary to produce water for producing oil.

- A continue surveillance is important for improving the oil production.
- Improving the water management process can extend the life of the mature fields.
- Add clay inhibitor and corrosion inhibitor to protect reservoir and facilities.
- Higher level treatment can be carried out if it is necessary based on the actual injection data and performance in future.
- EOR projects implementation could be an option for improving the recovery factor, but it will depend on the return on investment.

ACKNOWLEDGEMENT

The author would like to express his special thanks Dr. Zaw Htet Aung (Professor and Head, Department of Petroleum Engineering, Yangon Technological University) for giving permission for this paper. The author would be glad to express his thanks to his supervisor Dr. Naing Lynn (Professor, Department of Petroleum Engineering, Yangon Technological University) for helping to become this perfect study by his guidance and suggestions. The author is grateful to all Professors and Lectures from Department of Petroleum Engineering, Yangon Technological University and finally acknowledge to U Phone Thet Khaing (Executive Geologist, Chauk Field) the help for supporting the required data for this study.

REFERENCES

[1] J. F. B. A. R. J. W. STEPHEN C. ROSE, The design engineering aspects of waterflooding, Richardson, TX: Society of Petroleum Enginners, 1989.

[2] J. WILLIAN D. McCAIN, The properties of petroleum fluids, Tulsa, Oklahoma: PennWell Publishing Company, 1990.

[3] C. M. H. a. F. D. Bertomeu, Water Mangement Experience in Mature Field in South Argentian, Society of Petroleum Engineer, 2017.

[4] Water Flooding Pilot Test Scenarios, 2017.

Promote the Development of Renewable Energy in Myanmar

Khin Thi Aye
Deputy Director
PE (Water Resources) (0402)

Planning and Statistics Branch, Ministerial Office
Ministry of Electricity and Energy, Nay Pyi Taw, Myanmar

Khinthiaye2@gmail.com

Abstract _ **Myanmar has an abundance of renewable energy resources. Moreover, available energy resources in Myanmar are Hydropower, Solar Power, Wind Power, Biomass, Coal, Natural Gas and Crude Oil. Among them, hydropower, one of renewable energy resources in Myanmar is large contribution. Because, country's rivers, mainly four rivers, Ayeyawaddy, Chindwin, Sittaung and Thanlwin and its tributaries, can produce hydropower above 100,000 MW. And, other renewable energy resources, solar, wind and biomass are also available according to the geography condition of Myanmar. Now, Myanmar is growing fast and hence energy demand is significantly expanding. Therefore, Ministry of Electricity and Energy of Myanmar (MOEE) has been trying to generate the electricity from available energy resources to fulfill the electricity requirement. Moreover, MOEE has issued six objectives for electric power sector to meet the electricity demand and among them; the significant one is to generate more electricity from renewable energy resources. Myanmar Government formed the National Renewable Energy Committee on 6th February 2019, to promote and improve the Renewable Energy Sector, to get the international assistance for implementing the Renewable Energy Projects and to manage Renewable Energy Projects systematically when these are implemented by advanced technology. Myanmar has always promoted the Renewable Energy Sector; especially hydropower sector was promoted rapidly during the last decade of the 20th century. Therefore, at present, total installed capacity of hydropower stations, including large, medium and small scale is 3262 MW. Among them, 28 number hydropower stations with the total installed capacity of 3225 MW are connected to National Grid System and, 33 numbers small scale hydropower stations with the total installed capacity of 37 MW are off-grid. Moreover, MOEE has been carrying out studies to generate more electricity from Solar Power and Wind Power. In this paper, available energy resources in Myanmar, renewable energy resources in Myanmar, Existing Myanmar Electricity Condition (current generation mix, demand forecast, electricity consumption, planned and ongoing projects, strategic ways for power generation), developments of renewable energy (Hydro, Solar and Wind) and opportunities to invest in renewable energy sector are mainly described.**

Keywords: renewable energy resources, strategic ways for power generation, objectives and policies, developments of renewable energy and opportunities.

I. INTRODUCTION

Now, Myanmar Government has been trying to get balanced all round developments of States and Regions in the country. Therefore, generating electricity is very important to meet the electricity requirements of consumers, infrastructures, offices and all commercial and industrial works. Thus, renewable energy sector becomes vital role in Myanmar. Moreover, MOEE has been arranging by short term and long term plans to get electricity from available renewable energy resources.

II. AVAILABLE ENERGY RESOURCES IN MYANMAR

Myanmar has an abundance of renewable energy resources. Especially, hydropower resources are very plentiful. It has mainly four rivers, Ayeyawaddy, Chindwin, Sittaung and Thanlwin, these rivers and its tributaries are for Hydropower Resources. Country's rivers can be produced above 100,000 MW of hydropower. And, solar

power potential is 51973.8 Trillium Mega Watt Hour per year and Wind Power Potential is 365.1 Trillium Mega Watt Hour per year. In Myanmar, 52.5% of total land area is covered with forest and available annual yield of wood fuel is 19.12 million cubic ton for Biomass Potential. Available Coal potential has been 711 Million Metric Tons. Natural Gas for Onshore and Offshore will be 122.5391 Trillion Standard Cubic Feet and Crude oil for onshore and offshore will be 648.59 Million Barrels. These available energy resources are described in Table 1.

Table 1 Available Energy Resources

Particular	**Potential**
Hydropower	Above 100,000 MW
Solar Power	51973.8 TWH per year
Wind	365.1 TWH per year
Biomass	52.5 % of total land area covered with forest
	Potential available annual yield of wood-fuel 19.12 million cubic ton
Coal	711 Million Metric Tons
Natural Gas (offshore & Onshore) (Proven & Probable)	122.5391 TSCF
Crude Oil (offshore & Onshore) (Proven & Probable)	648.59 MMBBL

III. RENEWABLE ENERGY RESOURCES

There are many renewable energy resources in Myanmar. These are Hydropower, Solar Power, Wind Power, Geothermal Energy, Biomass, Waste to Energy and Ocean. Among them, hydropower, solar power and wind power are popular in Myanmar. MOEE has been trying to generate the electricity from these renewable energy resources.

IV. EXISTING ELECTRICITY CONDITION

In October 2019, the total installed capacity in power system is 5668.39 MW and the ratio of electric power (installed capacity) is 57 %(3225 MW) from hydro, 40% (2283.39 MW) from gas, 2 %(120 MW) from coal and 1 %(40 MW) from solar power respectively. According to the National Electricity Master Plan, the electricity consumption in 2015 was 2527 MW and the forecasted demand for the 2020, 2025 and 2030 are 4530 MW, 8121 MW and 14542 MW respectively. Besides, electricity consumption of year by year was increased from 15% to 19%. In December 2019, as electrified households became about 5.4 million, the electrification ratio became 50%. The total length of Existing Transmission Lines, 230 kV, 132 kV, 66 kV and 33 kV, up to October 2019 is about 16619 miles and the total length of planned and ongoing projects 500 kV Transmission line for Union Grid, Eastern, Western, Southern and Northern Grid is about 2665 miles. MOEE has also changed electric meter system from 1 meter system to 4 meter system to be easing public access and giving options for meter selection to electricity. And, Public call centers have been improved for responding to service with 1616 and 1717 contact numbers and doing business in Myanmar's ranking in Electricity Sector was improved. Moreover, Myanmar Government formed the National Renewable Energy Committee on 6th February 2019 with the Union Minister for Electricity and Energy as Chairman and having 6 Union Ministers from related ministries as members to improve Renewable Energy Sector, to get the international assistance for implementing the Renewable Energy Project and to manage Renewable Energy Project systematically when it is implemented by developed technology.

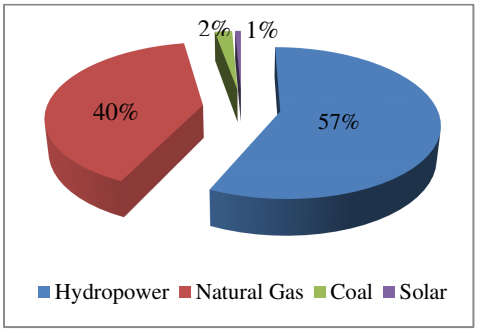

Figure 1 Generation Mix in Power System

V. POWER DEMAND AND ELECTRICITY CONSUMPTION

1. Power Demand Forecast

In Myanmar, annual demand of electricity is increased. According to the National Electricity Master Plan (NEMP), electricity demand (Peak Load) for 2030 will be 14542 MW and annual demand forecast for 20 years period, from year 2011 to year 2030, is shown in figure 5.

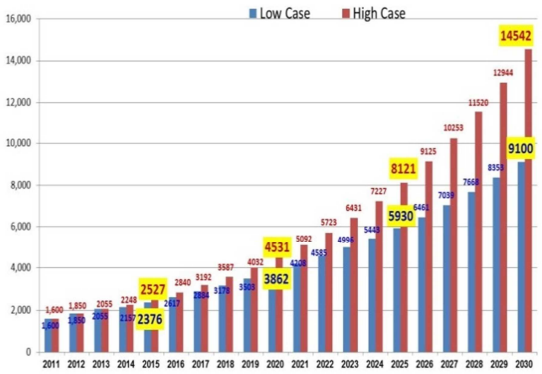

Figure 2 Demand Forecast for 20 years period (2011-2030)

2. Electricity Consumption

In Myanmar, electricity consumption was increased year by year. Now, its rate becomes from 15% to 19%. Total electricity consumption and per capita consumption year by year are shown in Table 2 and Figure 3. In December 2019, 50% of the total households (10.88 million) consume electricity.

Table 2 Electricity Consumption

Year	Total Electricity Consumption (GWh)	Per Capita Consumption (KWh)
2010-2011	6467.30	108
2011-2012	7876.72	131
2012-2013	8441.04	141
2013-2014	9795.09	163
2014-2015	11406.76	222
2015-2016	13550.81	263
2016-2017	15482.09	301
2017-2018	17251.91	335
2018-2019	19306.27 (sep 2019)	369

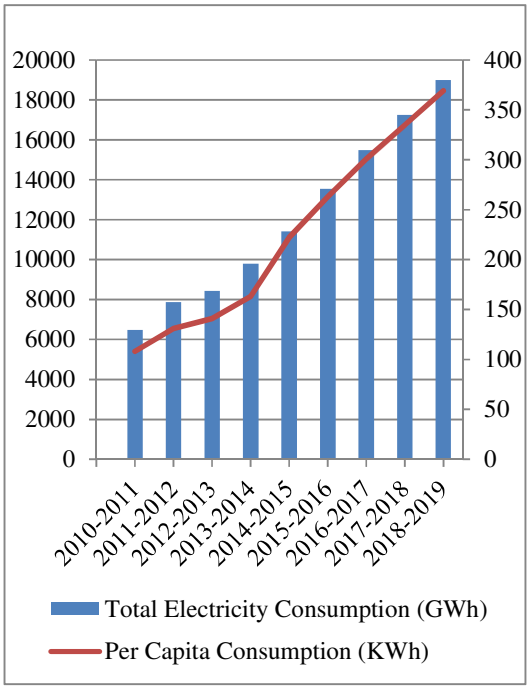

Figure 3 Electricity Consumption and Per Capita Consumption

VI. STRATEGIES WAYS FOR POWER GENERATION

Due to increased demands, to fulfill the electricity demand and reliable supplies of electric power is needed. Therefore, MOEE has laid down three strategies for power generation. Therefore, renewable energy projects are also implemented by three strategies ways; (1) sole investment by Ministry, (2) investment by local entrepreneurs on BOT basis and (3) investment by foreign companies on JV/BOT basis.

VII. OBJECTIVES AND POLICIES FOR ELECTRIC POWER SECTOR

MOEE has issued **six objectives** for electric power sector and significant one is **to generate more electricity from the renewable energy resources**. And MOEE has laid down **five policies** for electric power sector and the significant one is **to restructure the power sector with corporations, boards, private companies and regional organizations for more participation of local and foreign investments** and formation of competitive power utilities.

VIII. DEVELOPMENT OF RENEWABLE ENERGY (HYDROPOWER)

1. Hydropower Resources

Myanmar has abundant hydropower resources and the country's rivers can produce about 100,000 MW of hydroelectric power. Four major river basins are shown in figure 4. 92 numbers, medium and large scale hydropower projects, with the total installed capacity of about 46101 MW in river basin-wise are shown in Table 3.

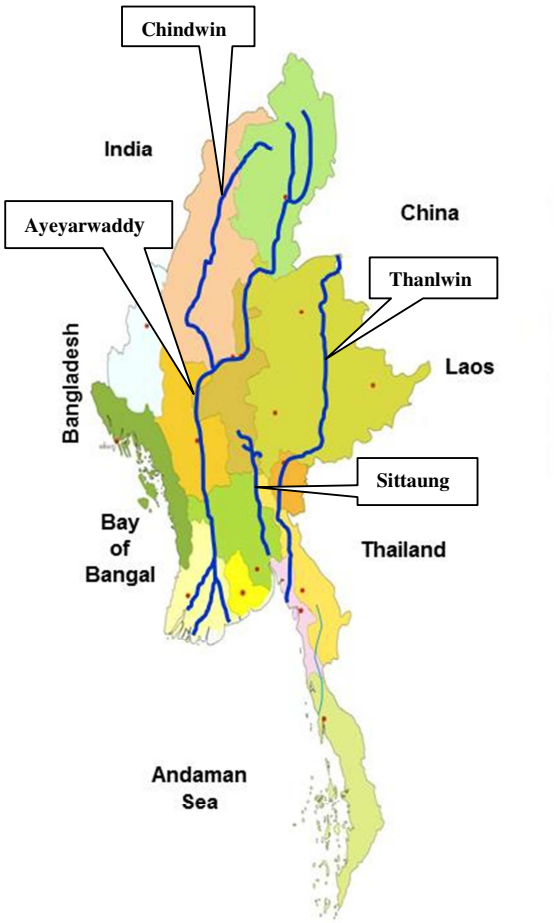

Figure 4 Four Major Rivers in Myanmar

Table 3 Hydropower Potential (River Basin-Wise)

Sr. No	River Basin	Number of Hydropower Projects	Installed Capacity (MW)
1	Ayeyarwaddy	34	21821
2	Chindwin	8	3015
3	Sittaung	11	1128
4	Thanlwin	21	17,641
5	Mekong	4	720
6	Others	14	1776
	Total	**92**	**46101**

2. Present Condition

At present, seven hydropower projects with the total installed capacity of 1355.4 MW, to connect the National Grid system are under implementation. And, three hydropower projects with the total installed capacity of 2655MW [Middle Yeywa-735 MW, Shweli(2)-520 MW and Upper Thanlwin-1400MW] have been carried out Feasibility Study. General information of the projects under implementation is described in Table 3. Total 28 numbers hydropower stations with the total installed capacity of 3225 MW have been connected to national grid and list of these Hydropower Stations in National Grid System is shown in Table 4. According to the future plan, 46 numbers hydropower projects with the total installed capacity of 36943.4 MW are arranged to be developed by local entrepreneurs and foreign investors.

Table 4 under implementation projects

Project Name	Location (State/ Region)	Capacity (MW)
Middle Paunglaung	Naypyitaw (Union Region)	152
Deedoke	Mandalay	60
Thahtay	Rakhing State	111
Shweli-3	Shan State(N)	671
Upper Yeywa	Shan State(N)	280
Upper Kengtawn	Shan State(S)	51
Upper Baluchaung	Shan State(S)	30.4
Total		1355.4

Table 5 existing hydropower station (connecting to National Grid)

No	Stations	Installed Capacity (MW)	Annual Genera-tion (Gwh)	Remark
1	Baluchaung(1)	28	200	
2	Baluchaung(2)	168	1190	
3	Kinda	56	165	
4	Sedawgyi	25	134	
5	Zawgyi(1)	18	35	
6	Zawgyi(2)	12	30	
7	Zaungtu	20	76	
8	Thaphanseik	30	117.2	
9	Mone Chaung	75	330	
10	Paunglaung	280	911	
11	Yenwe	25	123	
12	Kabaung	30	120	
13	Keng Taung	54	377.6	
14	Yeywa	790	3550	
15	Shwekyin	75	262	
16	Kun Chaung	60	190	
17	Kyee Ohn Kyee Wa	74	370	**Sole Invest-ment (2114 MW)**
18	Nancho	40	152	
19	Phyu Chaung	40	120	
20	Upper Paung laung	140	454	
21	Myogyi	30	135.7	
22	Myittha	40	170	
23	Yazagyo	4	96	
24	Thaukyegat(2)	120	604	**BOT (172 MW)**
25	Baluchaung(3)	52	334	
26	Shweli(1)	600	4022	**JV (939** MW)
27	Dapein(1)	240	1065	
28	Chipwe Nge	99	433	
	Total Installed	**3225**		

X. DEVELOPMENT OF RENEWABLE ENERGY (SOLAR POWER)

1. Solar Power Condition

Myanmar can use solar power according to the following situations:

- Myanmar is situated in the south eastern part of the Asian continent.
- The cooler, dry season lasts from November to April and the hotter, wet season from May to October.
- Sunshine is plentiful during the dry season average **7 to 10 hours a day.**
- During the rainy season, the weather is cloudier and daily sunshine amounts are average only **3 to 4 hours a day.**

2. Existing Solar Power Stations

Existing solar power stations in Myanmar are shown in table 5.

Table 6 Existing Solar Power Stations

Name	Location	Installed Capacity (MW)	Remark
Minbu	Magwe Region	40	1st Stage of Minbu 170 MW,
Thaton	Mon State	28.6	To be connected to Grid
Manaung	Rakhine State	3	Isolated
	Total	**71.6**	

Note: Off-grid Solar Home Systems excluded.

3. Planned and Ongoing Solar Projects

Nabuaing, Minbu and Wundwin solar projects, with the total installed capacity of 470 MW are planned and ongoing solar projects. Sagaing, Mandalay, Shwemyo and Thapyaysan solar projects with the total installed capacity of 990 MW are in investigation stage solar projects and the location of these solar projects are shown in figure 5.

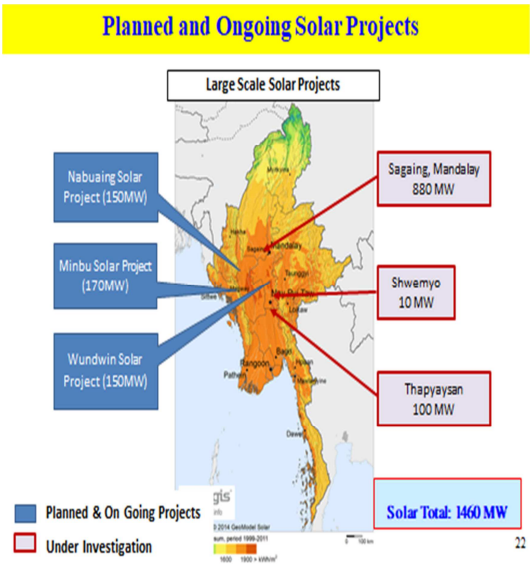

Figure 5 Solar Projects in Myanmar

4. Planned Floating Solar Projects

Three hydropower dams are planned as floating solar power projects. The location map of solar projects is shown in figure 6.

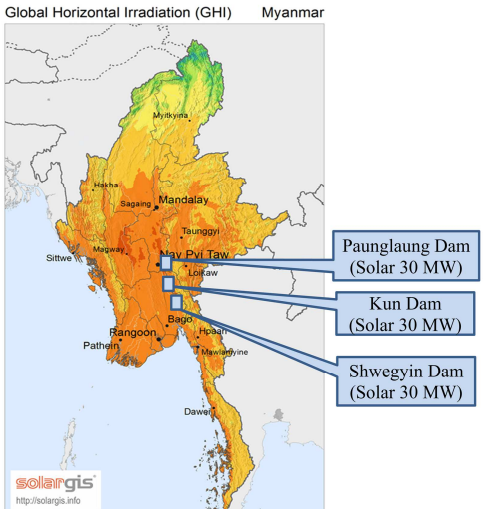

Figure 6 Location Map of Floating Solar Projects

XI. DEVELOPMENT OF RENEWABLE ENERGY (WIND POWER)

In Myanmar, wind power projects are under investigation. Wind power projects located in Rakhine, Ayeyawaddy and Yangon (Total installed capacity 830 MW) are in MOU stage and Chaung Thar (30 MW) is in MOA Stage. Therefore, total projected installed capacity of wind power project is 860 MW and all are in investigation stage.

X. CONCLUSION

In Myanmar, Electric Power Sector plays a vital role for all round development of the country. Now, more than 50% of households are electrified so the rest of households are needed to electrify. It is also needed to establish realistic generation mix to get the smart power system. Moreover, **opportunities** are open to invest in renewable energy sector because many hydropower potential remains and other renewable energy resources are plentiful. Since Myanmar has adequate energy resources and private sector has already invested in Power Sector, Myanmar is inviting the local and foreign investors to **invest more** in the electricity sector.

ACKNOWLEDGEMENTS

The author gratefully acknowledges to H.E U Win Khaing, Minister for Electricity and Energy and the author would also like to show her gratitude to Deputy Minister, Permanent Secretary, Deputy Permanent Secretary and Assistant Secretary from MOEE for their encouragement.

REFERENCES

Proceedings Paper

[1] Monthly Report for Electric Sector by DEPP, under MOEE, October 2019
[2] Monthly Report for Hydropower Projects by DHPI, under MOEE, November 2019
[3] Daily Generation Report by Power System Branch of DPTSC, under MOEE
[4] Power Sector Development in Myanmar, ADB Economics Working Paper Series No. 460, October 2015
[5] Overview of Hydropower Potential and Energy Sector in Myanmar and Sustainability of the Sector by MOEE for Strategic Environmental Assessment Workshop, October 2016

Transition of University to Prosumer Consortium Energy Model

Min Set Aung [2], Kaung Si Thu [1], Weerakorn Ongsakul [1], and Nimal Madhu Manjiparambil [1,*]

[1] Department of Energy, Environment and Climate Change,
School of Environment Resources and Development (SERD)
Asian Institute of Technology, Pathum Thani, 12120, Thailand

[2] Department of Information and Communication Technologies,
School of Engineering and Technology (SET)
Asian Institute of Technology, Pathum Thani, 12120, Thailand

*Corresponding author: mm-nimal@ait.ac.th

Abstract — **The conventional electricity grid system has many critical issues, which could lead to power instability, blackout, and many other issues. One main perspective is to consume the relative amount of distributed renewable energy in the adaptation system. Prosumer Consortium Model in a small community can be one of the solutions to reduce the price of electricity, increase efficiency and provide a better electronification for University, moreover, to solve the frequent blackout of electricity at university level in developing countries. It can be the learning opportunity for the researchers as well as the complementary benefit for the consumers inside university's grid.**

Keywords: Distributed energy, Energy trading, Prosumer consortium model, Renewable energy source, University grid.

I. INTRODUCTION

The increased of greenhouse gas emission and constantly high demand for energy encourage the mechanism of electricity generation to increase the production of green energy and high efficiency. The factors mainly cause the usage of renewable energy production with distributed generations (DG) through the macro/micro power grid. The current electricity system does not have the ability to maintain with DG as the main energy source, thus, only a backup or supplementary source. The key to play the prosumer consortium market model in the grid system is the support of distributed energy resources as in macro or microgrid, which can bring the energy balance in the grid. This implementation of prosumer consortium energy model allows the benefit to the local customers which allows from arranging dispatchable load at peak power consumption, reduce the load on distribution and transmission system.

The model is being conferred in the experimental studies in which many pilot projects are running in communities, nonetheless, an instant implementation can cause the current system to a revolution of operation, control and storage technology. The market is established on the supply and demand of the electricity especially volatile during peak hours. The comprising features of a university can be stated as a community grid. The model grid promotes the incorporation at the level of consumption of renewable energy sources (RES) and energy storage systems (ESS) targeting to increase power quality, reliability and performance.

II. CHARACTERISTIC OF TRADING MODEL

1. Integration of ICT in the market model

The characteristic of the model has to be changed from a unidirectional line to a bidirectional power exchange, as well as ICT infrastructure to transfer the data between customer nodes. The prosumer consortium model comprises DERs such as micro-wind generator, solar generator, biomass, EV station, different types of ESS and fuel cells. The

suitable preparation of the model has to be reliable and stable. When it comes to loads from a different consumer, they can be mainly distinguished into controllable load and uncontrollable load. The controllable load defines that the consumption of electricity can be stopped or start the operation in a matter of anticipated time, while incontrollable load does not have the flexible measure or control to operate in the time. Thus, these mentioned loads have to be aware of planning the demand response of the prosumer model. Sophisticated systems and advanced networking systems will have to the main part of transfer consumption/generation data, users' information and credit transfer. The aspects of the information system observe as software to approach the consumption information of building or node through web service as a worldwide web system to interact with the central monitoring of the prosumer consortium model. Then the web service can interact with the hardware interaction of the model, whether from the side of the consumer or supervisory unit. Communication of all the service intends to support the required and adequate bandwidth of the network as in an orthodox and reliable broadband power line technology. However, the convergence of 5G communication will be the future implication for the grid system. The complex control of the system is provided by the utilization of microprocessors to operate the load controllers, inverters and other components of the system.

2. Impact of Renewable Energy Production in University

The objective of energy generation is to shift from a conventional national grid system to take advantage of renewable energy production. However, the location of university and the available area, in order to obtain the required resources for RE production, depending on the method of power production such as biomass or wind energy. Those systems can be considered as a limitation to produce energy. Therefore, the popular source of supplying the required energy of the university can be powered by photovoltaic panels and microturbine, and besides, injections of power from electric vehicle can be an additional source of supporting RE. One of the important parts to maintain the RE power generation and local loads is a storage system – energy storage devices. The aggregated power from the surplus generation of RE will be solved by supplying back to the local demand or supporting the fulfill the local grid quality by discharging the storage devices. However, there is a thing that the implementation of energy storage system by itself cannot play as a vital part of the prosumer consortium model, thus the model can be designed without the storage. Since there are varieties of energy storage systems depending on the materials and energy, the effective system must be considered not only for financial assistance but the significant energy storage system to run the model. The application of energy storage system is mainly categorized into renewable energy integration, customer energy management, ancillary service and bulk energy. Typically, two configurations of energy storage system can be found in many systems, distributed and aggregated energy storage system. Generation output depends upon the cell temperature T and solar radiance G, nevertheless, the efficiency and power loss of the solar panel has to be considered. Normally, the solar generation inclines gradually from the morning and reaches the peak production at noon and falls back in the afternoon like a bell curve. A sudden rise in energy consumption of local load must be acutely considered that the consumption level reaches at less time. The microturbine can be another solution to provide the prosumer consortium model with a significant role as supplementary.

3. Prosumer Consortium in the system

A prosumer consortium microgrid is most likely to be found in regions with high retail electricity price or high MS financial support levels and both conditions are very likely to occur simultaneously. Individual or several prosumer bodies will own microgenerations and operate DERs to obtain profits from the integration. Individual or several prosumer bodies will own micro/macro sources and operate DERs to obtain profits from the integration. Microsource owners will get revenue from the sale and minimize the bill. The prosumer consortium market model for a small community as university might play a role since the model tends to have smaller DERs and discrete storage system. It will try to be more independent on the main grid and take no notice of network constraints. Figure 1 shows the prosumer consortium market model for a small community grid with the internal financial flow, which does not trade with wholesale market

and DSO, generally, the system works.

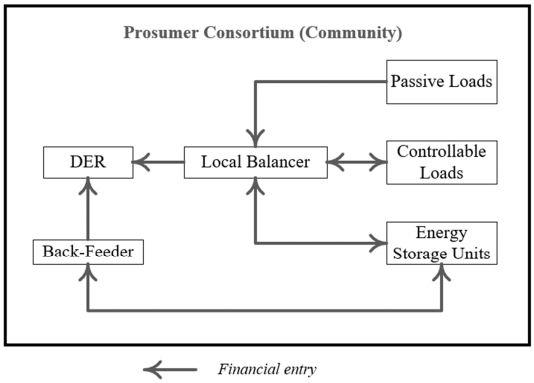

Figure 1 Financial entry in local prosumer consortium model.

III. FEASIBLE SYSTEM FOR THE MARKET MODEL

The form of DER and size of the generation mainly depends on the size of a university, funding and available resources to provide microgenerations. Meanwhile, a simple communication system with a small size of renewable energy generations can be premeditated. The installation of AMI at every consumer and prosumer node is necessary for data recording and operation of energy trade. The power line communication (PLC) broadband will be used while connecting to the central controller and smart meter, in which it will store the consumption/generation data and event statistics. The ability of BPL modems is to amplify the transmitted and received signal and perform the power converters gateway. The generation data of every generation units will be monitored by a central controller and thus make public to the participants from the university. Figure 2 presents the possible structure of prosumer market model at the university level, includes the rooftop solar panels which can be easily installed at the university buildings with battery system. Microturbine can be considered as a source, however, the availability of wind speed to produce an average power production is required, and necessary installation outside university compound is optional. Energy storage system can be used to maintain the system and backup even in the blackout or transition period. Electric vehicle station has to be one of the important sources to include in the prosumer consortium model though the accessible of EV will high depend on the location, nevertheless, as a dispersed storage system the injection of energy to the grid can be a benefit to the EV's owner. Usually, local consumer of university includes academic building, offices, residential units, lighting system and outreach buildings.

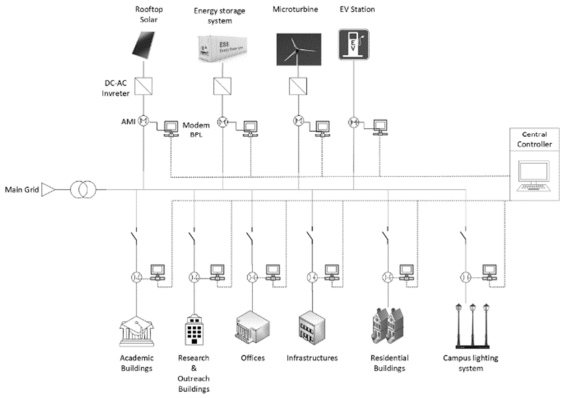

Figure 2 Feasible university grid system with a centralized controller.

Power line trading for prosumer and consumer nodes is assorted into substation level trading and centralized trading. Substation level trading depends on the total participants at each substation and one substation acts as one node of prosumer or consumer level. However, this research intends to emphasis centralized trading which all the nodes are connected at one communication line to central controller. Trading means good is a transfer between parties with a certain return with currency, currency shall be used on specified value of energy unit. Virtual currency will be a preferable system while performing the trading market. The central controller has an authority to has an interaction with a bank in order to inspect the purchasing of token by participants. The purchased token will be stored in the prosumer and consumer nodes.

During trading, the accessible power generation will be open to participants via website. The buyer has to make sure that has enough token to purchase the energy. When a buying request is made through the central control, it will make a decision based on energy production and token. Once the approval is passed, the token will be transferred to the destined seller account. Then the requested energy will be sent to the buyer node. The value of token on

energy assets will be decided due to the availability of DERs and local participants. At some cases, a certain fee has to be paid to the central control as a transaction fee but not considered in this study. The decision of other trading events will be made by centralized controlled and it has the right to resolve the violation of seller and buyer agreements. General idea of trading is explained in Figure 3.

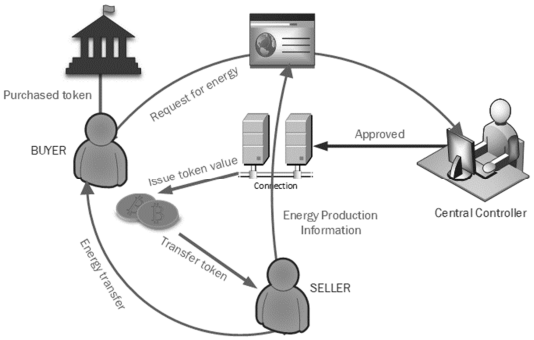

Figure 3 Actions of energy trading.

IV. CONCLUSION AND DISCUSSION

In this paper, the prosumer consortium market model for a university energy trading is presented. Many studies have been developed a community microgrid to create energy transferable mechanism and it has the nearly same architecture as this model. However, this proposed model can be tested in simulation case and then will be conducted in more research to be implemented. It has barriers to replace and upgrade an existing grid system and requires rigid ICT infrastructure in order to make strong and durable security. The use of hashing, cryptocurrency and encryption technology will be an optional method to solve trading and unauthorized access. A strong and transparent contract has to be made in order to accomplish integrity of the central controller and virtual account of each node must be protected from hacking and intrusion.

Advanced algorithms to make the prediction on renewable energy generation on prosumer or generation by hourly ahead or day ahead will be valuable information to purchase from consumers or buyers. Prediction of local demand is also an important factor to balance the local demand-supply. There is another research by authors that has been made a simulation in order to demonstrate the energy trading between prosumer nodes with virtual currency under the prosumer consortium market model. The local market model can provide financial benefit to the university and it can be assumed that can improve the understanding of energy market behavior to the learners from the university.

ACKNOWLEDGEMENTS

I would like to express my gratitude to Prof. Weerakorn Onngsakul for the guidance. Moreover, Dr. Jai Govind Singh, Dr. Chutiporn Anutrariya and Dr. Nimal Madhu Manjiparambil for their advice and encouragement for this research work. I would like to extend appreciation to Dr. Hien Vu Duc, supervisor of the AIT Energy laboratory for providing me the data.

REFERENCES

[1] Basak, P., Chowdhury, S., Dey, S. H. nee, & Chowdhury, S. A literature review on integration of distributed energy resources in the perspective of control, protection and stability of microgrid. Renewable and Sustainable Energy Reviews, 16(8), 2012,5545–5556.

[2] Dagdougui, H., Dessaint, L., Gagnon, G., & Al-Haddad, K. Modeling and optimal operation of a university campus microgrid. 2016 IEEE Power and Energy Society General Meeting (PESGM). doi: 10.1109/pesgm.2016.7741207, 2016.

[3] Dib, O., Brousmiche, K.-L., Durand, A., Thea, E., & Hamida, E. B. Consortium blockchains: Overview, applications and challenges. International Journal On Advances in Telecommunications, 11(1&2), 2018.

[4] Hadjidemetriou, L., Zacharia, L., Kyriakides, E., Azzopardi, B., Azzopardi, S., Mikalauskiene, R., … Tzovaras, D. Design factors for developing a university campus microgrid. 2018 IEEE International Energy Conference (ENERGYCON). doi: 10.1109/energycon.2018.8398791, 2018.

[5] Li, Z., Kang, J., Yu, R., Ye, D., Deng, Q., & Zhang, Y. Consortium blockchain for secure energy trading in industrial internet of things. IEEE transactions on industrial informatics,

14(8), 2017,3690–3700.

[6] Oh, S., Kim, M., Park, Y., Roh, G., & Lee, C. Implementation of blockchain based energy trading system. Asia Pacific Journal of Innovation and Entrepreneurship, 11(3), 2017,322–334.

[7] Soshinskaya, M., Crijns-Graus, W. H., Guerrero, J. M., & Vasquez, J. C. Microgrids: Experiences, barriers and success factors. Renewable and Sustainable Energy Reviews, 40, 2014,659–672.

[8] Tao, L., Schwaegerl, C., Narayanan, S., & Zhang, J. H. From laboratory microgrid to real markets—challenges and opportunities. In 8th international conference on power electronics-ecce asia , 2011,pp. 264–271.

[9] Available online at https://microgridknowledge.com/energy-storage-microgrid/

THE OPTIMAL COST OF AN OUTPATIENT DEPARTMENT BY USING SINGLE AND MULTIPLE SERVER SYSTEM

Dr. Win Lei Lei Aung
Associate Professor
Faculty of Computing, University of Information Technology, Hlaing , Yangon
wllaung@gmail.com

Abstract— Hospital management tradeoffs always exist between the costs in providing better service and waiting time of patients in any hospital. The objective of this study was to investigate whether increasing the cost for better service decreases the cost of patients waiting time or not, by using the technique of single and multiple servers which is based on the theory of Markovian queuing system. For this study, four weeks data has been taken from a public hospital. The results shows that as the service capacity level of doctors at the hospital increases from three to four servers then minimum total costs (include waiting and service costs) and the waiting time of patients as well as overutilization of doctors can be reduced. This paper also suggests that increasing the service units up to four servers will achieve lower cost as against two or more service units.

Keywords: ***Outpatient Department (OPD), Performance measures, the service cost, the waiting cost***

I. INTRODUCTION

Outpatient department (OPD) is one of the most important parts of hospital management and is visited by large section of community. This is the first point of contact between patient and hospital staff. The problems faced by the patients in that department are overcrowding, delay in consultation, lack of proper guidance etc. which lead to patients becoming dissatisfied. Every patient in each hospital is in search of hassle free and quick services in this fast growing world which is only possible with optimum utility of the resources through multitasking in a single server system in the OPD for better services. As patients flow increases because of that demands for hospitals and, better and quick services increases in [1] and [2].

In any hospital, patients come to the Outpatient Department without prior appointment and patients have to wait to receive medical service that may be waiting before, during or after being served. Generally queues are formed when the demand for a service exceeds its supply. For many patients or customers, waiting in lines or queuing is annoying or negative experience. A few of the factors that are responsible for long waiting lines or delays in providing service are: lack of passion and commitment to work on the part of the hospital staff, overloading of available doctors, doctors attending to patients in more than one clinic etc.

A good patient flow means that the patient queuing is minimized while a poor patient flow means patients suffer considerable queuing delays [**7]**. Considering these points mentioned above, our present study proposes to evaluate the patients waiting problems in terms of the performance measure and also to determine the level of service that minimizes the total cost of the expected cost of service and the expected cost of waiting.

II. MATERIALS AND METHODS

The study area is Yangon, which is a fast developing city in the MYANMAR. In every hospital, Yangon is actually facing a big issue of patient waiting time problem at every day. There is heavy inflow of sick patients in this region from neighboring rural areas or from smaller towns because of the availability of advanced health facilities. For our study we selected one of the leading public hospitals of the region, North Oaklapa General Hospital in Yangon where it was observed that there was a heavy flow of patients thought the week. Data was collected over a period of four Weeks from 15.10.2019 to 13.11.2019 as shown in Table 1. Table 1 shows the data collected for one week. These data represents the number of patients at OPD. Data was collected from the Patients who visited Out- Patient Department during day shift by using direct observation method.

In this observational study, the traffic intensity of the out patients at registration counters such as the arrival rate (λ), service rate (μ) and number of

servers was measured at hourly interval. The standard simple queuing model assumes that

1. Arrivals have the Poisson distribution
2. Service times have the exponential distribution
3. Arrivals and service times are all independent. (Independence means, for example, that: arrivals don't come in groups, and the server does not work faster when the line is longer.)

Table 1 measured data for one week

Time (hr) / days	9:00 AM to 10:00AM	10:00 AM to 11:00 AM	11:00AM to 12:00 AM	1:00 PM to 2:00 PM	2:00 PM to 3:00 PM	3:00PM to 4:00PM
15.10.19	60	70	80	65	50	45
16.10..19	43	63	70	100	45	55
17.10.19	33	56	50	120	55	65
18.10.19	23	88	45	80	65	77
19.10.19	12	102	35	90	78	78
20.10.19.	9	133	25	105	73	82
21.10.19	8	117	40	120	88	63

In this M/M/m queuing model, the 1st M indicates the inter-arrival time distribution arrivals follows Poisson distribution with parameter λ, and 2nd M indicates service time distribution [5]. Here, it is exponential distribution with parameter μ and 3rd m indicates number of servers available those are in parallel. The system has multiple servers and uses the FIFO service discipline. The waiting line is of infinite size. In the case M/M/1 queuing model, there is only one single server. It means that the system can process a single request at a time. But in this M/M/m queuing model, there are m numbers of servers that are connected in parallel [5]. Queuing model enable finding an appropriate balance between the cost of service and the amount of waiting. The ultimate goal of queuing analysis is to minimize two costs, which is service capacity cost and customer waiting cost.

These are analyzed for simultaneous efficiency in patient satisfaction and cost minimization through the use of a single server M/M/1(∞: FCFS) and multi-server queuing models, which are then compared for a number of queue performances such as; the average time each patient spends in the queue and in the system, average number of patients in the queue and in the system and the probability of the system being idle. In M/M/1(∞: FCFS) queuing model, the arrival of patients in a fixed time interval belongs to Poisson probability distribution at an average rate of λ patients per unit time. It is also assumed that the service time was exponentially distributed, with an average rate of μ patients per unit of time. The hypothetical structure of Single-server queuing model is shown in Figure 1.The hypothetical structure of Multi-server queuing system is as shown in Figure 2.

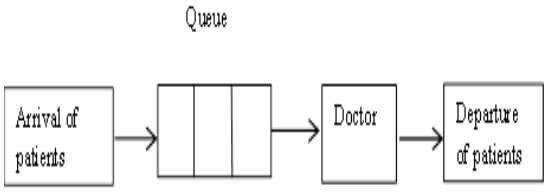

Figure 1 Single server queuing system.

The performance measures of single server system
Average server utilization factor in the system

$$\rho = \frac{\lambda}{\mu} \quad (1)$$

Probability that no patient in the system

$$P_0 = 1 - \rho \quad (2)$$

Average number of patients in the system

$$L_s = \frac{\rho}{1-\rho} \quad (3)$$

Average time a patient spends in the system

$$W_s = \frac{L_s}{\lambda} \quad (4)$$

Average number of patients in the queue

$$L_q = L_s - \rho \quad (5)$$

Average time a patient spends in the queue

$$W_q = \frac{L_q}{\lambda} \quad (6)$$

For the multi-server queuing model, the M/M/c (∞: FCFS) model has been adopted. The basic hypothetical structure of multi -server queuing model is shown in Figure 2.

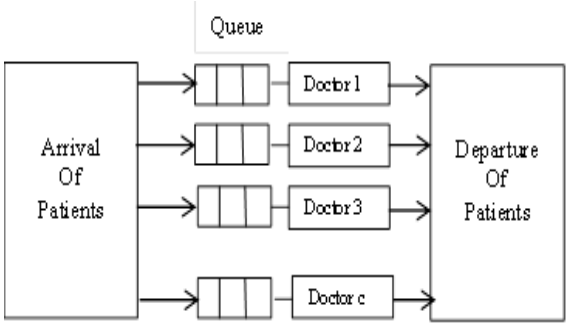

Figure 2 Multi server queuing system.

The performance measures of multi-server system
Average server utilization factor in the system

$$\rho = \frac{\lambda}{c\mu} \quad (7)$$

Probability that no patient in the system

$$P_0 = \left[\sum_{n=0}^{c-1} \frac{(c\rho)^n}{n!} + \frac{(c\rho)^c}{c!(1-\rho)}\right]^{-1} \quad (8)$$

Average number of patients in the queue

$$L_q = \frac{\rho(c\rho)^c}{c!(1-\rho)^2} P_0 \quad (9)$$

Average number of patients in the system

$$L_s = L_q + \rho \quad (10)$$

Average time a patient spends in the system

$$W_s = \frac{L_s}{\lambda} \quad (11)$$

Average time a patient spends in the queue

$$W_q = \frac{L_q}{\lambda} \quad (12)$$

In this queuing system, the arrival of patients is assumed to follow a Poisson process, and service times are assumed to have an exponential distribution. Let the number of servers be c, providing service independently of each other. It is also assumed that the arriving patients form a single queue and the one at the head of the waiting line enters into service as soon as a server is free. No server stays idle as long as there are patients to serve. If there are n patients in the queuing system, then two possibilities may arise:

Case.1: $k \leq c$. In this case no patient has to wait for service. However, (c-n) patients will be in queue and the rate of servicing will be $k\mu$.

Case.2: $k > c$. In this case, all the doctors will be busy and the maximum number of patients ρ will be (k-c) in the queue and the rate of service will be $c\mu$.

The Variables are analyzed by using the performance measures of the Queuing Models [M/M/1(∞: FCFS) and M/M/c (∞: FCFS)] as presented in equation (1) to (12). There are (5 x 4 weeks) working days in a month used in this study while the working hours per day are 24 hours for casualty service and 5 hours for outpatient service. Queuing models can be used to determine the operating performance of a waiting-line system.

In the economic analysis of waiting lines, we seek to use the information provided by the queuing model to develop a cost model for the waiting line under study. Then we can use the model to help the hospital management to make a trade-off between the increased costs of providing better service and the decreased waiting time costs of patients derived from providing that service. To determine the level of service that minimizes the total cost of the expected cost of service and the expected cost of waiting, we utilize the cost analyzing model.

In cost model, we consider the cost of patient time, both waiting time and servicing time, and the cost of operating the system.

Let C_w= the waiting cost per unit per patient and

C_s = Cost of providing service per doctors per unit of time

Therefore, the total cost per minute is

Total cost = $C_wL_s + C_s c$, where L_s is the average number of patients in the system and c is the number of servers/doctors.

III. RESULTS

Using equation (1) to equation (12), we get the performance measures of single doctor system and multi doctor system as shown in following Table 2 and Table 3. Table 2 shows the average server utilization in the department, the probability of no patient in the department, the average number of patient in the outpatient department and the average waiting time in this department.

Table 2 Summarized data ρ, P_0, L_s and W_s for single server and multi-server system

Doctors	Average patients Utilization in the system (ρ)	Probability that there are no patient in the system (P_0)	Average number of patients in the system (L_s)	Average time a patient spends in the system (W_s)
1	60%	0.40000	1.50000	0.50000
2	30%	0.53850	0.65935	0.11978
3	20%	0.54795	0.60616	0.20616
4	15%	0.54873	0.60062	0.20021
5	12%	0.54881	0.60006	0.20002
6	10%	0.54881	0.60001	0.20000
7	8.6%	0.54881	0.60000	0.20000

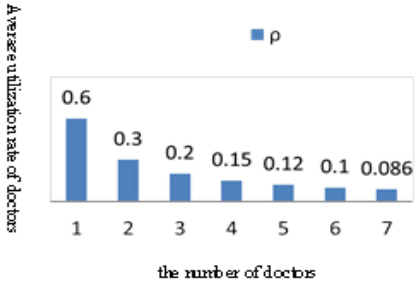

Figure 3 Utilization rate against the number of doctor.

In Figure 3, the average utilization rate of doctor decreases with increasing the number of doctor.Table 3 also summarizes the cost for the single server system and multiple-server system. We get the optimal cost from the data of Table 2.

Table 3 Summarized data L_q ,W_q and the total cost for single server and multi-server system

Patients	Average number of patients in the system (L_q)	Average time a patient spends in the system (W_q)	The total cost
1	0.90000	0.30000	2250 kyats
2	0.05935	0.01978	989 kyats
3	0.00616	0.00206	909 kyats
4	0.00062	0.00021	900 kyats
5	0.00006	0.00002	900 kyats
6	0.00001	0.00000	900 kyats
7	0.00000	0.00000	900 kyats

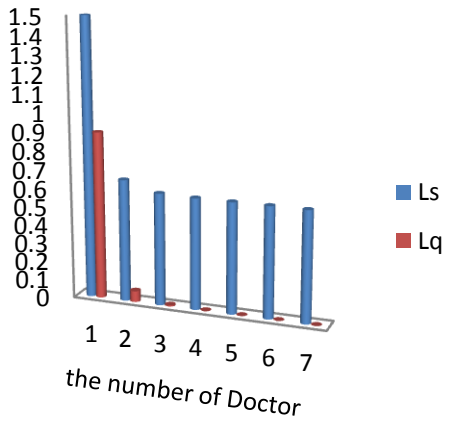

Figure 4 Average numbers of patients in the system and in the queue.

Figure 4 shows increased the number of doctor decreased the average number of patient in the queue. It saves time. For better graphical representations of the above summarized table, Figures 3-7 are shown. In Figure 3 we depict the average server utilization in the system against the number of doctors. As observed, server utilization rate decreases with increasing number of doctors. It is also noted in Figure 6 that the probability that there are zero patients rise upward as number of doctors increase and the expected length of the queue (L_q) and the system (L_s) in Figure 4 decline and rise upward respectively.

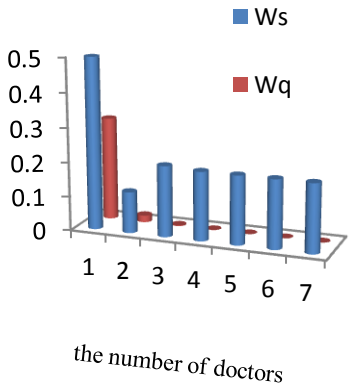

Figure 5 Average time a patient spends in the system and in the queue.

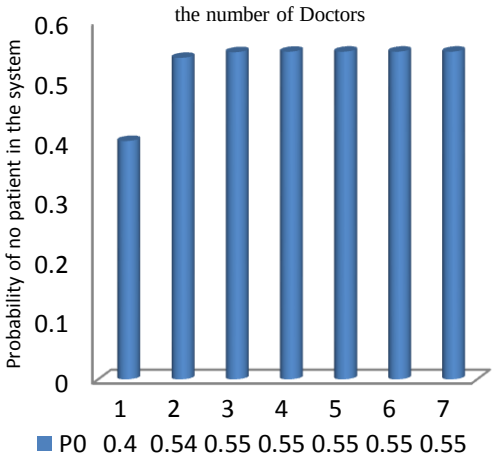

Figure 6 Probability of no patient in the system with the increased number of doctors.

Also the expected waiting time in the queue (W_q) and the expected time in the system (W_s) decrease in Figure 5. Figure 7 shows that the expected total cost and service cost fall downward and then rise upward. However, from the figures it is evident that the patients waiting time is optimum when the server is 4 as compared to server 2 and 3. It is also noted that patient's congestion and expected wait time is less than the optimum level. In optimizing of queue, there are optimizing over the number of servers, optimizing over the mean service rate and optimizing over the mean arrival rate [14]. In this paper, we get the optimal level from optimizing over the number of servers (doctors).

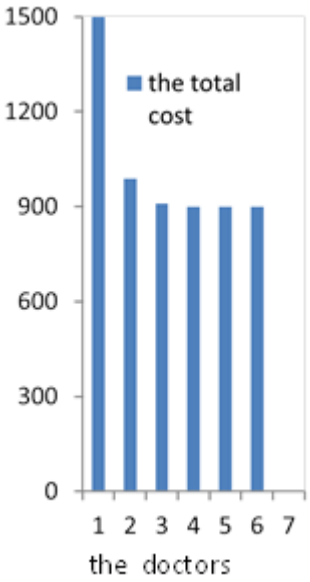

Figure 7 the optimal cost against the number of the doctors.

IV. DISCUSSION

Table 2 shows that a 4-server system is better than a single server, 2-server or 3-server system in terms of the performance criteria used. For instance, in terms of cost considerations, assume that the waiting cost is 1500 kyats per patient, for 4-server system records the lowest cost of 900 kyats compared to a 2-server and 3-server system that records 989kyats and 909 kyats respectively.These costs included the entire cost done by the hospital. The average time a patient spends in the system and in the queue are 0.2 minutes and 0.00021 minutes respectively for a 4-server system.

The probabilities of idleness are 30.0% and 20.0% respectively for 2 and 3 server systems respectively. The average time a patient spends in the queue and in the system for a single server system is 0.3 minutes and 0.5 minutes respectively while the system has 4.5 and 1.5 patients in the queue and in the system respectively. The system is likely to be idle for 0.4 minutes.

In [8], a survey comparing the performance of a single channel with multi-channel queuing models in achieving cost reduction and patient satisfaction using a hospital study, it was concluded that the 3-server system is better than a single server, 2-server or 4-server system. The average time a patient spends in the system and in the queue are 11 minutes and 1.79 minute.

However, another study revealed a positive correlation between arrival rates of customers and bank's service rates where it was concluded that the potential utilization of the banks service facility was 3.18% efficient and idle 68.2% of the time [9]. A One week survey revealed that 59.2% of the 390 persons making withdrawals from their accounts spent between 30 to 60 minutes while 7% spent between 90 and 120 minutes [10]. Further it was observed in another survey that although the mean time spent was 53 minutes by customers, they prefer to spend a maximum of 20 minutes only [11**]**. Their study revealed worse service delays in urban center's (average of 64.32 minutes) compared to (average of 22.2 minutes) in rural areas.

Moreover those customers spend between 55.27 to 64.56 minutes making withdrawal from their accounts Efforts in this study are directed towards application of queuing models in capacity planning to reduce patient waiting time and total operating costs [12].

V. Conclusion

The results of the analysis showed that that as the service capacity level of doctors at the hospital increases from three to four servers then minimum total costs (include waiting and service costs) and the waiting time of patients as well as overutilization of doctors can be reduced. The study also suggests that, to optimize the processing time for the patients it is necessary to rationalize the utilization of the servers for effective utilization of human resource. Otherwise, the service units may be increased to four to achieve better results at a lower cost as against two or three service units. A single server is not effective as much as compared to multiple servers. Whereas, five servers eliminates waiting cost but at a higher cost which is not optimal too.

ACKNOWLEDMENTS

Firstly, I would like to thank Dr. Pyke Tin who shares ideas and helpful suggestion. I am also grateful to Dr. Swe Swe Kyaw , head of Faculty of Computing , who motivates me to do this. And then, I appreciate to my mother for her patient, understanding and encouragement during my work that has to successful finish. Finally, I am also thankful for all my teachers and colleagues since my childhood and I sincerely thank all concerned persons of North Oaklapa General Hospital for their help and cooperation during the data collection

process.

REFERENCES

[1] Srinivasan, A. V. (2000). Managing a Modern Hospital, Response Books. A Division of Sage Publishers India (P) Ltd., New Delhi, 53-69.

[2] Llewelyn, R. and H. M. C. Davies.(1996). Macaulay Hospital Planning and Administration, WHO, Geneva, 105-11.

[3] Hiller, S.F. and Lieberman, J. G., Introduction to Operations Research, Boston: Mcgraw Hill, Eight Edition.pp.834-838, 2005.

[4] Singh V., "Use of Queuing Models in Health Care", Department of Health Policy and Management, University of Arkansas for Medicals Sciences, 2007.

[5] Raj Jian, "The Art Of Computer Systems Performance Analysis", John Wily & Sons Inc, computer press award winner, pp 592-604, 1992.

[6] Trivedi, Kishor S, "Probability and Statistics with Reliability, Queuing and Computer Application", John Wiley & Sons Inc, 2016.

[7] Hall, W. R. (2006). Patient Flow: The New Queuing Theory for Healthcare, OR/Ms, Today 2006.

[8] Brahma, P. K. An Appraisal of cost of queuing in healthcare sector a case study of IMS and SUM hospital, International Journal of Multidisciplinary Research, Vol. 2(4).

[9] Oladapo. (1998). Relationship between Arrival Rates of Customers and Bank's Service Rates, Seminar Paper Series, Obafemi Awolowo University, Ile-Ife.

[10] Elegalam. (1978). Customer Retention Versus Cost Reduction Technique, A Paper presented at the Bankers forum held at Lagos.

[11] Baale, A. F. (2002). Managerial Applications of Queuing Models in the Service Industry: A Int. j. sci. footpr. Dhar et al. (2014) Case Study of Afribank Nigeria Plc.,Ilorin Main Branch. A Research Paper submitted to Business Administration Department, University of Ilorin, Ilorin.

[12] Juwah. Operational Problems and Customers' Dissatisfaction, CBN Bullion, 1986.

[13] S Kalavathy, "Operations Research",Vikas Publishing House Pvt Ltd,pp411-440, 2000.

[14] Joseph G.Ecker and Michael Kupferschmid, "Introduction to Operations Research",John Wily & Sons, Inc, pp 409-413, 2014.

Analysis of Forecasting Techniques of Instant Noodle Manufacturing Company

Hsu Myat Tin[#1] , Kyaw Lin Thet[#2]

[#1]Department of Business and Management, Chindwin TU International College, Yangon,11162, Myanmar.

[#2]Department of Mechanical Engineering, Yangon Technological University, 11011, Myanmar

*Corresponding author: hsumyat.tin@gmail.com

***Abstract*— This paper is about the forecasting techniques of Yathar Cho Industry Limited (YUM YUM INSTANT NOODLE), Myanmar. Forecasting is a technique that uses historical data as inputs to make informed estimates that are predictive in determining the direction of future trends. Businesses utilize forecasting to determine how to allocate their budgets or plan for anticipated expenses for an upcoming period of time. The main aim of this paper is to show the forecasting techniques of Yum Yum noodle. The forecasting techniques is shown on two ways. The first way is the calculating of mean absolute percent Error calculating using the two period moving average method. The second way is the calculating of mean absolute percent error using exponential smoothing method.**

***Keywords*— Yathar Cho Industry Limited, Two-period moving average, Exponential Smoothing, Mean Absolute Percentage Error**

I. INTRODUCTION

A forecast is a statement about the future value of a variable such as demand. That is, forecasts are predictions about the future. The better those predictions, the more informed decisions can be. Some forecast are long range, covering several years or more. It describes the elements of good forecasts, the necessary steps in preparing a forecast, basic forecasting techniques and how to monitor a forecast.

Two aspects of forecasts are important. One is the expected level of demand; the other is the degree of accuracy that can be assigned to a forecast (i.e., the potential size of forecast error). The expected level of demand can be a function of some structural variation, such as a trend or seasonal variation Forecast accuracy is a function of the ability of forecasters to correctly model demand, random variation and sometimes unforeseen events.

Forecasts are the basic for budgeting, planning capacity, sales, production and inventory, personnel, purchasing, and more. Forecasts play an important role in the planning process because they enable managers to anticipate the future so they can play accordingly.

II. CASE STUDY

A case study is made at Yathar Cho Industry Limited (YUM YUM Instant Noodle), located at No (197,198,199), 10th Street, Yangon, Myanmar, which manufactures three different types of products. They are Original, Xcite and Premium. The machine can produce approximately 6000 boxes for one small production line and about 12000 boxes for large production line. For a day, they can produce around 35000 bags depending upon customer demand. The information and data are obtained from this factory for this paper.

III. MANUFACTURING

A. Functionally of raw materials/ ingredients

The main ingredients for instant noodles are wheat flour, salt or kansui (alkaline salt mixture of sodium carbonate, potassium carbonate and sodium phosphate), and water. Other ingredients like starch, gums, emulsifiers, stabilizers, antioxidants, coloring and flavoring agents are also added to improve the texture and eating quality. Nowadays instant noodles are also fortified with protein, minerals and vitamins to improve their nutrition value.

B. Role of critical unit operations

Noodle processing typically comprises mixing raw materials, resting the crumbly dough, sheeting the dough into two dough sheets, compounding the sheets into one, gradually the sheet into a specified thickness and slitting into noodle strands. For instant noodle preparation, strands are steamed and dehydrated by drying or frying followed by cooling and packing with the seasonings.

- Mixing: Ingredients other than flour are pre dissolved in water, stored at 20-30 ºC while salt water can be prepared separately. Wheat flour and water along with other weighted ingredients are mixed first at high speed and then a low speed, giving a total time of 15-25 minutes in industries. The mixing time, however also depends on the type of mixer used. Mixing is also influenced by the quality of flour, volume of water added, presence or absence and amount of certain ingredients (especially salt and alkaline salt) and temperature and humidity of processing environment. Mixing is usually followed by dough resting. Resting improves processing properties and facilitates gluten formation during sheeting.
- Sheeting: After mixing, the crumbly dough is compressto form continuous dough sheet, which is folded or compounded and passed through subsequent rolls. The sheeting process is intended to achieve a smooth dough sheet with desired thickness, and a continuous and uniform gluten matrix in dough sheet. Dough sheet are rest to allow gluten structure relaxation or mellow the gluten and make it more extensible by slow passage or zigzag conveyor in automobile plants.
- Cutting / slitting and Waving: The dough sheet is cut into noodle strands of desired width with a slitter. The width and shape of noodle strands are determined by cutting rolls. The speed differential between noodle feeding and net travelling result in a unique waving of noodle strands. Noodle strands are cut into a desirable length by a cutter.
- Steaming and Moulding: The cut and way noodle strands are conveyed to a steam chamber to cook them by exposing to a temperature of 100ºC for one-five minutes. The degree of cooking during steaming is critical and depends on the original moisture content of noodle; amount, pressure and temperature of steam and steaming time. Under steamed noodles will have a hard core and will be difficult to cook properly, whereas over steamed noodles are soft and sticky. Steaming is a key process in the manufacture of instant noodles. The cut noodles are placed in moulder of square, round, bowl, or cup shape, depending on the desired product shape before moving to the fryer or drier.
- Frying / Drying: After steaming and molding, noodle blocks are fed into frying baskets, which are mounted on the traveling chain of a tunnel fryer. The baskets filled with noodle blocks are immersed in hot oil for deep frying. Noodles drying can also be done by hot air to produce instant dried noodles. Frying is the preferred method of drying as nonfried instant noodles require a longer cooking time.
- Packaging: Frying or drying is followed by cooling the product to room temperature to avoid rapid oxidation and other changes. The cooled noodles are packed into a bag along with a soup base sachet. While for the cup noodles, powdered soup base is sprinkled over the noodles and sealed with shrink film. Seasonings and dehydrated vegetables are included in soup base. Higher fat content makes the noodles susceptible to oxidative changes and development of rancid flavour. Thus, proper packaging plays important role in extending the shelf life of the product. The packaging material used for noodles are polypropylene or polyethylene film for bag noodles and polyester for cup noodles.

Figure 1. New product of YUM YUM instant noodle

Figure 2. Wheat Flour Brands

IV. RESEARCH METHODOLOG Y

Data sheets were gathered for raw materials for the duration of three months. These data had been taken by the department of planning and a total of various wheat flour brands are checked from the production department. There are many different kinds of forecasting methods and inventory formulas in operation planning. For forecasting, the two most important factors are cost and accuracy. Two-period moving average and exponential smoothing are used to make forecast and forecast accuracy. For inventory management, the goal in ordering is to place an order when the amount on hand is sufficient to satisfy demand during the time it takes to receive that order (i.e., lead time).

A. Forecasting Methods

Demand forecasting is an important component of yield management, which relates to the percentage of capacity being used. There are two uses for forecasts. One is to help managers plan the system and the other is to help the use of the system. Forecasting techniques based on time series are made on the assumption that future values of the series can be estimated from past values. Three techniques for averaging are

Moving average

$$F_t = \mathrm{MA}_n = \frac{\sum_{i=1}^{n} A_{t-i}}{n} = \frac{A_{t-n} + \cdots + A_{t-2} + A_{t-1}}{n} \quad (1)$$

Weighted moving average

$$F_t = w_t(A_t) + w_{t-1}(A_{t-1}) + \ \ldots + \ w_{t-n}\,(A_{t-n}) \quad (2)$$

Exponential Smoothing

$$F_t \ = \ F_{t-1} + \ \alpha\,(\,A_{t-1} - \,F_{t-1}\,) \quad (3)$$

Forecast accuracy is significant factor when deciding among forecast alternatives. Accuracy is based on the historical error performance of forecast. Three commonly used measures for summarizing historical errors are the mean absolute deviation (MAD), the mean squared error (MSE), and the mean absolute percent error (MAPE). Difference between these measures is that MAD weights all errors evenly, MSD weights error according to their squared values, and MAPE weights according to relative error. Forecast error is the difference between the value that occurs and the value that was predicted for a given time period. Hence, Error = Actual-Forecast

$$\mathrm{MAD} \ = \frac{\sum|\mathrm{Actual}_t - \mathrm{Forecast}_t|}{n} \quad \text{or MAD} \ = \frac{\sum|e|}{n} \quad (4)$$

$$\mathrm{MSE} \ = \frac{\sum(\mathrm{Actual}_t - \mathrm{Forecast}_t)^2}{n-1} \ \text{or MSE} \ = \frac{\sum|e^2|}{n-1} \quad (5)$$

$$\mathrm{MAPE} = \frac{\sum[\frac{|e|}{\mathrm{Actual}}\mathrm{x}100]}{n} \quad (6)$$

Where,

F_t = Forecast for time period t

MA_n = n period moving average

A_{t-1} = Actual value in period t – 1

n = Number of periods (data points) in moving average

W_t = Weight for the period t

W_{t-1}= Weight for period t – 1

A_t = Actual value in period t

A_{t-1} = Actual value for period $t-1$

F_{t-1} = Forecast for the previous period (i.e., t -1)

α = Smoothing Constant

A_{t-1} = Actual demand or sales for previous period

V. RESULT AND DISCUSSIONS

(1) Calculating the forecast of wheat floor by using two-period moving average and exponential smoothing of Yathar Cho Industry. Wheat flour (1bag = 40kg)

A. Wheat Flour Forecasting based on monthly by using two-period and five- period moving average. All units were shown in tonnes. These forecast results were come from using the equation (1) and forecast accuracies were gained from using equation (4), (5) and (6)

Table 1. Forecasting of wheat flour

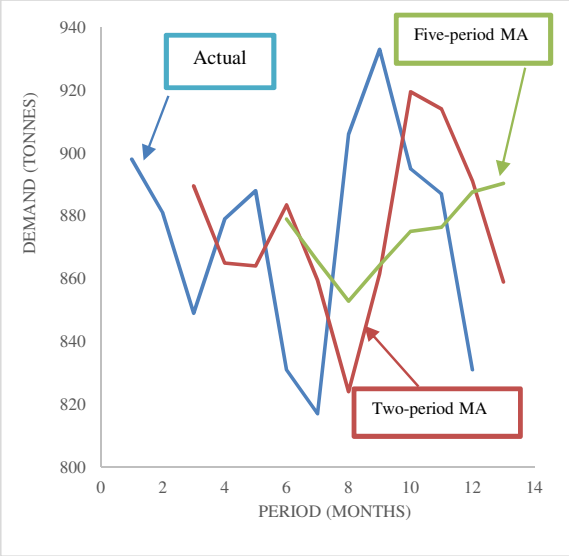

Figure 3. The more periods in moving average, the greater the forecast will lag (slow) changes in the data

A moving average forecast uses a number of the most recent actual data values in gathering a forecast. The moving average can incorporate as many data points as desired. The advantages of a moving average forecast are that it is easy to compute and easy to understand. A possible disadvantage is that all values weighted equally. For instance, in a 10 period moving average, each value has a weight of 1/10. In selecting the number of periods to include, we must take into account that the number of data points in the average determines its sensitivity to each new data point: The fewer the data points in an average, the more sensitive (responsive) the average tends to be. That is why, two- period moving average is more sensitive (responsive) than five-period moving average. If responsiveness is important, a moving average with relatively few data points should be used. This will permit quick adjustment to say, a step change in the data but it also will cause the forecast to be somewhat responsiveness even to random variations. Conversely, moving data points with five-period moving average will smooth more but less responsive to "real" changes. A review of forecast errors can help in this decision. Accuracy and control of forecasts is a vital aspect of forecasting, so forecasters want to minimize forecast errors. If lowest MAD is the criterion, the five-period moving average has the greatest accuracy; if lowest MSE is the criterion, two-period moving average works best; and if lowest MAPE is the criterion, the two-period

Month	Actual Demand	Two-period moving average		Five-period moving average	
		Forecast	Error	Forecast	Error
Jan	898	-	-	-	-
Feb	881	-	-	-	-
Mar	849	889.5	-40.5	-	-
Apr	879	865	14	-	-
May	888	864	24	-	-
June	831	883.5	-52.5	879	-48
July	817	859.5	-42.5	865.6	-48.6
Aug	906	824	82	852.8	53.2
Sep	933	861.5	71.5	864.2	68.8
Oct	895	919.5	-24.5	875	20
Nov	887	914	-27	876.4	10.6
Dec	831	891	-60	887.6	-56.6
Jan	-	859	-	890.4	-
MAD		43.85		43.69	
MSE		2638		2658	
MAPE		5.029%		5.03%	

moving average method is again best. Of course, it seems that two-period moving average performs better than five-period according to MSE, MAPE.

B. Wheat flour forecasting based on monthly by using exponential smoothing. All units were shown in tonnes. These results were come from using the equation (3).

Table 2. Calculation of wheat flour

Month	Actual	α = 0.1	α = 0.2	α = 0.3	α = 0.4
Jan	898	-	-	-	-
Feb	881	898	898	898	898
Mar	849	896.3	894.6	892.9	891.2
Apr	879	891.6	885.5	879.7	874.3
May	888	890.3	884.2	879.5	876.2
June	831	890.1	885	882.1	880.9
July	817	884.2	874	866.8	860.9
Aug	906	877.5	862.6	851.9	843.3
Sep	933	880.4	871.3	868.1	868.4
Oct	895	885.7	883.6	887.6	894.2
Nov	887	886.6	886	889.8	894.5
Dec	831	886.6	886.2	889	891.5
Jan	-	881	875.2	871.6	867.3
MAD		31.99	32.42	32.56	33.24
MSE		1745.6	1745.9	1794.5	1846.9
MAPE		3.74%	3.76%	3.76%	3.84%

Table 3. Calculation of Wheat Flour

Month	α = 0.5	α = 0.6	α = 0.7	α = 0.8	α = 0.9
Jan	-	-	-	-	-
Feb	898	898	898	898	898
Mar	880.5	887.8	886.1	884.4	882.7
Apr	869.3	864.5	860.1	856.1	852.4
May	874.2	873.2	873.3	874.4	876.3
June	881.1	882.1	883.6	885.3	886.8
July	856.1	851.4	846.8	841.9	836.6
Aug	836.6	830.8	825.9	822	819
Sep	871.3	876	882	889.2	897.3
Oct	902.2	910.2	917.7	844.2	929.4
Nov	898.6	901.1	901.8	884.8	898.4
Dec	892.8	892.6	891.4	886.6	888.1
Jan	862	855.6	849.1	842.1	836.7
MAD	33.9	35.79	36.28	37.28	35.45
MSE	1823.4	1914.7	1966.3	2052.7	1918.4
MAPE	3.9%	4.12%	4.17%	4.28%	4.07%

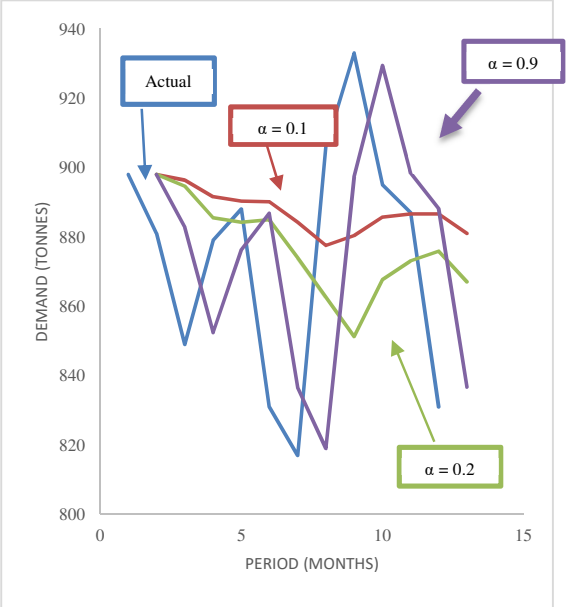

Figure 4. The closer α is zero, the greater the smoothing

Exponential smoothing is a sophisticated weighted averaging method that is still relatively easy to use and understand. Exponential smoothing is one of the most widely used techniques in forecasting, partly because of its ease of calculation, and partly because of the ease with which the weighting scheme can be altered-simply by changing the value of α. Each new forecast is based on the previous forecast plus a percentage of the difference between that forecast and the actual value of the series at that point. The quickness of forecast adjustment to error is determined by the smoothing constant error, α. The closer its value is to zero, the slower the forecast will be adjust to forecast errors (i.e., the greater the smoothing). Conversely, the closer the value of α is to 1.00, the greater the responsiveness and the less the smoothing. That is why, the value of α = 0.1 is more smoothing whereas the value of α = 0.9 is more

responsiveness and similar to actual trend. This is illustrated in figure 4. The goal is to select a smoothing constant that balances the benefits of smoothing random variations with the benefits of responding to real changes if and when they occur. Commonly used values of α range from .05 to .50. Low values of α are used when the underlying average tends to be stable; higher values are used when the underlying average is susceptible to change. Selecting a smoothing constant is basically a matter of judgement or trial and error, using forecast errors to guide the decision. From all of these data in exponential smoothing, α = 0.1 is the greatest accuracy because of the lowest MAD, MSE and MAPE.

C. Comparison of forecast accuracy of wheat flour

Table 4. Comparison of forecast accuracy

Methods	Two-period moving average	Exponential Smoothing		
		α = 0.1	α = 0.2	α = 0.3
Mean Absolute Deviation (MAD)	43.85	31.99	32.42	32.56
Mean Squared Error (MSE)	2638	1745.6	1745.9	1794.5
Mean Absolute Percent Error (MAPE)	5.029%	3.74%	3.76%	3.76%

One use for these measures is to compute the accuracy of alternative forecasting methods. For instance, we could compare the results to determine to one which yields the lowest MAD, MSE or MAPE for a given set of data. MAD is the easiest to compute, but weights errors linearly. MSE squares errors, thereby giving more weight to larger errors, which typically cause more problems. MAPE should be used when there is a need to put errors in perspective. Comparison of two-period moving average and exponential smoothing, the value of α = 0.1 is the best accuracy.

VI. CONCLUSION

The paper is studied on the operation planning of Yathar Cho Industry Limited (YUM YUM Instant Noodle Factory). Planning is the integral part of manager's job. If uncertainties cloud the planning horizon, managers will find it difficult to plan effectively. Forecasts help managers by reducing some of the uncertainty, thereby enabling them to develop more meaningful plans. A forecast is a statement about the future value of a variable such as demand. That is, forecasts are predictions about the future. The better those predictions, the more informed decisions can be. These are especially helpful in operation planning and scheduling day-to-day operations. This paper also describes the elements of good forecasts; the necessary steps in preparing a forecast, basic forecasting techniques, and how to monitor a forecast for wheat flour. Moreover, if demand was much less than the forecast, an action such as a price reduction or a promotion may be needed. If demand was much more than the forecast, increased output may be advantageous. This may involve working overtime, outsourcing, or taking other measures. Inventory management is also a core operation planning activity. Inadequate control of inventories can result in both under and overstocking of items. Understocking results in missed deliveries, lost sales, dissatisfied customers, and production bottlenecks; overstocking unnecessarily ties up funds that might be more productive elsewhere. If these procedures in operation fulfilled that requirement by operation planning, the factory will get the material smoothing and without interruption for operation process, prevent stock-out.

ACKNOWLEDGEMENT

The author would like thank all her teachers in Mechanical Engineering Department for their supporting, for thier encouragement, useful suggestion, invaluable guidance and help till the completion.

REFERENCES

[1] Handanhal V.Ravinder, Montaclair State University, "Forecasting with Exponential Smoothing- What's the Right Smoothing Constant",USA,Vol17,No 3,2013

[2] The Institute of Cost Account of India., "Operation Management and Strategic Management"

[3] William J.Stevenson., "Operations Management",Tenth Edition

[4] Jacobs Chase Aquiland., "Operations Management".2nd edition

[5] N.de P.Barbosa, E.da S.Christo, and KA.Costa, Department of Production Engineering "Demand Forecasting for Production Planning in a Food Company", Brazil, Vol 10,No 16,Sep,2015

[6] S.Anil Kumar, N.Suresh, "Operations Management", 2009

[7] Nigel Slack, Stuart Chambers, Robert Johnston, Alan Betts,

Towards Understanding Water Governance for Sustainable Urban Water Management in Yangon City

May Myat Mon[#1]

Water Resources and Water Supply Authority, Yangon City Development Committee

maymyatmon.thaethae@gmail.com[#1]

Abstract-Yangon City has already become water stressed due to the population growth, urbanization, industrial zones development, changing lifestyle pose serious challenges to water security. To access safe drinking water and distribute daily water demand for all city dwellers in Yangon is important for all water related organizations. This research focuses on understanding governance for sustainable urban water management under Yangon City Development Committee (YCDC). There are three approaches; Improvement of Institutional Management, Improvement of Non-Revenue Management and Improvement of Water Quality Monitoring are enhanced by Water Resources and Water Supply Authority (WRAWSA). According to that, capacity of YCDC on the management of water supply service is improved and set up strategies and actions plans to implement for sustainable urban water management.

Keywords: ***population growth, sustainable urban water management, Institutional Management, Non-Revenue Management, Improvement of Water Quality Monitoring***

I. INTRODUCTION

Myanmar's government, civil society, and population have recognized that water resources management systems must be put in place to ensure sustainable development of the country's economy and resources as well as human and cultural values.As population growth and economic development in urban and rural areas increase water demand in the country, it is important for all water related to collaborate and coordinate to set up strategies and action plans to implement for Integrated Water Resources Management.

Currently, the population in Yangon City is about 5.21 million (2014 Census Data) and the city is growing with increasing population by urbanization. Moreover Yangon City is forecasted to become a mega city with 10 million populations in 2040. The more population is increased, the more water demand is needed in future.Besides, accessing to safe drinking water and basic sanitation and other domestic needs is still a problem in many areas. To provide safe water, hygienic living, and sound water environment for all city dwellers is first priority of water vision in Yangon City. Therefore, future development plans for water supply and sanitation services are required to formulate as well as understanding water governance is needed for sustainable urban water management. This study empirically examines the governance needs SUWM in WRAWSA.

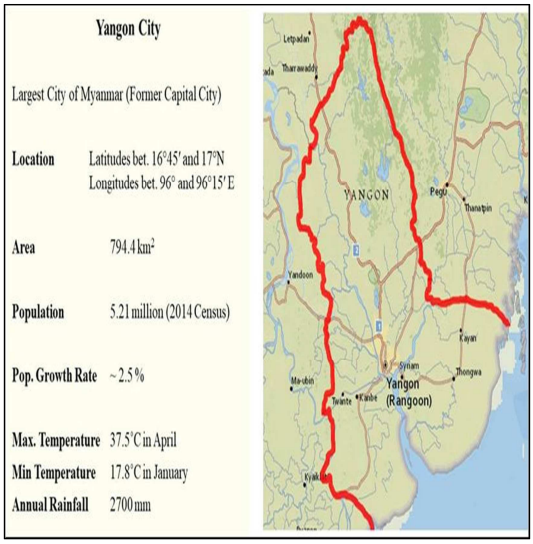

Fig 1 Location of Yangon City

II. OVERVIEW OFYANGON CITY WATER SUPPLY SYSTEM

2.1 Past Water Supply System in Yangon

Yangon city is the second capital of Myanmar. It is situated at the confluence of Bago River, Yangon River and Hlaing River. Yangon city water supply system has a long history of more than 150 years. In 1879, Kandawgyi Lake is the first used for water supply system. In 1884, Inya Lake is constructed for water supply system.

In 1894, the pumping station and service water tank is developed by the construction of Phoesein pumping station and Shwedagon service water tank (1MG storage capacity) in Yangon City.

The water delivered from Kandawgyi Lake to Phosein staion was pumped to the Shwedagon service tank.

In 1904, HlawgaReservoir(14MGD supply capacity) was constructed and the water from Hlawga Resevoir was pumped toYegu pumping station by booster pumping station Hlawga Reservoir.

In 1906, the construction of Yegu pumping station was completed. And then the water was pumped to Shwedagon Reservoir which water was distributed to the whole city.

In Kokkhine service water tank (20MGD storage capacity) was constructed and added to the existing water supply system to expand the served area.

In 1941, Gyobyu Reservoir (27 MGD supply capacity) and water was supplied through Yegu pumping station to Kokkhine service water tank.

In 1989, Phugyi Reservoir (54MGD supply capacity) was constructed and added to the water supply system by connecting with Hlawga Reservoir which is distributed to Yangon City.

At that time, the total amount of daily water supply was 85 MGD, including YCDC owned tube well (10 MGD). In 2000, Yangon Pauk ground water treatment project was completed and the water supply amount is 1MGD.

In 2005, Ngamoeyiek WTP project (Phase1 with 45 MGD supply capacity) was constructed by Ministry of Agriculture and Irrigation.

In 2009, South Dagon ground water treatment project (2MGD supply capacity) and Thaephyu ground water treatment project (11 MGD supply capacity) is added to the supply water. The second phase of Ngamoeyiek WTP in early 2014 and it started to supply daily water capacity 45MGD.

Now Kandawgyi Lake and Inya Lake are not used for water supply because the water quality is deterioration by rapid of urbanization. Phoesein pumping station is stopped, too.

2.2 Existing Current Yangon City Water Supply System

The current water supply amount is 205MGD. The source of surface water is about 92% from reservoir and 8% is the ground water from tube well for daily water supply.

The major water sources are Gyobyu Reservoir, Phugyi Reservoir, HlawgaReservoir, Ngamoeyeik Water Treatment (WTP) 1st and, 2nd phase and YCDC tube wells.

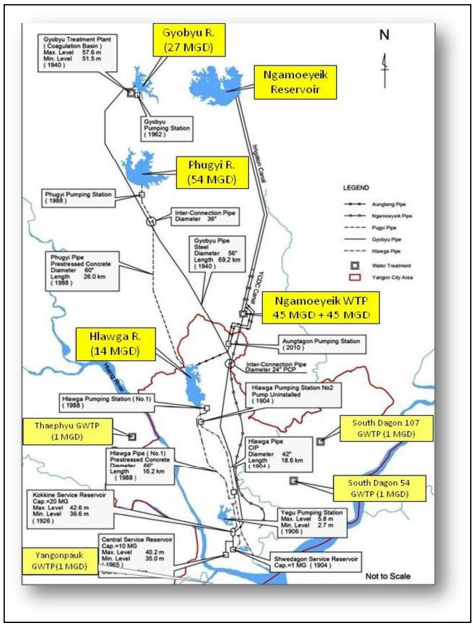

Fig 2 Existing Yangon City Water Supply System

Table 1 Daily Water Supply Capacity

No	Water Source	Million Gallons per Day (MGD)	Remark
1	Gyobyu Reservoir	27	YCDC
2	Phyugyi Reservoir	54	YCDC
3	Hlawga Reservoir	14	YCDC
4	Ngamoeyiek WTP (1st phase)	45	YCDC
5	Ngamoeyiek WTP (2ndphase)	45	YCDC
6	YCDC Tube Wells (425 nos)	20	YCDC
7	Total Water Supply Capacity	205	YCDC

2.3 Aged Transmission and Distribution Pipelines

Water Supply system in Yangon has a long history, the water supply services commenced in 1842. Transmission and distribution pipes have not been rehabilitated and the old age pipelines did not have enough flow capacity properly which results in large quantity of non-revenue water (NRW).

Moreover other water facilities have not been expanded last decades.

Table 2 Aged Transmission pipes

Start-up year	Pipe material	Diameter (in)	Length (mile)	Age (year)	Remark
1904	Cast iron	42	14.2	113	YCDC
1914	Cast iron	42	5	103	YCDC
1940	Mild Steel	56	43	77	YCDC
1989	Pre-stressed concrete	60	16	28	YCDC
1992	Pre-stressed concrete	66	10.4	25	YCDC

The total length of distribution and transmission pipelines in whole network is 2655 miles.

2.4 History Water Treatment Plant (WTP)

According to the history of water supply system, 90% of water came from reservoirs, and two thirds of them is distributed directly without any treatment.

In the old Gyobyu WTP, water is treated by sedimentation process without coagulant, Nyaunghnapin WTP is treated by rapid sand filtration and groundwater is treated by aeration method.

III IMPROVEMENT of WATER SUPPLY MANAGEMENT

3.1 Study Area

Water Resources and Water Supply Authority (WRAWSA)

3.2 Governance for Sustainable Urban Water Management (SUWM)

Water is the essential need of mankind for their life and living especially, the areas where the drinking water supply is systematically managed are more rapidly developing. It is not evenly distributed and well management leading to many problems and impacts in our environment. Based on these systemic and inter-related barriers **(Brown and Farrelly, 2009),** it can be surmised that there is a lackof insight intogovernance approaches required to support SUWM practices.

Governance describes the management of collectives issues, the stakeholders involved and process used **(Kjaer, 2004; Pierre and Peters, 2000; Stoker, 1998**).

Regarding good water governance for SUWM, WRAWSA is cooperating and collaborating with Japan International Cooperation Agency (JICA) Technical Assistance Team as well as implemented the project for “Improvement of Water Supply Management of YCDC” from 2016 to 2020.

3.3 Three Approaches

According to that, the three approaches often identified are Improvement of Institutional Management, Improvement of Non-Revenue Management and Improvement of Water Quality Monitoring.

3.4 Process of Preparation

Moreover, WRAWSA learns neighboring countries successful urban water supply system. Based on it, the findings, advantages, and disadvantages are compared and analyzed with past water supply situation. According to that, “Management Improvement Plan” proposal is designed and proposed to improve the YCDC water supply industry in more advanced and successful.

Improvement of Institutional Management; this article assesses the institutional prescriptions of adaptive (co-)management based on the literature review of water governance. The public participation, an experimental approach to water resources management and bioregional approach is essential for improvement of institutional management. The following are the management improvement area for Institutional Governance.

1. To practice Autonomous System
2. To get approval from respective ministry for budget allocation

It's also necessary to extend technology division to able to implement specific work operations and task allocation systematically. The extended Sections in New organization Structure are as follows.

Table 3 Objective of setting Sections

No	Section	Objectives
1	Planning	To manage overall planning of WRWSA
2	Transmission and Distribution	To maintain transmission and distribution pipes and to supervise its related works
3	GIS	To keep customer data and geometry information (tube wells, pipelines, service reservoirs SR, WTP)
4	NRW Management	To solve physical losses
5	Human Resources Development HRD	To promote capacity buildings management
6	WTP	To management water treatment facilities and water quality
7	Customer Service Division	To perform customers services and improve E-government

Improvement of Non-Revenue Water Management; it is rigid established and the activities to reduce NRW are continuously carried out by instruction of the trainers and based on NRW management plan.

Due to the old age pipelines, its capacity is low and it is happened leaking pipeswhich is so far cannot deliver as well as water losses by ways of physical damage and commercial loss. As a result of that, it is leading to NRW. Thus, the level of water losses can be determined by International Water Association standard water balance (IWA).

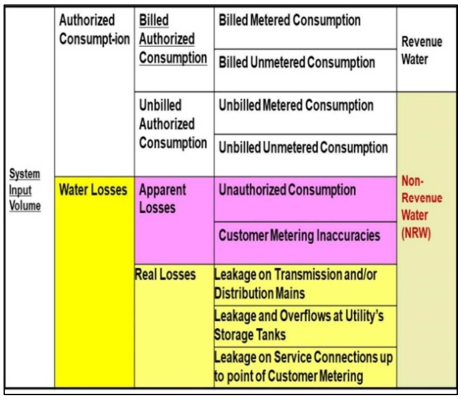

Fig 3 Standard IWA Water Balance

To protect the non-revenue water, develop and manage the water distribution with help of advantage technology, it is analyzed by new project.

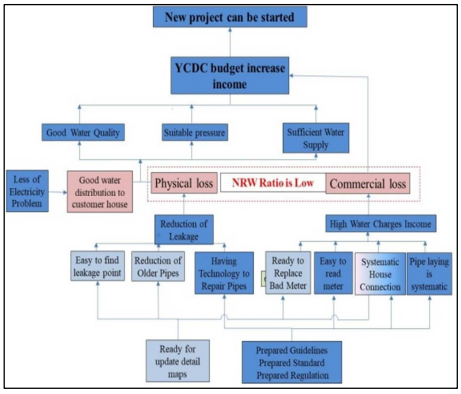

Fig 4 Flow Chart of New Project

Likewise; the update detail map and data, physical loss and commercial loss and management capacity improvement are the approaches for enhancement of NRW management. The following figures are as shown in below;

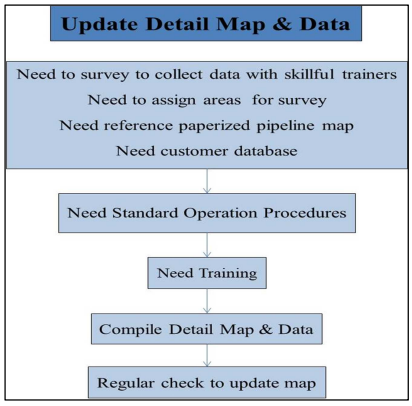

Fig 5 Update Detail Map and Data

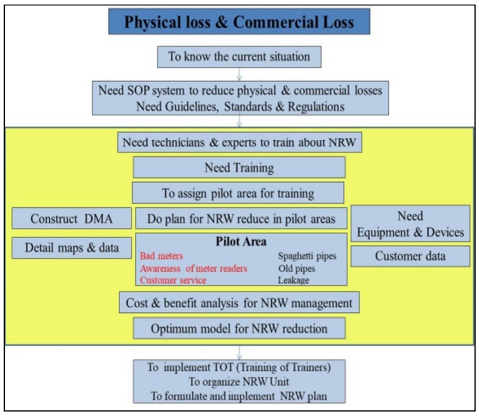

Fig 6 Physical Loss and Commercial Loss

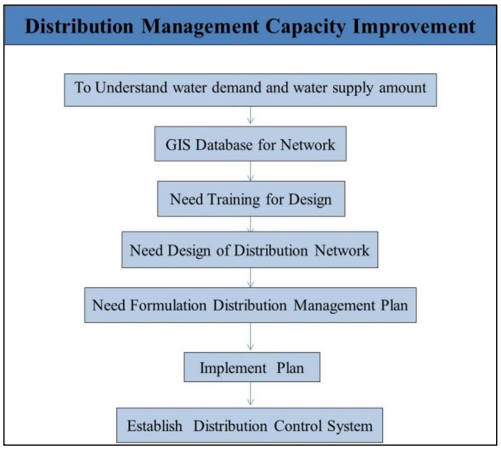

Fig 7 management capacity improvement

Improvement of Water Quality Management; acquiring and developing water treatment technology and capacity of planning, designing and operation and maintenance are required for producing safe and clean water.

.

Parameters for water quality monitoring

No	Parameters	Unit of measurement	Method of measurement
1	Total Coliform	MPN/100ml	multiple Tube Fermentation Technique(APHA9221A)
2	Fecal Coliform	MPN/100ml	ditto
3	Taste	mg/l	Sensory Evaluation Technique(APHA2160B)
4	Odor	mg/l	(APHA2150B)
5	Color	TCU	Spectro - photometric SingleWavelengthAPHA2120C
6	Turbidity	NTU	Nephelometric MethodAPHA2130B
7	Arsenic	mg/l	Hydride generation Atomic Absorption Spectrometric method
8	Lead	mg/l	Flame Atomic Absorption Spectrometric method
9	Nitrate	mg/l	Ultraviolet (UV) technique
10	Manganese	mg/l	Flame Atomic Absorption Spectrometric method
11	Chloride	mg/l	Argentometric method
12	Hardness	mg/l	EDTA Titrimetric method
13	Iron	mg/l	Flame Atomic Absorption Spectrometric method
14	pH	mg/l	Electrometric method
15	Sulphate	mg/l	Gravimetric method
16	Total Dissolved Solids(TDS)	mg/l	Dried at 180°C
17	Total Suspended Solids (TSS)	mg/l	Standard method (dried at 103-105°C)
22	Residual Chlorine	mg/l	DPD method
23	Calcium	mg/l	EDTA Titrimetric method
24	Magnesium	mg/l	EDTA Titrimetric method
25	Total Alkalinity	mg/l	Titrimetric method
26	Dissolved Oxygen	mg/l	DO meter

Fig 8 Parameters for Water Quality Monitoring

Fig 9 Sources of Water Quality Monitoring

Sampling Location	Monitoring item
Gyobyu Reservoir	Daily: Water temperature, pH, Turbidity and Color
	Weekly:TSS (Sampling)
Phugyi Reservoir	Daily: Water temperature, pH, Turbidity and Color
	Weekly:TSS (Sampling)
Hlawga Reservoir	Daily: Water temperature, pH, Turbidity and Color
	Weekly: TSS (Sampling)
Yegu PS	Daily: Water temperature, pH, Turbidity, Color and Residual chlorine*
	*Residual chlorine monitoring is done at After chlorine injection point.
	Weekly:TSS (Sampling)

Fig 10 Sampling Locations

These are the ways to provide safe water, hygienic living, and sound water environment to all citizens not only current situation but also in the future. Besides the perspective in planning, management and use of water resources about IWRM principles and participatory approach stand as a important role for IWRM.

IV. RESULTS AND DISCUSSION

Based on three approaches, it can be formulated again the problem solution to meet the improvement of water supply management as well as it can be developed 5 years plan and annual activity plan for WRAWSA.

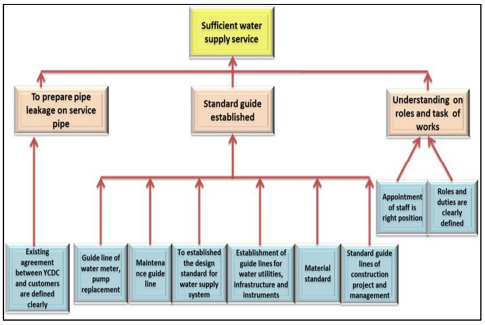

Fig 11 Sufficient Water Supply Services

According to NRW activities, WRAWSA could successful district meter area (DMA) for systematic water distribution pilot area in North Oakalapa Township (ward 2)

Meter Readings and NRW Ratio Calculation

No.	Date	Main Meter Units (m^3)	Service Meter Units (m^3)	NRW Ratio (%)	Remark
1.	19 . 6 . 2018	10480	9922	5.32	Only Phase-1 Finished
2.	20 . 7 . 2018	10740	10385	3.31	Only Phase-1 Finished
3.	19 . 8 . 2018	10360	10825	-4.49	Only Phase-1 Finished, Main Meter Block
4.	19 . 9 . 2018	37780	35347	6.44	Phase-1 & 2 Finished
5.	19 . 10 . 2018	31470	29547	6.11	Phase-1 & 2 Finished
6.	20 . 11 . 2018	29000	27150	6.39	Phase-1 & 2 Finished
7.	19 . 12 . 2018	107780	100106	7.12	Phase-1, 2 & 3 Finished
8.	19 . 1 . 2019	95540	88336	7.54	Phase-1, 2 & 3 Finished
9.	19 . 2 . 2019	91843	85478	6.93	Phase-1, 2 & 3 Finished
10.	9 . 8 . 2019	90119	97082	-7.73	Estimated Meter Reading
11.	9 . 9 . 2019	90000	95528	-6.14	Estimated Meter Reading
12.	7 . 10 . 2019	106584	90961	14.66	Actual Meter Reading

Fig 12 Result of Meter Readings and NRW Ratio Calculation

As a result of improvement of water quality monitoring, WRAWSA could establish standard operation parameters (SOPs), mini-laboratories in reservoirs and enhance the capacity of water quality analysis with advanced analytical equipment.

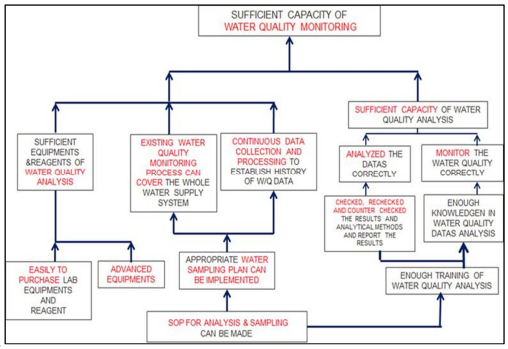

Fig 13 Sufficient Capacity of Water Quality Monitoring

V. CONCLUSIONS

Myanmar has many challenges in water quality, water supply services and sustainable development in natural resources. This research focuses on understanding governance for sustainable urban water management under Yangon City Development Committee (YCDC). The discipline knowledge, critical thinking and problem-solving water project management are important roles for realizing how strongly important of water governance is.

ACKNOWLEDGEMENT

First of all, the author would like to express thank to her Water Resources and Water Supply Authority under Yangon City Development Committee for supporting required data in research work and invaluable instruction throughout the study and research work.

The author would like to give extend thanks to Federation of Myanamr Engineering Socities for participating National Conference on Engineering Research.

The author is also sincerely thankful U Myint Zaw Than, Head of Water Resources and Water Supply Authority under Yangon City Development Committee for his kind and guidance.

The authour would like to thank to U Zaw Win Aung, Excutive Engineer of Water Resources and Water Supply Authority under Yangon City Development Committee for his advice and helpful sugesstions.

REFERENCES

[1] Book, W.J., 1990, December. Modeling, design, and control of flexible manipulator arms: A tutorial review. In 29th IEEE Conference on Decision and Control (pp. 500-506). IEEE.

[2] Franks, T.R. and Cleaver, F.D., 2009. Analysing water governance: a tool for sustainability.

[3] Wong, T.H. and Brown, R.R., 2009. The water sensitive city: principles for practice. Water science and technology, 60(3), pp.673-682.

[4] Book, JICA Master Plan., 2014, Preparatory Survey Report on The Project for The Improvement of Water Supply, Sewerage and Drainage System in Yangon City in The Republic of The Union of Myanmar.

FEDERATION OF MYANMAR ENGINEERING SOCIETIES
COMMEMORATION OF ANNUAL GENERAL MEETING OF FED.MES
16-1-2020
BUILDING OF FEDERATION OF MYANMAR ENGINEERING SOCIETIES

NATIONAL CONFERENCE ON ENGINEERING RESEARCH

Tentative Agenda

Function Hall

8:00 - 8:45	Registration
8:50 - 9:00	Opening
9:00 - 9:10	Opening Speech by U Aung Myint , President of Federation of Myanmar Engineering Societies

Function Hall

Session	Time	Presenter	Title
Keynote Speech	**9:10 -9:35**	**H.E Dr.Kyaw Linn**	PPP Analytical Framework for Infrastructure Asset Allocation
	9:35 - 10:00	**U Tin Myint**	Current Status of RE in Myanmar and its Future
	10:00 -10:25	**Prof.Dr.Hitoshi Tanaka**	Impact of Climate Change on River Delta Coastlines
	10:25 - 10:40		Coffee Break

Function Hall

Session	Time	Presenter	Title	Chairperson/ Moderator
Session (1)	**10:40 - 11:00**	**Khaing Chan Myae Thu**	Development of Flood Inundation Map for Upper Chindwin River Basin By Using HEC-HMS and HEC-RAS	**U Hla Baw/ Nan Theint Kham Ko Ko**
	11:00-11:20	**Kyaw Myo Htun**	Project Management and Construction Method for Different Types of Bridge in Various Locations of Myanmar. (From Naung Moon to Kawthaung)	
	11:20-11:40	**Shwe Pyi Tan**	Integrated Water Resources Management Plans for Sittaung River Basin	
	11:40-12:00	**Ei Khaing Zin Than**	Assessment of Crop and Irrigation Water Requirements for Some Selected Crops in Chaung Gauk Irrigation Scheme	
	12:00- 13:00		Lunch	

FEDERATION OF MYANMAR ENGINEERING SOCIETIES
COMMEMORATION OF ANNUAL GENERAL MEETING OF FED.MES
16-1-2020
BUILDING OF FEDERATION OF MYANMAR ENGINEERING SOCIETIES

NATIONAL CONFERENCE ON ENGINEERING RESEARCH

Tentative Agenda

Function Hall

Session	Time	Presenter	Title	Chairperson/ Moderator
Session (2)	13:00 - 13:20	Aung Aung Soe	Effect of Lime Content and Curing Condition on Strength Development of Lime-Stabilized Soil in Bogalay Township, Ayeyarwaddy Region	U Khin Maung Htaey/ Kyi Sin Thant
	13:20 - 13:40	Tin Tin Wai	Investigation on Performance Level of 10-storey R.C Building with Pushover Analysis	
	13:40 - 14:00	Aye Thet Mon	Comparative Study on Soft Storey Effect at Different Levels in Reinforced Concrete Buildings	
	14:00 - 14:20	Aung Myo Wai	Design of Water Distribution System Using Hydraulic Analysis Program (EPANET 2.0) for Tatkon Town in Myanmar	
	14:20 - 14:40	May Myat Mon	Towards Understanding Water Governance for Sustainable Urban Water Management in Yangon City	
	14:40 - 15:00		Coffee Break	

Function Hall

Session	Time	Presenter	Title	Chairperson/ Moderator
Session (3)	15:00 - 15:20	Chan Myae Kyi	Study on the Behavior of Spun Pile Foundation Becoming Due to Seismic Loading	U San Kyu/ Su Latt Twel Tar Bo
	15:20- 15:40	Hla Tun	Mathematical Analysis of Reservoir Flood Routing	
	15:40 - 16:00	Tun Min Thein	Key Factors for the Successful Construction of Tunnels and Shafts	
	16:00 - 16:20	Thi Thi Khaing	Transition of Urban Sustainability Approach	
	16:20 - 16:40	Wai Yar Aung	Earthquake Safety Assessment of RC Buildings in Myanmar	

FEDERATION OF MYANMAR ENGINEERING SOCIETIES
COMMEMORATION OF ANNUAL GENERAL MEETING OF FED.MES
16-1-2020
BUILDING OF FEDERATION OF MYANMAR ENGINEERING SOCIETIES

NATIONAL CONFERENCE ON ENGINEERING RESEARCH

Tentative Agenda

Function Hall

8:00 - 8:45	Registration
8:50 - 9:00	Opening
9:00 - 9:10	Opening Speech by U Aung Myint , President of Federation of Myanmar Engineering Societies

Function Hall

Session	Time	Presenter	Title
Keynote Speech	**9:10 -9:35**	**H.E Dr.Kyaw Linn**	PPP Analytical Framework for Infrastructure Asset Allocation
	9:35 - 10:00	**U Tin Myint**	Current Status of RE in Myanmar and its Future
	10:00 -10:25	**Prof.Dr.Hitoshi Tanaka**	Impact of Climate Change on River Delta Coastlines
	10:25 - 10:40		Coffee Break

Conference Room

Session	Time	Presenter	Title	Chairperson/ Moderator
Session (1)	**11:00-11:20**	**Dr.Htein Win**	Synthesis, Characterization and Application of Carbon Nanotubes in Conductive Ink	**U Kyaw Kyaw/ Yoon Thiri Zaw**
	11:20-11:40	**Dr. Saw Mya Ni**	Effect of Sintering Time on Properties and Shape Memory Behavior of Cu-Zn-Al Shape Memory Alloy	
	11:40-12:00	**Dr.Myat Myat Soe**	Recovery of Cobalt Metal From Spent LI-ION Battery by Combination Method of Precipitation and Reduction	
	12:00- 13:00		Lunch	

FEDERATION OF MYANMAR ENGINEERING SOCIETIES
COMMEMORATION OF ANNUAL GENERAL MEETING OF FED.MES
16-1-2020
BUILDING OF FEDERATION OF MYANMAR ENGINEERING SOCIETIES

NATIONAL CONFERENCE ON ENGINEERING RESEARCH

Tentative Agenda

Conference Room

Session	Time	Presenter	Title	Chairperson/ Moderator
Session (2)	13:00 - 13:20	Yu Nanda Hlaing	Microtremor Measurement at Some sites in Mandalay City, Myanmar, for Earthquake Disaster Mitigation	Dr.Zaw Htet Aung & U Khin Maung Than/ Aye Nyein Chan Moe
	13:20 - 13:40	Myint Aung	Assessment of Surface and Ground Water Quality around the Kyinsintaung Mine, Myanmar	
	13:40 - 14:00	Thaw Zin	Water Management for Waterflooding in Mature Field	
	14:00 - 14:20	Dr.Htay Htay Win	Theoretical and Numerical Modal Analysis of Six Spokes wheel's rim using ANSYS	
	14:20 - 14:40	Hsu Myat Tin	Analysis of Forecasting Techniques of Instant Noodle Manufacturing Company	
14:40 - 15:00			Coffee Break	
Session	**Time**	**Presenter**	**Title**	**Chairperson/ Moderator**
Session (3)	15:00 - 15:20	Khin Hnin Thant	Maritime Education, Training and Capacity Building in Myanmar Mercantile Marine College	Dr.Htin Lin/ Soe Moe Htet
	15:40 - 16:00	Thu Thu Aung	Capacity Building for Future-Oriented Education in Myanmar	
	16:00 - 16:20	Zin Thuzar Naing	Implementation of Sliding Mode Controller for Mobile Robot System	

FEDERATION OF MYANMAR ENGINEERING SOCIETIES
COMMEMORATION OF ANNUAL GENERAL MEETING OF FED.MES
16-1-2020
BUILDING OF FEDERATION OF MYANMAR ENGINEERING SOCIETIES

NATIONAL CONFERENCE ON ENGINEERING RESEARCH

Tentative Agenda

Function Hall

8:00 - 8:45	Registration
8:50 - 9:00	Opening
9:00 - 9:10	Opening Speech by U Aung Myint , President of Federation of Myanmar Engineering Societies

Function Hall

Session	Time	Presenter	Title
Keynote Speech	**9:10 -9:35**	**H.E Dr.Kyaw Linn**	PPP Analytical Framework for Infrastructure Asset Allocation
	9:35 - 10:00	**U Tin Myint**	Current Status of RE in Myanmar and its Future
	10:00 -10:25	**Prof.Dr.Hitoshi Tanaka**	Impact of Climate Change on River Delta Coastlines
	10:25 - 10:40		Coffee Break

Seminar Room

Session	Time	Presenter	Title	Chairperson/ Moderator
Session (1)	**10:40 - 11:00**	**Aung Kyaw Myint**	Implementation of SCADA System for Hydropower Station	**Daw Than Than Win/ Nay Htet Aung**
	11:00-11:20	**Nwe Ni Win**	Simulation and Analysis on Power Factor Improvement and Harmonic Reduction of High-voltage, High-frequency Power Supply for Ozone Generator	
	11:20-11:40	**Khin Thi Aye**	Promote the Development of Renewable Energy in Myanmar	
	11:40-12:00	**Min Set Aung**	Transition of University to Prosumer Consortium Energy Model	
	12:00- 13:00		Lunch	

FEDERATION OF MYANMAR ENGINEERING SOCIETIES
COMMEMORATION OF ANNUAL GENERAL MEETING OF FED.MES
16-1-2020
BUILDING OF FEDERATION OF MYANMAR ENGINEERING SOCIETIES

NATIONAL CONFERENCE ON ENGINEERING RESEARCH

Tentative Agenda

Seminar Room

Session	Time	Presenter	Title	Chairperson/ Moderator
Session (2)	**13:00 - 13:20**	**Zin Mar Htun**	Secure and Authenticated Data Hiding using Edge Detection	**Dr.Win Zaw / Lat yar La Pyae**
	13:20 - 13:40	**Dr.Aye Aye Thant**	Mathematical Approach to Stable Hip Trajectory for Ascending Stairs Biped Robot	
	13:40 - 14:00	**Khaing Thanda Swe**	Modeling Information Security System using Huffman Coding	
	14:00 - 14:20	**Dr. Phyo Thu Zar Tun**	Performance Evaluation for Classification on Dengue Fever	
	14:20 - 14:40	**Dr.Win Lei Lei Aung**	The Optimal Cost of an Outpatient Department by Using Single and Multiple Server System	

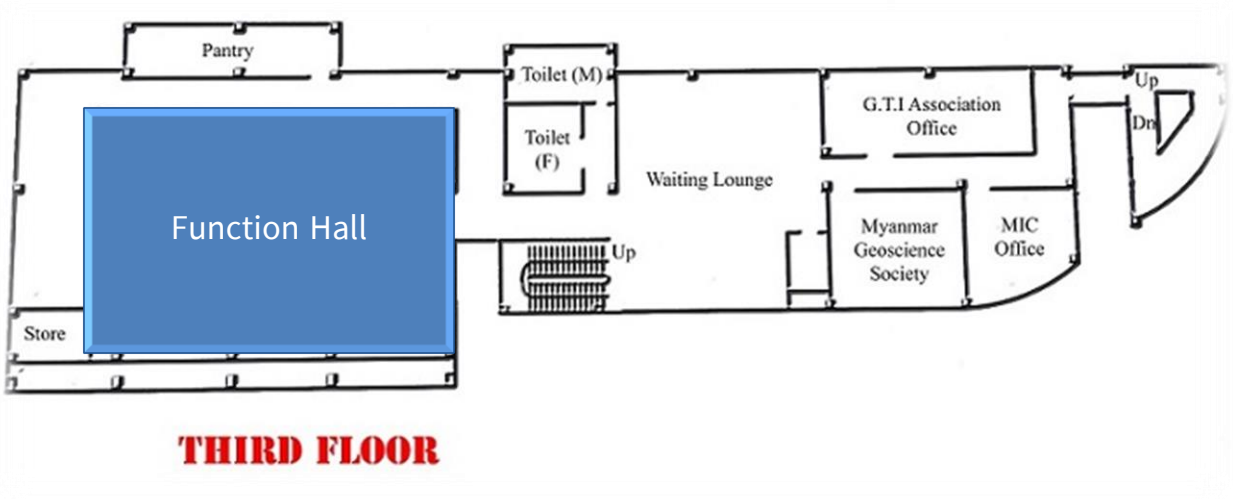
Pantry
Toilet (M)
Toilet (F)
Waiting Lounge
G.T.I Association Office
Up
Dn
Function Hall
Up
Myanmar Geoscience Society
MIC Office
Store
THIRD FLOOR

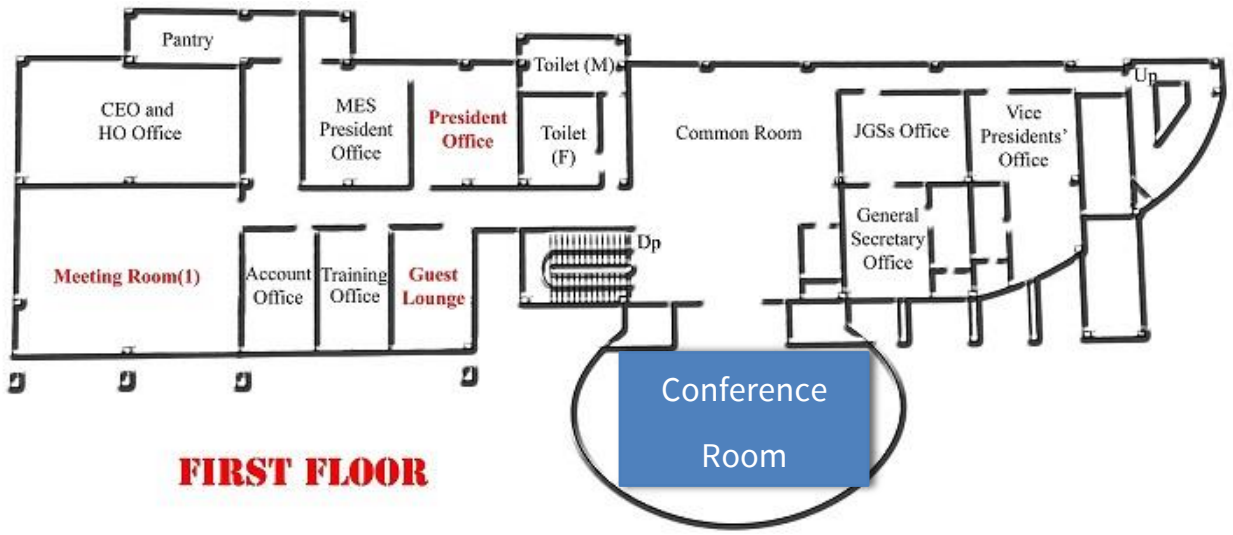
Pantry
CEO and HO Office
MES President Office
President Office
Toilet (M)
Toilet (F)
Common Room
JGSs Office
Vice Presidents' Office
Up
General Secretary Office
Meeting Room(1)
Account Office
Training Office
Guest Lounge
Dp
Conference Room
FIRST FLOOR

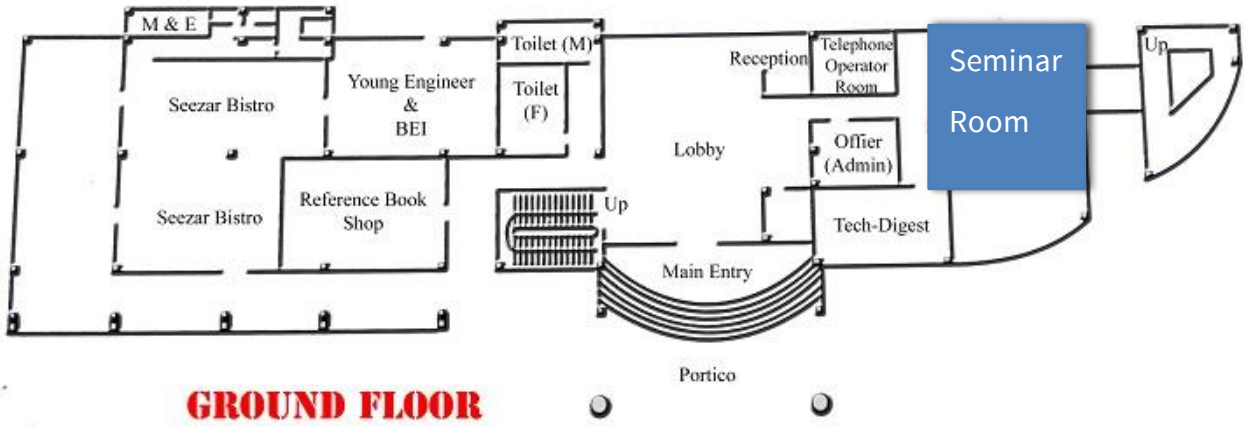
M & E
Seezar Bistro
Young Engineer & BEI
Toilet (M)
Toilet (F)
Reception
Telephone Operator Room
Seminar Room
Up
Lobby
Offier (Admin)
Seezar Bistro
Reference Book Shop
Up
Tech-Digest
Main Entry
Portico
GROUND FLOOR